

DOE/NV/10461--T66

TRAC *Technology and Resource Assessment Corporation*

3800 Arapahoe Avenue, Suite 225
Boulder, Colorado 80303
(303) 443-3700 FAX No. (303) 443-8626

RECEIVED

FEB 27 1993

**DIALOGS ON THE
YUCCA MOUNTAIN CONTROVERSY**

O.S.T.I

SPECIAL REPORT No. 10
CONTRACT No. 92/94.0004

SPECIAL REPORT Submitted to the
Nuclear Waste Project Office
State of Nevada

August, 1993

Assembled by:

C.M. Schluter
J. S. Szymanski

DISTRIBUTION OF THIS DOCUMENT IS UNLIMITED

JR

DISCLAIMER

This report was prepared as an account of work sponsored by an agency of the United States Government. Neither the United States Government nor any agency thereof, nor any of their employees, makes any warranty, express or implied, or assumes any legal liability or responsibility for the accuracy, completeness, or usefulness of any information, apparatus, product, or process disclosed, or represents that its use would not infringe privately owned rights. Reference herein to any specific commercial product, process, or service by trade name, trademark, manufacturer, or otherwise does not necessarily constitute or imply its endorsement, recommendation, or favoring by the United States Government or any agency thereof. The views and opinions of authors expressed herein do not necessarily state or reflect those of the United States Government or any agency thereof.

MASTER

**DIALOGS ON THE
YUCCA MOUNTAIN CONTROVERSY**

REPORT ORGANIZATION

PART 1

Introduction

Dr. C.B. Archambeau

PART 2

Letter to C.B. Archambeau

Dr. F. Press

PART 3

Letter to F. Press

Dr. C. B. Archambeau

PART 4

"Field Trip Report: Observations Made at Yucca Mountain,
Nye County, Nevada"

Carol A. Hill

PART 5

"The Origin of Sepiolite, Yucca Mountain, Nevada"

Carol A. Hill

PART 6

"Petrographic Description of Calcite/Opal Samples
Collected on Field Trip of December 5-9, 1992"

*Carol A. Hill and
Christine M. Schluter*

PART 7

"The Spatial and Chemical Diversity of Zeolitic Alteration
at Yucca Mountain, Nye County, Nevada"

Dr. Donald Livingston

PART 8

"Isotopic and Fluid Inclusion Study of Yucca Mountain Samples"

Dr. R.S. Harmon

PART 1

Introduction

INTRODUCTION

In an attempt to resolve the controversial issue of tectonic and hydrologic stability of the Yucca Mountain region, the National Academy of Sciences established a Panel on Coupled Hydrologic/Tectonic/Hydrothermal Systems. The Panel has recently released its findings in a report entitled *Ground Water at Yucca Mountain: How High Can It Rise?* The representation of data and the scientific validity of this report was the subject of comprehensive evaluations and reviews which has led to correspondence between Dr. Charles Archambeau and Dr. Frank Press, the President of the National Academy of Sciences. All such correspondence prior to April 9, 1993 is covered by TRAC Special Report #5, "Dialogs on the Yucca Mountain Controversy." The present report represents a continuation of the dialog between Dr. Archambeau and Dr. Press; specifically the letter from Dr. Press to Dr. Archambeau dated April 9, 1993 and Archambeau's response to Press, dated August 19, 1993.

In addition to the correspondence between Press and Archambeau, a series of recent reports by other investigators, referred to in the correspondence from Archambeau, are included in this report and document new data and inferences of importance for resolution of the question of suitability of the Yucca Mountain site as a high level nuclear waste repository. These reports also demonstrate that other scientists, not previously associated with the government's program at Yucca Mountain or the National Academy review of an aspect of that program, have arrived at conclusions that are different than those stated by the Academy review and DOE program scientists.

The focus of the controversy involves the origins of observed alkaline earth metasomatism and the abundant carbonate-opal-sepiolite mineral assemblages found throughout the mountain, from the surface to depths well below the water

table. The National Research Council report concluded that these observations could be accounted for by a combination of the large scale hydrothermal activity that occurred from 10 to 13 million years ago, which was associated with an episode of major (Timber Mountain) volcanism, and supergene processes involving the deposition of carbonates and silica by evaporation induced precipitation from downward percolating meteoric water.

On the other hand, a growing number of scientists (including Archambeau) point out that the young ages of the mineral deposits, including zeolites and zircons as well as opal-calcites from veins throughout the mountain, coupled with inferences of high fluid temperatures and degassing during deposition based on determinations of fluid inclusion formation temperatures, temperatures for zircon fission track annealing, paleo-temperature gradient inferences from oxygen isotope data, pervasive metasomatism, rare earth element abundances, zeolitic alterations and other observations, strongly indicate on-going hydrothermal activity; much younger than 10 to 13 million years ago and of a different type. Thus, these latter scientists take issue with the supergene hypothesis advanced in the NRC report, and with the similar interpretation of the DOE project scientists, and argue that a hypogene origin (involving upwelling ground water) is required based on the geologic and geochemical evidence. They also argue, based on the geophysical evidence of extensional tectonism at the site coupled with the seismic evidence for probable partial melt in the upper mantle and lower crust at and near the site, that continued episodic upwelling of ground water produced by convection and seismic pumping associated with volcanism and earthquakes has produced most of the observed young mineralization and metasomatism and that this phenomena can be expected in the future.

These differing conclusions have important consequences for the viability of Yucca Mountain as a permanent high level nuclear waste repository, since rapid intrusion of

upwelling ground water will lead to relatively rapid corrosion and break-down of containers followed by leaching and transport of the radionuclides into the biosphere, leading to serious health hazards. On the other hand, the conclusions of the Academy report, as well as the conclusion reached by most active DOE project scientists, is that intrusion of ground water has not happened at the site since at least 10 million years ago and that the likelihood that it will do so again within the next 10,000 years or so is vanishingly small. Consequently, leaching and transport by groundwater would be very unlikely to occur and is not, therefore, an issue that deserves concern or further investigation.

A review of the Academy report by M. Somerville et al., 1992 (*Critical Review of the National Research Council Report: "Ground Water at Yucca Mountain: How High Can It Rise"*, Technology and Resource Assessment Corporation, Report No. 2, Contract No. 92/94.0004, State of Nevada Nuclear Waste Project Office, August 1992) attacked the Academy report on the grounds that "the Panel has ignored multiple lines of evidence and does not justify the all-inclusive dismissal of hydrotectonic hazards at Yucca Mountain". Further the review stated that: "More importantly, analytical data (eg. radiometric ages, geothermometry and mineral and isotope abundances) not considered by the Panel provide evidence for recurrent invasions of the Yucca Mountain vadose zone by hydrothermal fluids". The review went on to present the data ignored by the NRC Panel and to argue that this data, if considered by the Panel, would have negated their arguments and conclusions and would have at least suggested, if not required, a very different conclusion; that is a hypogene origin for the observed mineralization and alteration at the site.

Archambeau (1992) in a report entitled *Review of the NAS/NRC Report; "Ground Water at Yucca Mountain: How High Can It Rise"* (Technology and Resource Assessment Corporation, Special Report No. 1, Contract No. 92/94.0004, State of Nevada, Nuclear Waste Project Office, December, 1992) summarized results and data described in the previous report by Somerville et al., while focusing on specific

problems with the Academy report that he considered to be fundamental and important. As stated in his report, these were: "First, the report ignores a considerable body of critical evidence relating to the ages and nature of hydrothermal alterations at the site; second, many of the strong conclusions expressed in the report are not reasonably supported by the evidence presented and, in some cases, are inconsistent with data and results available to the committee but which are not cited or used by them; and finally, there are statements describing field relationships and data that are not consistent with the facts or are made in such a way as to be misleading."

This report, along with a cover letter expressing his concerns with the NRC report was sent to Dr. F. Press in November of 1992. Dr. Archambeau suggested that the Academy President consider a re-evaluation of the issues covered by the NRC report.

Dr. Press responded in a letter to Dr. Archambeau in February of 1993 which stated that, based on his staff recommendations and a review report by Dr. J.F. Evernden of the United States Geological Survey, he declined to initiate any further investigations and that, in his view, the NRC report was a valid scientific evaluation which was corroborated by Evernden's report. He also enclosed, with his letter, a copy of the report he received from his staff.

In March of this year, Dr. Archambeau replied to the letter and NRC staff report sent by Dr. Press with a detailed point-by point rebuttal of the NRC staff report to Press. Also, in March, a critical review of Dr. Evernden's report by M. Somerville was submitted to the Nuclear Waste Project Office of the State of Nevada and this report, along with the earlier review of the NRC report by Somerville et al., was included as attachments to the letter sent to Dr. Press.

All of these reports and letters are contained in the reports entitled *Dialogs on the Yucca Mountain Controversy* (Technology and Resource Assessment Corporation, Special Report No. 5, State of Nevada Nuclear Waste Project Office, March 1993).

In April of 1993, Dr. Press responded to the second letter from Archambeau. This letter is reproduced as Part 2 of the present Dialogs report. Dr. Press continued to decline to re-evaluate the NRC Panel report and suggests that the controversy could be resolved when additional data becomes available. Dr. Archambeau replied to this letter in August, 1993, stating in part that the issue is not resolution using additional data, but whether the NRC Panel produced a fair and unbiased evaluation of all of the data available to it and whether the Panel's representations of conclusions by other researchers involved in the evaluation of Yucca Mountain were accurate. Dr. Archambeau also cited specific examples of omissions of critical data and misrepresentations of results and facts by the Panel which he felt justified re-evaluation of the Panel's report by the Academy. This letter is reproduced in Part 3 of this report. Subsequent sections (4 - 8), contain the recent reports referred to in Dr. Archambeau's letter.

The reviews of reports and of the NRC report, as well as the responses to these reviews, are considered to be an important part of the work being supported by the State of Nevada since they focus on the specific data and observations that are at the heart of the controversy over the suitability of the proposed Yucca Mountain Repository. In principal the opposing interpretations of the geologic data and observations could be directly compared with respect to their plausibility, completeness and overall scientific validity. Therefore, we have presented reviews and responses in the following sections of this report to provide interested readers with material which may enable them to contrast and assess the views of the opposing sides in this controversy. At the least, these documents reveal the character of the debate, which may be enlightening to those unfamiliar with this controversy.

PART 2

Letter to C. B. Archambeau from F. Press

NATIONAL RESEARCH COUNCIL

2101 CONSTITUTION AVENUE WASHINGTON, D. C. 20418

OFFICE OF THE CHAIRMAN

April 9, 1993

Dr. Charles Archambeau
Department of Physics
University of Colorado
Boulder, CO 80309

Dear Arch:

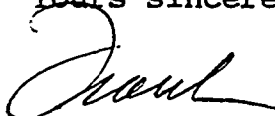
Thank you for the two reports produced by your firm, TRAC, which were sent with your response to my letter of January 7, 1993. Although I recognize the concerns you are raising, I still feel comfortable with the consensus reached by our panel that studied the rising groundwater hypothesis. I have taken the liberty, however, to distribute your response to the panel members. They are, of course, free to comment further as individuals to the points in your letter.

I take note of your criticism of the staff memorandum to me. You should be aware that this memorandum had input from several sources: panel members on the technical issues, staff on background, and the tapes of the meeting between the NAS panel and the DOE External Review Panel. Although there was a miscommunication between panel members and staff on the zircon dating method, the panel still strongly disagrees with your interpretation of the meaning of the range of zircon ages. As for your concern that the staff has mischaracterized your statements at the May 1991, I have been assured that the portrayal of your statements in their memo to me is fully supported by the tapes of your statements, which you are welcome to come and listen to when it is convenient for you to do so. With respect to your Point No. 1, the staff replies that there is no clue in Report No. 1, which you characterize as a "synopsis" of a larger review of the NAS panel's report, that it is not a standalone document. As you alone are listed as the author, there is also no evidence or acknowledgement that there was any input or review by anyone else. Indeed, the staff found it curious that the cover date of Report No. 2, the more comprehensive review, precedes that of Report No. 1 (August 1992 for No. 2 versus December 1992 for No. 1) and wonders why it was not sent with your earlier letter.

Dr. Charles Archambeau
April 9, 1993
Page 2

Although we may not be able at this time to reconcile the differences in viewpoint between you and your colleagues on the one hand and the NAS panel on the other, I'm sure we can agree that future site characterization activities are likely to produce the information necessary to resolve the issues now in controversy.

Yours sincerely,

A handwritten signature in cursive script, appearing to read "Frank Press".

Frank Press
Chairman

PART 3

Letter to F. Press from C. B. Archambeau

August 19, 1993

Dr. Frank Press
National Academy of Sciences
2101 Constitution Ave., N. W.
Washington, D. C. 20418

Dear Frank:

I received your reply to my letter of March 17, 1993 some time ago, in mid-April, but I've taken some time in replying since I thought I might also receive comments from some of the NRC panel members, inasmuch as you indicated that you had sent copies of my letter to them as well. However, I've received no response from any of them. I've therefore decided to send a reply to you, since I doubt I will hear from them in the near future, if ever.

You report in your letter that "The panel still strongly disagrees with your interpretation of the meaning of the range of zircon ages." However, I must point out to you once again that my criticism of the panel in this regard is not that my interpretation is different than their's, but that they misrepresented the conclusions of the authors of the paper they quote and that they then use this misrepresentation to buttress their arguments that the last hydrothermal event at Yucca Mountain was from 10 to 12 million years ago. There can be, in fact, no argument here, in that by simply comparing the conclusions of the authors of the zircon paper (Levy and Naeser) with those stated by the panel (on page 44 of their report) it is certain that misrepresentation has occurred. Therefore, your statement regarding my interpretations of zircon ages is not germane to the issue, what is at issue is whether there is misrepresentation by the panel. The evidence is clear in this regard and was stated in my original review of the Academy report and in all my letters to you. It involves no interpretation of scientific data by me, but merely the observation of inconsistency between the panel's statements regarding the results of Levy and Naeser's study and the statements of those authors themselves. In my view, given the importance of the data and the seriousness of misrepresenting it, a review of the NRC panel report is called for on these grounds alone and should be initiated by your office.

You state that you have been assured that the portrayal of my statements at the May 1991 meeting between the DOE review panel and the Academy panel is "fully supported by the tapes of your statements." This continued reference to these tapes leads me to request copies of the tapes. I would also like copies of written material that was distributed by the DOE panel to your panel and staff. I will then have the tapes transcribed as I wish to settle the issue as to what I did or did not say once and for all. I

do, in fact, know what I said and in what context I said it and I wish to make this clear and incontrovertible by distribution of the transcription. Since I believe I have been seriously misrepresented by your staff and through them by the Academy, I wish to leave no doubt as to the truth of the matter. I am particularly outraged by your staff's distribution of their allegations to the press— purportedly based on this tape. I intend to show that their statements are misrepresentations designed to discredit me. I can assure you that I don't intend to let these allegations stand.

I am continually amazed by the lack of logic displayed in your quotes from your staff. For example, you state that your staff informs you that "there is no clue in Report No. 1, which you characterize as a *synopsis* of a larger review of the panel's report, that it is not a stand alone document." But of course my report is exactly as I state, a synopsis of an earlier report (as well as other reports referenced in the earlier report, including the Minority Report of the DOE Review Panel by Neville Price and myself) and obviously it is a stand alone document as I wrote it and signed it as the sole author. In so doing I take full and personal responsibility for it. I clearly reference the earlier report and all your staff had to do was to request it. (Do you really believe that every referenced document should be sent along with the referencing paper or report?) If your staff was at all interested in the facts they obviously could have requested the report, instead they insinuated that no such report existed. Further, what does any of this have to do with the technical issues in question? If your staff was in any way interested in confronting the issues, and if I was, by their reasoning, off base because of a lack of background, it seems to me that they, along with the NAS panel and whoever else they could get to review the matter, could have easily pointed out the flaws, inconsistencies and errors of my arguments. However, on the contrary, in the one technical issue they chose to confront me with (the zircon data), they were shown to be not only plainly uniformed and confused, but incompetent since they were unaware of knowledge well known to undergraduates at the sophomore level.

Furthermore, I am frankly amazed that you would allow the first reply to me (which was also distributed to the press by your office) to see the light of day. It is clearly an attempt to discredit me, avoids issues of substance, is incorrect in essentially all respects and displays an obvious viciousness apparent to even casual, nontechnical readers (eg. the press people that called me about it.)

Finally, I also take issue with your last statement regarding this controversy between myself, along with others, and the NAS panel and others. The point of my correspondence with you, and indeed the emphasis I have placed on selecting issues in my communications with you, has been that the NAS panel has misrepresented published data and conclusions by others (eg. the zircon age data and the interpretation placed on the data by the authors of the paper) and omitted the most significant and critical data from their report, which, if included, would have made it impossible for them to draw the conclusions they draw.

The question is then, why did they misrepresent the results of the work on the zircon ages and why didn't they consider the important age and vein formation temperature data that was available to them during and well before they wrote their report. These

are not questions of technical interpretation, nor is new data an issue here. The facts are incontrovertible, they did misrepresent the zircon data and they did omit consideration of abundantly available temperature and age data. (Indeed, I personally reminded the chairman of the NAS panel of the existence of this data, so I know it was not an oversight nor, considering its abundance and importance, could it have been.)

To illustrate the magnitude and import of these omissions and misrepresentations, I've included two figures that show the critical vein formation temperature data and the age data for alterations of Yucca Mountain rocks, as well as vein calcite ages, all at various depths from throughout the mountain, as well as at the surface. It should be emphasized that this data was all published in reports and papers available to the NAS panel and that nearly all of it was obtained by DOE contractors, including (and predominantly) the USGS. (In this regard the reference to Szymanski, 1992, in Figure 1 refers to his compilation of results from a number of authors who were associated with the DOE program.) In looking at Figure (1) it is evident that none of the temperature data for vein formation, rock alteration or zircon annealing can possibly be due to rain water. Further the oxygen isotope data indicates high temperature gradients in the past, significantly higher than those at present, which are already quite high. (The lines on the left represent the present range of measured gradients/temperatures while the shaded zone just to the right of it represents the minimum gradients obtained from oxygen isotope data and the range of temperatures that could be expected. That is, paleo-gradients inferred from oxygen isotope data were greater than or equal to the gradients indicated in the figure.)

There can be no question that this data represents a very high temperature thermal history with alteration, annealing and vein formation by hydrothermal fluids from below. The only question is when it occurred, that is, was it 10 to 13 million years ago during the last major volcanic episode near Yucca Mountain, or was it more recently, or both. Figure 2 shows the age data relevant to this question. It represents ages of secondary calcites in veins from uranium series data (indicating the times of deposition), zeolite ages by K-Ar dating (indicating times of fluid alteration) and ages for annealing from the fission tracks (indicating times of high temperature annealing). These ages, obtained by independent methods from rocks and minerals from samples at essentially the same locations as were those used for the temperature results in Figure (1), all show a history of continuing deposition and alteration by fluids that spans the time from essentially the present to (and including) 13 million years ago. Clearly this age data shows that alteration and vein deposition has been on-going to the present throughout the mountain. The temperature data, at the least, strongly implies that this continuing alteration and deposition has been due to hydrothermal fluid intrusion and can not be attributed to percolation of rain water from above.

However, while it seems hard to escape the conclusion given above, the point I wish to make here is that none of the temperature data was used by the panel and none of the age data was used, except for the zircon data which was misrepresented as being compatible with a 10 to 12 million year age. Given the results shown here it is beyond belief that the panel could have missed the significance of this data or have dismissed it

without comment or justification when forming their conclusions. It is even more anomalous that they misrepresented the conclusions of Levy and Naeser regarding the zircon ages and did not state that their conclusions were at variance with those of the authors. I would again remind you that this is not a matter of scientific interpretation, but a matter of distortion by omission and misrepresentation. I believe that the Academy has the responsibility to ask why and how this happened and whether, if taken into account, this would change the panel's conclusions. New data from future site characterization studies is not needed, the old data is what is germane here.

Even though the issue I'm pressing here is the irrationality of the NAS report based on the evidence available to them, there is also new data that has been obtained that strongly implies conclusions quite different from those formulated by the panel. Further, along with the data there are conclusions, formulated by new investigators not previously involved in the DOE site characterization program, that contradict the NAS panel conclusions. I have taken the liberty to enclose copies of reports by these investigators that detail the data and illustrate their conclusions. These new reports, while not definitive in themselves, certainly do not support the NAS panel's strong conclusions and provide yet more evidence of the need for a thorough review of the panel's report.

Sincerely Yours,



Charles B. Archambeau
Department of Physics
Theoretical and Applied Geophysics Group
University of Colorado
Boulder, Colorado

cc: C. Raleigh, University of Hawaii
G. Thompson, Stanford University
W. Brace, Massachusetts Institute of Technology.
B. Brady, Dowell-Schlumberger
J. Bredehoeft, USGS
R. Burke, Humboldt State University
B. Fournier, USGS
S. Garg, S-Cubed
G. Hornberger, University of Virginia
R. McGuire, Risk Engineering, Inc.
A. Nur, Stanford University
H. Ramey, Stanford University
E. Roeder, Harvard University
D. Rumble, Carnegie Institution of Washington
W. Spaulding, Dames & Moore
B. Wernicke, California Institute of Technology
M. Zoback, USGS

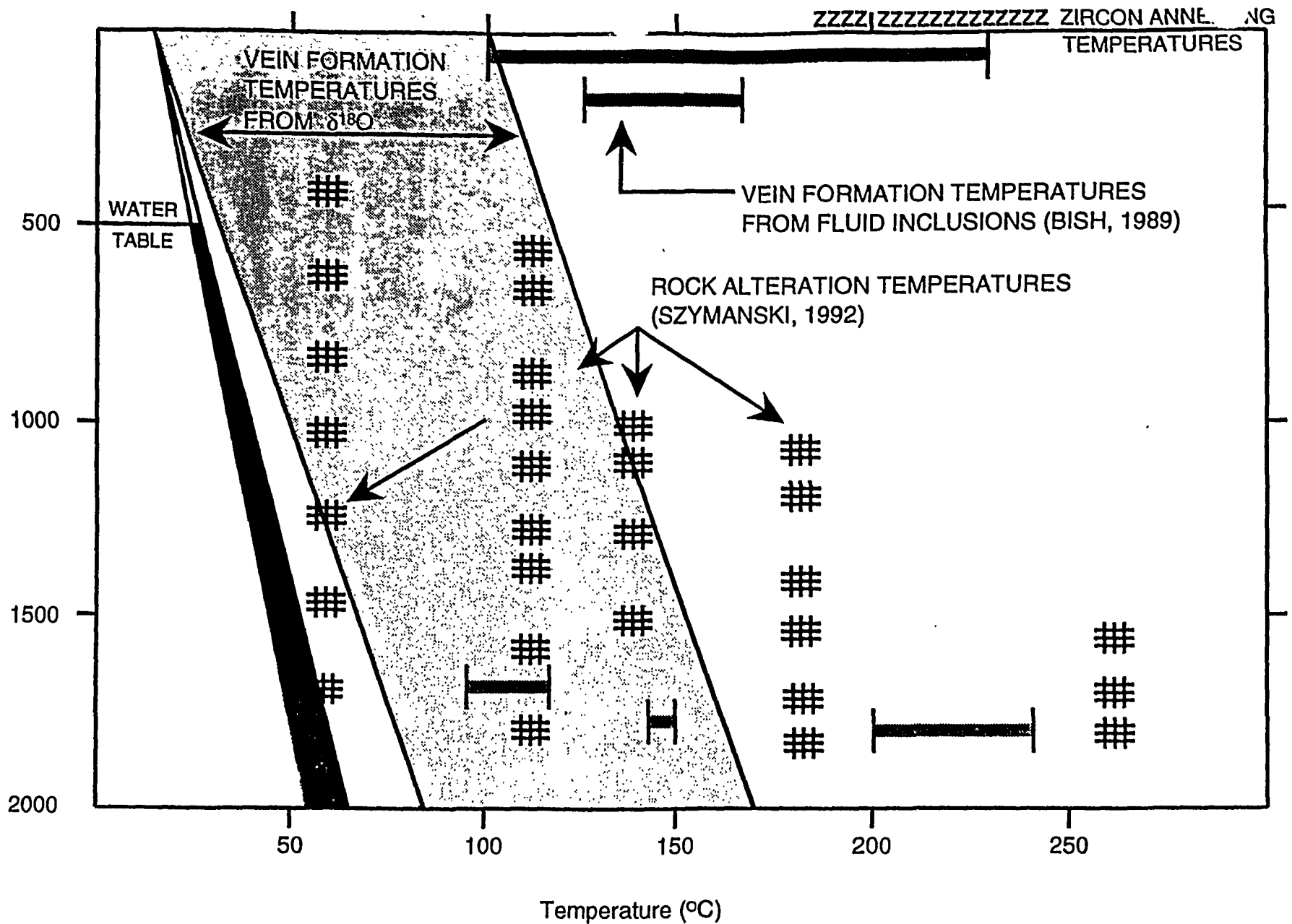


Figure 1. Borehole samples from Yucca Mountain reveal alteration products formed at high temperatures, indicating that the site has been invaded by high temperature fluids.

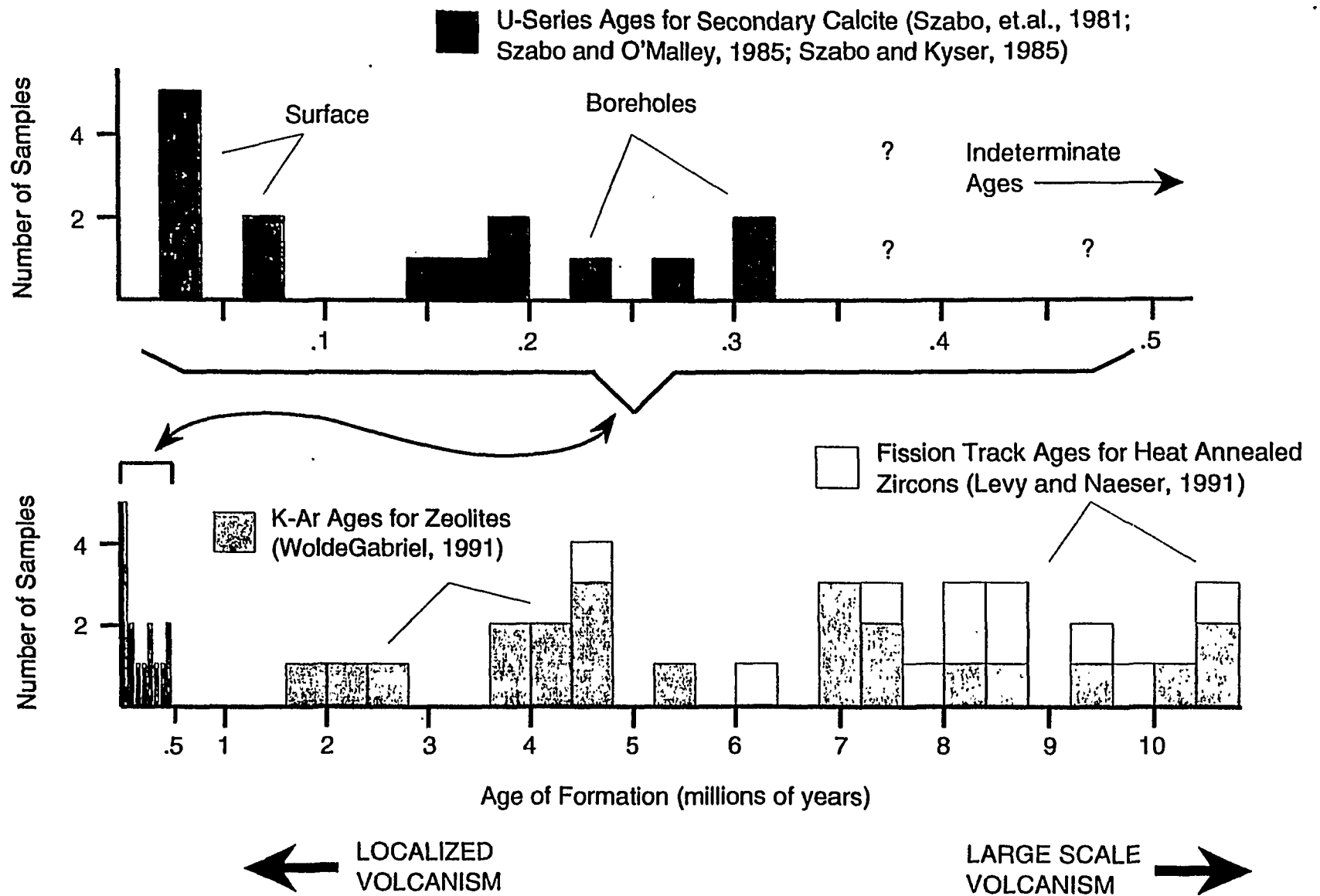


Figure 2. Ages of Fluid Alterations at Yucca Mountain

PART 4

**Field Trip Report: Observations Made at Yucca
Mountain, Nye County, Nevada**

TRAC *Technology and Resource Assessment Corporation*

3800 Arapahoe Avenue, Suite 225
Boulder, Colorado 80303
(303) 443-3700 FAX No. (303) 443-8626

**FIELD TRIP REPORT: OBSERVATIONS MADE
AT YUCCA MOUNTAIN, NYE COUNTY, NEVADA**

SPECIAL REPORT No. 2
CONTRACT No. 92/94.0004

SPECIAL REPORT Submitted to the
Nuclear Waste Project Office
State of Nevada

March, 1993

Authored by:

Carol A. Hill

**Field Trip Report: Observations Made at and Around Yucca Mountain,
Nye County, Nevada**

TABLE OF CONTENTS

INTRODUCTION	1
FIELD OBSERVATIONS	1
Calcite/Opal Travertine	1
Silica Types	8
Silica Fingers	11
Wahmonie Travertine/Gypsite Mound	12
Trench 14	14
Sand Ramps	18
Site 199	22
Ore Mineralization/Alteration	23
RECOMMENDATIONS	26
REFERENCES	28
APPENDIX 1 – Detailed List of Samples Collected	30
FIGURES (1, 2, and 3)	37

INTRODUCTION

A field trip was made to the Yucca Mountain area on December 5-9, 1992 by Jerry Frazier, Don Livingston, Christine Schluter, Russell Harmon, and Carol Hill. Forty-three separate stops were made and 275 lbs. of rocks were collected during the five days of the field trip. Key localities visited were the Bare Mountains, Yucca Mountain, Calico Hills, Busted Butte, Harper Valley, Red Cliff Gulch, Wahmonie Hills, Crater Flat, and Lathrop Wells Cone. This report only describes field observations made by Carol Hill. Drawings are used rather than photographs because cameras were not permitted on the Nevada Test Site during this trip. Figure 1 shows the location of all the sites (stops) mentioned in the text.

FIELD OBSERVATIONS

During the field trip various observations were made. Taken collectively, these preliminary observations may be used to infer origin of various calcite-silica deposits, known from Yucca Mountain. A summary of observations made by C. A. Hill is presented below.

CALCITE/OPAL TRAVERTINE

Deposits of calcite/opal were collected from nearly all of the localities visited (i.e., from about 40 separate sites). These will herein be referred to as "travertine" rather than as "calcrete" since the deposits are believed to have a spring origin rather than a pedogenic (soil-related) origin (i.e., they are calcareous or siliceous sinters or tufas). Although "calcrete" is a non-genetic term which can include spring or

travertine deposits (Machette, 1985), it is often interpreted to be strictly pedogenic in origin. The use of the term "travertine" will avoid this confusion.

The following observations were made concerning the travertine deposits in the Yucca Mountain region:

1. Calcite/opal travertine is localized along faults or fault zones. Faults were detectable by offset beds (e.g., Harper Valley), well-exposed and slickensided surfaces (e.g., Wailing Wall), or by brecciated and mineralized zones (e.g., Calico Hills and 2 km north of Mercury). In places where faults are well-exposed, the calcite/opal mineralization occurs primarily as seams or veins along or near the fault plane and dies out away from the fault (e.g., Wailing Wall). A number of the travertine deposits are located along major faults (e.g., the Bow Ridge Fault, Trench 14 calcite/opal and the Paintbrush Fault, Busted Butte calcite/opal). The nearly universal association of calcite/opal with faults implies that the travertine has a fault-related origin. If the calcite/opal were pedogenic in origin it should occur universally around Yucca Mountain and not be localized along fault zones.

2. Calcite/opal does not occur in soil horizons between fault zones. In an exposed soil horizon at the Highway 95 gate-gravel pit (shown on the map of Swadley and Carr, 1987) the soil contains no calcite-caliche whereas less than a kilometer north from the gate along this same road calcite mound deposits are locally abundant.

3. The calcite/opal does not occur within specific stratigraphic units or rock types.

Travertine was observed along fault zones in Paleozoic limestone (e.g., Bonanza King Limestone, Pull Apart Fault), in rhyolite tuffs (e.g., Bedded member of Paintbrush Tuff, Busted Butte), in basalts (e.g., Basalts Miocene, Tb₂, west of Mercury, Stop 27), and even in unconsolidated sand (e.g., Busted Butte sand ramps). That is, the source of calcium does not appear to be related to the amount of calcium in the host rock but to a subsurface travel route wherein calcium has been gained somewhere between recharge and discharge. It is suspected that the Bonanza King Limestone is the primary subsurface calcium source for the calcite/opal travertine as it is the most karstified unit in the region. Caves can be seen in the Bonanza King Formation along Highway 95 southwest of Mercury; also, regional discharge is at Ash Meadows and Devil's Hole in the cavernous Bonanza King.

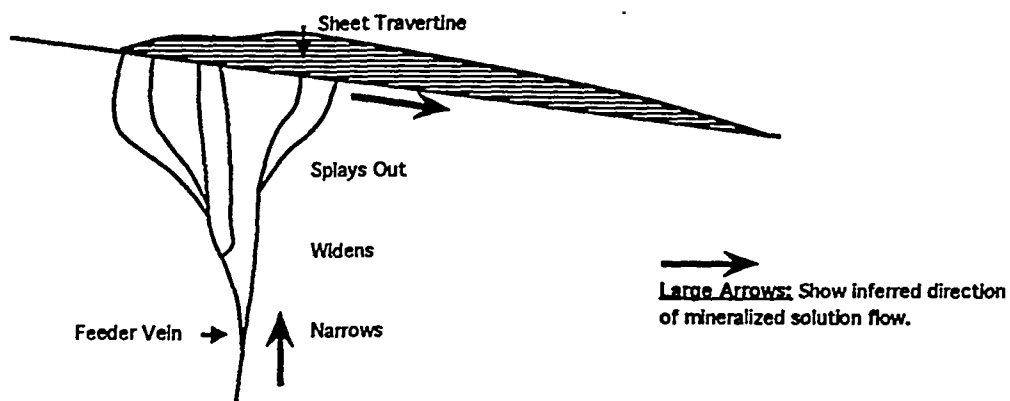
4. In some cases calcite/opal travertine occurs in conjunction with an aquiclude; that

is, a competent unit where carbonate-rich water has emerged as springs along the base of the unit. This can be observed on the western side of Busted Butte where the base of the Tiva Canyon member has acted as the aquiclude and where travertine occurs at the base of the Tiva but not in the stratigraphic units above the Tiva, at least in this location.

5. Calcite/opal travertine deposits are often associated with "feeder veins" where

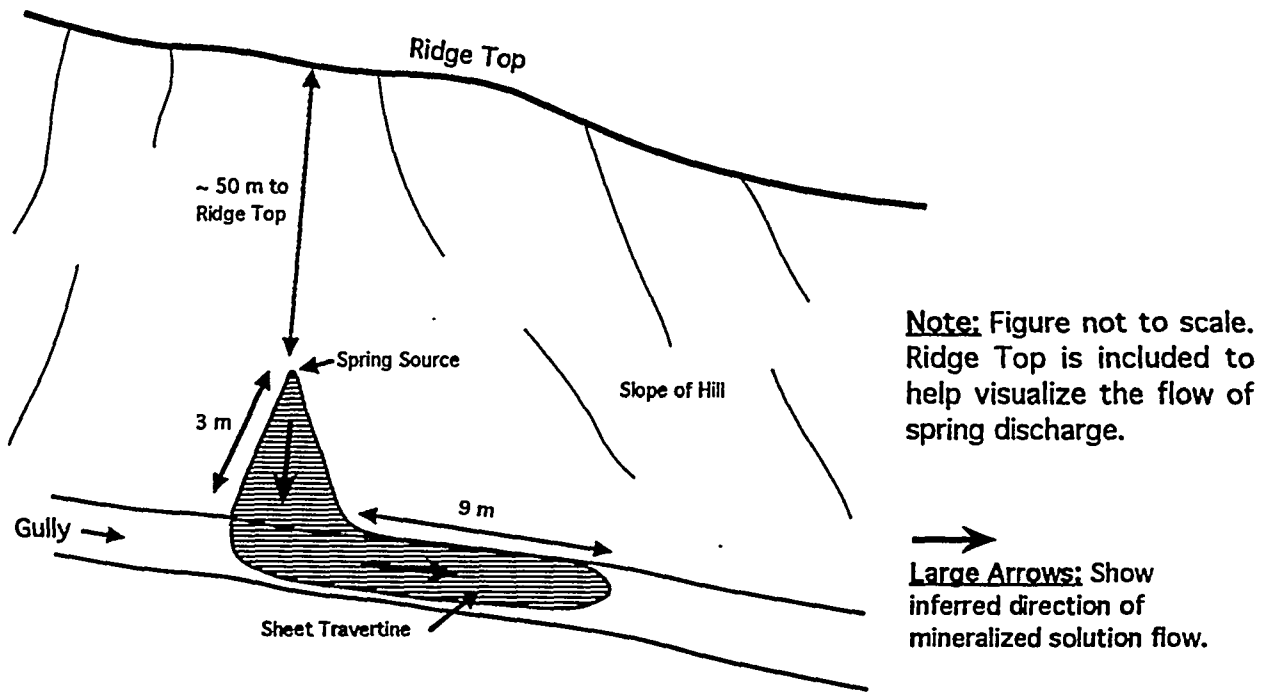
they have been vertically exposed by trenching or by valley downcutting. This

association can be seen at Trench 14 and at the fault scarp exposed at site 106 F, and is most dramatic on the west and east sides of Busted Butte where valley erosion has dissected sand ramps. As exposed in the sand ramps the veins narrow toward the base but thicken and splay out into multiple veins near (within a few meters of) the sand-ramp ground surface. Travertine continues along the surface downslope from these feeder veins:



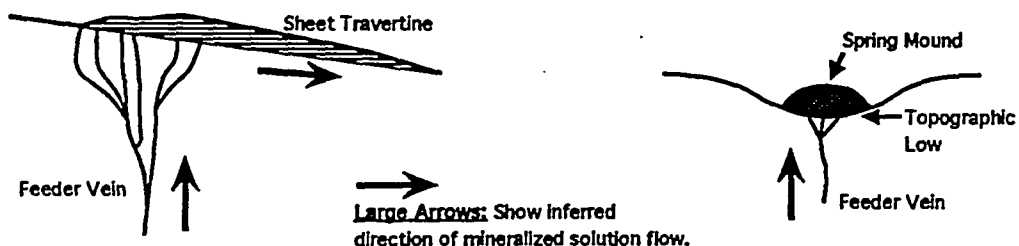
The direct correspondence in space between the feeder veins and the travertine downslope from the feeder veins is strong evidence that the veins were the source of mineralizing solutions from which the travertine deposited.

6. Calcite/opal deposits which have not been vertically exposed also sometimes have topologies that suggest a point-source spring origin. An excellent example of this can be seen in Harper Valley where carbonate-saturated water appears to have issued forth from a spring orifice, flowed downslope for 3 m before encountering a gully perpendicular to slope, and then continued down-gradient along the gully for another 9 m, all the while depositing a thin layer of carbonate travertine along its course:



7. Calcite/opal occurs as vein and fracture fillings, as material cementing breccia fragments, as matrix-supporting material cementing alluvium (e.g., Site 106 F) or colluvium/talus (e.g. Plug Hill), and as spring mounds (e.g., Site 199). The type of deposit can change over short distances (e.g., calcite/opal veins are exposed in Trench 14 whereas possible mound material is exposed in South Trench 14 located some 60 m or so south of Trench 14).

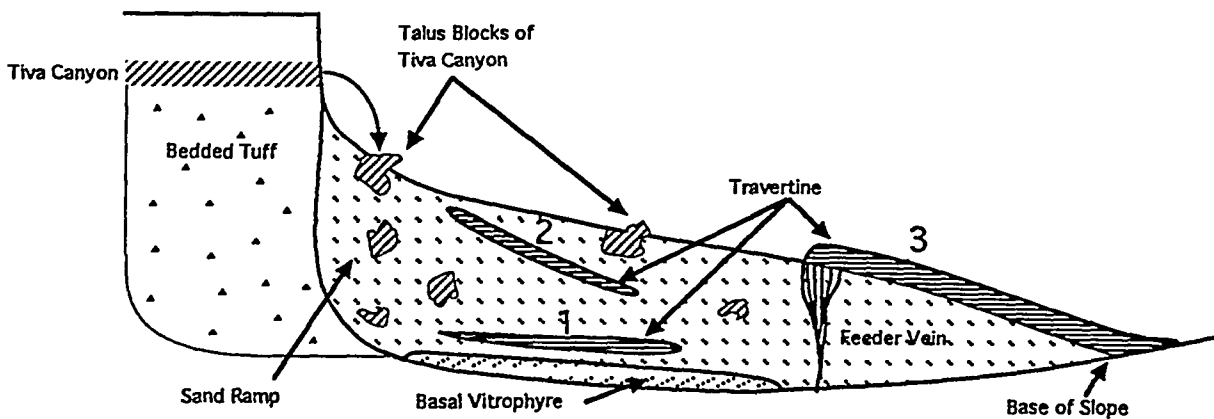
8. Spring mound-type travertine appears to have accumulated in topographic lows as compared to travertine which formed as sheet deposits downslope from feeder veins:



Mound-type deposits are composed of massive, unlayered, unconsolidated, chalk-like calcite in comparison to layered calcite/opal sequences such as characterize sheet travertine and vein material. Spring mound deposits on the present-day erosion surface are known to be young (e.g., ~30 Ka, Site 199; diatomaceous earth along Highway 95 which has camel, horse, and mammoth bones in it). Spring mounds overlain by later soil material are probably older than this (e.g., the massive calcite exposed in South Trench 14 and in the North and South Stagecoach trenches). The Stagecoach mound material may represent a time when Crater Flat was at a higher erosional level than it is today (i.e., it is an earlier equivalent of Site 199). The South Trench 14 mound material may have formed in a local topographic low associated with spring activity in nearby Trench 14.

9. Calcite/opal travertine deposition was both episodic and of varying intensity.

Various travertine episodes can be observed at Busted Butte where a number of travertine layers occur one above the other, separated by intervals of sand:



These travertine layers appear to have: (a) formed at different times (layer 1 being the oldest and layer 3 the youngest) and (b) represent different former ground-surface levels of the sand ramp. This is indicated by the presence of calcified root casts (and rare animal burrows) in all of the layers (1, 2, and 3). The calcite travertine layers of the sand ramps are oriented at different angles from the horizontal (from ~10-20°), which angles represent different angles of repose of the sand ramps at the time of each travertine event. Varying intensity of spring activity is indicated by some travertine layers extending all the way to the base of slope of the sand ramps and beyond (3); other travertine layers extend only part way down a former slope (1,2).

10. Calcite/opal deposits can increase in thickness and mass downslope. This can be observed on the hill just west of WT-7. Uphill the calcite/opal occurs as fracture fillings in the rock, but downhill the calcite/opal becomes a thin (a few cm or less) surface layer of travertine, and even further downslope along the road the travertine thickness increases to 15-30 cm.

11. Calcite/opal deposits display a variety of textures (e.g., laminated, vesicular, massive, etc.). A detailed description of these textures and field relationships between textural types will be provided in a separate report.

12. Calcite/opal deposits are microcrystalline which suggests rapid cooling and/or rapid degassing. This is in contrast to pedogenic carbonates which nearly always are "aggregates of silt-sized calcite crystals...the microcrystalline forms are readily

identified by optical microscope, either in thin section or grain mount" (Dixon and Weed, 1989, p. 281).

13. Density of calcite/opal travertine sheet deposits varies from a harder, more dense and shiny upper surface to a more porous, lower surface (e.g., Busted Butte, Trench 8). The travertine is often composed of an interwoven mass of root casts and sometimes displays algal- or pisolitic-like structures (e.g., Wailing Wall at the mouth of Red Cliff Gulch).

14. Some of the calcite/opal travertine must be relatively young since the deposits overlie and conform to present -day valley and gully slopes (e.g., Harper Valley)

SILICA TYPES

Five different types of opal (silica) were encountered during the course of this field trip. These five types display different textural relationships but they do not necessarily represent different episodes of mineralization. Four of the five silica types can occur with each other and these have been found in deposits of all ages (from ~30,000 ybp at the Wailing Wall to >400,000 ypb at Trench 14).

1. Opalite. "Opalite" is composed of a transparent to pearly opal (hyalite) which always fluoresces a brilliant green (i.e., it is an "uraniferous opal" such as described by Szabo and Kyser, 1985; U = 15-57 ppm). A number of specimens of opalite were collected from a number of different localities on this trip, but especially spectacular specimens were found at Harper Valley, on the hill above Trench 14, and at drill site

UE25p#1 (Stop 37-1). The Harper Valley opalite is translucent to white, opalescent, and botryoidal. It litters the hillsides and valleys of Harper Valley and has its source in the Tiva Canyon member where it occurs as veins filling fractures in the rock. The UE25p#1 opalite is massive, opaque, and displays conchoidal fracture and an opalescent sheen. This opalite occurs as veins in the bedrock (Topopah Spring member) and also crosscuts a soil horizon.

2. Silicified Breccia. Silicified breccia consists of breccia pieces floating in an opal matrix. This matrix is tan, opaque, hard (does not scratch with a knife) and dense, but it is not a pure opal as it contains variable amounts of intermixed calcite (it fizzes somewhat in acid). No samples of silicified breccia were observed to fluoresce. Silicified breccia was found at WT-7, Trench 14, and Harper Valley. At WT-7 the opal fills the spaces between fractured and brecciated rock. The silicified breccia at Trench 14 occurs as dikes and veins cut across by later calcite/opal veins. In both the WT-7 and Trench 14 occurrences, the silicified breccia appears to represent an early phase of brecciation and mineralization. The WT-7 opal has a U-series date of >300 Ka (R. Harmon, personal communication, 1992) and the Trench 14 silicified breccia is the first of five episodes recorded in the trench (Figure 3). In Harper Valley the silicified breccia occurs as a breccia dike which cross-cuts the Bedded Tuff member but which stops at the base of the more competent Tiva Canyon member.

3. Opal/Calcite Travertine. Opal exists interlayered or interlaminated with calcite in

many of the localities visited on the field trip. This opal is the same type as the opal in the matrix of the silicified breccia; it is tan, opaque, dense, hard, is intermixed with calcite, and never fluoresces. Particularly good exposures of opal/calcite exist at Trench 14 and Busted Butte. The laminations of opal and calcite are vertically oriented within feeder veins (e.g., Trench 14, Busted Butte), or they can be oriented near-horizontally within travertine sheet deposits downslope from feeder veins (e.g., Busted Butte). The opal laminations are distinguishable from interlaminated calcite by color (the opal is tan and the calcite white) and by hardness. Opal layers often stand out in relief between the more-porous and -powdery, less-hard layers of calcite.

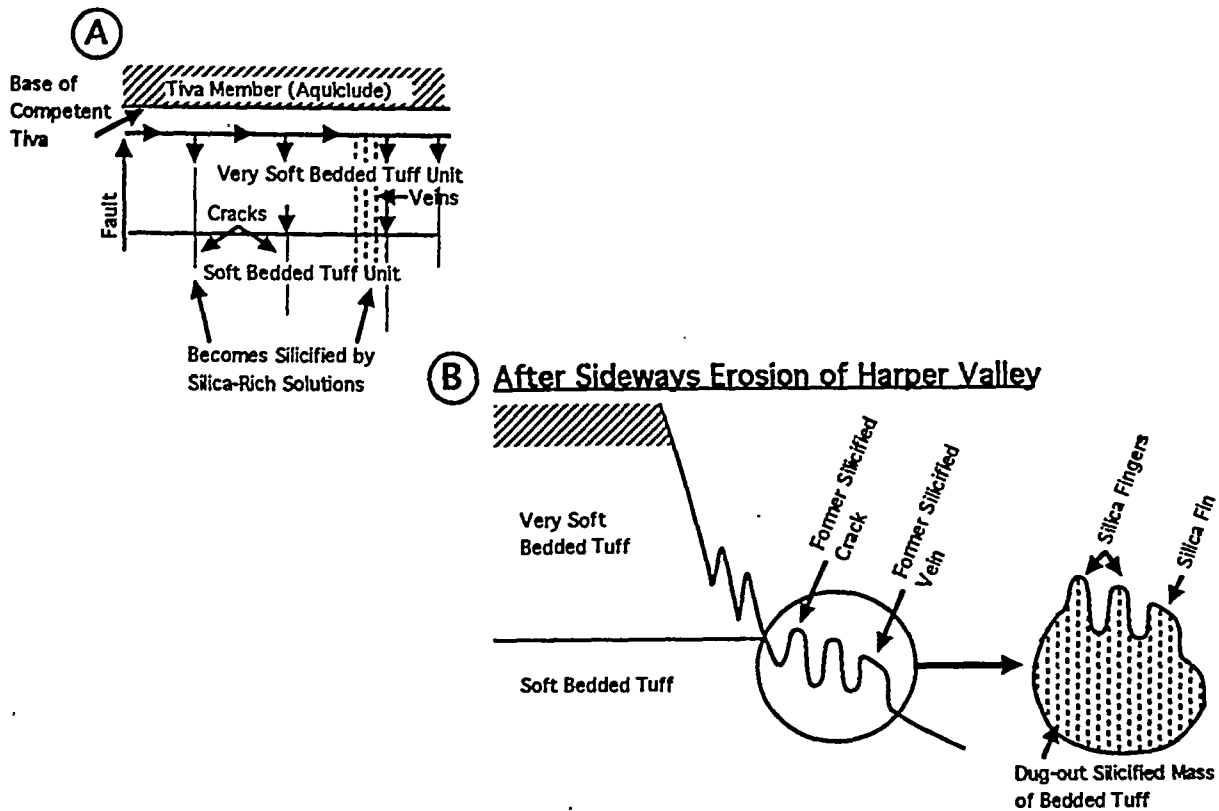
4. Powdery Opal. Powdery opal is a white, massive opal with a powdery-like texture and appearance. This type of opal was identified in samples collected from Trench 14, and while this type of opal was not positively identified in any other samples, it seems entirely possible that powdery opal may exist intermixed with powdery calcite in these layers.

5. Diatomaceous Earth (diatomite). Diatomaceous earth occurs along Highway 95 just northwest of the dirt road taking off to Site 199. This site was not visited on the field trip but reportedly the earth is siliceous rather than calcitic (J. Frazier, personal communication, 1992). This is the only silica type of the five listed that is not known to occur with the other types. The diatomaceous earth along Highway 95 contains camel, horse, and mammoth bones so it must be fairly young (25-30 Ka?).

SILICA FINGERS

Some unusual forms exist in the soft Bedded Tuff member, along the fault in Harper Valley. These are finger-like projections of silicified tuff a few centimeters or so high and wide which have been informally been given the name "silica fingers." Hill (1992) mistakenly thought that these forms might be miniature "tent rocks" which were perhaps syngenetic with deuteritic gas activity. During this field trip two other silica-finger localities were examined. The silica fingers are actually erosional remnants of more extensive blocks of silicified tuff which, in addition to the finger shapes, display fin-like shapes where the tuff became silicified along cracks.

The author now believes that the silica fingers in Harper Valley formed in a manner analogous to "sand stalagmites" in caves except that sand stalagmites are cemented with calcite brought in by dripping water whereas the silica fingers are cemented with silica brought in by silica-rich water ascending from below. Sand stalagmites and compound sand-stalagmite forms are caused by calcite-saturated water seeping preferentially through vertical and horizontal porous zones in sand on the cave floor (Hill and Forti, 1986). The calcite cements the porous zones causing them to become harder than the surrounding sand and to better resist subsequent erosion. When the uncemented sand becomes eroded away, the harder cemented portions of sand are left in relief. In an analogous manner the silica fingers in Harper's Valley are believed to have formed as follows:



Contrary to speculation that silica fingers may represent late-stage degassing (deuteric) at Yucca Mountain, the silica fingers are actually part of a consistent story of epithermal (epigenetic) mineralization along fault zones. The silica fingers formed by silica-bearing solutions ascending along the Harper Valley fault zone, which solutions then permeated into cracks within the Bedded Tuff. As the valley walls eroded away, the harder silica fingers and fins were left in relief, becoming eroded on the very top into rounded "finger" shapes.

WAHMONIE TRAVERTINE/GYPSITE MOUND

This site was specifically visited because of reports of "crystalline-gypsum beehive-shaped mounds" in the Wahmonie Hills. The Wahmonie mound is a travertine/gypsite block ~6 m long, 4 m wide, and 2 m high composed of ~70-80%

calcite and ~20-30% gypsum (5 samples tested). Rather than being crystalline in character the mound is massive and contains a somewhat harder, more-dense exterior and a softer, more-porous, friable interior. Thin (1-3 mm) botryoidal crusts of gypsum line the travertine/gypsite block in places where cavities in the block have not been exposed to weathering. These crusts represent diffusion of the more soluble gypsum component toward the outside of the block caused by evaporation of solutions at the air/block surface. Sepiolite has been reported as being present in the mound (Vaniman et al., 1988 and Somerville et al., 1992), but was not observed.

The Wahmonie travertine/gypsite mound is also not indicative of special processes occurring at Yucca Mountain but is consistent with the concept of region-wide epithermal (epigenetic) mineralization along fault zones. The only difference between this site and other mounds in the Yucca Mountain area is that the Wahmonie mound is composed partially of gypsum. The reason for this variation in mineralogy is because the Wahmonie mound is located within the Wahmonie Mining District, directly overlying a prominent N30°E- trending fault. Quade and Tingley (1983) reported both sulfide and gypsum mineralization in the Wahmonie Mining District and it seems logical that hydrothermal solutions ascending from depth through sulfide-rich intrusives along the fault picked up sulfate and deposited it in the Wahmonie travertine/gypsite spring-mound.

Because the Wahmonie mound is composed partially of gypsum and because it is extremely friable, it is believed to be very young (<30,000 years?). The Wahmonie

mound is especially important because it demonstrates the principle: "What's on top reflects what's below." The gypsum mound on the surface reflects the presence of a sulfide-rich intrusive body below, and this, in turn, implies ascending water along a fault rather than sulfate carried in by descending water (i.e., the gypsite is not of pedogenic origin). **Editorial Note by J. S. Szymanski:** By itself, the Wahmonie mound seems to successfully challenge the notion of a quiescent steady-state description of the local hydrologic system. This mound occurs at an attitude of about 4,700 ft above mean sea level, in an area where the contemporary water table is very deep. In two wells the water table was found at altitudes 2,784 ft (to the east) and 3,755 ft (upstream) (Winograd and Thordarson, 1975). In this setting, the young and unequivocally hypogene mound cannot be dismissed without recognizing that, for one reason or another, the local hydrologic system can exhibit diverse behavior, including discharge of mineralized and deep-seated solutions at the topographic surface.

TRENCH 14

Trench 14 was mapped in some detail (Figure 2 & 3) and a number of samples (36a to 36z) were collected at this site. Trench 14 is located directly along the Bow Ridge Fault, a normal fault which trends north-south along the eastern flank of Yucca Mountain. At Trench 14 the Rainer Mesa member of the Timber Mountain Tuff has been downfaulted against the Tiva Canyon member of the Paintbrush Tuff (Figure 3). A complex sequence of crosscutting veins filled with calcite/opal has been exposed by the trench.

At least five crosscutting episodes of epithermal mineralization are exposed in Trench 14. The first episode (1, Figure 3) is represented by the silicified breccia which has been crosscut by later calcite opal veins. Pieces of silicified breccia have been sheared off by later movement along the fault and incorporated as "float" into calcite/opal which was injected during that movement (sbf = silicified breccia float in Figure 3). The remaining four episodes are represented by calcite/opal veins which consecutively crosscut each other (2, 3, 4, 5; Figure 3). During the last episode (5) mineralizing solutions appear to have used the same vein conduits as during episodes 2, 3 and 4 but mineralization extended farther to the surface, crosscutting everything else. Following the five mineralization episodes was a later period of extension during which the veins were opened a centimeter or more causing cavities to form in the mass (cav = cavities in Figure 3). In some of these cavities tiny (a few mm in diameter) calcite "popcorn" nodules have formed as crustal linings.

Veins 2, 3, 4, and 5 consist of alternating laminae of calcite and opal. The calcite is the lighter-colored, more friable component of the couplets and the opal is the tannish-colored, denser, chert-like component of the couplets. Individual laminae vary substantially in width but the opal layers on the average are thinner (~a few mm) than the calcite layers (~1 cm). However, opal layers up to 2-3 cm thick and calcite layers as narrow as a few mm were noted. The intimately-laminated sequences of calcite/opal do not resemble textures which could have been caused by all of the opal forming first and all of the calcite last. The calcite/opal sequences within each episode (e.g., 2-4) may represent sub-episodes of opal and then calcite

precipitation, but the textures more readily suggest that the opal and calcite laminae within the veins precipitated nearly simultaneously for each episode of crosscutting.

The Trench 14 calcite/opal veins are interpreted by the author to be feeder veins for ascending mineralized solutions. Morphologically they are identical to the feeder veins observed at Busted Butte, only they are larger and more complexly-episodic. Like the veins at Busted Butte the Trench 14 veins narrow (but do not pinch out) toward the base and splay outward near the ground surface. Also, travertine material (~0.5 m thick) is present downslope from the feeder veins at Trench 14 as is the case for the Busted Butte veins. The morphology of the veins at Trench 14 is consistent with the concept of ascending mineralized solutions which become injected into cracks along the unloaded ground-surface zone (hence the splaying out of the veins near the surface).

The author does not interpret the vein material at Trench 14 to be of pedogenic origin, despite numerous reports to the contrary (e.g., Quade and Cerling, 1990).

Objections to a pedogenic model are:

1. The veins and localized travertine at Trench 14 do not look like caliche/pedogenic-calcrete deposits. Calcic soils are those that contain a significant amount of secondary carbonate in the form of horizontal or nearly-horizontal layers (i.e.; see the figures of Wiede, 1985, which show calcic soil horizons in desert climates).

2. The author cannot visualize how pedogenic processes could have produced the cross-cutting vein morphology at Trench 14 or how the vertical laminations of calcite and opal could have been produced by soil-forming processes.

3. If the calcite/opal were pedogenic then calcrete/caliche-type mineralization should not be localized as vein deposits but should occur everywhere in the vicinity of Trench 14.

4. Sepiolite has been reported as occurring at Trench 14 (Vaniman et al., 1988 and Levy and Naeser, 1991). It has been argued that this sepiolite may have a pedogenic origin as is supposed for the sepiolite playa deposits south of Yucca Mountain (The "Amargosa Sepiolite Mine"). However, a pedogenic origin for these playa deposits is not supported by the evidence. Rather, this sepiolite occurs with opal CT in areas of spring discharge along faults in the Amargosa Valley. (A discussion of sepiolite occurrences in the Basin and Range will be provided in a separate report.)

5. Finally, a pedogenic model does not adequately provide for the source of calcium for the calcic veins at Trench 14. There are no wind-blown dust accumulations in the immediate area of Trench 14 nor are there large windblown deposits anywhere at Yucca Mountain (see the following discussion on the origin of the so-called "eolian" sand ramps).

SAND RAMPS

Sand ramps were observed at Busted Butte, Fran Ridge, and Harper Valley. Sand ramps are long (500 m or so) and thick (50-90 m or so) masses of sand which slope away from the sides of valleys, ridges, or buttes. Sand ramps have been commonly thought to be eolian in origin (e.g., Whitney et al., 1985; Vaniman et al., 1988). In turn, windblown "dust" has been deemed the source of calcium for the "pedogenic calcite/opal calcretes" in otherwise calcium-poor volcanic rock (Stuckless et al., 1991, 1992).

The sand ramps at Busted Butte are interpreted by the author to be apron debris.

This interpretation is based on the following observations:

1. The sand ramps go all the way around Busted Butte. They have not piled up in a consistent prevailing-wind direction. This is in contrast to uncontroversial sand dune deposits (e.g., the Lathrop Wells Cone dunes which have accumulated only along the eastern side of the cone).
2. The sand ramps all emanate from approximately the same level on Busted Butte; that is, from the Bedded Tuff member of the Paintbrush Tuff. Burchfiel (1966, p. 4) described this stratigraphic unit as "approximately 45 feet of yellow-brown pumiceous airfall tuff and tuffaceous sandstone. The pumice fragments in the tuff are about 1 inch in diameter and may form as much as 80 percent of the rock...Most of the tuff is friable and weathers into low relief between the more resistant welded tuffs of the Topopah Spring and Tiva Canyon Members."

3. The sand ramps contain large talus clasts from the competent Tiva Canyon member of the Paintbrush Tuff but no talus pieces from the incompetent Bedded Tuff member (See Figure on p. 7). Therefore, the sand must represent the erosion of this soft member.

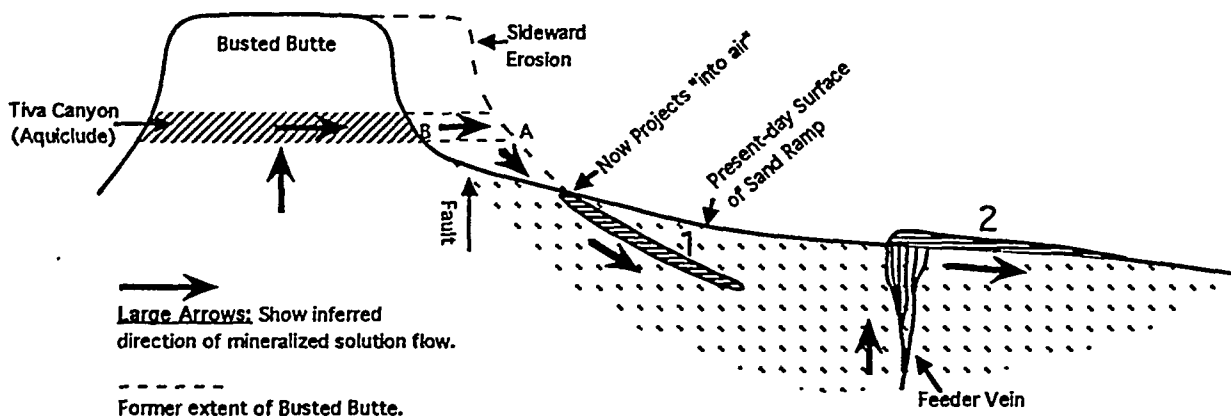
4. The sand ramps can be traced directly to their source; that is, to the very soft, pumice-rich, Bedded Tuff member. The Bedded Tuff member is so unconsolidated that wind pockets (up to a meter high and several meters wide) have formed in this unit (seen in Harper Valley and at Busted Butte). In-situ wind erosion of the unwelded Bedded Tuff has helped to produce the apron-debris sand of the ramps -- this "in situ" wind erosion should not be confused with an "eolian" origin for the sand where sand particles have been transported for great distances. This point is of extreme importance because in the case of apron-debris (in-situ sand) there is no source of calcium brought into the system, whereas in the case of an eolian origin calcium could be brought from a distant carbonate source.

5. The sand ramps have few characteristics of wind-blown deposits. There are no characteristic dune shapes and no cross-bedded sequences. The angle of repose of the sand ramps is ~15-20° and does not approach the 34° angle reached by sand dunes. Talus pieces of all sizes occur in the ramps and the sand is not well sorted as is characteristic of wind-blown deposits. In addition, the color of the sand ramps matches (or is slightly darker than) the Bedded Tuff member and is not light-colored as are the other known sand dunes in the area (e.g., the Lathrop Wells Cone sand dunes). Wind has no doubt played a minor role in the formation of the sand ramps,

with the wind reworking the sand and piling up small dunes <1 m in height (as seen on the western side of Busted Butte), but in the author's estimation probably less than 1% of the sand of the ramps had a wind-blown, eolian origin where wind has transported material for great distances. It is also possible that reworking by wind may have been partly responsible for creating higher-angled ramps on the eastern side of the butte than on the western side.

The sand ramps are interpreted to be apron deposits which have been dissected by valley erosion. Where crosscut by faults, the dissecting valleys make a jog along the fault (e.g., on the eastern side of Busted Butte). The origin of the sand ramps and associated calcite/opal vein and travertine deposits is proposed as follows:

1. Earthquake activity and faulting along the Paintbrush Fault caused mineralized water to rise along the fault.



2. The base of the Tiva Canyon member acted as an aquiclude for epithermal solutions ascending along the Paintbrush Fault. Springs issued forth along the base of the Tiva Canyon and flowed downhill. Progressive sideward erosion of Busted

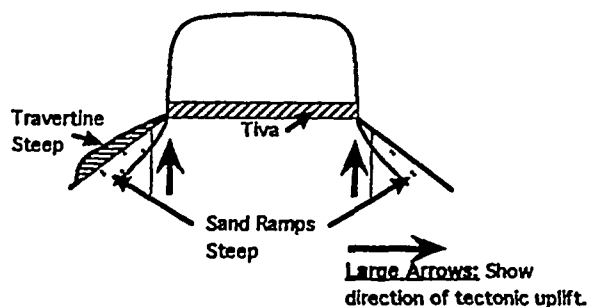
Butte caused past travertine flows to project "into the air" (i.e., when Busted Butte was at A, the #1 travertine flow issued forth from the base of the Tiva Canyon aquiclude).

3. Other springs occurred along faults after the Tiva Canyon had eroded past their extent; in these cases the feeder veins extended directly to the surface and travertine-precipitating flows occurred downslope from the veins (2).

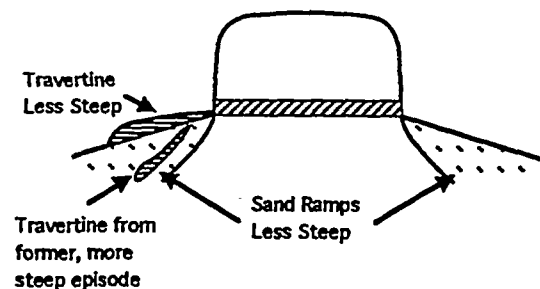
4. All of the travertines (1,2) formed as spring deposits at the surface of the sand ramps. This is indicated by the presence of root casts in all of the travertine, whether in the older units which formerly deposited on a past surface of the sand ramps (1), or younger surficial units now at the surface of the sand ramps (2).

5. The differently angled travertine represents the slope of the sand ramps at the time the travertine formed. The different angles may relate to differential displacement along the Paintbrush Fault, minor eolian activity, or both. During times of tectonic displacement the sand ramps (and travertine formed on the surface of the ramps) would have become steeper sloped and during times of tectonic quiescence the sand ramps would have been less steep.

A. Tectonic Uplift



B. Tectonic Quiescence



6. The calcite/opal filling the feeder veins in the sand ramps are not considered to be "of pedogenic, infilling origin along faults" as specified by Stuckless and Whitney (1990, p. 25). Why would the so-called "wind-blown" sand of the sand ramps not have infilled fault openings? Why would they have remained open to become filled with slowly-accumulating, pedogenic calcite and opal instead of with sand? The calcite/opal of the veins and downslope sheet deposits contain sand in places where they contact the sand (i.e., at the base of the sheets and sides of the veins), but they are relatively sand-poor where they have not come into direct contact with pre-existent sand.

7. The age of the sand ramps/travertine is not known with certainty, but Whitney et al. (1985) and Stuckless and Whitney (1990) reported that the ~740 Ka Bishop Ash appears near the base of the sand ramps at Busted Butte and so the overlying travertine layers must be younger than this.

SITE 199

Site 199 was the most puzzling stop of the field trip. Calcite spring mounds exist at the site along with rock of the very-brecciated, Cambrian Bonanza King and Carrera Formations. Swadley and Carr (1987), Swadley and Parrish 1988), and Frizzel et al. (1990) portrayed these Paleozoic units to be landslide deposits (T_{1g}) and they may be. However, it seems suspicious that only a few kilometers to the northeast are the thrust faults of the Bare Mountain. On the Bare Mountain Quadrangle the Bonanza King Formation is shown thrust to the south and the east, in the direction of the so-called Paleozoic "landslide deposits" overlying Tertiary rock (the Ammonia Tank

member, ~11 Ma). Could local thrust faulting possibly have happened as late as the Miocene? Might thrust faulting have caused the shattering of the brecciated Bonanza King and Carrera Formations at Site 199? Could the presence of the calcareous and diatomaceous spring mound deposits in the immediate vicinity of these "landslide" deposits be related to late-stage (Quaternary) solutions moving up along these Tertiary thrust faults?

Another problem related to Site 199 is the nearby presence of Pliocene/Pleistocene lake deposits. Might the springs at Site 199 (and along the road between the gate and Site 199) have fed the lake with water? Might the high mark of this lake be correlative with higher water input along the fault plus higher runoff during the Wisconsin glacial?

Site 199 is most curious and may be a key that helps unlock some of the geologic history of the Yucca Mountain area.

ORE MINERALIZATION/ALTERATION

There is evidence of ore mineralization and alteration in the Yucca Mountain region: to the west in the Bare Mountain Mining District, to the east in the Wahmonie Mining District, to the northeast in the Calico Hills, and at Yucca Mountain.

1. Yucca Mountain. Not only is calcite/opal travertine localized along fault zones at Yucca Mountain, but also alteration of bedrock has been localized along these same fault zones. Alteration in the Yucca Mountain area seems to consist primarily of iron

which colored the tuffaceous rock honey yellow to orange to bright red. Such iron enrichment can be seen in the Bedded Tuff member at Busted Butte and in Harper Valley. In Harper Valley the altered areas contain elevated levels of iron (1.45%) and manganese (130 ppm) and also elevated levels of lead and zinc (Pb = 34 ppm; Zn = 20 ppm).

2. Calico Hills. The Calico Hills area has been especially subject to alteration by silicification, alunitization, and kaolitization. Cubic hematite (after pyrite) and reniform hematite was found in the Calico Hills; hematite and disseminated iron cause the entire Calico Hills to be colored various shades of red, orange, and tan (like calico). Along the fault zone (at the site visited) the Topopah Spring member of the Paintbrush Tuff is so silicified and hardened by silica that it resembles quartzite more than it does tuff.

3. Bare Mountain Mining District. Mineralization also occurs along Tertiary intrusive rhyolite dikes and faults in the Bare Mountains located about 15 km west of Yucca Mountain. The Diamond Queen Mine is located at a thrust-fault contact between the Precambrian Johnnie Formation and the Cambrian Nopa Formation. Mineralization seen at the Diamond Queen Mine and vicinity includes fluorite, calcite, opal, and kaolinite. In places the calcite occurs as large bladed sheaths or Iceland spar and the opal occurs as rounded nodules. In other places (at "Slide mine", just north of the Diamond Queen Mine) calcite/opal textures closely resemble those found at Yucca Mountain.

Breccia dikes were also found in the Bare Mountain Mining District. These are most likely explosion breccias as they are heterogeneous in breccia-fragment type (i.e., material has come from different stratigraphic units) and heterogeneous in shape (some of the fragments are rounded, some are angular). These breccias differ from the silicified breccias at Yucca Mountain which are much more homogeneous with respect to composition, size, and shape of the breccia fragments (i.e., the breccias are typically in place or have not been carried far from a host bedrock source).

4. Wahmonie Mining District. In the Wahmonie Mining District quartz is plentiful and calcite and fluorite are rare. A small amount of an opaque mineral was observed with the quartz; this may be either a sulfide mineral or cerargyrite.

RECOMMENDATIONS

The following recommendations are made pertaining to the analysis of samples for the purpose of using such information in forthcoming publications:

1. $^{87}\text{Sr}/^{86}\text{Sr}$. Perform strontium analyses on all 18 of the collected Precambrian, Paleozoic, and Tertiary rock samples. Perform strontium analyses on at least some of the calcite/opal deposits collected at key spots at Yucca Mountain and compare these values with bedrock values in order to determine the provenance of the strontium. Also compare these with calcite/opal deposits already analyzed for $^{87}\text{Sr}/^{86}\text{Sr}$.

2. U-Series dates. It is recommended that as much dating as possible be done on the samples collected. Dating of a number of samples would allow one to determine: (a) if some of the calcite is very young, (b) if there is a clustering of ages around discrete hydrothermal events, and (c) if the dates on calcite and opal couplets are equivalent. This would require a great deal of money but would provide important, even definitive, information.

3. Fluid inclusions. From the analyses done so far on the WT-7 and Wailing Wall opal, the fluid inclusion method does not appear promising in establishing a hypogene origin for the calcite/opal. However, only the opal has been tested and perhaps some of the calcite filling cavities in the opal can be analyzed for fluid inclusions. It is worth some effort to do this because not only must it be proved that the calcite/opal is young, it must also be proved that the deposits are hypogene (i.e.,

of deep-seated origin).

4. Trace element analyses. Trace element analyses may also be a way to show that the calcite/opal travertine is hypogene. High amounts of metals (Hg, Mo, etc.) in the travertine would tie it to the ore deposits of the surrounding region (e.g., the Bare Mountains). Trace element analyses are not that expensive: a 32 element package costs \$5.50/sample.

5. Carbon-oxygen isotope analyses. Carbon-oxygen isotope analyses need to be done on the calcite of both the Wahmonie mound and the Bare Mountain Mining District where the calcite is known to be hydrothermal; these deposits can then be compared to the controversial vein deposits at Yucca Mountain. Also, carbon-oxygen isotope analyses should be performed on different types of travertine deposits (feeder vein, sheet, mound deposits, etc.) in order to compare the isotopic signatures of these different morphological types. In addition, known pedogenic crusts coating volcanic clasts in Lathrop Wells Cone should be isotopically compared with respect to the so-called "pedogenic" deposits at Trench 14, Busted Butte, etc.

REFERENCES

- Burchfiel, B.C., 1966. *Reconnaissance geologic map of the Lathrop Wells 15-minute quadrangle, Nye County, Nevada*. U. S. Geological Survey Miscellaneous Geologic Investigations Map I-474, scale 1:62,500. Six pages of accompanying notes.
- Dixon, J. B., and S. B. Weed, 1989. *Minerals in soil environments*. Soil Science of America. Madison, Wisconsin, 1244 pp.
- Frizzel, V. A., and J. Shulters, 1990. *Geologic map of the Nevada Test Site*. U. S. Geological Survey Miscellaneous Investigation Series, Map I-2046, scale 1:100,000.
- Hill, C. A., 1992. *Report of field trip of 2-27 and 2-28, 1992*. Unpublished report to Technology and Research Assessment Corporation, 10 pp.
- Hill, C. A., and P. Forti, 1986. *Cave minerals of the world*. National Speleological Society. Huntsville, Alabama, 238 pp.
- Levy, S., and C. Naeser, 1991. *Bedrock breccias along fault zone near Yucca Mountain, Nevada*. Draft Los Alamos-USGS paper.
- Machette, M. N., 1985. *Calcic soils of the southwestern United States*. In Weide, D. L., Soils and Quaternary geology of the southwestern United States, pp. 1-21.
- Quade, J., and T. E. Cerling, 1990. *Stable isotopic evidence for a pedogenic origin of carbonates in Trench 14 near Yucca Mountain, Nevada*. Science. v. 250, pp. 1549-1552.
- Quade, J., and J. V. Tingley, 1983. *A mineral inventory of the Nevada Test Site and portions of the Nellis Bombing and Gunnery Range, southern Nye County, Nevada*. Department of Energy Report, DOE/NV/10295-1.
- Somerville, M. R., J. S. Szymanski, G. A. Frazier, C. B. Archambeau, C. M. Schluter, and D. E. Livingston, 1992. *Critical review of the National Research Council report: groundwater and Yucca Mountain: how high can it rise?* Quarterly Report prepared by TRAC for the Nuclear Waste Project Office, State of Nevada.
- Stuckless, J. S., Z. E. Peterman, and D. R. Muhs, 1991. *U and Sr isotopes in ground water and calcite, Yucca Mountain, Nevada: evidence against upwelling water*. Science. v. 254, pp. 551-554.

- Stuckless, J. S., Z. E. Peterman, R. L. Forester, J. F. Whelan, D. T. Vaniman, B. D. Marshall, and E. M. Taylor, 1992. *Characterization of fault-filling deposits in the vicinity of Yucca Mountain, Nevada*. Proceedings of Waste Management '92. Tucson, Arizona, March 1-5. Rough draft.
- Stuckless, J. S., and J. Whitney, 1990. *Field trip to Yucca Mountain and surrounding region for the National Academy of Sciences Panel on coupled processes*. October 18-20, pp. 25-26.
- Swadley, W. C., and W. J. Carr, 1987. *Geologic map of the Quaternary and Tertiary deposits of the Big Dune Quadrangle, Nye County, Nevada, and Inyo County, California*. U.S. Geological Survey Miscellaneous Investigations Map I-1762, scale 1:48,000.
- Swadley, W. C., and L. D. Parrish, 1988. *Surficial geologic map of the Bare Mountain Quadrangle, Nye County, Nevada*. U.S. Geological Survey Miscellaneous Investigations Map I-1826, scale 1:48,000.
- Szabo, B. J., and T. K. Kyser, 1985. *Uranium, thorium isotopic analyses and uranium-series ages of calcite and opal, and stable isotopic compositions of calcite from drill cores UE25a#1, USW G-2, and USWG-3/GU-3, Yucca Mountain, Nevada*. U. S. Geological Survey, Open File Report 85-224, 25 pp.
- Vaniman, D. T., D. L. Bish, and S. Chipera, 1988. *A preliminary comparison of mineral deposits in faults near Yucca Mountain, Nevada, with possible analogs*. Los Alamos National Laboratory, Report LA-11289-MS, 54 pp.
- Weide, D. L., 1985. *Soils and Quaternary geology of the southwestern United States*. Geological Society of America, Special Paper 203, 150 pp.
- Whitney, J. W., W. C. Swadley, and R. R. Shroba, 1985. *Middle Quaternary sand ramps in the southern Great Basin, California and Nevada*. Geological Society of America. Abstracts with Programs, v. 17, p. 750.
- Winograd, I. J., and W. Thordarson, 1975. *Hydrogeologic and hydrochemical framework, South-Central Great Basin, Nevada-California, with special reference to the Nevada Test Site*. USGS Professional Paper 712-C. Washington, D. C. pp. C1-C126.

APPENDIX 1

Detailed List of Samples Collected

Note: Appendix 1 is a detailed list of the samples collected at each stop. (Provided by C. M. Schluter) An "X" in the column identifies the samples selected for analyses. All Trace Element and REE analyses have been completed.

		STATUS:	To Do	To Do	To Do	Done	To Do	Done
	SAMPLE	TYPE	87Sr/86Sr	U-series	Fluid Inclusions	Trace element	Carbon-oxygen	REE
STOP #1	US 95 mile 10							
1a	dolomite	Nopah Fromation	X					
1b	silica	breccia zone						
1c	calcite							
1d	dolomite	organic lithofacies						
1e	silica	vein						
1f	calcite	vein						
1g	calcite							
STOP #2	US 95 mile 12.47							
2a	quartzite (clean)	Stirling Quartzite	X					
2b	quartzite (dirty)	Stirling Quartzite	X					
2c	epidote	vein						
2d	calcite	vein						
STOP #3	US 95 mile 18.8							
3a	dolomite/lmst		X					
STOP #4	Pull Apart Fault							
4a	limestone	fault related alteration	X			X	X	
4b	calcite	coating						
4c	calcite-opal-breccia					X		
4d	calcite-opal	bulk samples	X				X	
4e	opal breccia							
4f	calcite	riverbed						
4g	carb.-coated rock							
STOP #5	WT - 7							
5a	calcrete-coated rock							
5b	calcite-opal	surficial deposit						
5c	opaline layer	on breccia	X				X	
5d	calcite-silica					X		X
5e	calcite	fracture fill						
5f	breccia							
5g	breccia							
5h	calcium crystals	Carol's sample			X			
STOP #6	USW H - 6							
6a	carbonate crust	surficial coating						
STOP #7	roadside (WT-7)							
7a	calcite	caliche?/calcrete						
7b	silica-calcite							
7c	opal							
7d	indurated layer	coating on surface roc						
STOP #8	Plug Hill							
8a	carbonate	coating on colluvium						

STOP #	SAMPLE	TYPE	87Sr/86Sr	U-series	Fluid Inclusions	Trace element	Carbon-oxygen	REE
STOP #9	roadside (WT-7)							
9a	calcite	coating						
STOP #10	Bare Mountain							
10a	calcite-opal	loose material	X			X	X	
10b	lmst/opal	brecciated, cemented						
10c	calcite-lmst					X		
10d	limestone	Ely Springs	X					
10e	opal	siliceous						
10f	carbonate	in stream bed						
STOP #11	Diamond Queen M.							
11a	white mineral	filling, metamorphosed						
11b	calcite	float sample						
11c	phyllite	Johnnie Formation	X					
11d	carbonate	incrustations						
11e	Nopah formation		X					
11f	Iceland spar	massive					X	
11g	calcite	vein						
11h	quartz							
11j	fluorite							
11k	fluorite							
11m a	calcite	coating						
11m b								
11n	calcite	crust						
11o	kaolinite clay	from breccia pipe						
11p	chert nodule	in fluorite breccia						
11q	porphyry	volcanic breccia						
11r	fluorite breccia							
11s	chert nodule							
STOP #12	Chuckwalla Canyon							
12a	Iceland spar	massive					X	
12b	opal-calcite	inter-layers						
12c	carbonate	white & black mineral						
12d	dolomite	Lone Mt.	X					
12e	calcite							
12f	calcite	fracture filling						
12g	calcite	columnar crystals						
STOP #13	Tarantula Canyon							
13a	limestone	Meiklejohn	X					
13b	rhyolite							
STOP #14	Trench 8							
14a	calcite	root casts						
14b	ash							
14c	calcite-opal-silica							
14d	calcite-opal	fault infilling						
14e	black glassy material	in altered vitrophyre						

STOP #	SAMPLE	TYPE	87Sr/86Sr	U-series	Fluid Inclusions	Trace element	Carbon-oxygen	REE
STOP #14	Trench 8 (cont.)							
14f	carb., some silica	cement						
14g	silica-calcite	vein	X			X	X	
STOP #15	roadsie (trench 8)							
15a	carbonate	matrix						
STOP #16	New Trench							
16a	carbonate	vein						
16b	ash							
16c	carbonate	matrix	X			X	X	
STOP #17	Site 106							
17a	tufa	spring						
17b	carbonate	spring						
STOP #18	Livingston Scarp							
18a	carbonate	fracture fillings						
18b	opal-carbonate	vein	X			X	X	
STOP #19	Wailing Wall							
19a	opal-calcite	coating	X			X	X	
19b	carbonate	vein						
19c	carbonate	coating						
19d	algal?							
19e	opal-calcite	Carol's sample			X			
STOP #20	roadside ("scarp")							
20a	glass	volcanic	X			X		X
STOP #21	Red Cliff Gulch							
21a	carbonate	surface coatings				X		
STOP #22	Stagecoach Trench							
22a	carbonate	root casts				X		
22b	tuff	calcite overlies				X		
22c	quartz?	calcite overlies						
22d		full of clasts						
22e	carbonate	surficial						
STOP #23	Stagecoach Trench							
23a	carbonate	root casts						
23b	glass	vitrophyre						
STOP #24	Site 199							
24a	silicified material	some clasts						
24b	breccia (Carrera)	conglomerate	X				X	
24c	breccia	Bonanza King	X					
24d	tufa	some brecciated carb.	X			X	X	

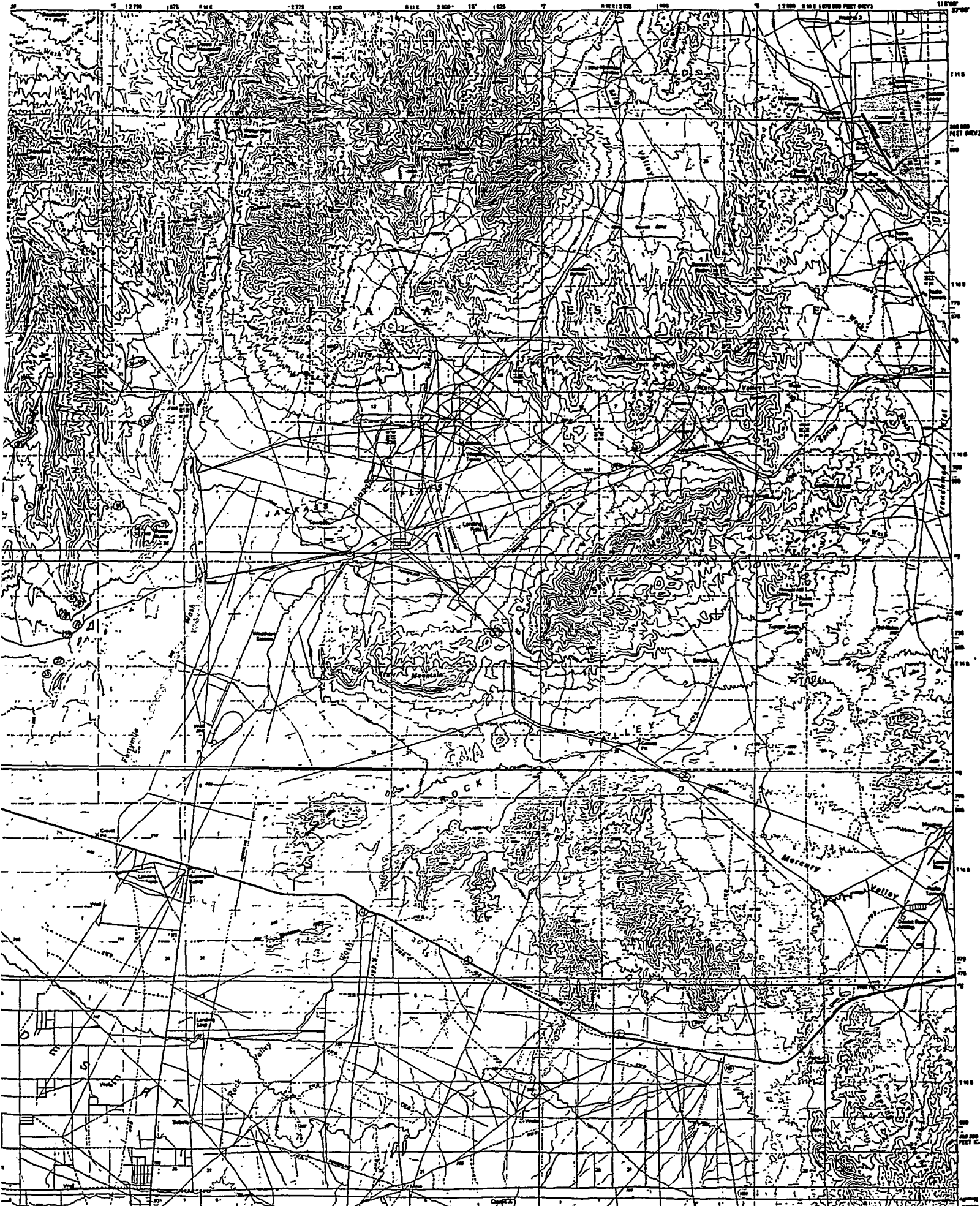
STOP #	SAMPLE	TYPE	87Sr/86Sr	U-series	Fluid Inclusions	Trace element	Carbon-oxygen	REE
STOP #25	roadside (site 199)							
25a	carbonate	root casts (burrows?)						
25b	seds.	marsh/lake						
STOP #26	roadside (FOC)							
26a	lmst, dolomite	Bonanza King	X					
STOP #27	roadside (FOC)							
27a	calcite	secondary						
27b	carbonate? in basalt	cement filling						
27c	travertine	surficial cap				X		
STOP #28	East Busted Butte							
28a	silica	vein						
28b	sand							
28c	carbonate?	root casts						
28d	carbonate?	vert. vein	X	X?		X	X	
28e	opaline-coral	slope deposit		X?				
28f	travertine	upslope						
STOP #29	East Busted Butte							
29a	calcrete							
29b	rat midden							
29c	sheet deposit							
29d	vitrophyre		X					
29e	travertine, breccia	sheet deposit						
29f	carbonate?	root casts						
STOP #30	West Busted Butte							
30a	carbonate?	vert. vein		X?				
30b	carbonate?	root casts						
30c	opal-calcite		X			X	X	
30d	carbonate?	vein						
30e	carbonate?	vein						
30f	calcite	vein						
30g	carbonate?	punchbowl						
30h	carbonate?	root casts						
STOP #31	roadside (Mercury)							
31a	calcite	coating						
STOP #32	Wahmonie Mounds							
32a	gypsum with calcite							
32b	carbonate							
32c	calcite-gypsum							
32d	calcite		X?			X		
32e	gypsum	crust on carbonate						

STOP #	SAMPLE	TYPE	87Sr/86Sr	U-series	Fluid Inclusions	Trace element	Carbon-oxygen	REE
STOP #33	Mines (Wahmonie)							
33a	carbonate?	vein						
33b	fluorite? in quartz					X		
33c	calcite crystal in qua							
STOP #34	Calico Hills							
34a	shale	Eleana	X					
34b	limestone	Eleana	X					
34c	pyrite	cubes						
34d	pumice and silicified	Calico Hills						
34e	kaolinitized clay							
34f	ironized tuff	Calico Hills				X		
34g	calcite	slslickenside	X			X	X	
34h	yellow hot rock							
STOP #35	Shoshone Mt. road							
35a	kaolinite							
35b	Topopah	red sample						
35c		cavity fillings						
STOP #36	Trench 14							
36a	carbonate							
36b	opaline							
36c	carbonate	finely laminated						
36d	carbonate	vein		X?				
36e	silica	vein	X			X	X	
36f	carbonate	vein						
36g	carbonate	vein		X?				
36h	silica	vein	X			X	X	X
36i	carbonate	vein						
36j	opal	vein						
36k	opal-breccia-carbonate	finely laminated		X?			X	
36m	calcite	vein	X			X	X	X
36n	carbonate	vein		X				
36o	carbonate	vein						
36p1	calcite-opal	vein						
36p2	calcite-opal	vein		X?				
36r	carbonate	vein						
36s	opal	vein						
36t	carbonate	vein						
36v	carbonate	vein						
36w	opal	vein						
36x		Calico Hills?						
36y	breccia-calcite							
36z	breccia		X			X		
JP #37-1	UE 25 p#1							
37-1a	opal	opaline	X			X	X	
37-1b	opal	Carol's sample						

STOP #	SAMPLE	TYPE	87Sr/86Sr	U-series	Fluid Inclusions	Trace element	Carbon-oxygen	REE
STOP #37-2	Mercury							
37-2a	dolomite	fault zone	X					
37-2b	carbonate	vein						
37-2c	brecciated dolomite	red altered zone						
STOP #	SAMPLE	TYPE	87Sr/86Sr	U-series	Fluid Inclusions	Trace element	Carbon-oxygen	REE
STOP #38	West Busted Butte							
38a	sand	windblown						
38b	travertines							
38c	opal-calcite							
38d	pumice tuff	bedded tuff						
38e	tuff	red altered				X		X
38f	travertine		X			X	X	
38g	carbonate	caps tuff						
STOP #39	Harper Valley							
39a	carbonate	in streambed	X	X		X	X	
39b	silica	botryoidal (opalite)						
39c	Tiva	partially welded						
39d	flowstone	laminated						
39e	carbonate	vein filling						
39f	opal	botryoidal						
39g	calcite	vein						
39h	some opal	pinnacles						
39i	carb?-silica	"Z" veins						
39k	tuff	red altered						
39m	carbonate	vein						
39n	opal	Carol's sample						
STOP #40	Trench 14							
40a1	mostly carbonate	vein						
40a2	carbonate?	vein						
40a3	carbonate?	vein						
40b	calcite	vein	X			X	X	
40c	calcite	subsurface						
STOP #41	Lathrop Cone							
41a	sulfur or jarosite							
41b	carbonate	coatings	X				X	
41c	sulfur?							
STOP #42	Lathrop Cone							
42a	sand							

Figure 1. Locations of Stops are located on the map as circled numbers (Red). Please see Appendix 1 for a detailed list of samples collected at each stop.

Map: USGS--Beatty (Nevada-California),
No. 36116-E1-TM-100 (1986)



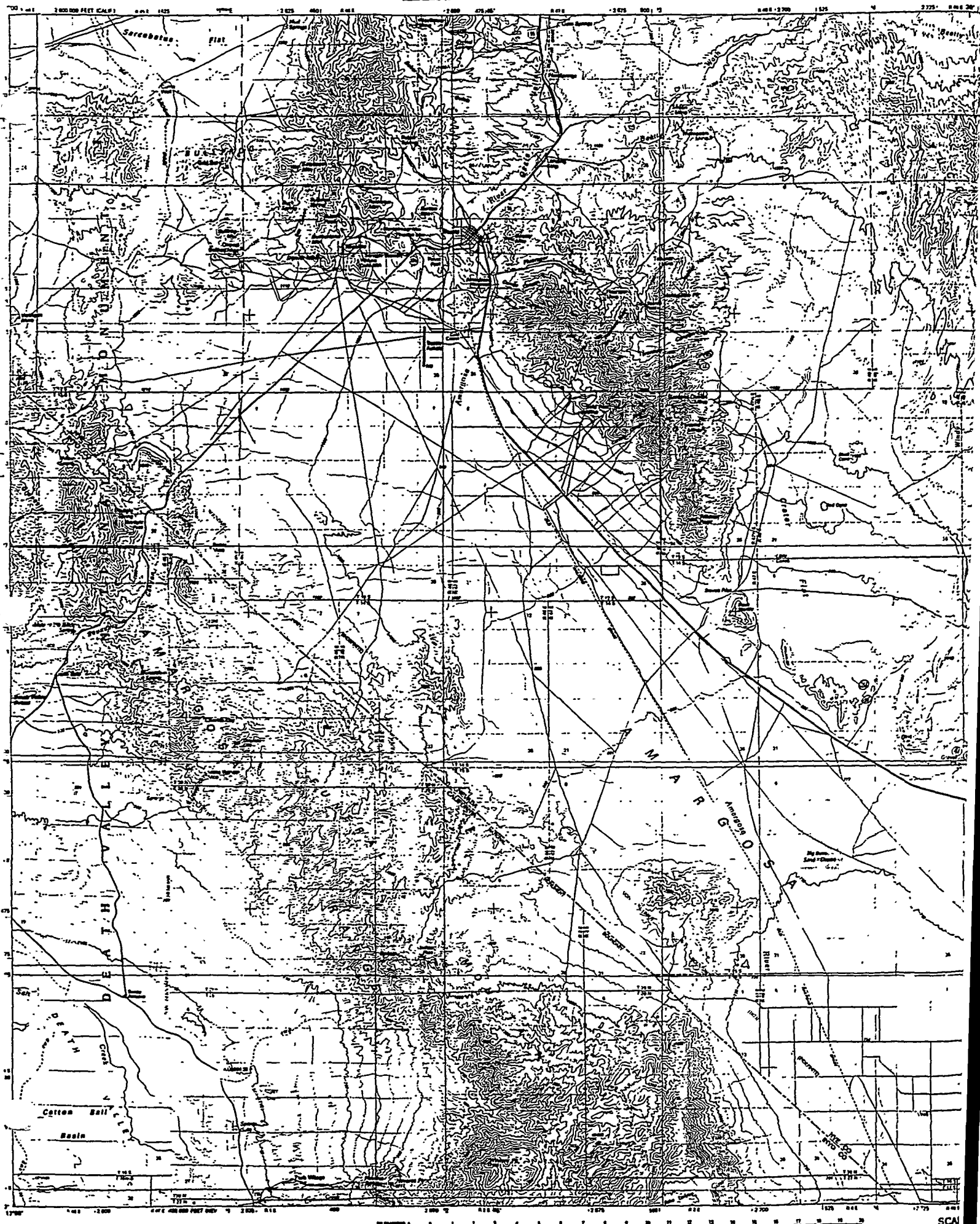




Figure 2. Actual photograph of the south wall of Trench 14 taken from an unclassified, United States Department of Energy negative — No. YM-284.

PART 5

The Origin of Sepiolite, Yucca Mountain, Nevada

3800 Arapahoe Avenue, Suite 225
Boulder, Colorado 80303
(303) 443-3700 FAX No. (303) 443-8626

THE ORIGIN OF SEPIOLITE, YUCCA MOUNTAIN, NEVADA

SPECIAL REPORT No. 6
CONTRACT No. 92/94.0004

SPECIAL REPORT Submitted to the
Nuclear Waste Project Office
State of Nevada

June, 1993

Authored by:

Carol A. Hill

THE ORIGIN OF SEPIOLITE, YUCCA MOUNTAIN, NEVADA

TABLE OF CONTENTS

INTRODUCTION	1
NEVADA/UTAH/CALIFORNIA/ARIZONA SEPIOLITE	1
LAS VEGAS, NEVADA SEPIOLITE	2
AMARGOSA VALLEY SEPIOLITE	3
YUCCA MOUNTAIN SEPIOLITE	5
DISCUSSION	6
REFERENCES	9
FIGURES	11

INTRODUCTION

Quade and Cerling (1990), among others, have concluded that the calcite/opal vein deposits along the fault at Trench 14, Yucca Mountain, Nevada are of supergene-pedogenic origin. Yet, the mineral sepiolite ($\text{Mg}_4\text{Si}_6\text{O}_{15}(\text{OH})_2 \cdot 6\text{H}_2\text{O}$) is known to occur with calcite and opal at Trench 14, a mineral which may be of hypogene origin in this setting. A review of the literature shows that many of the sepiolite deposits in the Basin and Range of Nevada, Utah and California are related to hydrothermal spring water upwelling along fault zones, even in the case of so-called "playa" deposits. Therefore, the Trench 14 calcite/opal/sepiolite mineral suite may have a similar hydrothermal/hypogene origin.

NEVADA/UTAH/CALIFORNIA/ARIZONA SEPIOLITE

Ehlmann et al. (1962) were among the first to report on the sepiolite deposits of the Basin and Range, western United States. These authors studied four occurrences of sepiolite: (1) Maxfield Mine, Utah (M; Fig. 1), (2) Ferber Mining District, Nevada (F), (3) Cane Springs Mine, Utah (CS), and (4) Mineral Range, Beaver County, Utah (B). In all four of these districts, the sepiolite occurs with calcite, quartz, and /or opal in sulfide-mineralized ore veins and is associated with dolomite and intrusive volcanic rock. It was the opinion of Ehlmann et al. (1962) that the sepiolite in these four districts was formed by low-temperature, hydrothermal solutions during the last stages of sulfide-mineral deposition in carbonate beds.

Sepiolite has also been found along the Eleana thrust fault just northeast of Yucca

Mountain (EF; Fig. 1). Jones (1983, p. 4) attributed this sepiolite and associated carbonate mineralization to "spring waters brought to the surface along a thrust of quartzite over argillite in the Mississippian Eleana formation."

Hay and Wiggins (1980) reported sepiolite in fanglomerates of the Argus Range, California, near Wickieup, Arizona, and in Kyle Canyon, Nevada (AR, W, KC; Fig. 1). In all of these localities the sepiolite was determined to be of pedogenic origin, the mineral having formed in semi-horizontal calcrete layers within the fanglomerates. In addition, Bachman and Machette (1977) noted sepiolite in calcic soils, pedogenic calcretes, and other surficial carbonates in other semi-arid Southwest settings.

LAS VEGAS, NEVADA SEPIOLITE

Post (1978) reported four different types of sepiolite deposits in the region of Las Vegas, Nevada, just east and southeast of Yucca Mountain (Fig. 1): (1) North Las Vegas (LV); (2) Two Crows (2C); (3) Chamber Mine (CM); and (4) Amargosa Playa (AP). The North Las Vegas sepiolite occurs as an alluvial terrace deposit at a depth of about 3 m. The Two Crows is a vein deposit, up to 0.6 m wide and 450 m long, which occurs along a fault cross-cutting volcanic ash. The Chambers mine sepiolite is along a vein in dolomite.

Post (1978, p. 58) was of this opinion concerning the origin of these deposits: "Each of the sepiolite deposits appears to be formed in a somewhat different manner, although they all appear to be brought about by groundwater movement in areas of

high Mg concentration with high pH conditions...The mineral source in each case must have been derived from some depth in circulating groundwater." (emphasis added)

AMARGOSA VALLEY SEPIOLITE

Papke (1972) was one of the first to describe the sepiolite deposits in the Amargosa Valley area of Nevada just south of Yucca Mountain (AP; Fig. 1). Post (1978) also discussed these deposits, as did Regis (1978). Regis (1978) showed sepiolite deposits located at AV (Fig. 1); however, this location is probably misplaced--Regis was probably describing the Amargosa playa deposits further southeast (AP; Fig. 1). Regis found tridymite, cristobolite, and calcite associated with this playa sepiolite. Khoury et al. (1982) studied the sepiolite deposits of Amargosa Flat (AP; Fig. 1) and those of nearby Ash Meadows (AM), and Hay et al. (1986) studied the Amargosa sepiolite and carbonate playa deposits in detail and related them to stratigraphy and structure.

All of the above authors favored a spring-discharge origin for the sepiolite at Amargosa Flat. Regis (1978, p. 31) said of the Amargosa Valley sepiolite: "Introduction of late Pleistocene and recent hot spring activity and subsequent faulting did much to produce the clay mineral assemblage occurring here and also the high magnesium content of the clays. This (sepiolite) deposit is probably the result of the alteration of Tertiary volcanic sediments by hot, magnesium-rich water." Khoury et al. (1982, p. 327) concluded that the sepiolite had precipitated directly

from solution and that "mineral precipitation probably occurred during a pluvial period in shallow lakes or swamps fed by spring water from Paleozoic carbonate aquifers." Hay et al. (1986, p. 1488) described the Amargosa Desert of Nevada-California as "an area of major spring discharge that contains large amounts of spring-related carbonate deposits and Mg clays." The "spring-related carbonate deposits" consist of "seepage mounds" and "caliche breccias" and the Mg clays consist of sepiolite, all of which may be silicified where the silica fills pores and fractures and replaces carbonates and Mg clays.

Most important, Hay et al. (1986) found that the carbonate seepage mounds, caliche breccias, and sepiolite deposits of the Amargosa Valley playa all occur along fault zones (Fig. 2). The seepage mounds and caliche breccias fall along two linear zones, the southern one being the eastward extension of a fault (Fig. 2A). Slow groundwater discharge along this fault supplied the solutes for the mounds, breccias, and silica (opal-CT). Likewise, the sepiolite at East Playa was deposited near probable areas of spring discharge, and the sepiolite at Dry Lake pit lies along the eastward extension of the fault-controlled linear zone of spring-related carbonate deposits (Fig. 2B). According to Hay et al. (1986) the sepiolite at Dry Lake pit was precipitated in fractures from groundwater seeping upward (emphasis added). Discharge was from Paleozoic dolomite aquifers, which rock supplied the Mg for the sepiolite.

Hay et al. (1986) also performed isotopic analyses on sepiolite and associated silica

minerals of the playa. These isotopic values indicated that crystallization of the sepiolite had taken place at low temperatures ($< 35^{\circ}\text{C}$). The difference in $\delta^{18}\text{O}$ values of co-existing silica and calcite corresponded to an equilibrium temperature of about 27°C and formation from water having a $\delta^{18}\text{O}$ value near -10.0 . This low-temperature, hydrothermal origin is consistent with known temperatures of water at nearby Paleozoic carbonate-aquifer discharge points (e.g., 34°C at Devil's Spring, from the Cambrian Bonanza King Formation). This hydrothermal origin is not consistent with a pedogenic model where water temperatures should be $< 20^{\circ}\text{C}$.

YUCCA MOUNTAIN SEPIOLITE

In the vicinity of Yucca Mountain, sepiolite has been reported as occurring with calcite and/or opal at Trench 14 and Busted Butte (Vaniman et al., 1988; Levy and Naeser, 1991), and in at least five additional locations (Jones, 1983). At Busted Butte, sepiolite occurs as pore fillings in crushed-tuff-matrix (CTM) breccias and with fine-grained calcite and silica as fracture and vesicle fillings in authigenic-mineral-cement (AMC) breccias (Levy and Naeser, 1991). At Trench 14, sepiolite occurs as a $< 2\mu\text{m}$ fraction in a matrix of calcite/opal-CT (Vaniman et al., 1988), and also with silica fracture fillings as discrete pods of material scattered along relict fractures along which the pods lie (Levy and Naeser, 1991). The sepiolite of the pods has a platy to fibrous texture, locally with an overall elongate fabric matching the elongation of the pods themselves. In other places at Trench 14, a mixture of silica-sepiolite is the most common pore-filling cement surrounding the AMC breccias.

Sepiolite was also briefly noted by Jones (1983) from the following five localities in

the Yucca Mountain area: southern Striped Hills, southern Crater Flat, central Crater Flat, Jackass Divide, and Mercury Valley (SH, SCF, CCF, JD, MV; Fig. 1). A number of the samples collected by Jones were from trenches dug "across fault traces" and in which calcite/opal mineralization is exposed (Jones, 1983, p. 2). Other samples were collected from alluvial terraces and erosion surfaces consisting of calcretes and calcic soils. These sepiolite deposits were believed by Jones (1983, p. 11) to have been precipitated from "percolating waters with the same solute source (Paleozoic carbonates and Tertiary volcanics) as the discharge from the regional groundwater system at Ash Meadows."

DISCUSSION

The occurrence of sepiolite at Yucca Mountain is important because it relates to the hypogene-supergene debate, where the calcite/opal vein deposits at Yucca Mountain (e.g., at Trench 14) have alternatively been attributed to supergene-pedogenic processes (e.g., Quade and Cerling, 1990) or to hypogene processes (e.g., Szymanski et al., 1993). Far from being of esoteric concern, the ultimate outcome of this dispute will determine the future of Yucca Mountain as being the site for the permanent disposal of high-level nuclear waste. Therefore, the question of whether sepiolite (which occurs associated or intermixed with the controversial calcite/opal deposits) is of hypogene or supergene origin is an important one.

Vaniman et al. (1988), working on the calcite/opal/sepiolite vein deposits at Trench 14, thought that these deposits were of supergene-pedogenic origin and made the

statement (p. 18) that: "the commonest occurrences of sepiolite in southern Nevada appear to be either playa-formed or pedogenic." Contrary to this statement, the sepiolite deposits of the Basin and Range seem to be characterized by the following:

(1) Most of the reported sepiolite in the Basin and Range occurs as fault (EF, AP, AM, TR, CCF) or vein (M, F, CS, B, 2C, CM) deposits (Fig. 1).

(2) Even the "playa-formed" sepiolite deposits occur along fault zones (Fig. 2).

(3) A few deposits are known to be pedogenic (AR, W, KC, and perhaps LV). In other cases it is not clear from their descriptions whether the sepiolite is pedogenic or hypogene (LV, SH, SCF, JD, MV). The known pedogenic deposits (AR, W, KC) occur as semi-horizontal calcrete layers within fan conglomerates (Hay and Wiggins, 1980), not as vertical vein fault deposits.

(4) The universal source of Mg and Si for sepiolite in the Basin and Range seems to be dolomite and volcanic rock, respectively. In this regard, it should be pointed out that at Yucca Mountain the Paleozoic carbonates (dolomite) are located in the subsurface beneath the controversial calcite/opal/sepiolite deposits and therefore the mineral (Mg) source must have come from depth. (i.e., be of hypogene origin). In other places, such as in Kyle Canyon in the Spring Mountains west of Las Vegas (KC; Fig. 1), dolomite outcrops can provide a direct source of magnesium to supergene-pedogenic sepiolite.

(5) Some of the deposits appear to be associated with sulfide mineralization of unquestionable hydrothermal origin (M, F, CS, B; Fig. 1).

(6) In all of the sepiolite occurrences along fault zones, the origin of these deposits

has been attributed to low-temperature, hydrothermal spring-water which has ascended from Paleozoic aquifers along these faults to form either vein or playa deposits. In no case has the fault-related sepiolite been attributed to a pedogenic origin.

The pertinent questions that need to be asked now are: If many or most of the sepiolite deposits in the Basin and Range are of a hydrothermal, spring- and fault-related origin, then why would the fault-related Trench 14 and/or Busted Butte sepiolite be considered pedogenic? And, if the sepiolite is hypogene rather than pedogenic, then how can the associated/intermixed calcite/opal be considered to be supergene-pedogenic?

REFERENCES

- Bachman, G. O., and M. N., Machette, 1977. *Calcic Soils and Calcretes in the Southwestern United States*. USGS, OFR 77-794. 163 pp.
- Ehlmann, A. J., L. B. Sand, and A. J. Regis, 1962. *Occurrences of Sepiolite in Utah and Nevada*. Economic Geology. v. 57, pp. 1085-1094.
- Hay, R. L., R. E. Pexton, T. T. Teague, and T. K. Kyser, 1986. *Spring-Related Carbonate Rocks, Mg Clays, and Associated Minerals in Pliocene Deposits of the Amargosa Desert, Nevada and California*. Geological Society of America, Bulletin. v. 97, pp. 1488-1503.
- Hay, R. L., and B. Wiggins, 1980. *Pellets, Ooids, Sepiolite and Silica in Three Calcretes of the Southwestern United States*. Sedimentology. V. 27, pp. 559-576.
- Jones, B. F., 1983. *Occurrence of Clay Minerals in Surficial Deposits of Southwest Nevada*. in Nahon, D. (ed.), Colloque Nationale Research Sciences. Colloquim on Petrology of Weathering and Soils. Paris. 13 pp.
- Khoury, H. N., D. D. Eberl, and B. F. Jones, 1982. *Origin of Magnesium Clays from the Amargosa Desert, Nevada*. Clays and Clay Minerals. v. 30, No. 5, pp. 327-336.
- Levy, S. S., and C. W. Naeser, 1991. *Bedrock breccias along fault zones near Yucca Mountain, Nevada*. Draft report submitted for publication by the USGS. Los Alamos National Laboratory. Los Alamos, New Mexico.
- Papke, K. G., 1972. *A Sepiolite-Rich Playa Deposit in Southern Nevada*. Clays and Clay Minerals. v. 20, pp. 211-215.
- Post, J. L., 1978. *Sepiolite Deposits of the Las Vegas, Nevada Area*. Clays and Clay Minerals. v. 26, No. 1, pp. 58-64.
- Quade, J., and T. E. Cerling, 1990. *Stable Isotopic Evidence for a Pedogenic origin of Carbonates in Trench 14 Near Yucca Mountain, Nevada*. Science. v. 250, pp. 1549-1552.
- Regis, A. J., 1978. *Mineralogy, Physical and Exchangeable Chemistry Properties of Bentonites from the Western United States, Exclusive of Montana and Wyoming*. U. S. Bureau of Land Management, Technical Note. v. 315, 35 pp.

Szymanski, J. S., C. M. Schluter, D. E. Livingston, M. R. Somerville, and J. B. Davies, 1993. *Investigations of Natural Groundwater Hazards at the Proposed Yucca Mountain High Level Nuclear Waste Repository*. 1992 Annual Report. Submitted to the State of Nevada Agency For Nuclear Projects, Nuclear Waste Project Office. Technical and Resource Assessment Corporation. Boulder, Colorado.

Vaniman, D. T., D. L. Bish, and S. Chipera, 1988. *A Preliminary Comparison of Mineral Deposits in Faults Near Yucca Mountain, Nevada, With Possible Analogs*. Los Alamos National Laboratory Report [LA-11289-MS]. 54 pp.

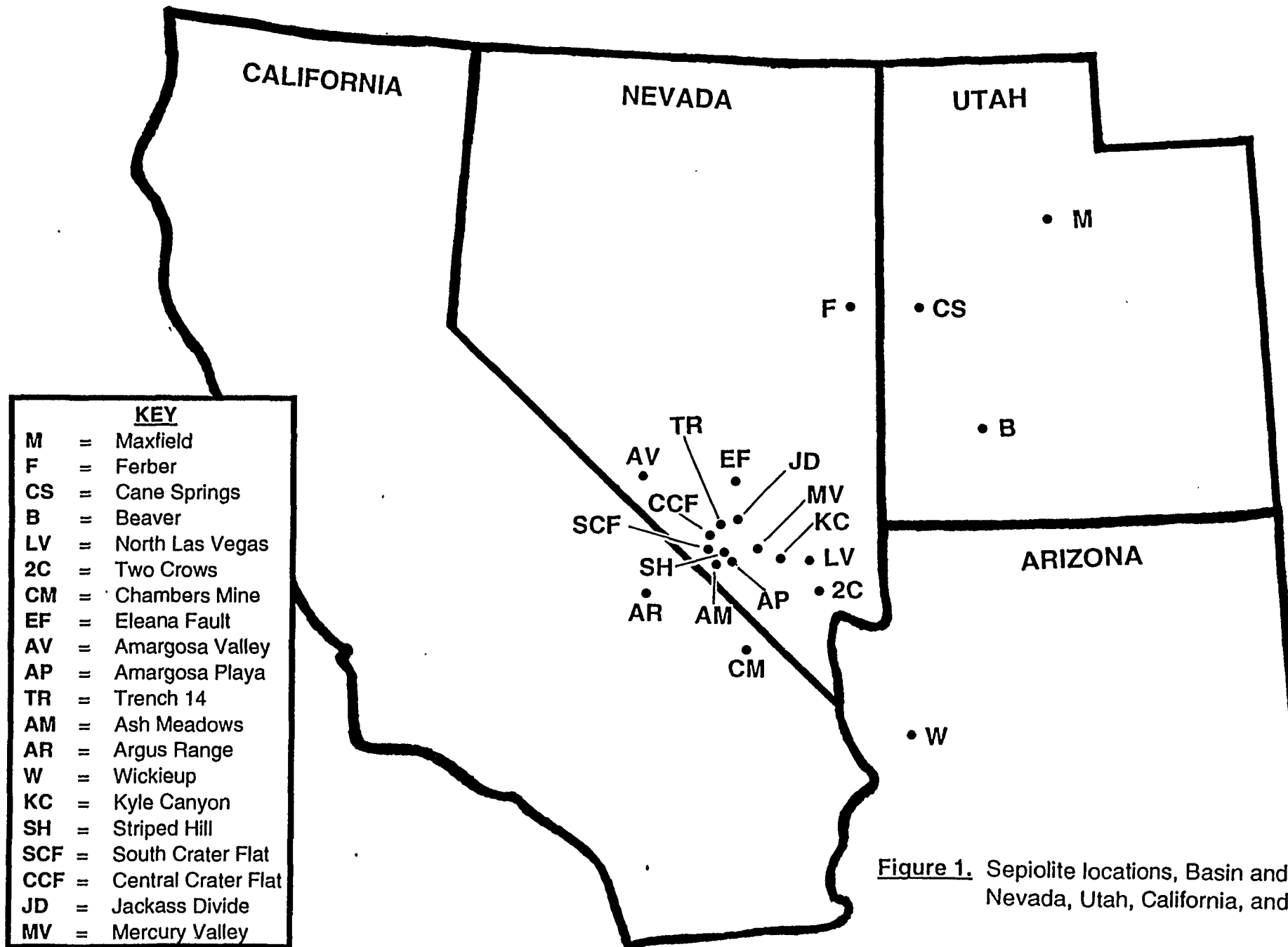


Figure 1. Sepiolite locations, Basin and Range; Nevada, Utah, California, and Arizona.

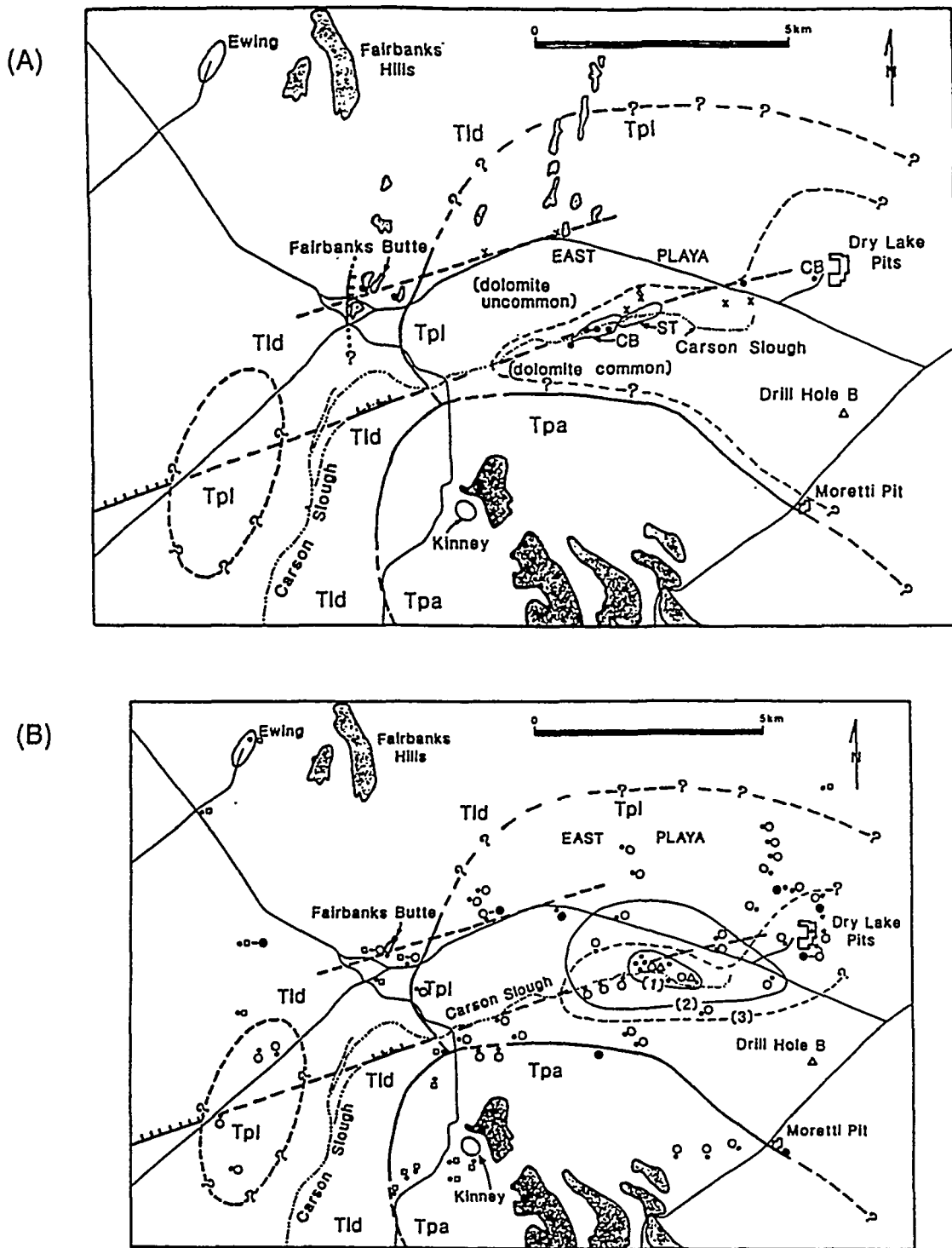


Figure 2. (A) Map of east-central Amargosa Desert showing the position of caliche breccias (CB), seepage mounds (x), and silicification (solid circles) and their relationship to east-northeast, west-southwest fault zones of inferred groundwater seepage (dashed lines). (B) Same map showing clay mineral localities. Sepiolite occurrences are indicated by the solid circles and are located along or near fault zones of inferred groundwater seepage. From Hay et al. (1986).

PART 6

**Petrographic Description of Calcite/Opal Samples
Collected on Field Trip of December 5-9, 1992**

TRAC *Technology and Resource Assessment Corporation*

3800 Arapahoe Avenue, Suite 225
Boulder, Colorado 80303
(303) 443-3700 FAX No. (303) 443-8626

**PETROGRAPHIC DESCRIPTION OF CALCITE/OPAL SAMPLES
COLLECTED ON FIELD TRIP OF DECEMBER 5-9, 1992**

SPECIAL REPORT No. 7
CONTRACT No. 92/94.0004

SPECIAL REPORT Submitted to the
Nuclear Waste Project Office
State of Nevada

June, 1993

Authored by:

**Carol A. Hill
Christine M. Schluter**

**PETROGRAPHIC DESCRIPTION OF CALCITE/OPAL SAMPLES
COLLECTED ON FIELD TRIP OF DECEMBER 5-9, 1992**

TABLE OF CONTENTS

INTRODUCTION	1
GENERAL OBSERVATIONS	1
PETROGRAPHIC TEXTURES	2
FIELD RELATIONSHIPS OF CALCITE/OPAL	9
IMPORTANT QUESTIONS RAISED BY THE TEXTURAL TYPES	11
REFERENCES	15
APPENDIX 1	16
FIGURES	20

INTRODUCTION

A field trip was made to the Yucca Mountain area on December 5-9, 1992 by Don Livingston, Jerry Frazier, Russell Harmon, Christine Schluter, and Carol Hill to collect rock samples for analyses and measurement of isotopic properties. This study is part of the research program of the Yucca Mountain Project intended to provide the State of Nevada with a detailed analysis and assessment of the water-deposited minerals of Yucca Mountain and adjacent regions. Forty-three separate stops were made and 203 samples were collected during the five days of the field trip. This report describes petrographic observations made on the calcite/opal samples.

GENERAL OBSERVATIONS

Collection sites for the 203 samples are shown in Figure 1. For a listing of the location, brief description, and sample number of each sample refer to Appendix 1. Of the 203 samples collected, about 25 samples were bedrock and miscellaneous material (sand, etc.): all the rest were calcite/opal travertine ("calcrete" or "caliche").

In the past, petrographic observations on Yucca Mountain calcite/opal material have been limited. Vaniman et al. (1988) previously described calcite/opal from two faults (Trenches 14 and 17). Levy and Naeser (1991) discussed texture, mineralogy, field relationships of crushed-tuff-matrix (CTM) breccias and authigenic-mineral-cemented (AMC) breccias and cements. This is the first petrographic study which includes a large number of calcite/opal samples collected from many sites in and around Yucca Mountain. Observations on these samples were made with hand lens and petrographic microscope; fluorescence observations were made using a UVS-12 and UVG-54 (115 volts) Mineralights.

The most striking aspect about the calcite/opal deposits of Yucca Mountain and vicinity is their simplicity of mineralogy but diversity in texture. Calcite, opal, and gypsum were the only minerals found in the many travertine samples collected. Sepiolite was looked for, but not found, in the samples. This does not mean that the mineral was not there, only that it may not have been obvious by optical means. Vaniman et al. (1988) and Levy and Naeser (1991) both reported sepiolite (from Trench 14 and/or Busted Butte); however, the sepiolite fraction in these deposits was small and the mineral was identified by X-ray diffraction techniques.

PETROGRAPHIC TEXTURES

Texture is the size, shape, and arrangement (packing and fabric) of the component elements of a rock or mineral material. The crystal size of the calcite/opal travertine collected from the Yucca Mountain area is consistently very fine-grained (in the millimicron or less size range). The only exception to this are millimeter-sized calcite crystals filling vugs or veins within the finer-grained calcite/opal groundmass.

While the crystal size and mineralogy of the samples are simple and consistent, textures are diverse. The following describes a number of different textures observed in the calcite/opal samples collected at or near Yucca Mountain. Sample numbers in bold represent textures shown in the photographs (figures).

(1) **Pure texture.** This type of texture refers to either pure opal or pure calcite, with little or no mixing of the two minerals. Pure opal (hyalite) usually occurs in narrow (<1 cm) bands, but it can also occur as pods or isolated seams in a matrix of

dense, buff-colored, mixed calcite/opal (Figures 2a, b, c; 3a). The pearly to vitreous, pure opal fluoresces a brilliant green under ultraviolet light (Figures 2B, a, b, c, 3B, a), but wherever the opal is mixed with calcite it never fluoresces (Figures 2B, d, e, h, 3B). Pure calcite consists of crystals (sometimes a few millimeters in size) which occurs within vugs and veins. These fluoresce green and were also observed to phosphoresce (for a few seconds).

Vaniman et al. (1988, p. 15) described "almost-pure" transparent opal which may be equivalent to our "pure texture" opal. These authors identified this transparent opal as "opal-A" and it is possible that much (or all?) of our pure-textured, fluorescent opal is of the opal-A type.

Samples: fluorescent opal: WT-7 (3), 5b, 5c, 5d, 7c, 10c, 19a, 28e, **36b, 36j, 36z**, 37-1a, 37-2, 39b, 39n.

Samples: fluorescent calcite: 1b, 1c, 1f.

(2) **Mixed texture.** Mixed texture is one that consists of a mixture of calcite and opal. This mixture varies in density and color depending on the relative amounts of calcite and opal. The denser, darker-tan samples contain more opal and the less-dense, light-colored samples contain more calcite (the relative amounts of these two minerals within a sample was estimated by the amount of fizzing in acid). Most samples of calcite/opal are fairly-dense and buff-colored (Figures 2A, d; 3, 4, 5, 6, etc.). Samples which display a mixed texture never fluoresce as do the pure-textured opal and calcite. Most of the calcite/opal samples collected in the Yucca Mountain region fall into this mixed category.

Vaniman et al. (1988, p.46) also noted that most calcite/silica bands are composed of an intergrowth of calcite and opal. These authors reported (p. 20) that the dense,

buff-colored, silica component of the mixture was “opal-CT” and it is possible that much (or all?) of our opal intermixed with calcite is of the opal-CT type.

Samples: many including 5e, 7 a, 17a, 36 b, 36 j.

(3) **Banded/laminated texture.** Banded/laminated texture describes layered sequences of calcite/opal, calcite/opal. Layers within these sequences contain various amounts of mixed-textured calcite and opal, the darker layers containing more opal and the lighter ones containing more calcite (Figures 5 and 6). Layering can vary in thickness from millimeters (laminations; Figure 6A) to centimeters (bands; Figure 6B), and it can vary in orientation from the horizontal (Figure 5A) to the vertical (Figure 5B). Layers can be concisely banded or laminated, or they can be roughly banded or laminated. The layers can be aligned perfectly parallel to one another, or they can be aligned roughly parallel to one another. A majority of the calcite/opal deposits in and around Yucca Mountain display banded/laminated texture.

Vaniman et al. (1988) described banded samples collected from Trench 14. Their sample T14F was comprised of two bands representing two episodes of deposition: (1) an earlier, mixed calcite and opal-CT band, and (2) a later, pure opal-A band. In addition, their sample T14-10 displayed vertically-oriented, laminated texture.

Samples: vertical bands/laminations: Trench 14 and Busted Butte “feeder” veins, **28 d**

Samples: horizontal bands/laminations: Trench 14 and Busted Butte “sheet” deposits, **5 a, 5 d, 8a, 10a, 10f, 19 a, 39d.**

(4) **Massive texture.** Massive texture describes unlayered or very-roughly layered calcite/opal or calcite/gypsum deposits. Massive texture consists of material which is powdery to porous and light-weight and which resembles tufa travertine (Figures 2A, e; 7). Usually massive-textured deposits are composed mostly of calcite, with smaller amounts of opal, but at the Wahmonie travertine/gypsite mound, the massive-textured deposits are composed mostly (70-80%) of calcite with smaller amounts (20-30%) of gypsum (Hill, 1993). Massive texture is typical of “mound” deposits such as are deposited at springs.

Samples: Stagecoach Trenches A and B, Site 199, South Trench 14, 2d, 16c, 17b, 22a, 22e, 32a, 36b.

(5) **Powdery texture.** Powdery texture refers to unlayered calcite/opal which is very powdery, even more so than massive-textured samples. Often powdery texture is found with, or grades into, massive texture, but in many other occurrences powdery texture can overlie (Figure 14B, b), be banded in-between (Figure 8), or be invasive of (Figure 16B, a) denser, buff-colored, calcite/opal layers. Usually the powder is composed primarily of calcite, but it can also be composed of some opal or even mostly opal.

Samples: 4d, 5b, 5d, 7a, 7d, 8a, 10e, 19b, 36b, 36f, 36g, 36h, 36j, 40c.

(6) **Patchy texture.** Patchy texture is where pieces of lighter (or darker) calcite/opal material occur within a groundmass of darker (or lighter), calcite/opal. The clasts may be rounded or angular (breccia-like), and these included pieces give the samples a patchy or mottled appearance (Figures 9; 15b).

Vaniman et al. (1988, p. 14) may have been referring to “patchy texture” when they

described patchy, mineral-clast rich, fragmental and ooidal layers (their sample T14B). This texture indicated to these authors that an earlier episode of calcite/opal deposition had occurred followed by brecciation and then recementation by calcite/opal during a later episode.

Samples: 4 d, 4 e, 5b, 8a.

(7) **Brecciated texture.** Brecciated texture is where foreign pieces of material are surrounded by a calcite/opal matrix. This type of texture differs from patchy texture in that the clasts are not composed of calcite/opal, but instead are composed of fractured and filled bedrock (e.g., Figure 10B), or fragments of bedrock (e.g., talus clasts from the Tiva Canyon; Figure 4). Subtypes of brecciated texture are (a) *floating-brecciated texture*, where the foreign pieces are isolated from one another and look like they are “floating” in a groundmass of calcite/opal (Figures 4a, b; 10A), and (b) *mosaic-brecciated texture*, where the clasts resemble pieces of a puzzle which can be “fitted” back together” into their original position (Figures 10B; 11).

Samples of mosaic-brecciated texture: Wailing Wall, WT-7, Trench 14, 5 g, 36z, WT-7 (3).

Samples of floating-brecciated texture: 5 g, 7 a, 10b, 14g, 22a, 22e.

(8) **Flow texture.** Flow texture is where darker and lighter bands of calcite/opal exhibit a marbly or wavy pattern (Figures 6; 12). These undulatory bands give the appearance that the calcite/opal groundmass was once in a plastic or fluid state. Often holes or vugs (sometimes filled with calcite crystals) are aligned along the flow bands (Figures 13A, c, d).

Samples: WT-7, 5d, 10 a, 36 z.

(9) **Vesicular/phenocrystic texture.** Vesicular/phenocrystic texture is where the calcite/opal matrix material is full of holes. Sometimes the holes are empty (vesicular texture); less often they are filled with calcite and/or opal (phenocrystic texture). The holes may be randomly spaced within the calcite/opal matrix or they may be aligned in rows along roughly-banded sequences or flow texture (Figures 2A, f, g, h, i; 14A, a, b, c, d). The holes themselves can be ellipsoidal, the ellipsoids being elongated in the direction of the flow bands or layering. Rarely, the holes are aligned in swirl-shaped rows. Holes usually occur in a dense, mixed-texture, calcite/opal groundmass (Figures 2A, f, g; 14B, a), but they can also occur in a powdery- or massive-textured groundmass (Figures 2A, h; 14B, b).

Levy and Naeser (1991, p. 12) reported vesicular texture in the fine-grained, carbonate cements of AMC (authigenic-mineral-cemented) breccias. Some of these vesicles contained residual void space but most were completely filled with silica. Other vesicle-filling material included sparry and acicular calcite and a possible mixture of sepiolite and minor silica (Levy and Naeser, 1991, p. 14).

Samples: WT-7 (3), 5a, 5h, 10a, 10e, 19e, 36b, 36h, 36p.

(10) **Veined texture** Veined texture is where calcite/opal veins crosscut the calcite/opal matrix (Figure 15). This type of texture was not commonly observed in our samples, but Levy and Naeser (1991, p. 14) reported abundant fracture fillings composed mainly of silica in their samples from Trench 14.

Sample: 4e.

(11) **Invasive texture.** Invasive texture is where a “blob” or “finger” of calcite/opal material penetrates the main mass of calcite/opal (Figure 16). The

invasive material can be distinguished from the matrix by its lighter (or darker) color and its more calcitic (or opalitic) composition.

Samples: 7c, 7d, 10e, 19b, 36b.

(12) **Botryoidal texture.** This type of texture is where the mineral deposits assume a botryoidal appearance. Botryoidal opal is quite common in the Yucca Mountain area (e.g. Harper Valley; Figure 17A), occurring as fracture fillings within the Tiva Canyon or other stratigraphic units. This textural type also occurs as surface coatings on calcite or gypsum. Botryoidal gypsum occurs at the Wahmonie mound as crusts overlying the main mass of travertine/gypsite (Figure 17C). These crusts represent diffusion of the more soluble gypsum component of the mass toward the outside of the mound due to an evaporation gradient at the air/mound-surface interface (i.e., these form similar to “popcorn” botryoids in caves; Hill, 1993, p. 13). Calcite “popcorn” crusts were also observed at Trench 14 in small cavities within the calcite/opal vein mass (Hill, 1993, p. 13).

Levy and Naeser (1991, p. 8) reported botryoidal silica fillings within large fractures at Busted Butte, Yucca Mountain.

Samples: 4d, 5f, 32a, 32e, 39b, 39f, 39n.

(13) **Algal/ooidal texture.** Algal (or ooidal) texture is where algae- or pea-shaped bodies comprise the main mass of calcite/opal (Figure 18). This type of texture may actually be produced by algae or other types of biota. At Cane Springs, a presently-active spring located about 25 km east of Yucca Mountain, small calcite mounds are associated with live algae.

Vaniman et al. (1988, p. 14) reported "ooidal" layers in calcite/opal bands at Trench 14 (their sample T14-FB). This may (or may not) be equivalent to what we are calling algal/ooidal texture.

Samples: 16c, 17b, 19a, 19d, 36a, 36i.

(14) **Root-cast texture.** Root-cast texture is where plant roots have grown into the calcite/opal deposits and where they have become incorporated into the travertine mass. Root-cast texture is particularly well displayed in the sheet travertines of Busted Butte (Figure 19), but it also occurs within many other travertine deposits at Yucca Mountain (Figure 20).

Vaniman et al. (1988, p. 46) reported root-cast texture at Trench 14 and thought that organic materials such as root casts were perhaps responsible for the deposition of opal-A.

Samples: 22a, 23a, 28c, 29f, 30b, 30h.

(15) **Speleothemic texture.** Speleothemic texture is where dripstone- or rimstone-like forms are produced where calcite from the main mass of travertine has been dissolved and reprecipitated on the undersides of the travertine or on below-lying bedrock (Figure 21).

Samples: 4f, 17b.

FIELD RELATIONSHIPS OF CALCITE/OPAL

The calcite/opal deposits at or near Yucca Mountain were observed to have the following field relationships:

(1) There appears to be no correlation between location and textural type of a calcite/opal deposit. Different textural types are found throughout the region - even in the Bare Mountain mining district to the west of Yucca Mountain. For example, powdery, laminar, vesicular/phenocrystic, and floating-brecciated textures were all observed in calcite/opal travertine associated with ore mineralization at Bare Mountain (Figures 8 and 13A).

(2) Various textures of calcite/opal do not appear to be correlative with a specific host-rock type (e.g., rhyolite, limestone, dolomite).

(3) Different textural types exist in close proximity to one another. For example, at Plug Hill, powdery, laminated, and mottled texture was seen in the same sample (within a centimeter or so of each other).

(4) Where calcite/opal directly overlies host bedrock, the first layer in a banded/laminated sequence may be opal, it may be calcite, or it may be of mixed texture (i.e., one mineral does not seem to consistently appear first in a precipitative sequence). This observation is in contrast to that of Levy and Naeser (1991, p. 11) who reported that "most tuffaceous clasts (in AMC breccias) have complex, crudely-interlayered coatings of silica and calcite, with silica as the innermost layer."

(5) The calcite/opal can occur as sheet travertine, vein- or fault-filling travertine, coatings over colluvium or alluvium, or cementing material.

(6) The calcite/opal travertine cemented whatever lay in its way as it was deposited: talus/colluvium, alluvium (sand to cobble sizes), breccia fragments, or bedrock (Hill, 1993). For example, at Busted Butte, sheet travertine has cemented sand, breccia fragments of rhyolite and opal, and the soft tuff of the Bedded

member. At WT-7, Wailing Wall, and Plug Hill, the calcite/opal travertine has cemented talus/colluvium, and at Livingston Scarp, it has cemented alluvium (cobbles).

(7) How “sandy” the calcite/opal travertine is (e.g., at Busted Butte) seems to have been dependent on whether the travertine was in direct contact with a sandy stratum; that is, wherever solutions flowed over sand, some sand was incorporated into the precipitated travertine.

IMPORTANT QUESTIONS RAISED BY THE TEXTURAL TYPES

The calcite/opal deposits at Yucca Mountain have been interpreted by many investigators to be of supergene-pedogenic origin (e.g., Quade and Cerling, 1990). However, the textures described in this report raise some important questions as to the validity of this model:

(1) The diversity and heterogeneity of textures displayed by the calcite-opal deposits, even within centimeters of each other, favor a dynamic fluid system rather than a pedogenic system. For example, pure-textured opal seams can occur interbanded with mixed-textured, vesicular-textured, calcite/opal layers (Figure 2). These opal bands do not seem to have come in a later or earlier episode than the calcite/opal; yet, the opal is pure (not mixed with calcite) and is uraniferous (fluorescent).

Such a situation might be explained if a highly-dynamic fluid system is invoked where variations in the chemistry of precipitating solutions are reflected in mineral-content gradations ranging from essentially pure calcite to pure opal. A plausible

precipitation scenario for the above might be: (a) degassing of carbon dioxide from solution caused the vesicular texture of a precipitating calcite/opal mass (Figure 2f, g), (b) solutions out of which the mixed calcite/opal deposited were then enriched in calcite leading to massive-textured calcite/opal (Figure 2h), and (c) pure silica was left in solution, leading to the pure-opal seams high in uranium (Figure 2a, b).

While the above specific scenario is speculative, it is at least tenable that a dynamic fluid system could have produced the above combination of textures and other textures described in this report. It can also explain the closeness (a few centimeters) of different textural types. In contrast, it is extremely difficult to imagine how pedogenic processes could have produced the diversity of textures seen in the calcite/opal deposits at Yucca Mountain.

(2) The very-fine grain size of the calcite/opal travertine is in direct contrast to pedogenic carbonates which are “nearly always aggregates of silt-sized calcite crystals” (Dixon and Weed, 1989, p. 281). Why is the calcite/opal travertine at Yucca Mountain so fine-grained if it is pedogenic? Such a small grain size is more indicative of material precipitated as a result of fast cooling and/or degassing of solutions.

(3) How can one get pure, fluorescent (uraniferous) opal from pedogenic processes? How could a pedogenic process have concentrated the uranium and constrained the purity of the opal to separate bands or seams? Hydrothermal solutions, however, such as those which were responsible for altering volcanic rock (Livingston, 1993), could have precipitated pure opal veins and layers.

(4) How could flow texture be produced by any mechanism other than fluid injection? Pedogenic processes might be expected to produce massive, laminated, or algal/ooidal textures, but not flow texture. Elevated fluid pressures are indicated by dilated and brecciated flow textures.

(5) How could vesicular/phenocrystic texture be produced by pedogenic processes? The holes look like they are gas cavities created by the degassing of fluids out of which the calcite/opal precipitated. Vesicular swirl textures are especially indicative of flow and degassing.

(6) How could the puzzle-brecciated texture be produced by any process other than fluid injection (e.g., sample 36z)? Not only have the breccia fragments been forced apart in this sample, they have also been moved sideways from their original position (i.e., sample 36z shows flow texture in addition to mosaic-brecciated texture; Figures 12; 13).

(7) How could the floating-brecciated texture be produced by a pedogenic process? Floating textures indicate that the calcite/opal was precipitated from solution at a faster rate than erosional detritus was being introduced by seasonal storms.

(8) Likewise, invasive and patchy textures show penetration of later fluids of slightly different composition after sections of the main calcite/opal matrix had partially "hardened" or become brecciated. It seems like this penetration could occur by fluid injection of heterogeneous fluids, but not by a pedogenic build-up of material.

(9) Calcite/opal samples from the Bare Mountain mining district display the same textural types as those at Yucca Mountain, even though the Bare Mountain samples are more enriched in metal than samples from Yucca Mountain (e.g., metal content of the Bare Mountain calcite/opal was measured at: As = 96 ppm, Cd = >100 ppm, W = 130 ppm, Zn = >10,000 ppm). It may be that metals were more accessible at depth in the vicinity of Bare Mountain, but that the process of deposition of the calcite/opal (i.e., from hypogene solutions) was the same over the region.

(10) All of the textural types which make a pedogenic origin questionable were found at Trench 14.

REFERENCES

- Dixon, J. B., and S. B. Weed, 1989. *Minerals in Soil Environments*. Soil Science of America. Madison, Wisconsin. 1244 pp.
- Hill, C. A., 1993. *Field Trip Report: Observations at Yucca Mountain, Nye County, Nevada*. Special Report No. 2. Submitted to the State of Nevada Agency For Nuclear Projects, Nuclear Waste Project Office. Technology and Resource Assessment Corporation. Boulder, CO.
- Levy, S. S., and C. W. Naeser, 1991. *Bedrock Breccias Along Fault Zones Near Yucca Mountain, Nevada*. Draft Report submitted for publication by the USGS. Los Alamos National Laboratory. Los Alamos, New Mexico.
- Livingston, D. E., 1993. *A Review of the Major Element Geochemistry of Yucca Mountain, Nye County, Nevada*. Quarterly Report No. 4. Submitted to the State of Nevada Agency For Nuclear Projects, Nuclear Waste Project Office. Technology and Resource Assessment Corporation. Boulder, CO.
- Quade, J., and T. E. Cerling, 1990. *Stable Isotopic Evidence for a Pedogenic Origin of Carbonates in Trench 14 Near Yucca Mountain, Nevada*. Science. v. 250, pp. 1549-1552.
- Vaniman, D. T., D. L. Bish, and S. Chipera, 1988. *A Preliminary Comparison of Mineral Deposits in Faults Near Yucca Mountain, Nevada, With Possible Analogs*. Los Alamos National Laboratory. Los Alamos, New Mexico. Report LA-11289-MS. 54 pp.

APPENDIX 1

**Detailed List of Samples Collected
at Each Stop**

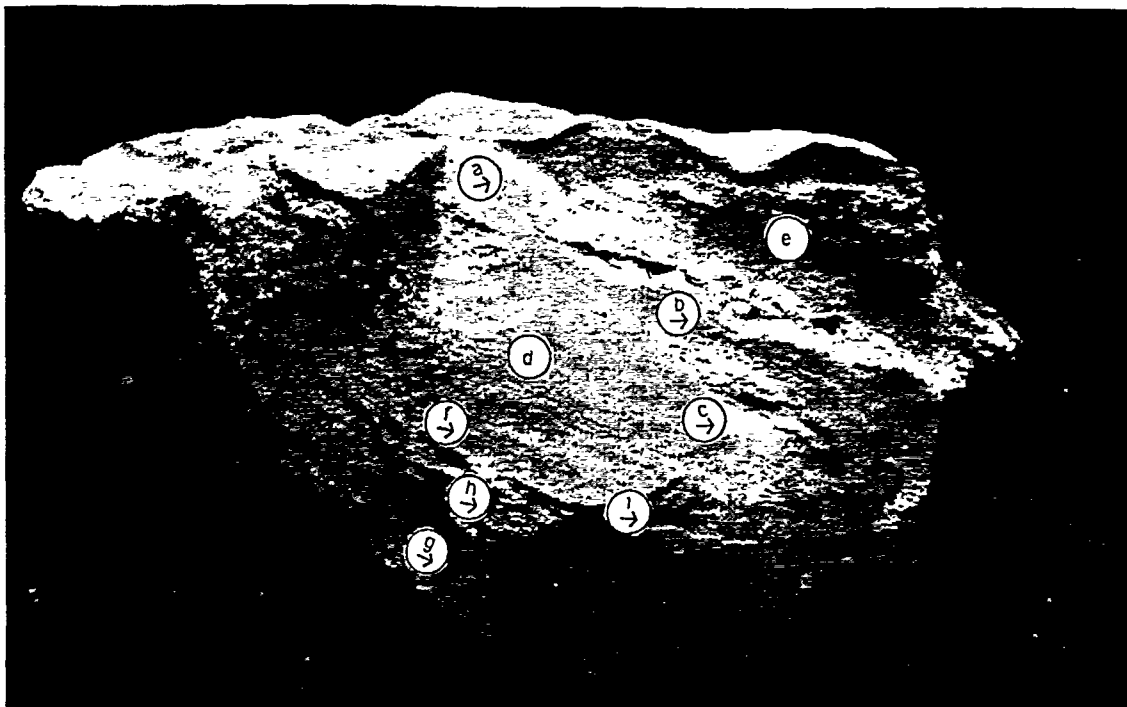
STOP #	SAMPLE	TYPE	STOP #	SAMPLE	TYPE
STOP #1	US 95 mile 10		STOP #10	Bare Mountain	
1a	dolomite	Nopah Fromation	10a	calcite-opal	loose material
1b	silica	breccia zone	10b	lmst/opal	brecciated, cemented
1c	calcite		10c	calcite-lmst	
1d	dolomite	organic lithofacies	10d	limestone	Ely Springs
1e	silica	vein	10e	opal	siliceous
1f	calcite	vein	10f	carbonate	in stream bed
1g	calcite				
			STOP #11	Diamond Queen M.	
STOP #2	US 95 mile 12.47		11a	white mineral	filling, metamorphosed
2a	quartzite (clean)	Stirling Quartzite	11b	calcite	float sample
2b	quartzite (dirty)	Stirling Quartzite	11c	phyllite	Johnnie Formation
2c	epidote	vein	11d	carbonate	incrustations
2d	calcite	vein	11e	Nopah formation	
			11f	Iceland spar	massive
STOP #3	US 95 mile 18.8		11g	calcite	vein
3a	dolomite/lmst		11h	quartz	
			11j	fluorite	
STOP #4	Pull Apart Fault		11k	fluorite	
4a	limestone	fault related alteration	11m a	calcite	coating
4b	calcite	coating	11m b		
4c	calcite-opal-breccia		11n	calcite	crust
4d	calcite-opal	bulk samples	11o	kaolinite clay	from breccia pipe
4e	opal breccia		11p	chert nodule	in fluorite breccia
4f	calcite	riverbed	11q	porphyry	volcanic breccia
4g	carb.-coated rock		11r	fluorite breccia	
			11s	chert nodule	
STOP #5	WT - 7				
5a	calcrete-coated rock		STOP #12	Chuckwalla Canyon	
5b	calcite-opal	surficial deposit	12a	Iceland spar	massive
5c	opaline layer	on breccia	12b	opal-calcite	inter-layers
5d	calcite-silica		12c	carbonate	white & black minerals
5e	calcite	fracture fill	12d	dolomite	Lone Mt.
5f	breccia		12e	calcite	
5g	breccia		12f	calcite	fracture filling
5h	calcium crystals	Carol's sample	12g	calcite	columnar crystals
STOP #6	USW H - 6		STOP #13	Tarantula Canyon	
6a	carbonate crust	surficial coating	13a	limestone	Meiklejohn
			13b	rhyolite	
STOP #7	roadside (WT-7)				
7a	calcite	caliche?/calcrete	STOP #14	Trench 8	
7b	silica-calcite		14a	calcite	root casts
7c	opal		14b	ash	
7d	indurated layer	coating on surface rock	14c	calcite-opal-silica	
			14d	calcite-opal	fault infilling
STOP #8	Plug Hill		14e	black glassy material	in altered vitrophyre
8a	carbonate	coating on colluvium	14f	carb., some silica	cement
			14g	silica-calcite	vein
STOP #9	roadside (WT-7)				
9a	calcite	coating			

STOP #	SAMPLE	TYPE	STOP #	SAMPLE	TYPE
STOP #15	roadsie (trench 8)		STOP #26	roadside (FOC)	
15a	carbonate	matrix	26a	lmst, dolomite	Bonanza King
STOP #16	New Trench		STOP #27	roadside (FOC)	
16a	carbonate	vein	27a	calcite	secondary
16b	ash		27b	carbonate? in basalt and	cement filling
16c	carbonate	matrix	27c	travertine	surficial cap
STOP #17	Site 106		STOP #28	East Busted Butte	
17a	tufa	spring	28a	silica	vein
17b	carbonate	spring	28b	sand	
			28c	carbonate?	root casts
STOP #18	Livingston Scarp		28d	carbonate?	vert. vein
18a	carbonate	fracture fillings	28e	opaline-coral	slope deposit
18b	opal-carbonate	vein	28f	travertine	upslope
STOP #19	Wailing Wall		STOP #29	East Busted Butte	
19a	opal-calcite	coating	29a	calcrete	
19b	carbonate	vein	29b	rat midden	
19c	carbonate	coating	29c	sheet deposit	
19d	algal?		29d	vitrophyre	
19e	opal-calcite	Carol's sample	29e	travertine, breccia	sheet deposit
			29f	carbonate?	root casts
STOP #20	roadside ("scarp")		STOP #30	West Busted Butte	
20a	glass	volcanic	30a	carbonate?	vert. vein
STOP #21	Red Cliff Gulch		30b	carbonate?	root casts
21a	carbonate	surface coatings	30c	opal-calcite	
			30d	carbonate?	vein
STOP #22	Stagecoach Trench	(North)	30e	carbonate?	vein
22a	carbonate	root casts	30f	calcite	vein
22b	tuff	calcite overlies	30g	carbonate?	punchbowl
22c	quartz?	calcite overlies	30h	carbonate?	root casts
22d		full of clasts			
22e	carbonate	surficial	STOP #31	roadside (Mercury)	
			31a	calcite	coating
STOP #23	Stagecoach Trench	(South)	STOP #32	Wahmonie Mounds	
23a	carbonate	root casts	32a	gypsum with calcite	
23b	glass	vitrophyre	32b	carbonate	
STOP #24	Site 199		32c	calcite-gypsum	
24a	silicified material	some clasts	32d	calcite	
24b	breccia (Carrera)	conglomerate	32e	gypsum	crust on carbonate
24c	breccia	Bonanza King			
24d	tufa	some brecciated carb.	STOP #33	Mines (Wahmonie)	
			33a	carbonate?	vein
OP #25	roadside (site 199)		33b	fluorite? in quartz	
25a	carbonate	root casts (burrows?)	33c	calcite crystal in quartz	
25b	seeds.	marsh/lake			

STOP #	SAMPLE	TYPE	STOP #	SAMPLE	TYPE
STOP #34	Calico Hills		STOP #37-2	Mercury	
34a	shale	Eleana	37-2a	dolomite	fault zone
34b	limestone	Eleana	37-2b	carbonate	vein
34c	pyrite	cubes			
34d	pumice and silicified	Calico Hills	STOP #38	West Busted Butte	
34e	kaolinitized clay		38a	sand	windblown
34f	ironized tuff	Calico Hills	38b	travertines	
34g	calcite	slslickenside	38c	opal-calcite	
34h	yellow hot rock		38d	pumice tuff	bedded tuff
			38e	tuff	red altered
STOP #35	Shoshone Mt. road		38f	travertine	
35a	kaolinite		38g	carbonate	caps tuff
35b	Topopah	red sample			
35c		cavity fillings	STOP #39	Harper Valley	
			39a	carbonate	in streambed
STOP #36	Trench 14		39b	silica	botryoidal (opalite)
36a	carbonate		39c	Tiva	partially welded
36b	opaline		39d	flowstone	laminated
36c	carbonate	finely laminated	39e	carbonate	vein filling
36d	carbonate	vein	39f	opal	botryoidal
36e	silica	vein	39g	calcite	vein
36f	carbonate	vein	39h	some opal	pinnacles
36g	carbonate	vein	39i	carb?-silica	"Z" veins
36h	silica	vein	39k	tuff	red altered
36i	carbonate	vein	39m	carbonate	vein
36j	opal	vein	39n	opal	Carol's sample
36k	opal-breccia-carbonate	finely laminated			
36m	calcite	vein	STOP #40	Trench 14	
36n	carbonate	vein	40a1	mostly carbonate	vein
36o	carbonate	vein	40a2	carbonate?	vein
36p1	calcite-opal	vein	40a3	carbonate?	vein
36p2	calcite-opal	vein	40b	calcite	vein
36r	carbonate	vein	40c	calcite	subsurface
36s	opal	vein			
36t	carbonate	vein	STOP #41	Lathrop Cone	
36v	carbonate	vein	41a	sulfur or jarosite	
36w	opal	vein	41b	carbonate	coatings
36x		Calico Hills?	41c	sulfur?	
36y	breccia-calcite				
36z	breccia		STOP #42	Lathrop Cone	
			42a	sand	
STOP #37-1	UE 25 p#1				
37-1a	opal	opaline			
37-1b	opal	Carol's sample			

FIGURES

A)



B)

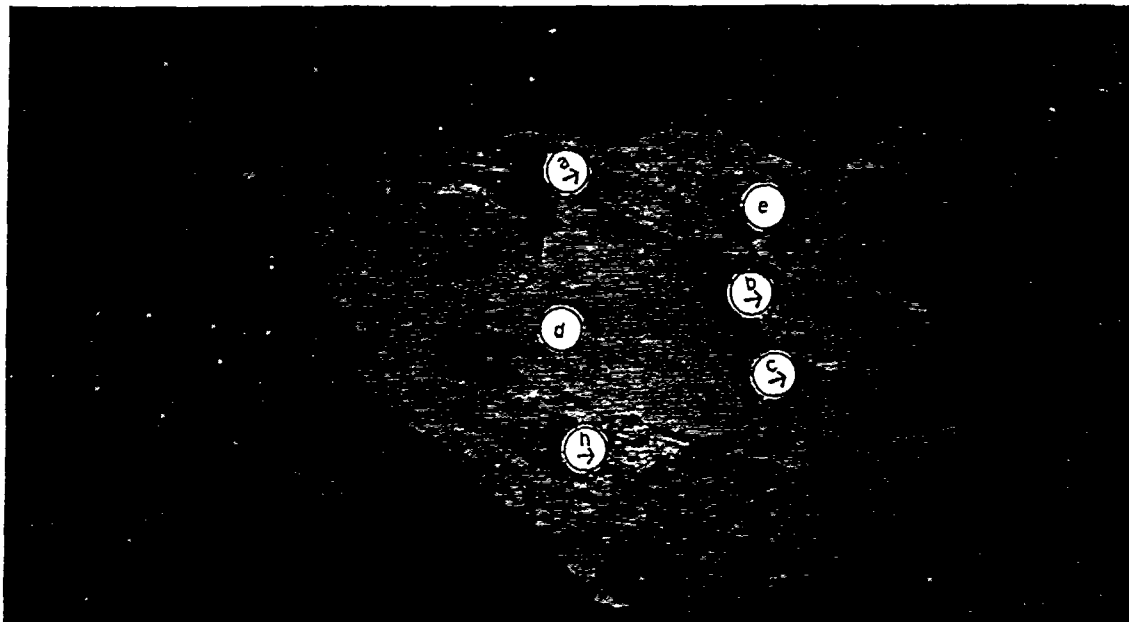
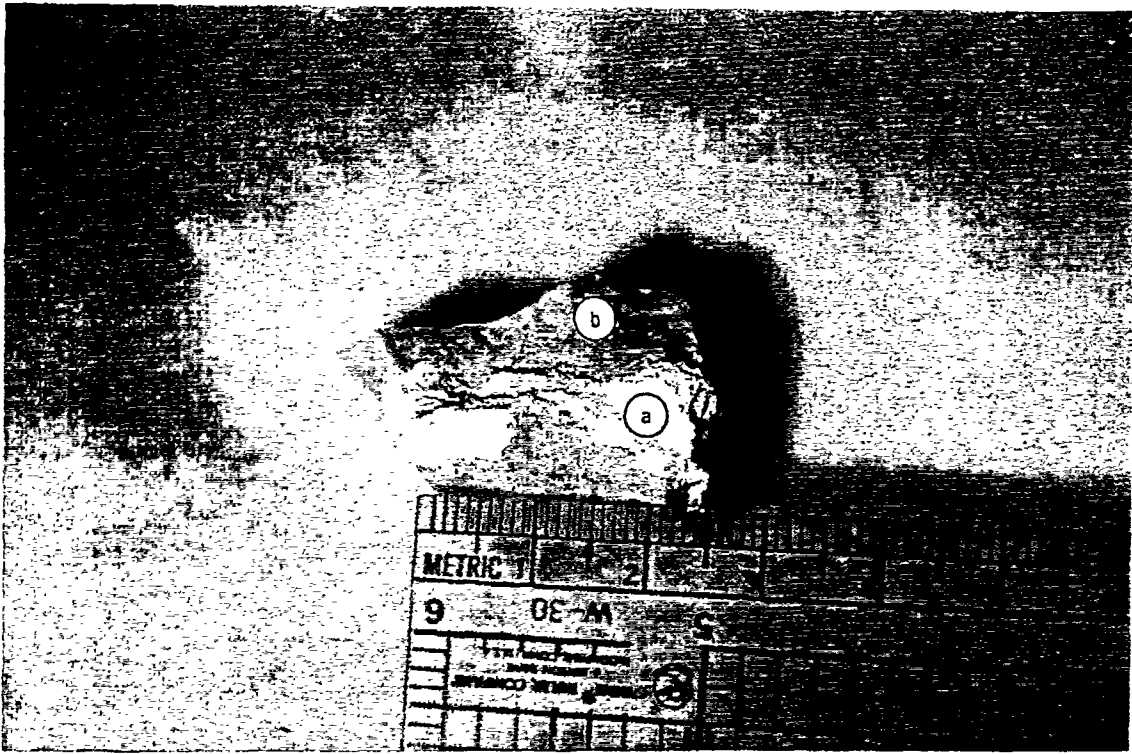


Figure 2. (A) Pods and seams of pure-texture, pearly opal (a, b, c) in a matrix of dense, buff-colored, mixed-textured calcite/opal (d). Lighter-colored sections are very soft and porous (easily scratched), massive-textured calcite/opal (e). Note the holes (vesicular/phenocrystic texture) throughout the mass, especially in the dense, buff-colored calcite/opal (f, g), but also in the massive-textured calcite/opal (h). Also note how the vesicles seem to line up in bands (i and elsewhere). (B) Using a UVG-54 Mineralight, this photo (same position as A) illustrates bands of pure opal fluorescing a brilliant green (a, b, c) in the mixed-textured calcite/opal which does not fluoresce (d, e, h). Photos by Christine Schluter; Sample 36b, Trench 14).

A)



B)

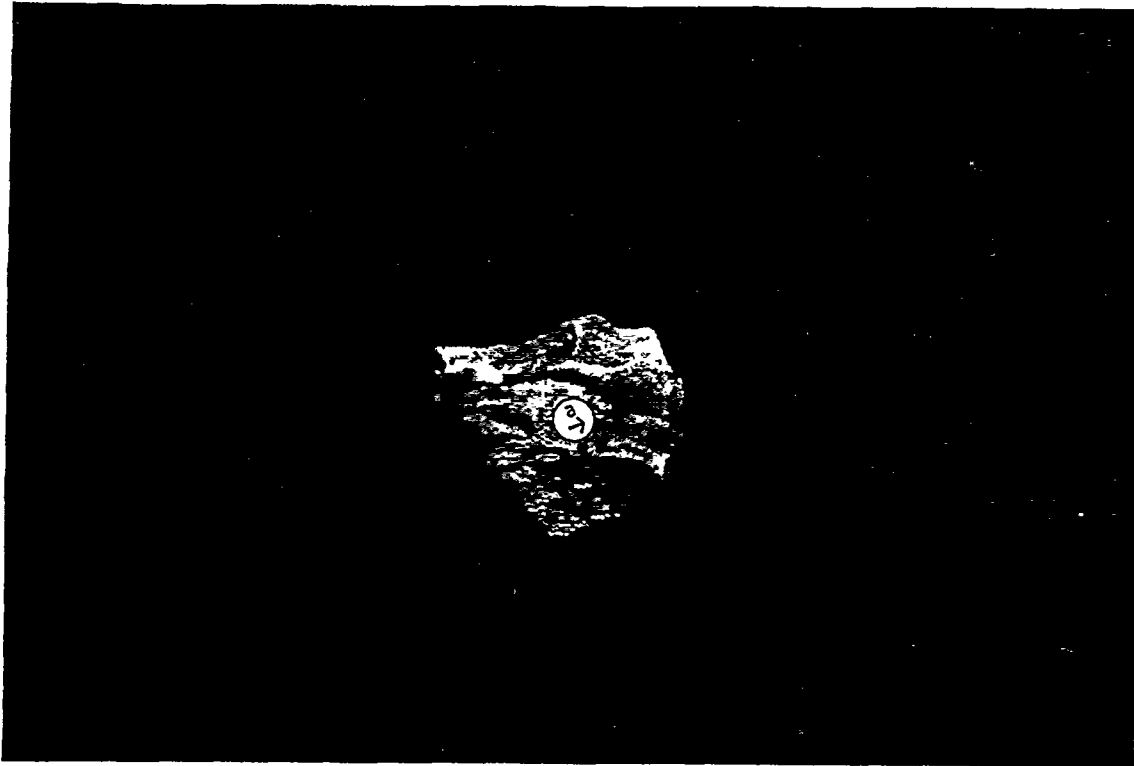


Figure 3. (A) Close-up of pearly, pure-textured opal (a) in a dense, buff-colored, mixed-texture matrix (b). (B) The same sample using a UVG-54 Mineralight, which illuminates the bands of pure opal (a). Photos: Christine Schluter; Sample 36j, Trench 14.

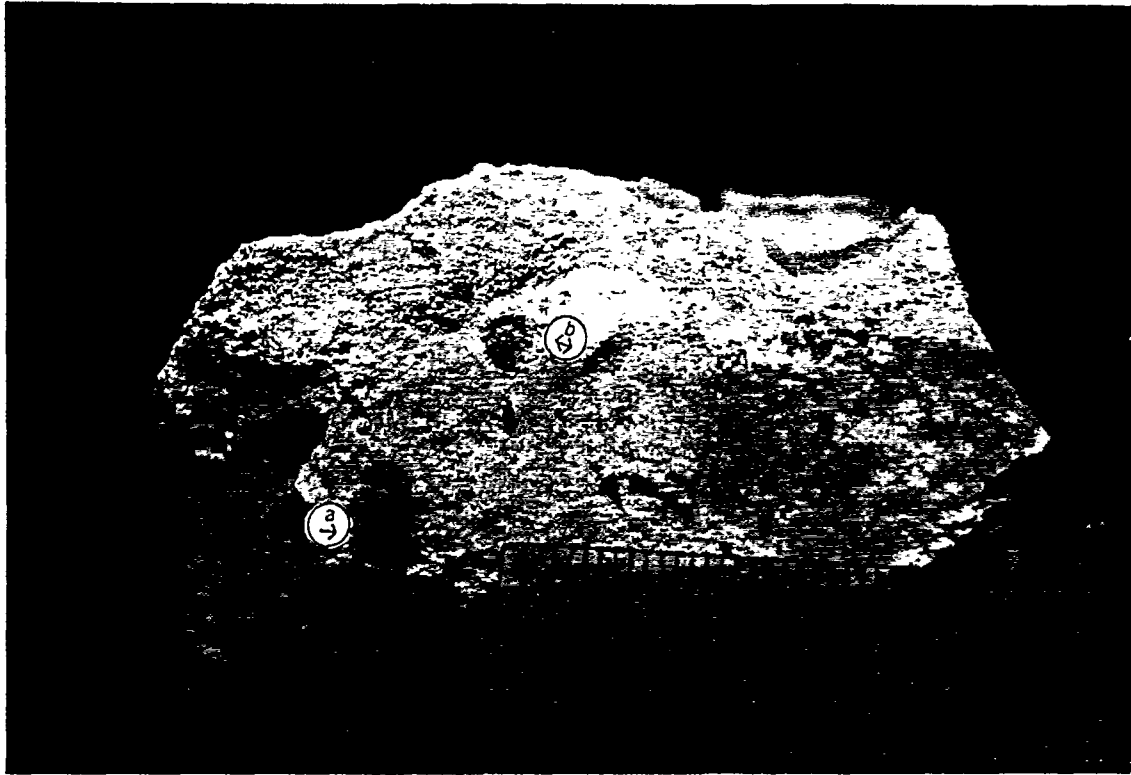


Figure 4. This sample is an example of both mixed texture and floating-brecciated texture. The buff-colored matrix contains varying amounts of calcite and opal; the lighter-colored upper part contains relatively more calcite, and the darker-colored lower part contains relatively more opal. Note the tuffaceous foreign clasts (a, b) which seemingly “float” in the mixed-textured matrix. Photo by Christine Schluter; Sample 7a, downhill from WT-7.

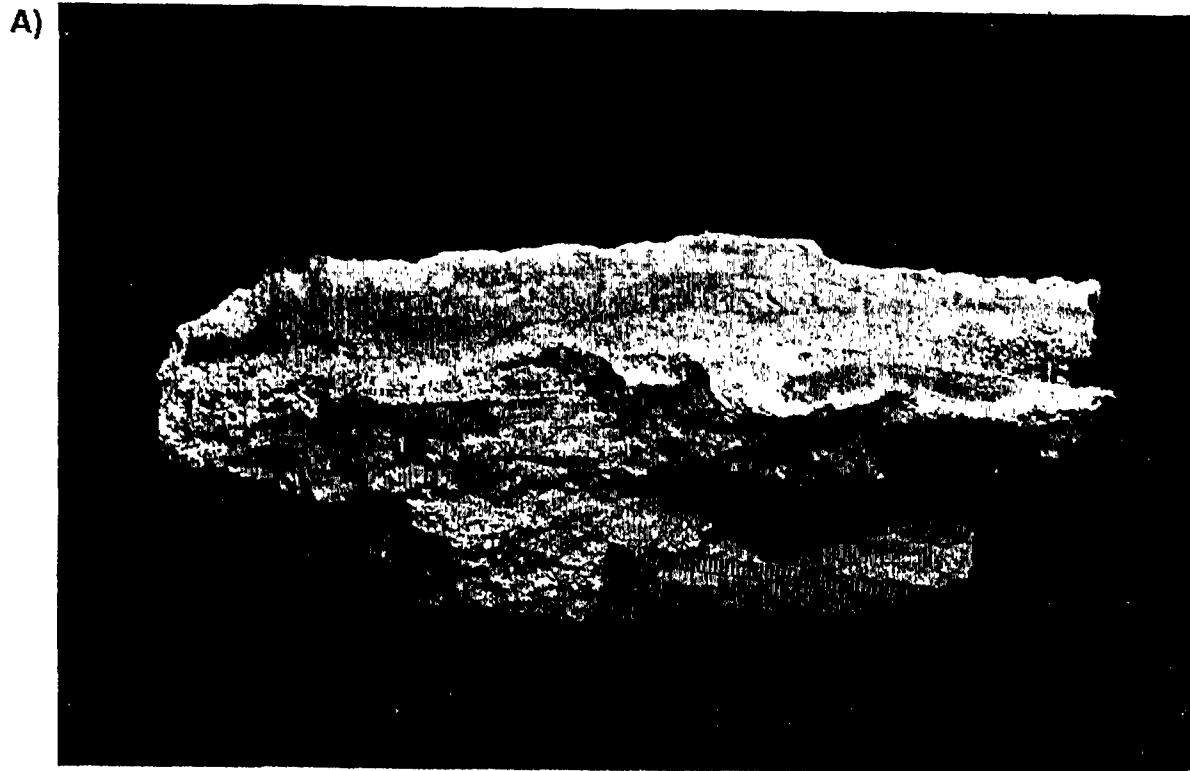
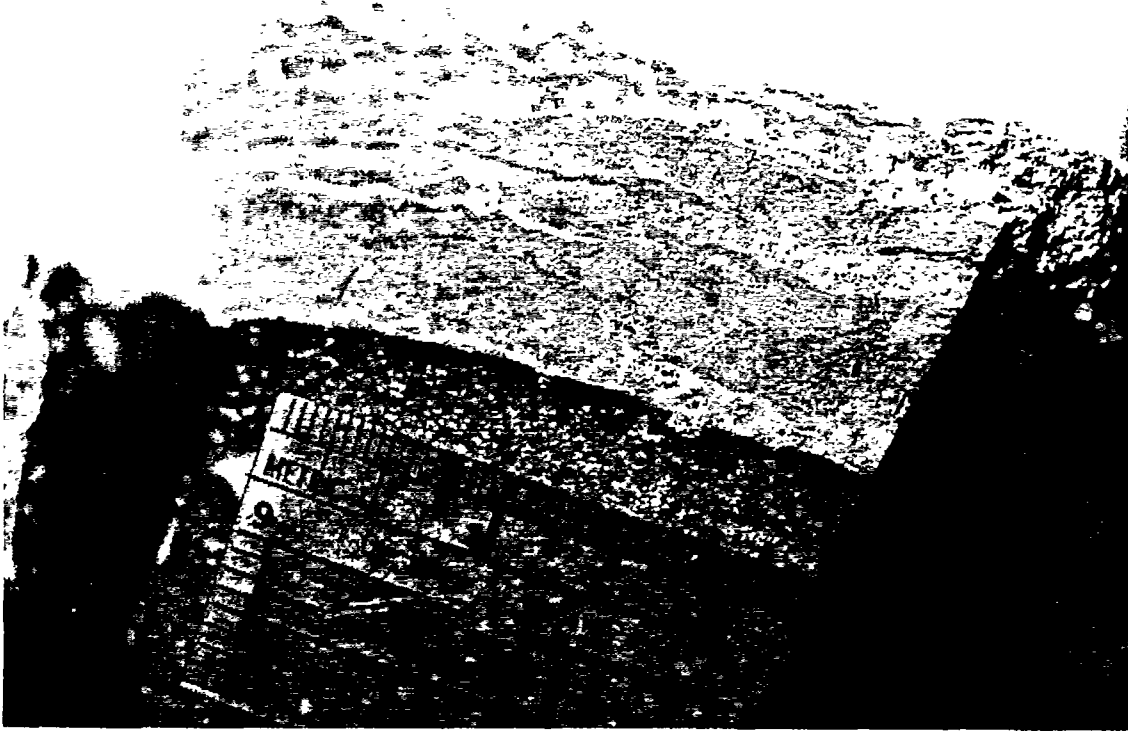


Figure 5 - Banding in a mixed-textured calcite/opal matrix. Banding represents different mixtures of calcite and opal. (A) Horizontal banding, Sample 5d, WT-7 drill pad, and (B) vertical banding, Sample 28d, from east side of Busted Butte. Photos by Christine Schluter.

A)



B)



Figure 6. Two more examples of banded/laminated texture. (A) Laminated texture where the individual layers are narrow (a few millimeters). This sample also displays flow texture, where darker and lighter bands exhibit a marbly or wavy pattern. Note the dark reaction rim at the edge of the Tiva Canyon tuff where it comes in contact with the calcite/opal matrix. Under thin section this rim does not appear to have been altered or invaded by calcite/opal; rather, it appears to be a “baked” rim possibly caused by hot calcite/opal solutions. (B) Two banded textures from the Wailing Wall. Photos by Christine Schluter; (A) = 5a; (B) = 19a.

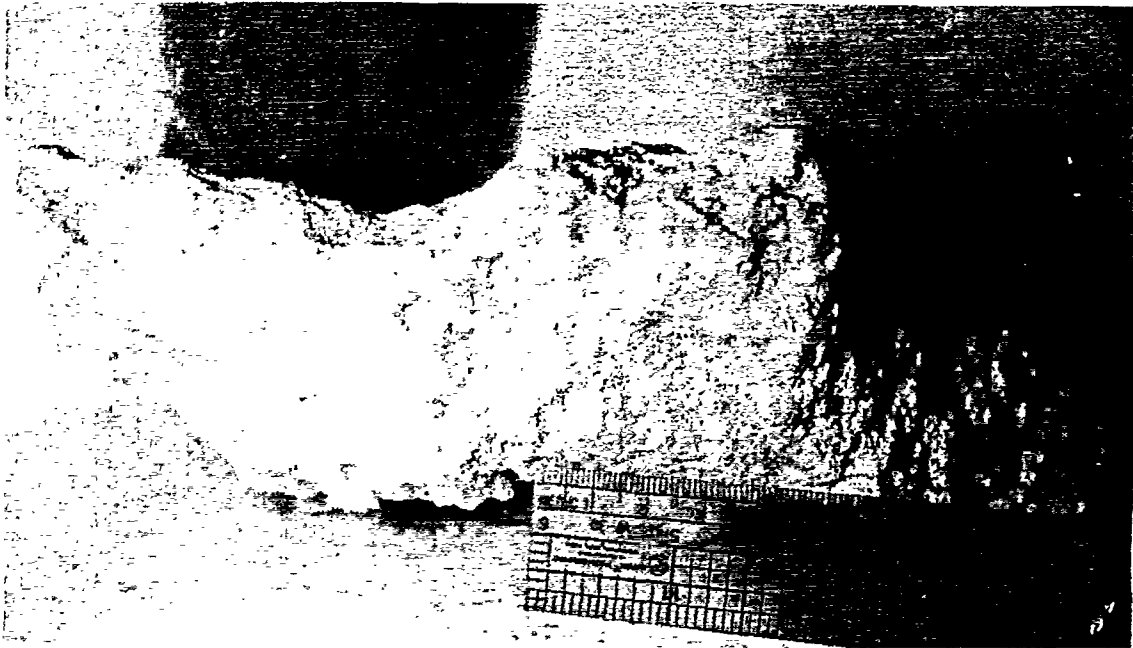


Figure 7. Massive texture showing porous, unlayered to roughly-layered, calcite/gypsum. This sample (32a) was collected from the Wahmonie travertine/gypsite mound and consists of about 70-80% calcite and 20-30% gypsum. Photo: Christine Schluter.

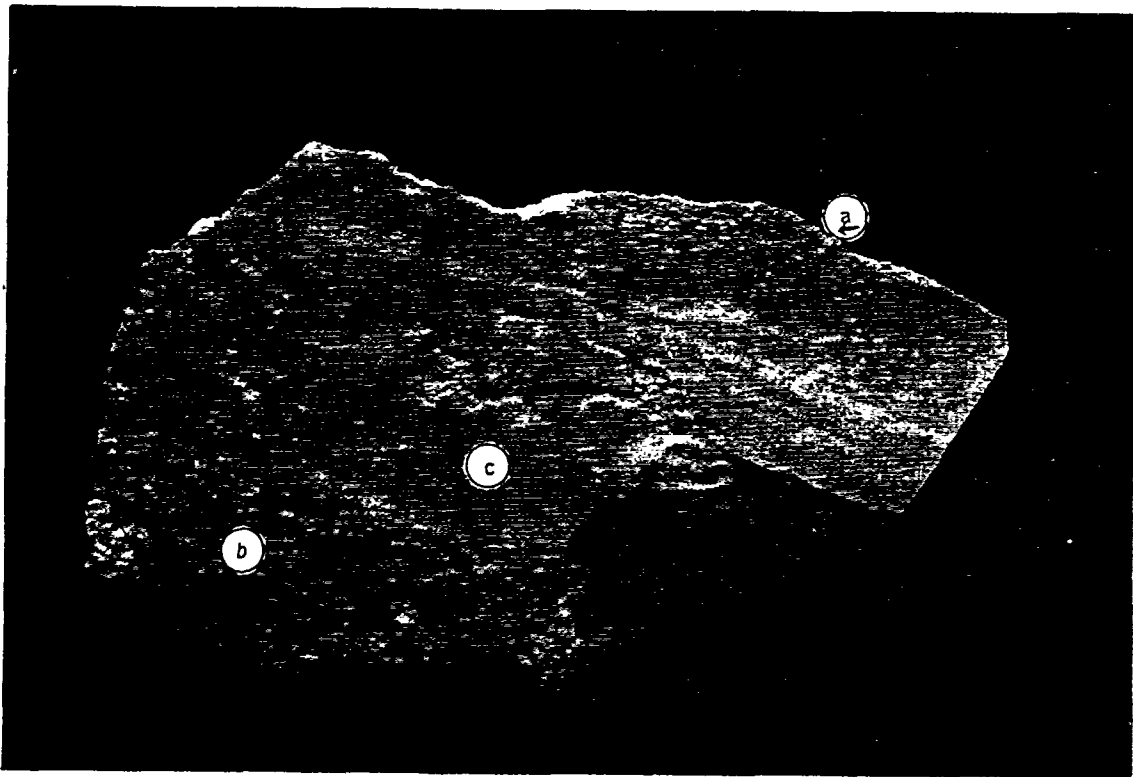


Figure 8. Powdery-textured calcitic layers (a, b) interbedded with dense, buff-colored, mixed-textured calcite/opal (c). This sample (10e) was collected from the Bare Mountain mining district west of Yucca Mountain, yet it displays identical textures to samples collected at Yucca Mountain. Photo: Christine Schluter.

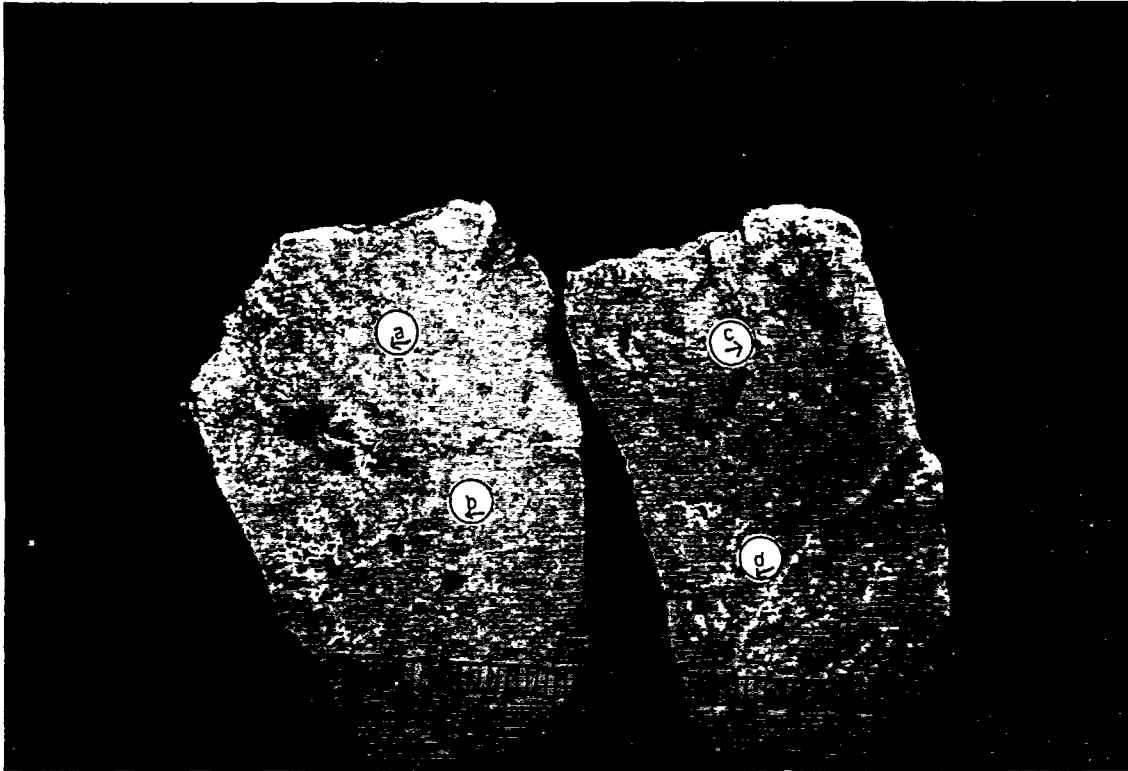
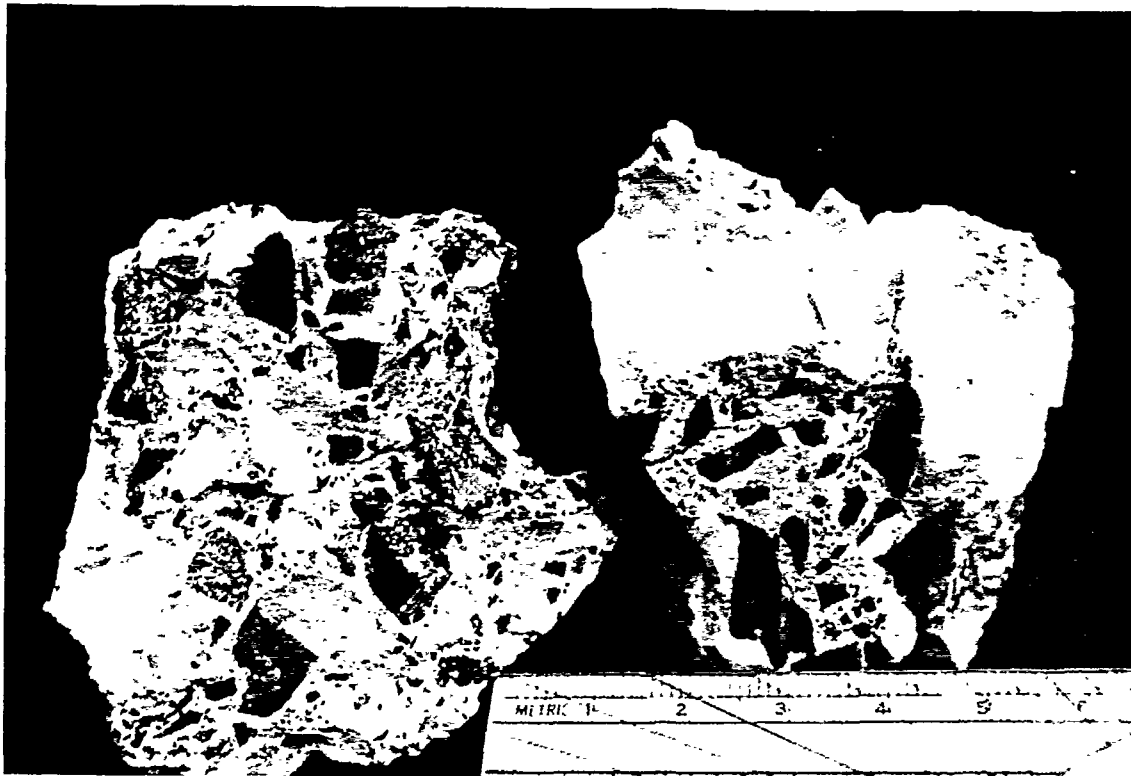


Figure 9. Patchy texture contains clasts of calcite/opal (a, b, c, d) within a mixed-textured calcite/opal matrix. The clasts (both rounded and angular) of calcite/opal must have been at least partially-hardened and brecciated before a later engulfment by the calcite/opal matrix. Photo: Christine Schluter; Sample 4d, Pull Apart Fault.

A)



B)



Figure 10. Brecciated texture: (A) Floating-brecciated texture where the Tiva Canyon clasts seem to “float” in a calcite/opal matrix, and (B) Mosaic-brecciated texture where the Tiva Canyon has become fractured and filled with (and wedged apart by?) calcite/opal. Both (A) and (B) are part of Sample 5g, WT-7 drill site, showing that floating- and mosaic-brecciated texture can occur together. Photos by Christine Schluter.



Figure 11. Mosaic-brecciated texture, WT-7 drill pad, Sample WT-7 (3). Note how many of the clasts can be “fitted back together” like the pieces of a puzzle. This type of breccia has alternately been considered to be an “explosion breccia” or the result of “chemical brecciation.” Photo: Carol Hill.

A)



B)

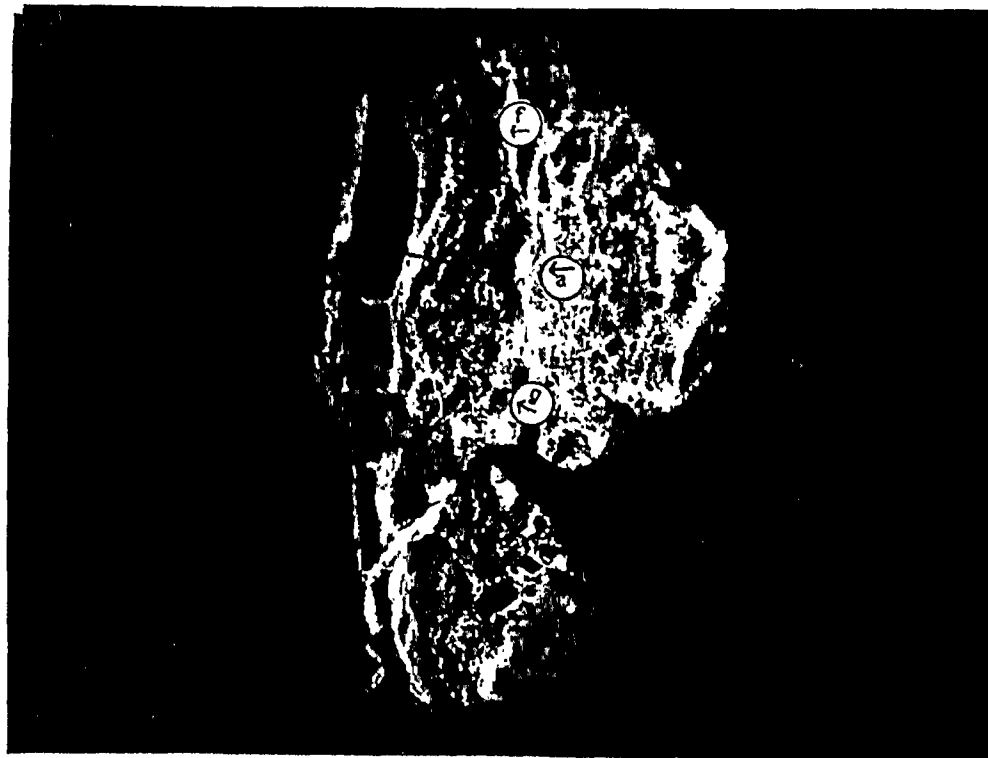
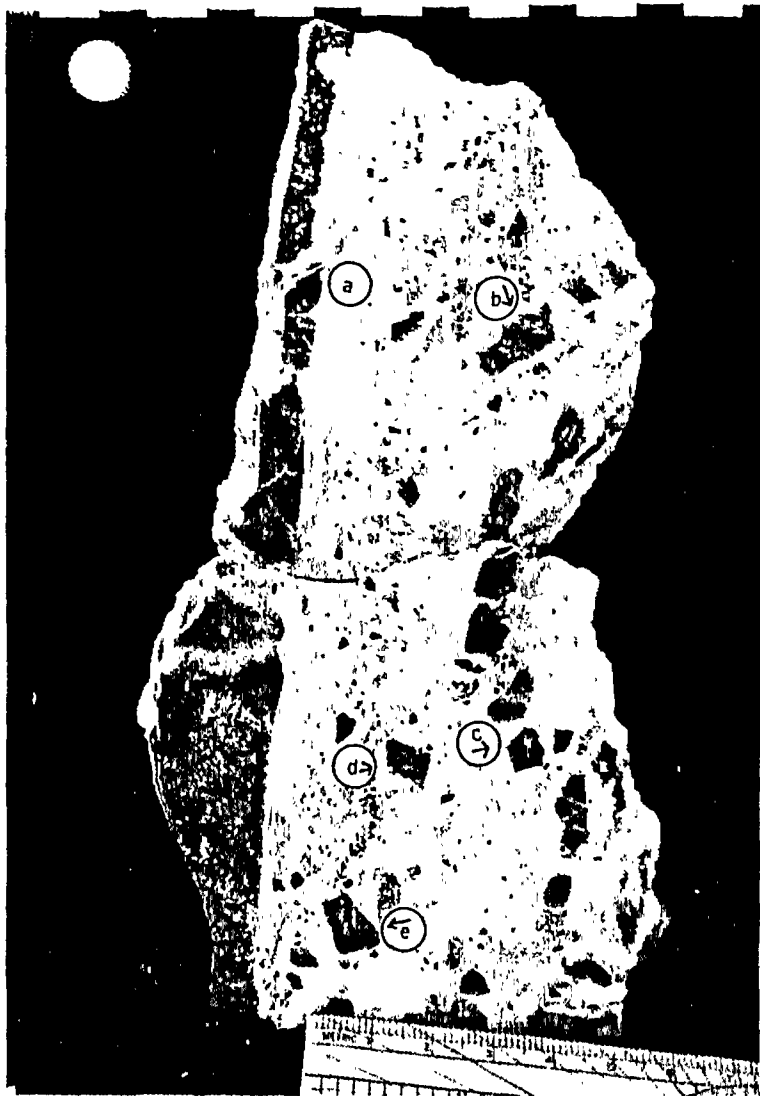


Figure 12. (A) This sample displays many textural types: pure texture (the seams of pearly opal; a), mixed texture (the buff-colored matrix material; b), floating-breccia texture (c), mosaic - breccia texture (d), and flow texture (e). Note how in the flow texture the calcite/opal appears to have "flowed" conformable to the Tiva Canyon breccia clast to the left of it. Note also the seam of pearly opal (follow seam from f to g). This piece is part of an almost-vertical dike cutting the Tiva Canyon at Trench 14 (Sample 36z). (B) Using a UVG-54 Mineralight, this fluorescent photo illustrates flow texture; where bands of pure opal (a, f, g) exhibit a wavy pattern. Photos: Christine Schluter.

A)



B)

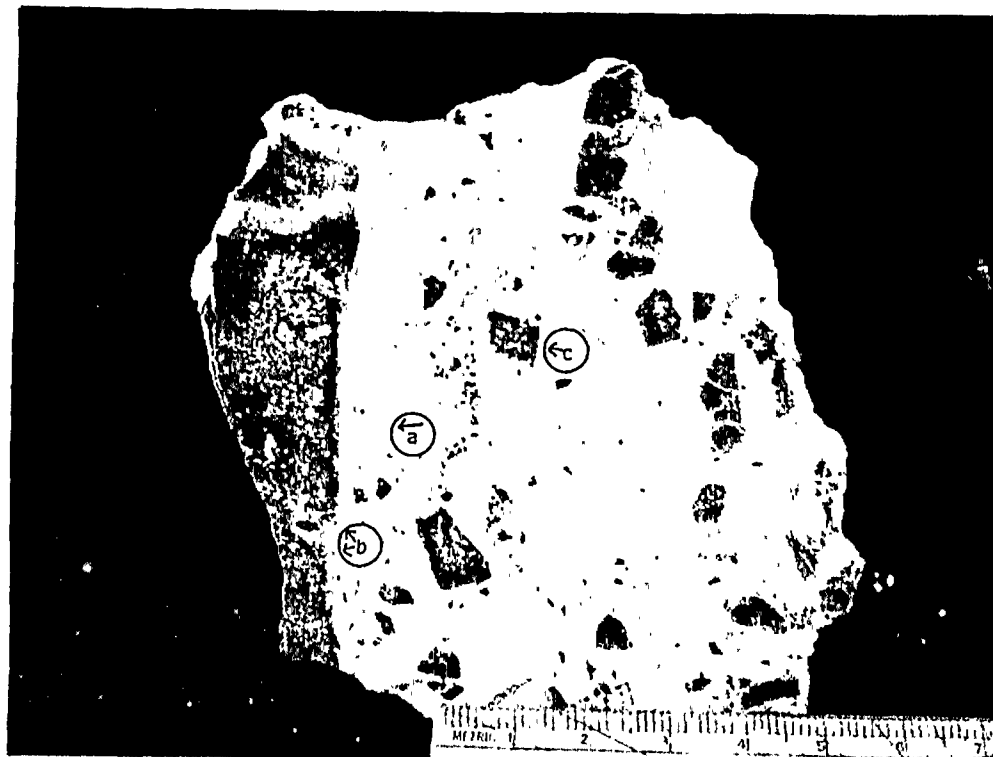


Figure 13. Mosaic- and floating-brecciated texture, Sample 36z, Trench 14. (A) Note the mosaic-brecciated texture on the left and how the clasts at (a) have been cross-cut by calcite/opal material and offset slightly to the right. Note also the mosaic- to floating-brecciated textures on the right; how the clast at (b) has been turned about 30° to the vertical and how the "line of clasts" veers to the right at (c). Clasts (d) and (e) may have been part of the "line" but were swept to the left. (B) Close-up of bottom part of (A) which shows the marbled flow-texture of the calcite/opal matrix (e.g., at a). Note the possible reaction (baked?) rims surrounding clasts (b) and (c). Photos: Christine Schluter.

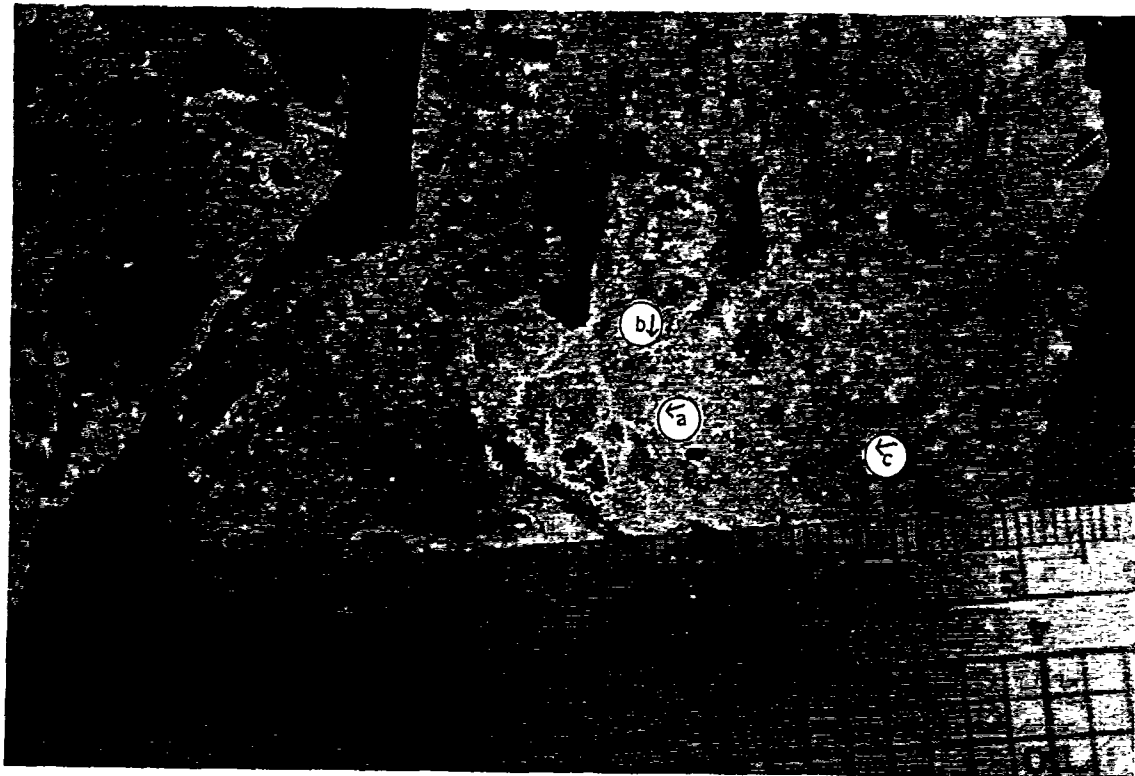


Figure 15. Veined texture where calcite/opal veins cross-cut calcite/opal matrix (a). This is also a good example of patchy texture (see calcite/opal clasts at b and elsewhere), and floating-brecciated texture (e.g., see foreign clasts at c). Sample 4e, Pull Apart Fault. Photo by Christine Schluter.

A)



B)



Figure 16. Two examples of invasive texture: (A) where dense, buff-colored, calcite/opal of mixed texture (a) has invaded a powdery-textured mass composed primarily of calcite (b), Sample 19b, Wailing Wall; (B) where a "blob" displaying powdery texture (a) has invaded a calcite/opal banded mass of mixed texture (b), Sample 7d, downhill from WT-7 drill site. Photos by Christine Schluter.

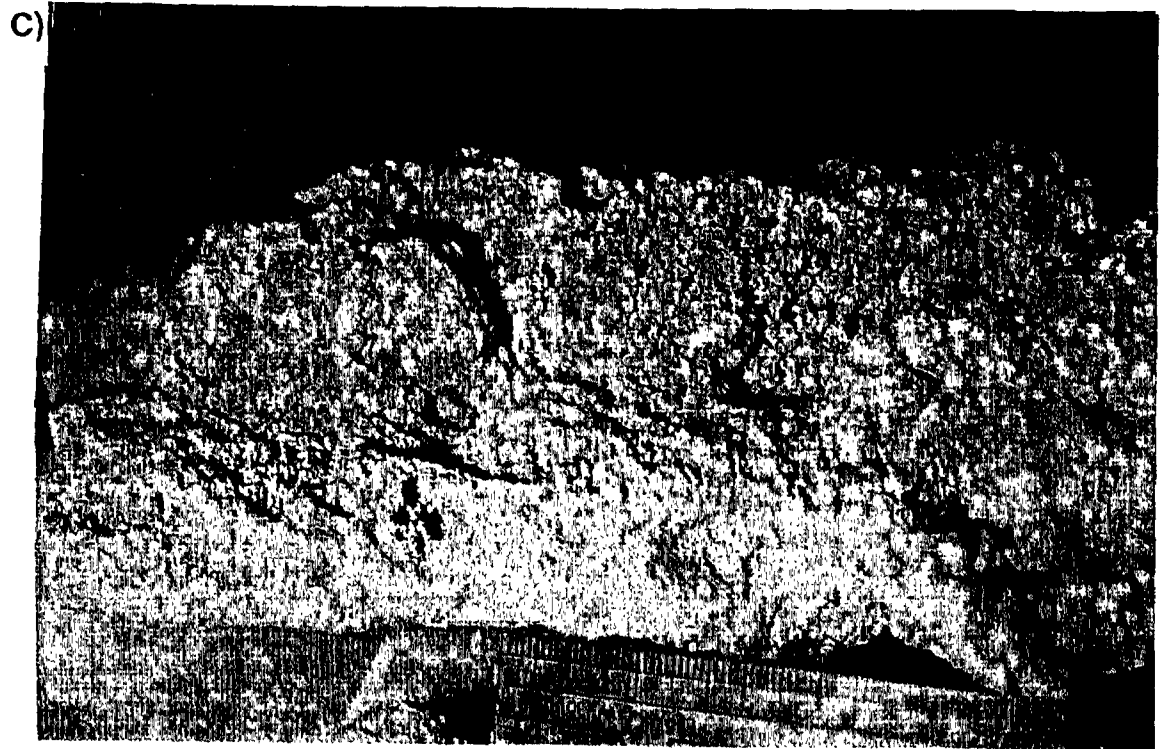
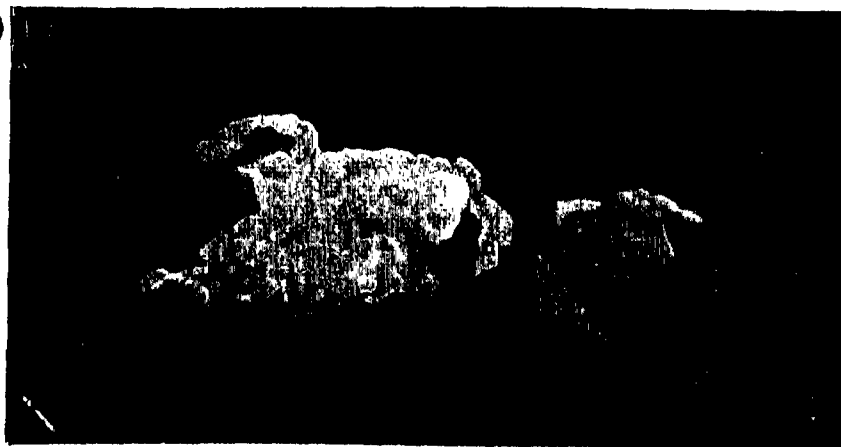
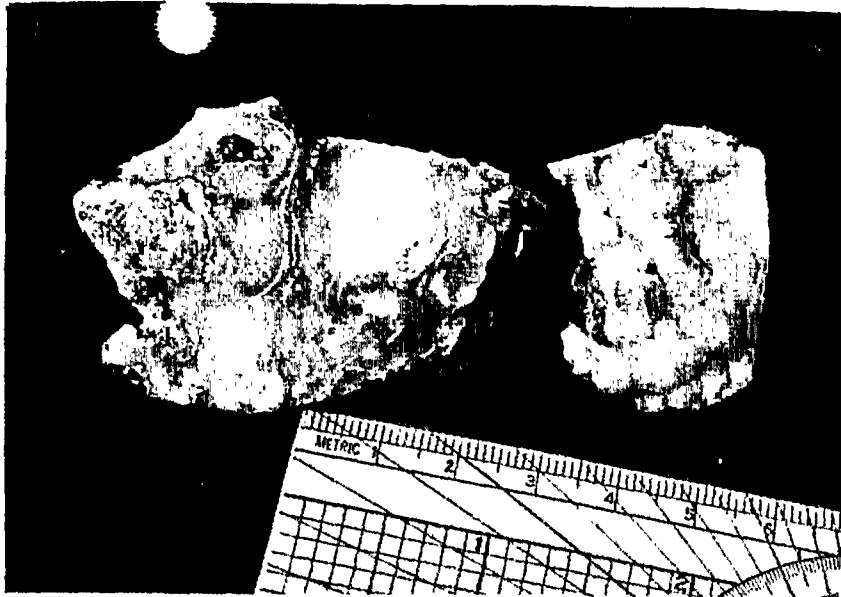


Figure 17. Two examples of botryoidal texture: (A) Botryoidal opal that fills fractures in the Tiva Canyon tuff, Harper Valley (B) fluorescent photo of same sample (Sample 39b); (C) botryoidal gypsum crusts overlying the main mass of calcite/gypsum, Wahmonie travertine/gypsite mound (Sample 32a). Photos by Christine Schluter.

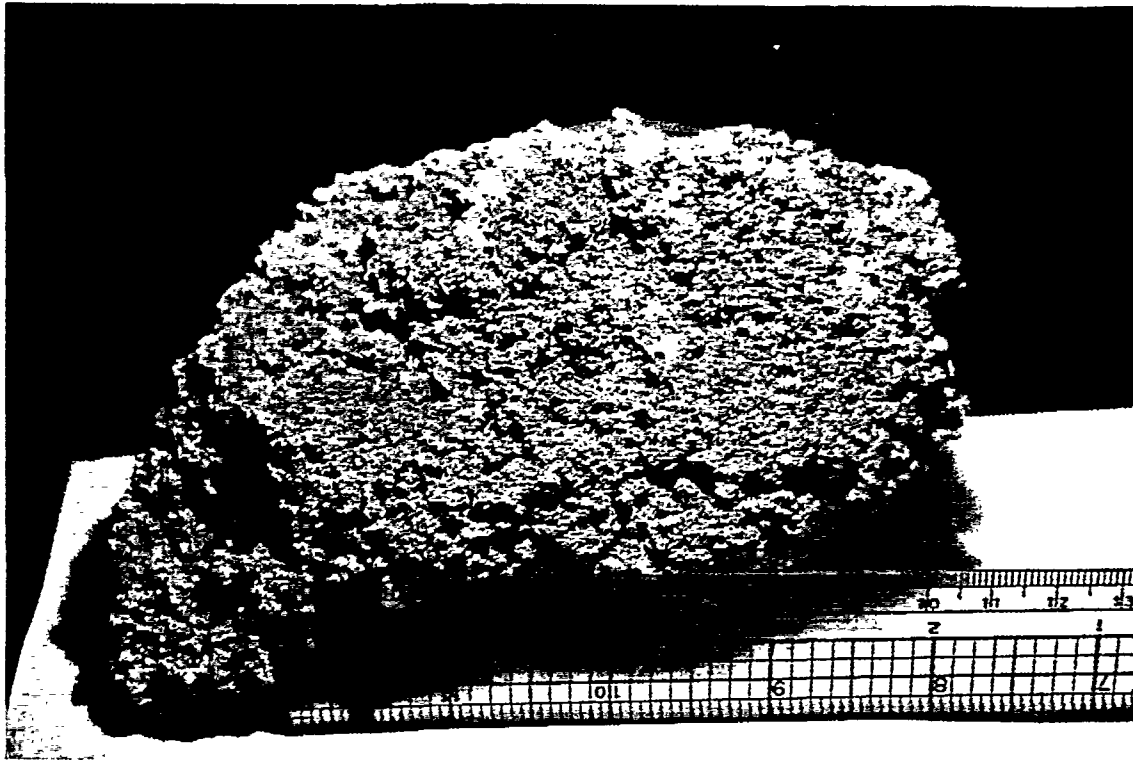


Figure 18. Algal-oid texture, Sample 19d, Wailing Wall. Sample may have precipitated from spring water in which algae were growing, much as the actively-growing spring travertine at Cane Springs (east of Yucca Mountain) has live algae in it today. Photo: Christine Schluter.

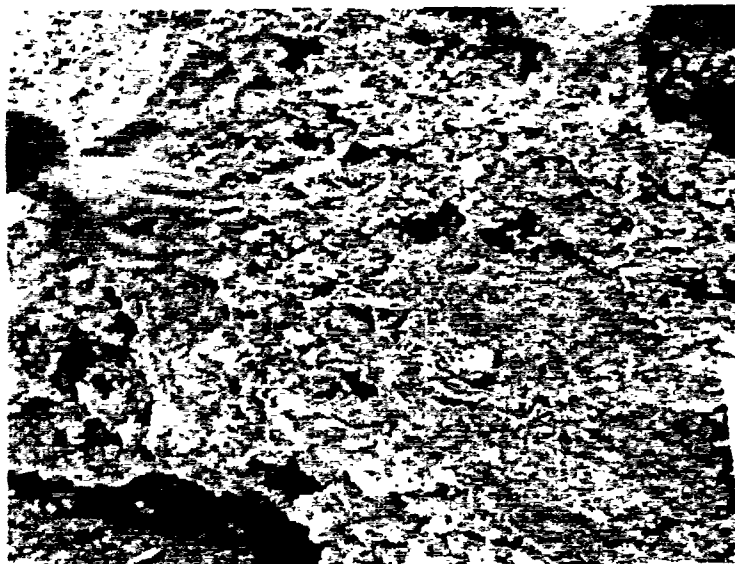


Figure 19. Root-cast texture in sheet travertine, West Busted Butte. Photo: from Johnson Control World Services (taken from a video).

A)

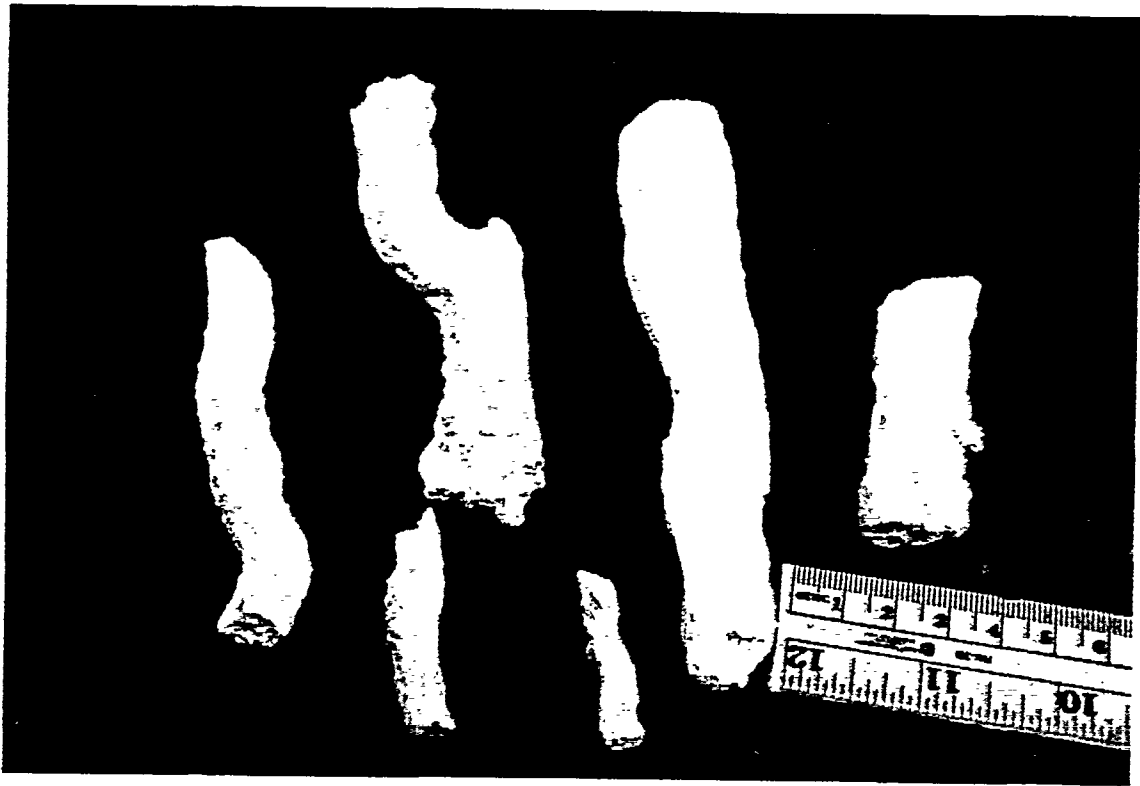


B)



Figure 20. Root casts collected from a variety of locations, Yucca Mountain. (A) Sample 22a, Stagecoach Trench North, Trench A, (B) Sample 23a, Stagecoach Trench South, Trench A,

c)



D)

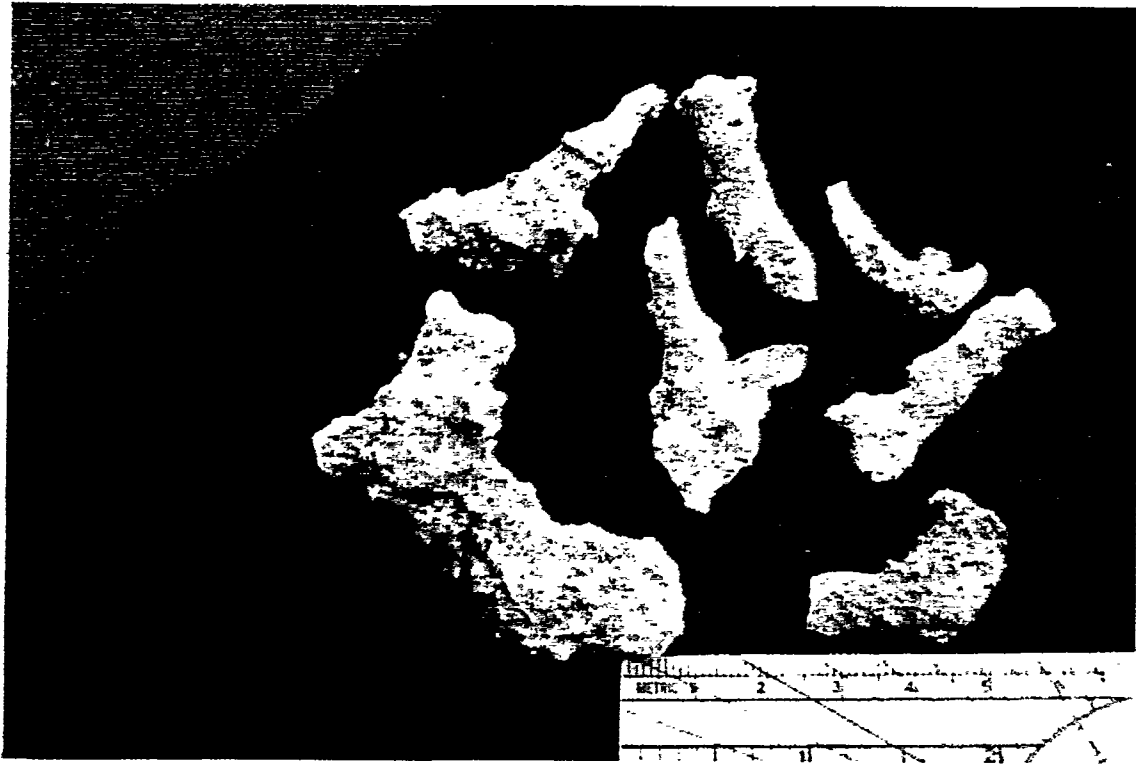


Figure 20. (C) Sample 28c, East side of Busted Butte, (D) Sample 30b, West side of Busted Butte. Photos by Christine Schluter.

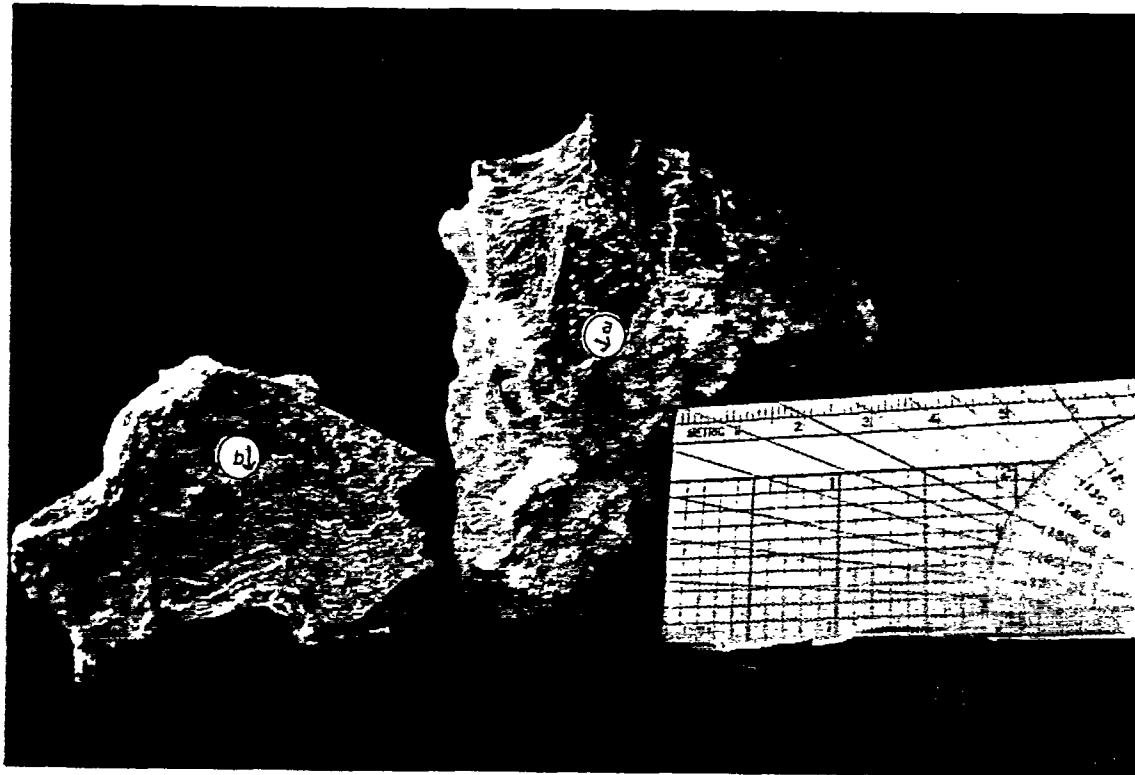


Figure 21. Speleothemic texture, Sample 4f, Pull Apart Fault. Calcium carbonate was leached from above-lying calcite/opal mass and redeposited as dripstone or rimstone on the undersides of the travertine mass or rock. Growth of the travertine was in thin layers (a, b), similar to travertine deposition in caves. Photo by Christine Schluter.

PART 7

**The Spatial and Chemical Diversity of Zeolitic
Alteration at Yucca Mountain, Nye County,
Nevada**

TRAC *Technology and Resource Assessment Corporation*

3800 Arapahoe Avenue, Suite 225
Boulder, Colorado 80303
(303) 443-3700 FAX No. (303) 443-8626

**THE SPATIAL AND CHEMICAL DIVERSITY OF
ZEOLITIC ALTERATION AT
YUCCA MOUNTAIN, NYE COUNTY, NEVADA.**

QUARTERLY REPORT No. 5
CONTRACT No. 92/94.0004

QUARTERLY REPORT Submitted to the
Nuclear Waste Project Office
State of Nevada

July, 1993

Authored by:

Dr. Donald E. Livingston

**The Spatial and Chemical Diversity of
Zeolitic Alteration at
Yucca Mountain, Nye County, Nevada.**

CONTENTS

LIST OF FIGURES	1
LIST OF TABLES	2
I. INTRODUCTION	3
A. General	3
B. Purpose	4
C. Location and Geography	5
D. Stratigraphy and Sample Distribution	5
II. NORMALIZATION AND PRESENTATION OF DATA	7
A. Normalization of Data	7
B. Presentation of Data	9
III. CHEMICAL AND SPATIAL DIVERSITY OF ALTERATION MINERALS AT YUCCA MOUNTAIN, RESULTS	25
A. Diversity Within Boreholes and Surface Locations	25
1. USW G-1	25
2. USW G-2	26
3. USW G-3	27
4. USW G-4	28
5. USW H-3	29
6. USW H-4	30
7. USW H-5	30
8. UE-25 a&b#1	31
9. UE-25 p#1	32
10. J-13	33
11. Prow Pass	33
12. Summary of Chemical and Spatial Diversity within Boreholes	34

B. Large Scale Spatial and Chemical Diversity of Clinoptilolites	58
1. Geographic Diversity	58
a. North-South Cross Section along Yucca Mountain	58
b. Central Yucca Mountain	58
c. Southern Yucca Mountain	59
d. Deep Calcium Rich Clinoptilolite	59
2. Relation to the Water Table	59
3. Relation to Elevation	59
4. Relation to Stratigraphy	59
5. Summary of Large Scale Spatial and Chemical Diversity of Clinoptilolites	60
C. Authigenic Analcime and Feldspar	61
1. Analcime and Feldspar in USW G-1	61
2. Analcime in J-13	62
3. Analcime in UE-25 b#1	62
4. Analcime in UE-25 p#1	62
5. Albites and Adularia in USW G-2	63
6. Feldspar in Boreholes USW G-3 and USW G-4	63
7. Adularia at Prow Pass	63
8. Summary of the Spatial Distribution of Analcime and Feldspar	63
 IV. SUMMARY OF RESULTS, CHEMICAL AND SPATIAL DIVERSITY AT YUCCA MOUNTAIN	 72
 V. DISCUSSION OF GENETIC IMPLICATIONS	 73
A. Historical Perspective	73
B. Interpretive Options	78
1. The Supergene (Pedogenic) Hypothesis	79
2. The Hypogene Hypothesis	80
C. Supergene vs. Hypogene	80
 VI. CONCLUSIONS	 82
 VII. REFERENCES	 83

LIST OF FIGURES

- Figure 1. Location Map.
- Figure 2. Borehole and Sample Locations, Yucca Mountain, Nevada.
- Figure 3. Comparison of Normalized and Unnormalized Oxides for Glass, Whole Rock and Clinoptilolite.
- Figure 4. Comparison of Framework Oxides and Sum of Interstitial Oxides for Glass, Whole Rock and Clinoptilolite.
- Figure 5. Cross Plots of Interstitial Cation Oxides for Glass, Whole Rock and Clinoptilolite.
- Figure 6. USW G-1, Clinoptilolite Chemistry.
- Figure 7a. USW G-2, Clinoptilolite Chemistry.
- Figure 7b. USW G-2, Clinoptilolite Chemistry, detail, Tpp and Tpt.
- Figure 7c. USW G-2, Clinoptilolite Chemistry, detail, Tht and Tcp.
- Figure 8a. USW G-3, Clinoptilolite Chemistry.
- Figure 8b. USW G-3, Clinoptilolite Chemistry, detail, Tcb and Tcb.
- Figure 8c. USW G-3, Clinoptilolite Chemistry, detail, Tct.
- Figure 9a. USW G-4, Clinoptilolite Chemistry.
- Figure 9b. USW G-4, Clinoptilolite Chemistry, detail, Tht and Tcp.
- Figure 9c. USW G-4, Clinoptilolite Chemistry, detail, Tcb.
- Figure 10. USW H-3, Clinoptilolite Chemistry.
- Figure 11a. USW H-4, Clinoptilolite Chemistry.
- Figure 11b. USW H-4, Clinoptilolite Chemistry, detail, Tht and Tcp.
- Figure 12. USW H-5, Clinoptilolite Chemistry.
- Figure 13a. UE-25 a&b#1, Clinoptilolite Chemistry.
- Figure 13b. UE-25 a&b#1, Clinoptilolite Chemistry, detail, Tpt and Tht.
- Figure 13c. UE-25 a&b#1, Clinoptilolite Chemistry, detail, Tcp and Tcb.
- Figure 14. UE-25 p#1, Clinoptilolite Chemistry.
- Figure 15a. J-13, Clinoptilolite Chemistry.
- Figure 15b. J-13, Clinoptilolite Chemistry, detail, Tpt and Tht.
- Figure 16. Prow Pass, Clinoptilolite Chemistry.
- Figure 17. N-S Cross Section of Boreholes along Yucca Ridge.
- Figure 18. Boreholes of Central Yucca Mountain.
- Figure 19. Boreholes of Southern Yucca Mountain.
- Figure 20a. Cross Plots of Interstitial Cation Oxides for Tpp, Tpt and Tht.
- Figure 20b. Cross Plots of Interstitial Cation Oxides for Tcb, Tcb and Tct.
- Figure 20c. Cross Plots of Interstitial Cation Oxides for Tfb and Tlr.
- Figure 21. Analcime and Feldspars at Yucca Mountain.

LIST OF TABLES

- Table 1. Table of Stratigraphic Units.**
- Table 2. Locations for Samples and Boreholes and Borehole Data.**
- Table 3a. Sample Distribution, Glass.**
- Table 3b. Sample Distribution, Whole Rock.**
- Table 3c. Sample Distribution, Clinoptilolite.**
- Table 3d. Sample Distribution, Sample Type.**
- Table 3e. Sample Distribution, Analcime.**
- Table 3f. Sample Distribution, Albite.**
- Table 3g. Sample Distribution, Adularia.**

INTRODUCTION

General

In a previous report (Livingston, 1993) it has been advocated that the zeolitic chemical alteration of tuffs at Yucca Mountain is best characterized as metasomatic (open system chemical alteration), hypogene, polygenetic and epigenetic with respect to the eruption, deposition, compaction and devitrification of the ash flow tuffs. The great diversity of the chemical compositions of clinoptilolites indicates that chemically diverse waters have invaded the mountain episodically over the entire history of its existence. Direct infiltration of meteoric precipitation, a supergene hypothesis, does not account for this diversity of chemical alteration. Significantly, the zeolitic alteration is mostly calcic in character and much of it is associated with secondary silica (Livingston, 1992). Thus the alteration of the tuffs displays a chemical affinity with the calcite and silica deposits that form veins and surficial deposits that cross cut and overlie both tuffaceous bedrock and unconsolidated Quaternary deposits. The zeolitic and carbonate-silica alterations may be, at least in part, cogenetic. The conclusions of that report support the conclusions of Szymanski (1992) that both the silicate alteration and the carbonate and silica veins and surficial deposits are hypogene in character and that they record repeated invasions of ground water into rocks that constitute the present day vadose zone of Yucca Mountain. These episodic invasions of ground water have occurred throughout the history of Yucca Mountain and have continued into the late Quaternary. K-Ar dating of clinoptilolites (WoldeGabriel, 1990), ~ 10 my. to ~ 2 my., indicates that the zeolites were formed or altered over most of the entire history at

Yucca Mountain. Uranium series isotopic dating of carbonate veins and surficial deposits indicate that many have been formed during the late Quaternary.

Purpose

In this report we examine the spatial distribution of the various types of chemical alteration indicated by the data reported in Broxton, *et al.* (1986) in order to evaluate the location, spatial character and extent of the alteration with the hope of shedding light on the origin of the altering fluids and to test the hypogene hypothesis of Szymanski (1992). In this regard, it is of prime importance to evaluate whether the metasomatic alteration reflects supergene or, conversely, hypogene processes.

The data are presented in graphical format so that the reader is relieved of the tedium of studying lengthy tables of data. In addition to the data reviewed in the previous report (112 microprobe analyses of glass, 63 x-ray fluorescence analyses of whole rock and 436 microprobe analyses of clinoptilolite, Appendices E, A and F respectively of Broxton, *et al.*, 1986) the distribution of 82 analcime and 64 authigenic feldspars (Appendices G and H of Broxton *et al.*, 1986) is examined. It is important to note here that the full extent of the chemistry of zeolitic alteration can not be treated with the data set under consideration. Mordenite has been identified as a major zeolite alteration phase by Bish and Chipera (1989). Broxton *et al.* (1986) state *"Mordenite has been identified in many altered tuffs at Yucca Mountain by x-ray diffraction (Bish and Vaniman 1985), but its chemistry has not been studied. Individual mordenite crystals are so fine grained and intergrown with other authigenic*

phases that analysis by electron microprobe is not feasible." This report is then a part of a larger study that will include both the mineralogy and chemistry of Yucca Mountain.

Location and Geography

Yucca Mountain is located in southern Nye county, Nevada about ninety kilometers northwest of the city of Las Vegas and about fifteen kilometers north of the crossroad community of Amargosa Valley, formerly known as Lathrop Wells. Figure 1 shows the important geographical features of the region. The mountain is located partly on each: the U. S. Department of Energy Nevada Test Site, the U. S. Air Force Nellis Test Range and federal land administered by the U. S. Bureau of Land Management. The regions surrounding Yucca Mountain are sparsely populated and very arid. It is located along the margin between the Great Basin and the Mojave Desert regions of the Basin and Range physiographic province.

Stratigraphy and Sample Distribution

Except for those samples that were collected from surface exposures at Prow Pass in the northwestern part of the mountain, all of the samples were taken from boreholes at and near Yucca Mountain. Chemical analyses are available for each of the stratigraphic units shown on Table 1. The stratigraphic symbols of this table, as given in the original report, are used to identify the stratigraphic source of the samples in tables of the sample distributions, Tables 3a to 3g, and the figures showing the distribution in the individual boreholes, Figures 6 through 20. The

geographic distribution of the surface sample sites and the sampled boreholes are shown in Figure 2. Data for locations and borehole features are given in Table 2. The number of samples and their geographic and stratigraphic settings are given in Tables 3a through 3g. The correlation between the major three sample types is given in Table 3d. Although the number of chemical analyses is a very large data set, it can be seen from these tables that the data set is sparse and spotty with respect to the number of sampled boreholes and stratigraphic units present at Yucca Mountain. The most completely sampled stratigraphic units are the Topopah Spring member (Tpt) of the Paintbrush tuff, the tuff of Calico Hills (Tht) and the Prow Pass member (Tpc) of the Crater Flat tuff. The best correlation of the three major sample types also occurs in these same stratigraphic units. Glass is more heavily represented in the younger (upper) units of the stratigraphic section in keeping with well known greater alteration of the older (lower) units of the section. The occurrences of analcime and feldspar are usually at greater depth than clinoptilolite, an exception is the occurrence of analcime in the Tiva Canyon member (Tpc) of the Paintbrush tuff in borehole J-13 Figure 21. In this borehole analcime occurs 727 feet above the shallowest reported occurrence of clinoptilolite, at a depth of 608 feet.

NORMALIZATION AND PRESENTATION OF DATA

Normalization of Data

For the purposes of the previous report (Livingston, 1993) the data reported by Broxton, *et al.* (1986) were manually keyed into a data base for graphical presentation. Among the critiques by colleagues was that it would be more appropriate to evaluate the data on a volatile-free basis. This has been done for this report. The results are illustrated in Figure 3 where the top three diagrams present the reported results of Broxton, *et al.* (1986), and used in Livingston (1993), for SiO_2 vs. Al_2O_3 in glass, whole rock and clinoptilolite. The bottom three diagrams present the results normalized to the sum of the metal oxides as indicated in the figure caption. A remarkable improvement in the coherence of the data is readily noted. In addition Livingston (1993) noted that, during zeolitic alteration, iron and titanium are excluded from clinoptilolite relative to the parent material, glass. Thus it is likely that iron and titanium are not essential components of clinoptilolite at Yucca Mountain and reasonably can be excluded from further consideration.

Because it is the purpose of this report to examine the internal variations among only the essential elements in clinoptilolite, the data used in this report have been normalized to the sum of SiO_2 , Al_2O_3 , MgO , CaO , Na_2O and K_2O then recalculated as molar quantities of oxides. Molar oxide quantities are preferred because the electrostatic charge of these oxides (Al_2O_3 , MgO , CaO , Na_2O and K_2O) in aluminosilicate minerals are equal in absolute value and the amount of the interstitial cations is limited by the charge deficiency of the framework elements which is determined by

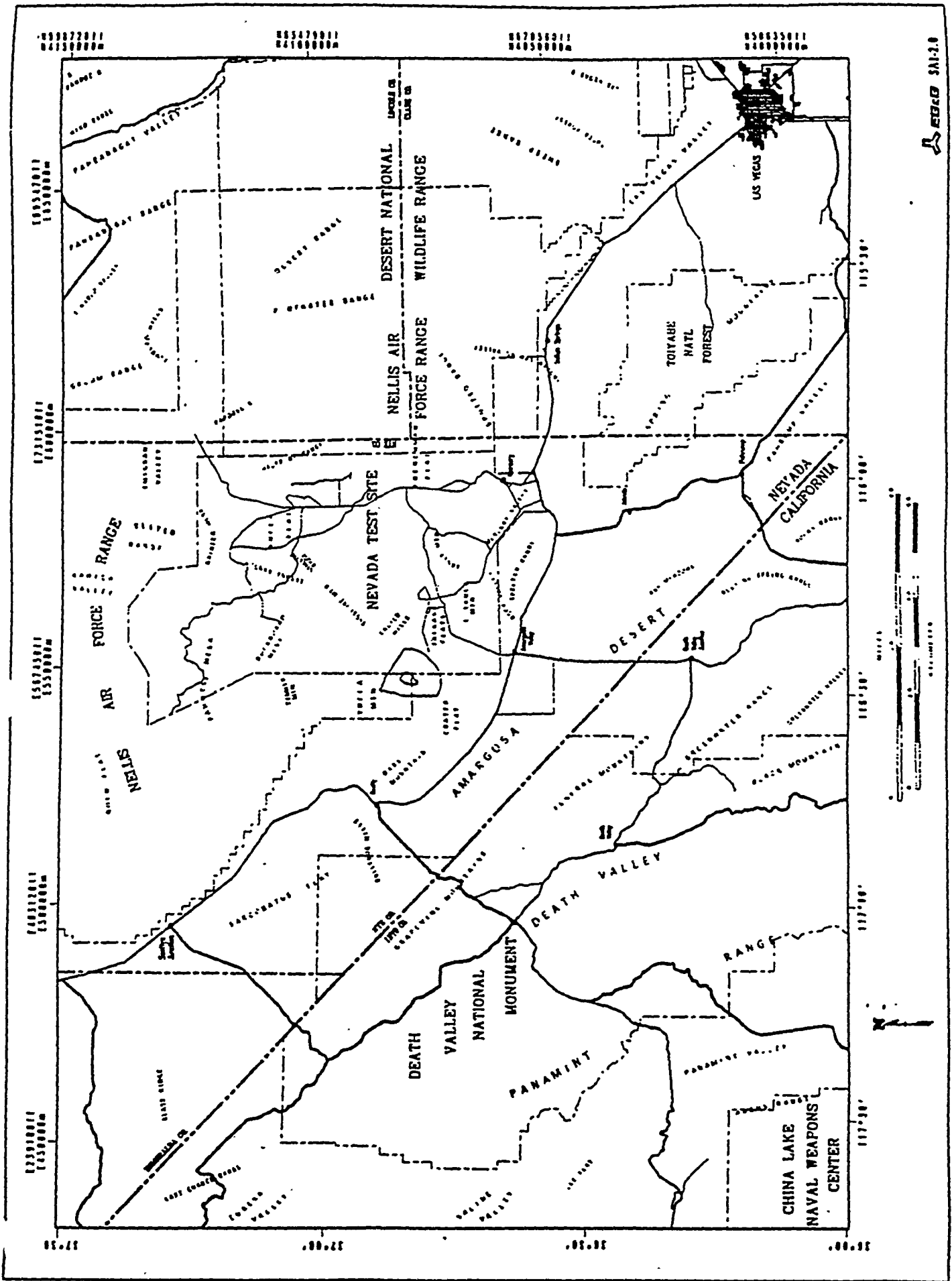
the abundance of Al_2O_3 . The results of this normalization are shown in Figure 4. The upper three diagrams show the results for glass, whole rock and clinoptilolite as SiO_2 vs. Al_2O_3 . Little difference is noted from the similar plots of normalized oxides shown in Figure 3. The utility of using molar oxide quantities is shown in the lower three diagrams of Figure 4. Here the molar concentration of alumina is plotted against the sum of the molar quantities of MgO , CaO , Na_2O and K_2O . The glass compositions plot close to the line of equal abundance while the whole rock analyses show considerable scatter as might be expected from the presence of minor and trace minerals included in results of the whole rock x-ray fluorescence analyses. The clinoptilolite compositions plot parallel to the equal abundance line but slightly and systematically to the left. This could be caused by the omission of trace alkali and alkaline earth elements in the analyses or by volatilization of sodium during microprobe analyses as discussed by Broxton, *et al.* (1986). Barium concentrations in glass and clinoptilolite were reported by Broxton, *et al.* (1986) and examined by Livingston (1993). Little difference in the barium distributions for glass and clinoptilolite were noted but the glass does have a greater proportion of values at zero percent BaO than does clinoptilolite. Might the clinoptilolite have a greater abundance of alkali and alkaline earth trace elements than the glass? This question remains unanswered. Regardless of the answer to this question the diagrams do attest to the very excellent quality of the chemical analyses reported by Broxton, *et al.* (1986) and serve to justify the use of normalized values to eliminate variations in the data that would otherwise be present due to dilution by volatile constituents and other elements which are nonessential to the chemistry of the zeolites.

Figure 5 shows the results of normalization of the interstitial cation oxides for glass, whole rock and clinoptilolite. The normalization is the same as used for the individual boreholes of the main body of this report. This figure is referenced as appropriate in the discussions of the distribution of the chemical composition of clinoptilolite at each location. Note that the glass, 112 analyses, has a very restricted chemical composition, that is nearly pure alkali oxides with nearly equal molar abundances of both Na_2O and K_2O . CaO and MgO are very low. The 63 whole rock analyses, in the center of the figure are mostly of altered rocks and clearly show the enrichment of MgO and CaO and the diminishment of Na_2O and K_2O with respect to glass. The 436 analyses of clinoptilolite show a most remarkable range of chemical abundances, ranging from pure alkali oxides to pure alkaline earth oxides.

Presentation of Data

Following sections present the main body of the data that is the subject of this report. The data are presented graphically so that the chemical and spatial variabilities can be examined readily. All of the samples from each borehole (or location) are presented in one figure of four diagrams, Figures 6 through 16. Detailed figures follow the respective main figure when necessary. The main figure for each borehole presents the mole fraction of the interstitial cation oxides in the left-hand diagram, in borehole log format, plotted as a function of the elevation of the sample above mean sea level. The dashed horizontal line indicates the elevation of the ground surface for that particular borehole, the present day water table is noted by

the horizontal dotted line. The elevations used for the topographic surface and the present day water table are given in Table 2. The solid curve gives the mole fraction of MgO. The curve second from left (dashed) is the sum of MgO and CaO. Thus the difference between the two curves indicates the mole fraction of CaO. The third curve (dotted) is the sum of MgO, CaO and K_2O . The abundance of K_2O is the difference between the second and third curves and the abundance of Na_2O is the difference between the third (dotted) curve and the right hand edge of the diagram. A different symbol is used for each of the individual stratigraphic units of the tuffs as indicated in Table 1. The middle diagram, labeled as the legend, uses the same symbol as the left-hand diagram and indicates the elevation of the sample in feet and the stratigraphic unit as indicated in Table 1. The two diagrams on the right-hand side of the figure are cross plots of the mole fraction of the four interstitial cation oxides. In the top diagram the axes are the mole fraction of the alkali oxides, the origin represents 100 % of CaO and MgO. The diagonal line from 1.0 to 1.0 represent 100 % of alkali oxides. The bottom diagram presents the mole fractions of CaO and MgO. The origin is 100 % alkali oxides and the line from 1.0 to 1.0 represents 100 % alkaline earth oxides. The symbols in these two diagrams are the same as in the two other diagrams of the figure to facilitate visual correlation among the four diagrams. Detailed figures, labeled with b and c, follow the main figure for each borehole when needed for clarity. The detailed figures present cross plots of individual stratigraphic units which are ordered by sample elevation. They immediately follow the main figure for the respective borehole.



EDGE 3412.8

Figure 2
 BORE HOLE AND SAMPLE LOCATIONS
 Yucca Mountain, Nevada

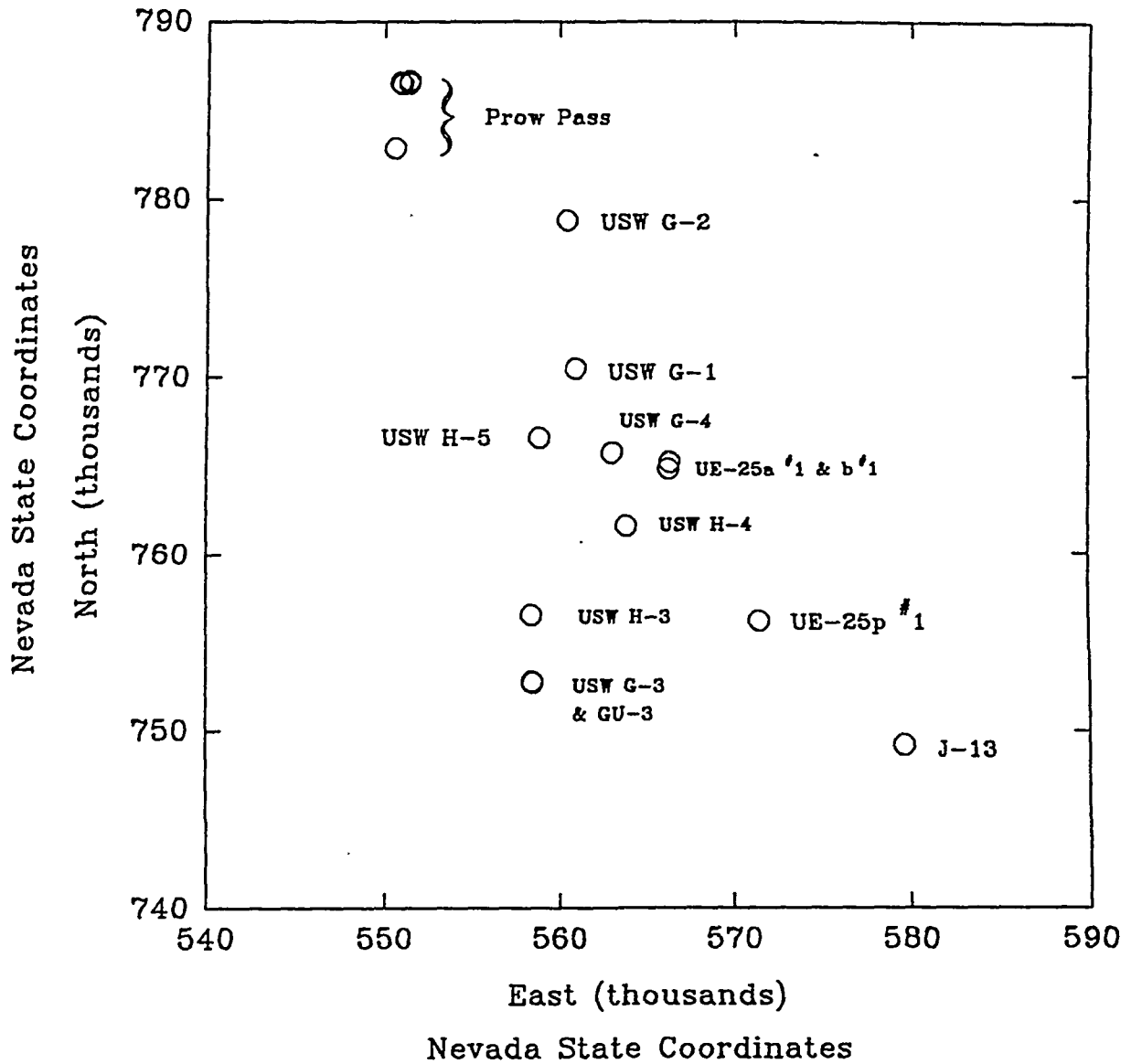


TABLE 1
TABLE OF STRATIGRAPHIC UNITS

formation	member	symbol
Paintbrush Tuff	Tiva Canyon	Tpc
	Yucca Mountain	Tpy
	bedded tuff	Tb
	Pah Canyon	Tpp
	Topopah Spring	Tpt
Tuff of Calico Hills		Tht
Crater Flat Tuff	Prow Pass	Tcp
	Bullfrog	Tcb
	Tram	Tct
Dacite Flow Breccia		Tfb
Lithic Ridge Tuff		Tlr
	bedded tuff	Tb
Older Tuffs and Lavas		Tot

TABLE 2. LOCATIONS FOR SAMPLES AND BORE HOLES AND BORE HOLE DATA

Bore Hole	North	East	G. L. Elev.		Depth		Water Table			
			(Nev. St. Coordinates)	(feet)	(meters)	(feet)	(meters)	WT depth (meters)	WT elev. (meters)	WT depth (feet)
J-13	749,209.00	579,651.00	3,318.00	1,011.28	3,488.00	1,063.09	283.00	728.00	928.24	2,387.84
UE-25a #1	764,900.20	566,349.90	3,934.40	1,199.15	2,501.00	762.27	469.00	731.00	1,538.32	2,397.68
UE-25b #1	765,243.40	566,416.40	3,939.00	1,200.55	4,002.00	1,219.75	470.00	731.00	1,541.60	2,397.68
UE-25p #1	756,171.20	571,484.50	3,654.60	1,113.87	5,923.00	1,805.24	362.00	752.00	1,187.36	2,466.56
USW G-1	770,500.20	561,000.50	4,348.60	1,325.39	6,000.00	1,828.71	572.00	753.39	1,876.16	2,471.11
USW G-2	778,824.20	560,503.90	5,098.40	1,553.92	6,006.00	1,830.54	525.00	1,029.00	1,722.00	3,375.12
USW G-3	752,779.80	558,483.10	4,856.50	1,480.19	5,031.00	1,533.37	750.00	731.00	2,460.00	2,397.68
USW GU-3	752,690.10	558,501.30	4,856.60	1,480.22	2,644.00	805.85	*	*	*	*
USW G-4	765,807.10	563,081.60	4,166.90	1,270.01	3,003.00	915.27	540.00	730.00	1,771.20	2,394.40
USW H-3	756,542.10	558,451.70	4,866.40	1,483.21	4,000.00	1,219.14	752.00	732.00	2,466.56	2,400.96
USW H-4	761,643.60	563,911.10	4,096.50	1,248.55	4,000.00	1,219.14	518.00	730.00	1,699.04	2,394.40
USW H-5	766,634.30	558,908.70	4,850.80	1,478.45	4,000.00	1,219.14	703.00	775.00	2,305.84	2,542.00
Prow Pass	786,500.00	551,000.00	*	*	0.00	0.00	*	*	*	*
Prow Pass	786,700.00	551,400.00	*	*	0.00	0.00	*	*	*	*
Prow Pass	786,550.00	551,400.00	*	*	0.00	0.00	*	*	*	*
Prow Pass	782,850.00	550,625.00	*	*	0.00	0.00	*	*	*	*
Prow Pass	786,600.00	550,900.00	*	*	0.00	0.00	*	*	*	*

TABLE 3a.
SAMPLE DISTRIBUTION
(Number of analyses)

<u>Glass</u>	Statigraphic Unit													<u>Sum</u>
	<u>Tpc</u>	<u>Tpy</u>	<u>Tb</u>	<u>Tpp</u>	<u>Tpt</u>	<u>Tht</u>	<u>Tcp</u>	<u>Tcb</u>	<u>Tct</u>	<u>Tfb</u>	<u>Tlr</u>	<u>Tb</u>	<u>Tot</u>	
<u>Borehole</u>														
USW G-1	*	*	*	*	*	*	*	*	*	*	*	*	*	0
USW G-2	*	9	5	3	*	*	*	*	*	*	*	*	*	17
USW G-3	*	*	*	*	*	*	*	*	*	*	*	*	*	0
USW GU-3	3	*	*	*	19	5	1	*	*	*	*	*	*	28
USW G-4	*	*	*	*	*	3	*	*	*	*	*	*	*	3
USW H-3	*	*	*	*	*	*	*	*	*	*	*	*	*	0
USW H-4	*	*	*	*	*	6	*	*	*	*	*	*	*	6
USW H-5	4	*	*	*	1	6	3	*	*	*	*	*	*	14
UE-25a#1	2	*	18	*	1	*	1	*	*	*	*	*	*	20
UE-25b#1	*	*	*	*	*	*	*	*	*	*	*	*	*	0
UE-25p#1	*	*	*	*	*	*	*	*	*	*	*	*	*	0
J-13	*	*	*	*	8	5	*	*	*	*	*	*	*	13
Prow Pass	*	*	*	*	11	*	*	*	*	*	*	*	*	11
<u>Sum</u>	9	9	21	3	40	25	5	0	0	0	0	0	0	<u>112</u>

 Includes 7 high alumina (13.4 % or greater) and low silica (70.5 % or less) samples.

TABLE 3b.
SAMPLE DISTRIBUTION

Whole Rock

(Number of analyses)

Statigraphic Unit

<u>Borehole</u>	<u>Tpc</u>	<u>Tpy</u>	<u>Tb</u>	<u>Tpp</u>	<u>Tpt</u>	<u>Tht</u>	<u>Tcp</u>	<u>Tcb</u>	<u>Tct</u>	<u>Tfb</u>	<u>Tlr</u>	<u>Tb</u>	<u>Tot</u>	<u>Sum</u>
USW G-1	*	*	*	*	*	*	*	*	*	*	*	*	*	0
USW G-2	*	*	*	1	*	2	2	2	2	1	1	1	1	13
USW G-3 &														
USW GU-3	*	*	*	*	*	1	2	1	2	*	4	*	2	12
USW G-4	*	*	*	*	1	2	2	1	1	*	*	*	*	7
USW H-3	*	*	*	*	*	*	*	*	*	*	*	*	*	0
USW H-4	*	*	*	*	*	*	*	*	*	*	*	*	*	0
USW H-5	*	*	*	*	*	*	*	*	*	*	*	*	*	0
UE-25a#1	*	*	*	*	2	3	1	1	*	*	*	*	*	7
UE-25b#1	*	*	*	*	*	*	*	2	4	*	1	*	*	7
UE-25p#1	*	*	*	*	*	*	3	3	*	*	*	*	2	8
J-13	*	*	*	*	*	2	2	1	2	*	*	*	*	7
Prow Pass	*	*	*	*	*	2	*	*	*	*	*	*	*	2
<u>Sum</u>	0	0	0	1	3	12	12	11	11	1	6	1	5	<u>63</u>

TABLE 3c.
SAMPLE DISTRIBUTION

Clinoptilolite

(Number of analyses)

Statigraphic Unit

<u>Borehole</u>	<u>Tpc</u>	<u>Tpy</u>	<u>Tb</u>	<u>Tpp</u>	<u>Tpt</u>	<u>Tht</u>	<u>Tcp</u>	<u>Tcb</u>	<u>Tct</u>	<u>Tfb</u>	<u>Tlr</u>	<u>Tb</u>	<u>Tot</u>	<u>Sum</u>
USW G-1	*	*	*	*	1	7	4	1	*	4	*	*	*	17
USW G-2	*	*	*	17	3	18	16	*	*	*	*	*	*	54
USW G-3	*	*	*	*	6	*	20	10	18	*	2	*	*	56
USW GU-3	*	*	*	*	*	*	*	*	*	*	*	*	*	0
USW G-4	*	*	*	*	*	18	31	10	*	*	*	*	*	59
USW H-3	*	*	*	*	*	*	5	*	*	*	*	*	*	5
USW H-4	*	*	*	*	*	16	7	*	*	*	*	*	*	23
USW H-5	*	*	*	*	2	14	4	*	*	*	*	*	*	20
UE-25a#1	*	*	*	*	11	28	25	*	*	*	*	*	*	64
UE-25b#1	*	*	*	*	*	*	*	22	*	*	*	*	*	22
UE-25p#1	*	*	*	*	*	15	18	*	3	*	12	*	*	48
J-13	*	*	*	*	22	14	*	*	*	*	*	*	*	36
Prow Pass	*	*	*	*	8	24	*	*	*	*	*	*	*	32
<u>Sum</u>	0	0	0	17	53	154	130	43	21	4	14	0	0	<u>436</u>

 All high alumina (14.5 % or greater)
and high lime (5.5 % or greater) samples.

Table 3d.

SAMPLE DISTRIBUTION

(g = glass, r = whole rock, c = clinoptilolite)

<u>Borehole</u>	<u>Stratigraphic Unit</u>													
	<u>Tpc</u>	<u>Tpy</u>	<u>Tb</u>	<u>Tpp</u>	<u>Tpt</u>	<u>Tht</u>	<u>Tcp</u>	<u>Tcb</u>	<u>Tct</u>	<u>Tfb</u>	<u>Tlr</u>	<u>Tb</u>	<u>Tot</u>	
USW G-1	*	*	*	*	c	c	c	c	*	c	*	*	*	
USW G-2	*	g	g	grc	c	rc	rc	r	r	r	r	r	r	
USW G-3 &														
USW GU-3	g	*	*	*	gc	gr	grc	rc	rc	*	rc	*	r	
USW G-4	*	*	*	*	r	grc	rc	rc	r	*	*	*	*	
USW H-3	*	*	*	*	*	*	c	*	*	*	*	*	*	
USW H-4	*	*	*	*	*	gc	c	*	*	*	*	*	*	
USW H-5	g	*	*	*	gc	gc	gc	*	*	*	*	*	*	
UE-25a#1	g	*	g	*	grc	rc	grc	r	*	*	*	*	*	
UE-25b#1	*	*	*	*	*	*	*	rc	r	*	r	*	*	
UE-25p#1	*	*	*	*	*	c	rc	r	c	*	c	*	*	
J-13	*	*	*	*	gc	grc	r	r	r	*	*	*	*	
Prow Pass	*	*	*	*	gc	rc	*	*	*	*	*	*	*	

TABLE 3e.
SAMPLE DISTRIBUTION
(Number of analyses)

Analcime

Statigraphic Unit

<u>Borehole</u>	<u>Tpc</u>	<u>Tpy</u>	<u>Tb</u>	<u>Tpp</u>	<u>Tpt</u>	<u>Tht</u>	<u>Tcp</u>	<u>Tcb</u>	<u>Tct</u>	<u>Tfb</u>	<u>Tlr</u>	<u>Tb</u>	<u>Tot</u>	<u>Sum</u>
USW G-1	*	*	*	*	*	*	*	*	11	*	23	*	24	58
USW G-2	*	*	*	*	*	*	*	*	*	*	*	*	*	0
USW G-3	*	*	*	*	*	*	*	*	*	*	*	*	*	0
USW GU-3	*	*	*	*	*	*	*	*	*	*	*	*	*	0
USW G-4	*	*	*	*	*	*	*	*	*	*	*	*	*	0
USW H-3	*	*	*	*	*	*	*	*	*	*	*	*	*	0
USW H-4	*	*	*	*	*	*	*	*	*	*	*	*	*	0
USW H-5	*	*	*	*	*	*	*	*	*	*	*	*	*	0
UE-25a#1	*	*	*	*	*	*	*	*	*	*	*	*	*	0
UE-25b#1	*	*	*	*	*	*	*	*	8	*	*	*	*	8
UE-25p#1	*	*	*	*	*	*	*	5	*	1	*	*	*	6
J-13	4	*	*	*	*	*	6	*	*	*	*	*	*	10
Prow Pass	*	*	*	*	*	*	*	*	*	*	*	*	*	0
<u>Sum</u>	4	0	0	0	0	0	6	5	19	0	24	0	24	82

TABLE 3f.
SAMPLE DISTRIBUTION
(Number of analyses)

Albite

Statigraphic Unit

<u>Borehole</u>	<u>Tpc</u>	<u>Tpy</u>	<u>Tb</u>	<u>Tpp</u>	<u>Tpt</u>	<u>Tht</u>	<u>Tcp</u>	<u>Tcb</u>	<u>Tct</u>	<u>Tfb</u>	<u>Tlr</u>	<u>Tb</u>	<u>Tot</u>	<u>Sum</u>
USW G-1	*	*	*	*	*	*	*	*	*	*	3	*	28	31
USW G-2	*	*	*	*	*	*	*	*	*	*	4	*	5	9
USW G-3	*	*	*	*	*	*	*	*	*	*	*	*	*	0
USW GU-3	*	*	*	*	*	*	*	*	*	*	*	*	*	0
USW G-4	*	*	*	*	*	*	*	*	*	*	*	*	*	0
USW H-3	*	*	*	*	*	*	*	*	*	*	*	*	*	0
USW H-4	*	*	*	*	*	*	*	*	*	*	*	*	*	0
USW H-5	*	*	*	*	*	*	*	*	*	*	*	*	*	0
UE-25a#1	*	*	*	*	*	*	*	*	*	*	*	*	*	0
UE-25b#1	*	*	*	*	*	*	*	*	*	*	*	*	*	0
UE-25p#1	*	*	*	*	*	*	*	*	*	*	*	*	*	0
J-13	*	*	*	*	*	*	*	*	3	*	*	*	*	3
Prow Pass	*	*	*	*	*	*	*	*	*	*	*	*	*	0
<u>Sum</u>	0	0	0	0	0	0	0	0	3	0	7	0	33	<u>43</u>

TABLE 3g.
SAMPLE DISTRIBUTION

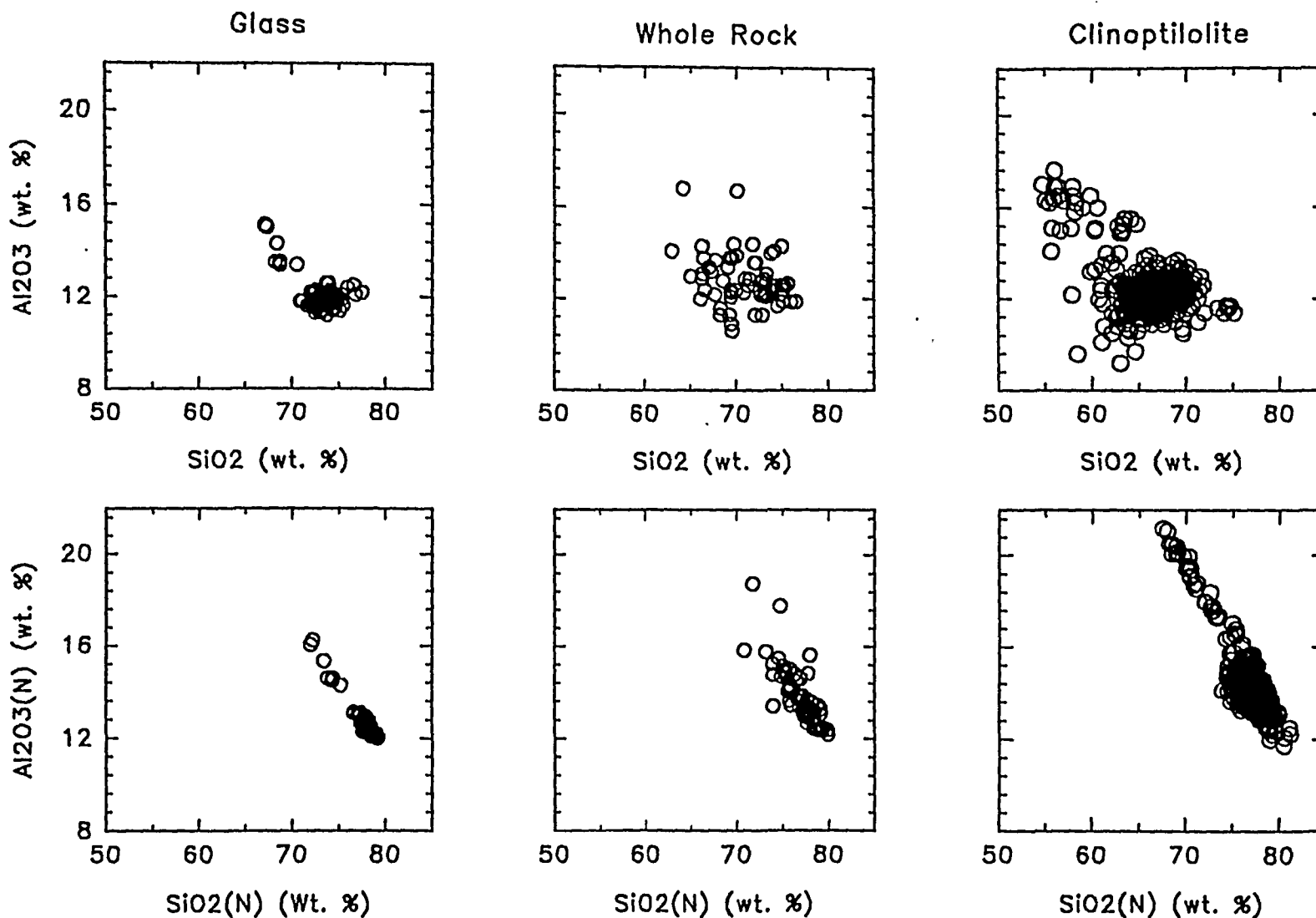
Adularia

(Number of analyses)

Statigraphic Unit

<u>Borehole</u>	<u>Tpc</u>	<u>Tpy</u>	<u>Tb</u>	<u>Tpp</u>	<u>Tpt</u>	<u>Tht</u>	<u>Tcp</u>	<u>Tcb</u>	<u>Tct</u>	<u>Tfb</u>	<u>Tlr</u>	<u>Tb</u>	<u>Tot</u>	<u>Sum</u>
USW G-1	*	*	*	*	*	*	*	*	*	*	3	*	6	9
USW G-2	*	*	*	*	*	5	*	*	*	*	2	*	1	8
USW G-3	*	*	*	*	*	*	*	*	*	*	1	*	*	1
USW GU-3	*	*	*	*	*	*	*	*	*	*	*	*	*	0
USW G-4	*	*	*	*	*	*	*	1	*	*	*	*	*	1
USW H-3	*	*	*	*	*	*	*	*	*	*	*	*	*	0
USW H-4	*	*	*	*	*	*	*	*	*	*	*	*	*	0
USW H-5	*	*	*	*	*	*	*	*	*	*	*	*	*	0
UE-25a#1	*	*	*	*	*	*	*	*	*	*	*	*	*	0
UE-25b#1	*	*	*	*	*	*	*	*	*	*	*	*	*	0
UE-25p#1	*	*	*	*	*	*	*	*	*	*	*	*	*	0
J-13	*	*	*	*	*	*	*	*	*	*	*	*	*	0
Prow Pass	*	*	*	*	*	2	*	*	*	*	*	*	*	2
<u>Sum</u>	0	0	0	0	0	7	0	1	0	0	6	0	7	<u>21</u>

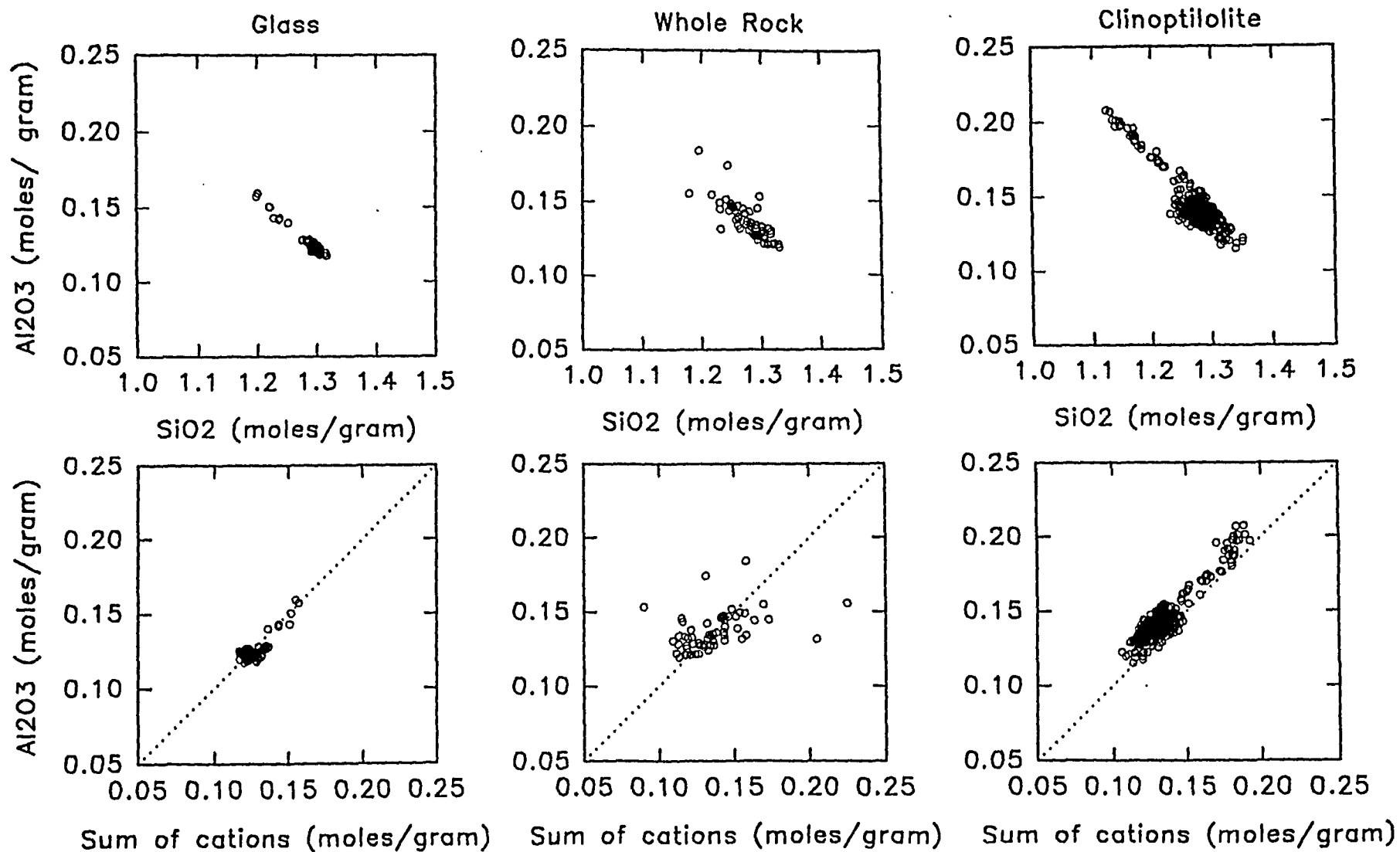
Figure 3. Comparison of Normalized and Unnormalized Oxides for Glass, Whole Rock and Clinoptilolite.



8

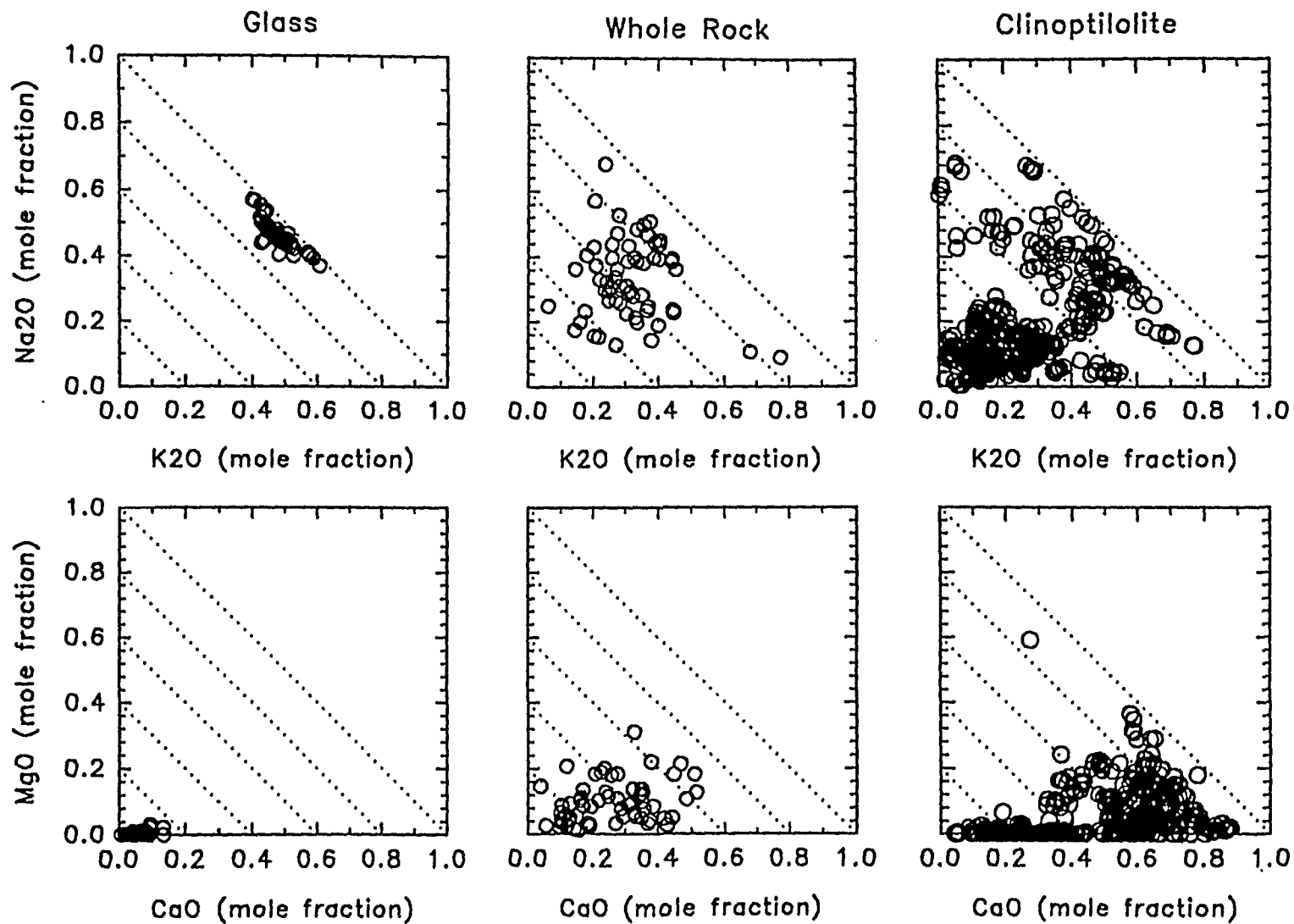
Comparison of reported oxide values with values normalized to the sum of oxides, (SiO₂+ TiO₂+Al₂O₃+Fe₂O₃+MgO+CaO+BaO+Na₂O+K₂O) for glass and clinoptilolite, (SiO₂+ TiO₂+ Al₂O₃+Fe₂O₃+MnO+MgO+CaO+Na₂O+K₂O+P₂O₅) for whole rock.

Figure 4. Comparison of Framework Oxides and Sum of Interstitial Oxides for Glass, Whole Rock and Clinoptilolite.



Plots of molar abundances of oxides normalized to the total moles of SiO₂+Al₂O₃+MgO+CaO+Na₂O+K₂O. Sum of cations = MgO+CaO+Na₂O+K₂O.

Figure 5. Cross Plots of Interstitial Cation Oxides for Glass, Whole Rock and Clinoptilolite.



Comparison of oxides normalized to (MgO+CaO+Na₂O+K₂O) for glass, whole rock and clinoptilolite.

CHEMICAL AND SPATIAL DIVERSITY OF ALTERATION MINERALS AT YUCCA MOUNTAIN, RESULTS

Diversity within Boreholes and at Surface Locations

This section presents the principal data that are the subject of this review. The data are that given in Appendix F of Broxton, *et al.* (1986). The samples were collected from ten boreholes and one surface location at Yucca Mountain.

USW G-1

Borehole USW G-1 (Figure 2) is located along the northern boundary of the potential repository in the central part of Yucca Mountain in Drill Hole Wash. The ground surface elevation is at 4,348.6 feet and the present day water table is at 2,471.1 feet (Table 2). Seventeen samples of clinoptilolite from eleven different elevations were analyzed (Figure 6). The shallowest sample, from the Topopah Spring member (Tpt) of the Paintbrush tuff, is exceedingly rich in CaO and very poor in MgO, Na₂O and K₂O. All analyses in this borehole are low in MgO. There is a general increase of Na₂O with increasing depth. The deepest samples, from the dacite flow breccia (Tfb), are very high in Na₂O but have negligible K₂O. Intermediate samples from the tuff of Calico Hills (Tht) and the Prow Pass and Bull Frog members (Tcp and Tcb) of the Crater Flat Tuff are alkali rich with similarly large amounts of Na₂O and K₂O, CaO is generally low. No significant changes in chemistry are obviously related to the present day water table but there could be some significant changes in chemistry related to some of the boundaries between lithologic-stratigraphic units. The diversity of chemistry in this borehole marks out at least a three end member field in

the upper right hand diagram of Figure 6, Na_2O vs. K_2O . The samples from the Paintbrush tuff (Tpt) and the flow breccia (Tfb) are markedly different in chemical composition from that of the glass (compare with Figure 5). Some of the analyses from the tuff of Calico Hills (Tht) and the Prow Pass member (Tcp) of the Crater Flat tuff are not too different from that of the parental glass.

USW G-2

Borehole USW G-2 is located in the northern part of Yucca Mountain (Figure 2) south of Yucca Wash and just to the east of the Solitario Canyon Fault near the head of Solitario Canyon. The ground elevation is 5,098.4 feet and the water table elevation is 3,387.8 feet (Table 2). Fifty four analyses of clinoptilolite from thirteen different elevations are reported (Figures 7a, 7b and 7c). The shallowest samples are from the Pah Canyon member (Tpp) of the Paintbrush tuff, see left-hand diagrams of Figure 7a. These samples are very high in CaO and MgO, see lower right-hand diagram of Figure 7a. The immediately subjacent top bed of the Topopah Spring member (Tpt) is similar in composition but richer in K_2O and poorer in CaO. The base of the Topopah Spring member has negligible MgO, higher Na_2O and K_2O and lesser CaO. The base of the Topopah Spring member is very similar in chemical composition to the underlying tuff of Calico Hills (Tht) but distinctly different from the upper beds of the Topopah Spring member. All samples above 2,668 feet of elevation are rich in CaO, see lower right hand diagram of Figure 7a. All samples in the Prow Pass member (Tcp) of the Crater Flat tuff are very low in MgO and high in Na_2O while K_2O is very low to moderate. No change in chemical composition of

the clinoptilolites occurs at the location of the present day water table and strong changes in chemical composition are not systematically related to stratigraphic boundaries.

Because of the overlap of data points on the two right hand cross plots of Figure 7a, detailed cross plots for each stratigraphic unit, by sample elevation, are included in the following two figures (Figures 7b and 7c). The compositions of the clinoptilolites of the Pah Canyon member (Tpp, Figure 7b) of the Paintbrush tuff and from the tuff of Calico Hills (Tht, Figure 7c) are tightly grouped. The differences in chemical composition of the samples from the top and bottom of the Topopah Spring member (Tpt) are shown in the two right-hand diagrams of Figure 7b. The calcic nature of these beds of the Paintbrush tuff has been pointed out by Broxton, *et al.* (1986). The differences among the samples from the Prow Pass member (Tcp) of the Crater Flat tuff are shown in the two right-hand diagrams of Figure 7c. Especially notable is the difference among samples from the same elevation, 2,031 feet. Very clearly this demonstrates that, even at the same elevation and below the present day water table, clinoptilolite samples can be out of equilibrium with one another.

USW G-3

Borehole USW G-3 (Figure 2) is located along Yucca Ridge south of the potential repository. The ground surface elevation is 4,856.6 feet and the water table is at 2,397.7 feet of elevation (Table 2). Fifty six samples of clinoptilolite from fourteen different elevations were analyzed (Figures 8a, 8b and 8c). Again, the samples

from the Topopah Spring member of the Paintbrush tuff (Tpt), are very rich in CaO and moderately rich in MgO. A general increase in Na₂O is noted with increasing depth of the borehole. Both CaO and K₂O vary irregularly but in a complementary fashion with respect to one another. The lowest concentration of CaO occurs in clinoptilolites from the Prow Pass member (Tcp) of the Crater Flat tuff at 2,871 feet of elevation. MgO is generally low throughout most of the borehole. Large differences can be noted for both CaO and K₂O within the Bull Frog member (Tcb) of the Crater Flat tuff, see upper and lower right-hand diagrams of Figure 9a. This substantial change in clinoptilolite chemistry occurs 60 to 100 feet below the present day water table. K₂O is nearly absent at the deepest level (Tlr, 434 feet). Significant changes do not seem to be related to stratigraphic boundaries, however, sample spacing is inadequate to determine if this is truly so. Detail diagrams for this borehole are shown in Figures 8b and 8c for members of the Crater Flat tuff (Tcp, Tcb and Tct). The Prow Pass member (Tcp) is more potash rich and soda poor than the Tram member (Tct). Both members show that there are distinct differences in total alkali content at different elevations within each unit. In each case the samples from lower elevations are richer in alkalis than those from upper elevations and possibly significant differences of the Na₂O to K₂O ratio occur at individual elevations (2,871 feet for Tcp and 1,185 feet for Tct). The intermediate member, the Bull Frog member (Tcb), is moderately rich in lime.

USW G-4

Borehole USW G-4 (Figure 2) is located in the central part of Yucca Mountain. The

ground surface elevation is 4,166.9 feet and the water table is at 2,394.4 feet of elevation (Table 2). Fifty nine samples of clinoptilolite from nine different elevations were analyzed (Figures 9a, 9b and 9c). Samples collected from below the water table are rich in CaO but contain only minor concentrations of MgO, Na₂O and K₂O. Samples above the water table are rich in Na₂O and K₂O and low in MgO and CaO. Clinoptilolite compositions from the upper part of the Prow Pass member (Tcp) of the Crater Flat tuff are very similar to the overlying beds of the tuff of Calico Hills but markedly different from lower beds of the Prow Pass member. The marked chemical changes are not associated with stratigraphic boundaries and, importantly, are distinctly different from the patterns of marked chemical changes observed in boreholes USW G-1, USW G-2 and USW G-3. The detailed figures, 9b and 9c, show the uniform character of the chemical composition of the clinoptilolites from the tuff of Calico Hills (Tht), which are not markedly different from the composition of glass (see Figure 5). The Bull Frog member (Tcb) of the Crater Flat tuff is markedly CaO rich. The marked contrast of the chemical analyses between different levels of the Prow Pass member (Tcp) of the Crater Flat tuff are shown in the right-hand diagrams in Figure 9b. Samples from the upper elevation, 2,405 feet, are alkali rich while those from the lower elevations, 2,035 to 1,928 feet, are markedly rich in calcium.

USW H-3

Borehole USW H-3 (Figure 2) is located along Yucca Ridge south of the potential repository. The ground surface elevation is 4,866.4 feet and the water table is at

2,466.6 feet of elevation (Table 2). Five samples of clinoptilolite from a single elevation of the Prow Pass member (T_{cp}) of the Crater Flat tuff were analyzed (Figure 10). All five chemical analyses show a high content of CaO, very little MgO and only moderate amounts of Na₂O and K₂O.

USW H-4

Borehole USW H-4 (Figure 2) is located near the central part of Yucca Mountain. The ground surface elevation is 4,096.5 feet and the water table is at 1,699.0 feet of elevation (Table 2). Twenty three analyses from four different elevations are available (Figures 11a and 11b). Samples from above the water table (all from the tuff of Calico Hills, T_{ht}) are variable in CaO, MgO and K₂O content and low in Na₂O while those below the water table (all Prow Pass member, T_{cp}, of the Crater Flat tuff) are very high in Na₂O and K₂O and very low in MgO and CaO. The diversity of the chemical compositions of the clinoptilolites from the tuff of Calico Hills (T_{ht}) are well illustrated in the left-hand diagrams of Figure 11b. The samples are CaO rich but with distinctly different compositions at different elevations. The compositions of the clinoptilolites from the Prow Pass member (T_{cp}) of the Crater Flat tuff are alkali rich and very similar to the analyses of glass (compare with Figure 5). Distinctly different chemical compositions may or may not be related to the boundaries of the stratigraphic units and to the position of the present day water table.

USW H-5

Borehole USW H-5 (Figure 2) is located along Yucca Ridge near the central part of

Yucca Mountain. The ground surface elevation is 4,850.8 feet and the water table is at 2,542.0 feet of elevation (Table 2). Twenty analyses from four different elevations are available (Figure 12). All samples were collected from above the present day water table. The most shallow samples, from the Topopah Spring member (Tpt) of the Paintbrush tuff, are very rich in CaO, contain moderate amounts of MgO but are very poor in both Na₂O and K₂O. The clinoptilolites from the tuff of Calico Hills (Tht) and the Prow Pass member (Tcp) of the Crater Flat tuff are similar in chemical composition and rich in Na₂O and K₂O with nearly no MgO and little CaO.

UE-25 a#1 & UE-25 b#1

Boreholes UE-25 a#1 and UE-25 b#1 are located in Drill Hole Wash, to the east of the potential repository site. The ground surface elevation is 3,934.4 feet and the water table is at 2,397.7 feet of elevation (both values for UE-25 a#1, Table 2). These two drill holes are treated as one for the purposes of this review. Results of eighty six analyses from fifteen different elevations are available, Figures 13a, 13b and 13c. Again, the uppermost samples, the Topopah Spring member of the Paintbrush tuff (Tpt), are rich in CaO but the shallowest sample (2,655 feet) is exceedingly rich in MgO (the highest value reported for Yucca Mountain), see lower right-hand diagram of Figure 13a and the lower left-hand diagram of Figure 13b. Most of the samples from the Topopah Spring member (Tpt) and the tuff of Calico Hills (Tht) are similar to one another in their chemical composition and similar to most of the samples from the Prow Pass member (Tcp) of the Crater Flat tuff. One

of two samples from the tuff of Calico Hills (Tht) at 2,469 feet is richer in K_2O and lower in CaO than the other sample from the same elevation. One sample from the Prow Pass member (Tcp), at an elevation of 1,821 feet, is markedly low in CaO and high in Na_2O and K_2O , see the right-hand diagrams of Figure 13a and the left-hand diagrams of Figure 13c. This sample is not very different from the parent glass, see upper left-hand diagram of Figure 5. The lowermost samples, from the Bull Frog member (Tcb) of the Crater Flat tuff (see right-hand diagrams of Figure 13c), are also similar in chemical composition to most of the other samples from this borehole. Marked changes in chemical composition are not related to either stratigraphic boundaries nor to the present day water table. Other than the previously mentioned anomalies, there is no overall changing trend of the chemical compositions of the clinoptilolites with depth at this locality. MgO , Na_2O and K_2O show some slight variations but are consistently of low abundance.

UE-25 p#1

Borehole UE-25 p#1 (Figure 2) is located south and east of the potential repository. The ground surface elevation is 3,654.6 feet and the water table is at 2,466.6 feet of elevation (Table 2). Forty eight samples of clinoptilolite from seven different elevations were analyzed (Figure 14). All samples were collected from below the present day water table. CaO is by far the most abundant interstitial cation oxide and shows a regular increase with increasing depth. Na_2O and K_2O show a regular decrease with increasing depth and MgO is very low and irregular.

J-13

Borehole J-13 is located east of Yucca Mountain and Forty Mile Wash on the western edge of Jackass Flat, see Figure 2. The ground surface elevation is 3,318.0 feet and the water table is at 2,387.8 feet of elevation. The results of thirty six analyses of clinoptilolites from six different elevations are available, see Figures 15a and 15b. Most samples are generally high in CaO except for those from 1,897 feet of elevation which are relatively high in K₂O. This marked change in chemistry occurs within beds of the lower Topopah Spring member (Tpt) of the Paintbrush tuff. Most of the samples from each different elevation seem to have their own distinctive chemical compositions, see Figure 15b. Interestingly, analcime occurs both above and below the clinoptilolite analyses shown here, at 2,710 feet of elevation in the Tiva Canyon member (Tpc) of the Paintbrush tuff (above the present day water table) and at 1,323 feet of elevation in the Prow Pass member (Tpc) of the Crater Flat tuff.

Prow Pass

Thirty two samples from four stratigraphic horizons were collected from surface exposures at Prow Pass northwest of the repository site (Figure 2). Ground elevations are not reported by the authors (Broxton, *et al.*, 1986). The data are presented graphically in Figure 16 in the same format as previous figures but in this case elevation is not a parameter. The several horizons are presented in stratigraphic order along the vertical axis. The results show a systematic decrease of MgO and CaO downward through the section. K₂O increases down section while

Na₂O is variable. The lowest horizon (Tht) has the highest K₂O reported for Yucca Mountain. The upper and lower horizons have their own distinctive chemistry but the two middle horizons have abundances of the several oxides that overlap one another in the two right-hand diagrams.

Summary of Chemical and Spatial Diversity within Boreholes

The following observations of the chemical alteration at the several localities are noted.

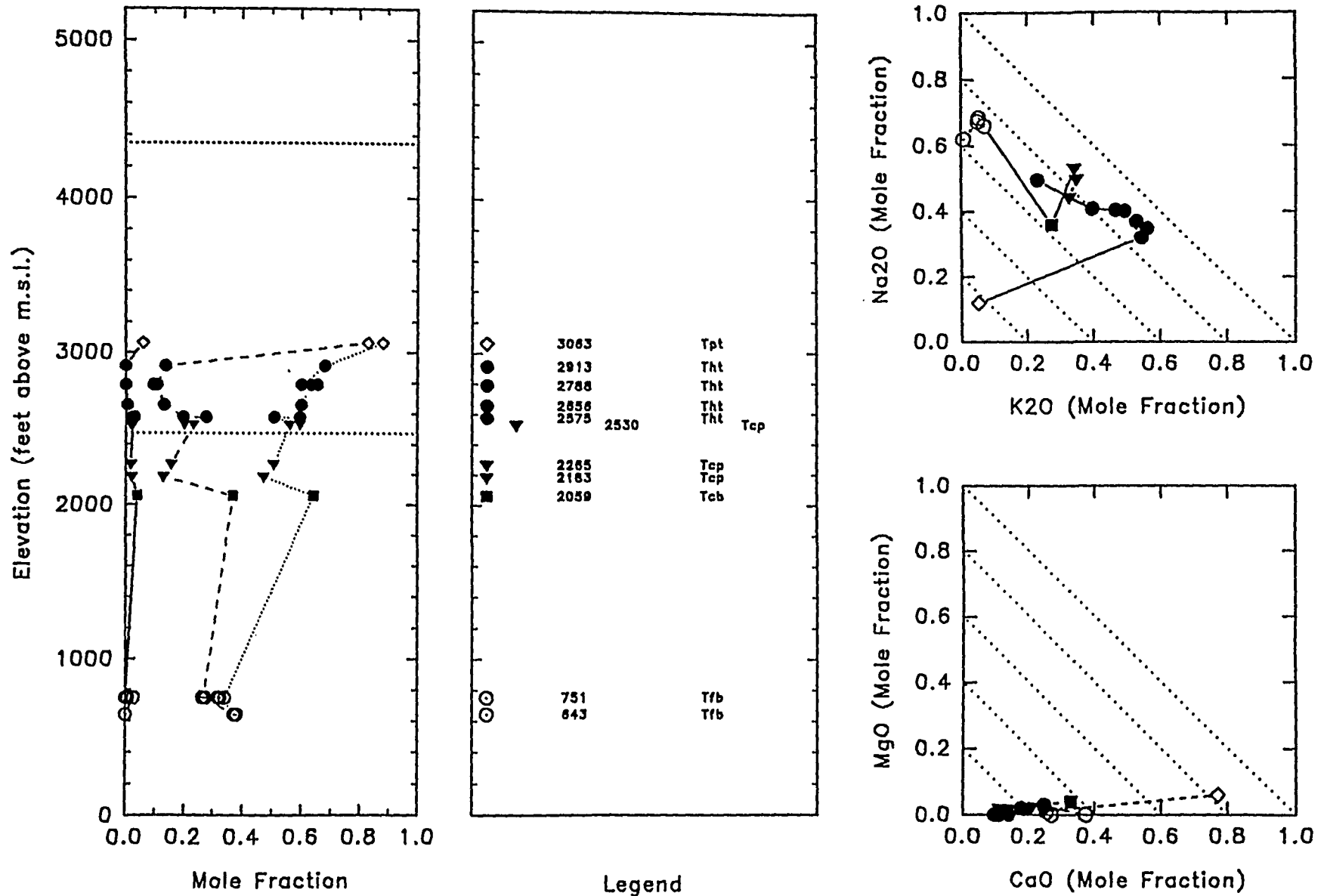
1. Most of the clinoptilolites of Yucca Mountain are calcic in character which differs markedly from the composition of the parent glass which is alkalic in character. The alteration is largely metasomatic, that is to say caused by open system water-rock interaction.
2. Distinctly divergent chemical compositions of interstitial cation metal oxides occur at discretely different elevations for all boreholes at Yucca Mountain that have been sampled and analyzed at more than one elevation.
3. Strongly divergent chemical character of clinoptilolite is displayed within a few feet in a single borehole, for example: USW G-3, Tcb, at 2,280 feet and 2,242 feet elevation .
4. Strongly divergent chemical character of clinoptilolite is displayed even at a single depth of individual boreholes, for example: USW G-2, Tcb, at 2,031 feet elevation and UE-25 a#1, Tht, at 2,469 feet of elevation (possible diversity within single thin sections ?).

5. Strongly divergent chemical character of clinoptilolite is displayed within a single stratigraphic unit in a borehole, for example: UE-25 a#1, Tpt, 2,655 feet of elevation and USW G-4, Tcp, 1,928 feet to 2,405 feet of elevation.
6. Strongly divergent chemical character of clinoptilolite is displayed even at a single level within a stratigraphic unit between levels of alteration of a different kind in a single borehole, for example: UE-25 a#1, Tcp, 1,821 feet of elevation and J-13, Tpt, 1,897 feet of elevation.
7. Strong changes in chemical composition of clinoptilolite do not have a systematic relation to stratigraphic boundaries.
8. The chemical compositions of clinoptilolites may occur in two or more clusters or groups within single stratigraphic units within individual boreholes.
9. The chemical composition of clinoptilolite can be similar across stratigraphic boundaries, USW G-4, Tht at 2,460 feet and Tcp at 2,405 feet.

The above listing of chemically diverse and distinct characteristics, "anomalies", observed within the data reported for the several boreholes support the concepts of polygenesis and epigenesis for at least some of the zeolitic metasomatic chemical alteration at Yucca Mountain. In situ pore waters would not likely have provided sufficient calcic chemical elements to have caused the observed wholesale chemical changes. Much of the calcic chemical constituents of the altered rocks must have been introduced into the rocks from sources outside of the tuffs themselves and the

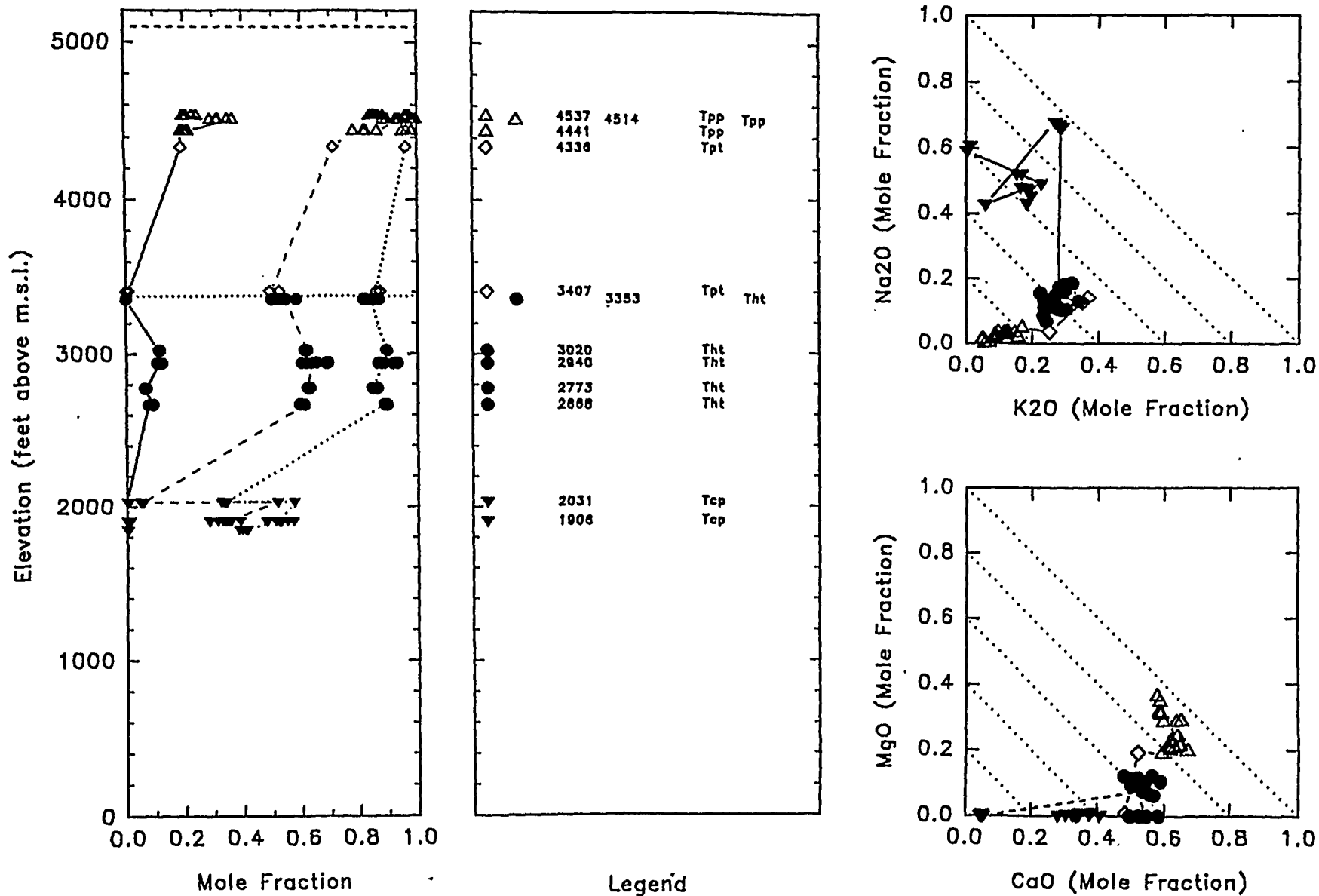
alkalic constituents must have been removed. This process, or these processes, require a great abundance of water to have been moving into, through and out of the zones of alteration. The smaller spatial scale chemical anomalies had to have been introduced into the system from sources other than the sources for the alteration of contrasting chemical composition which enclose them. The contrasting chemical alterations also must have occurred at different times from one another, because waters of distinctly different chemical composition from different sources cannot occupy the same space at the same time. The small scale anomalies of chemical alteration must have been introduced into and through discrete zones of high permeability such as faults, fractures, thin strata and breccias.

Figure 6. USW G-1, Clinoptilolite Chemistry.



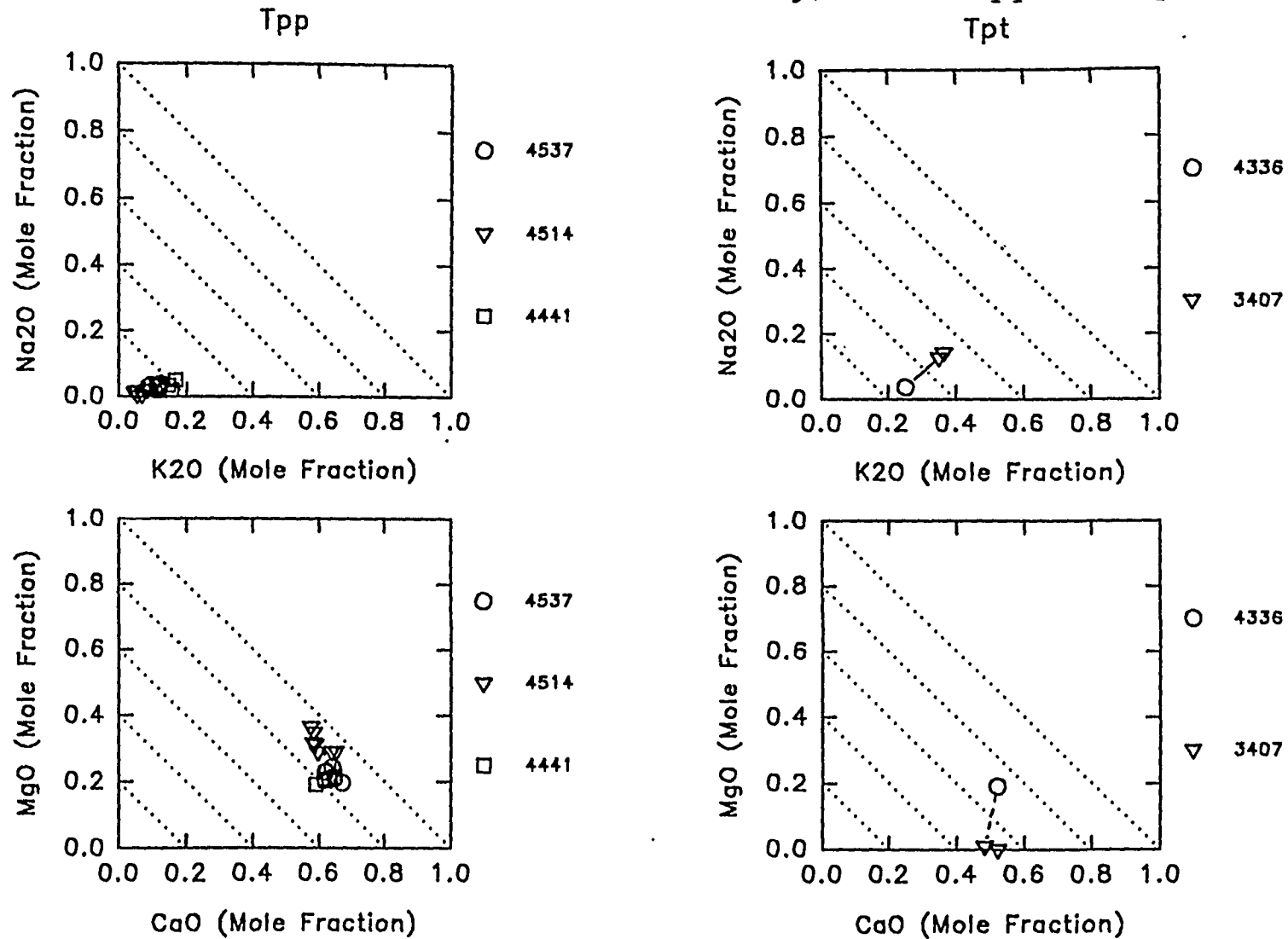
For lefthand diagram: The solid, dashed and dotted lines represent MgO, MgO+CaO and MgO+CaO+K₂O respectively divided by (MgO+CaO+K₂O+Na₂O). Horizontal dotted line = water table. Horizontal dashed line = land surface.

Figure 7a. USW G-2, Clinoptilolite Chemistry.



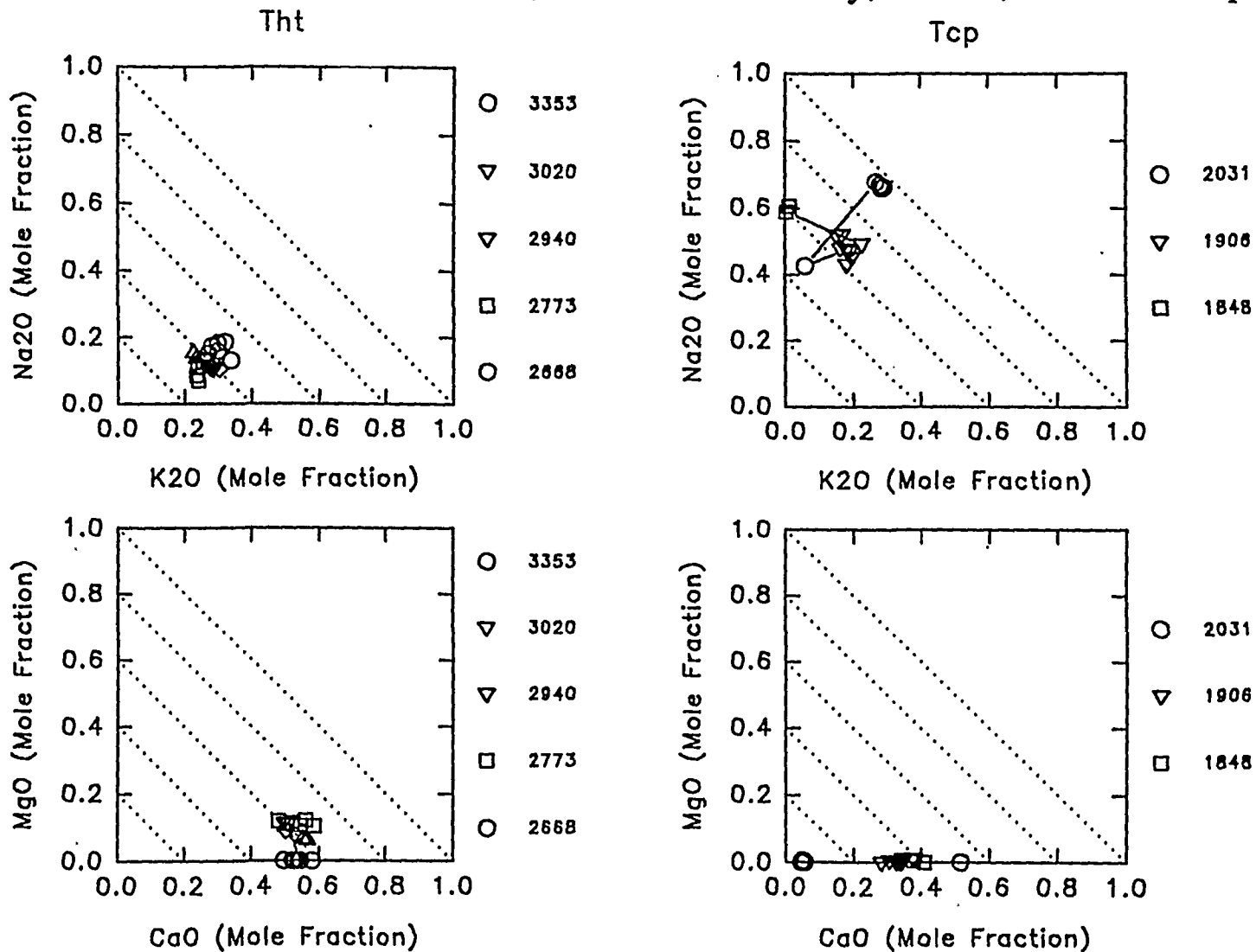
For lefthand diagram: The solid, dashed and dotted lines represent MgO, MgO+CaO and MgO+CaO+K₂O respectively divided by (MgO+CaO+K₂O+Na₂O). Horizontal dotted line = water table. Horizontal dashed line = land surface.

Figure 7b. USW G-2, Clinoptilolite Chemistry, Detail, Tpp and Tpt.



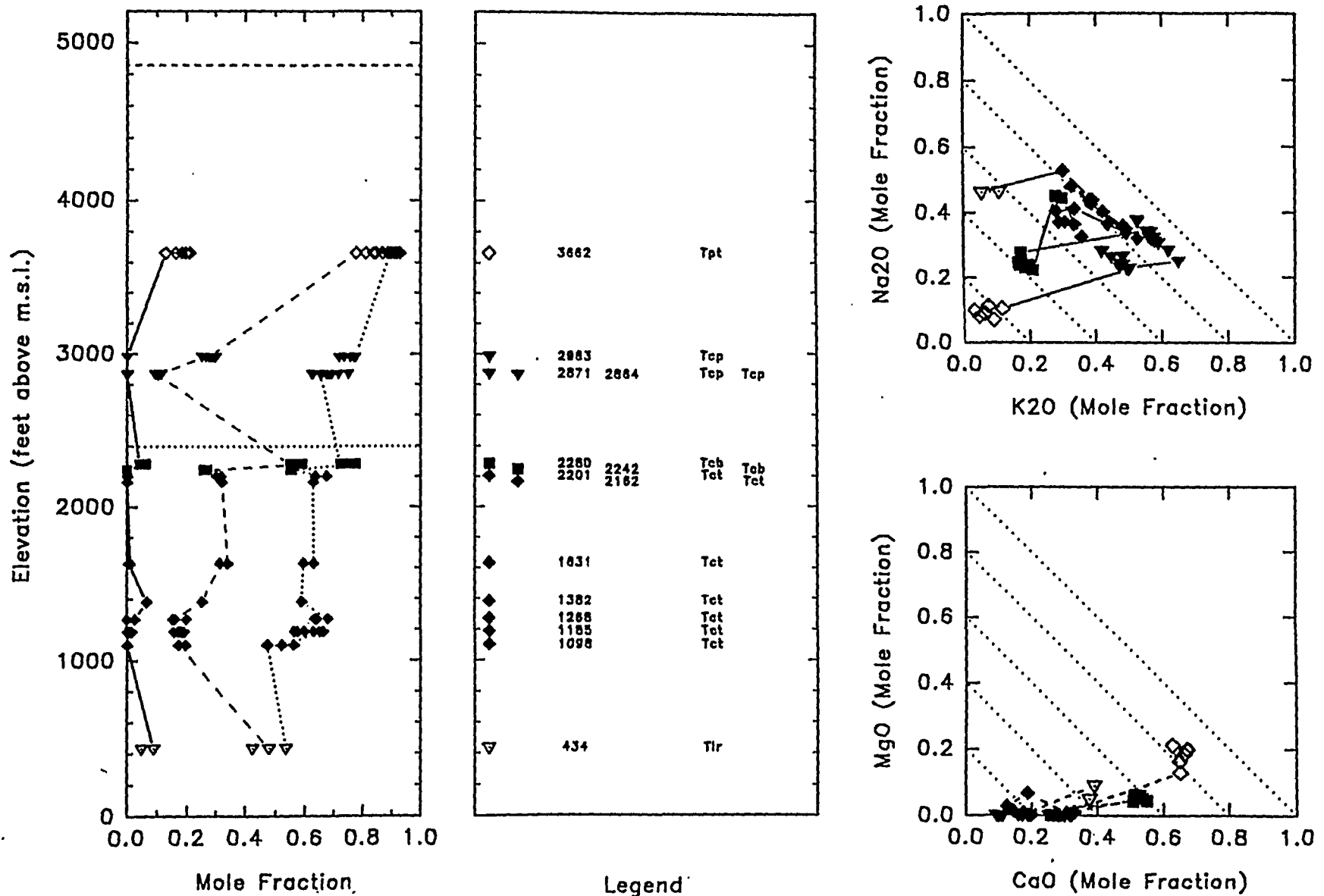
Detailed crossplots by elevation of samples for stratigraphic units, borehole USW G-2.

Figure 7c. USW G-2, Clinoptilolite Chemistry, Detail, Tht and Tcp.



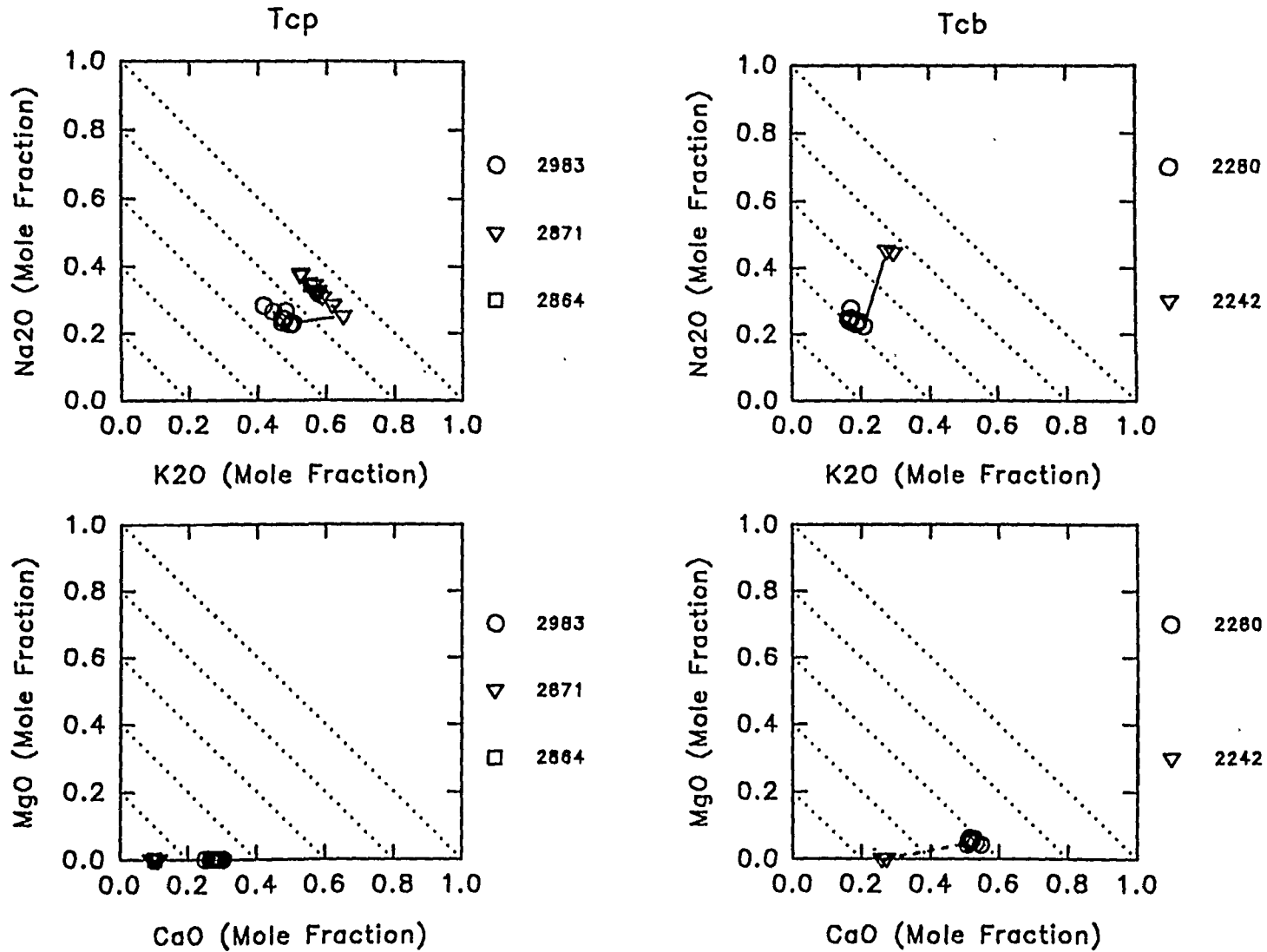
Detailed crossplots by elevation of samples for stratigraphic units, borehole USW G-2.

Figure 8a. USW G-3, Clinoptilolite Chemistry.



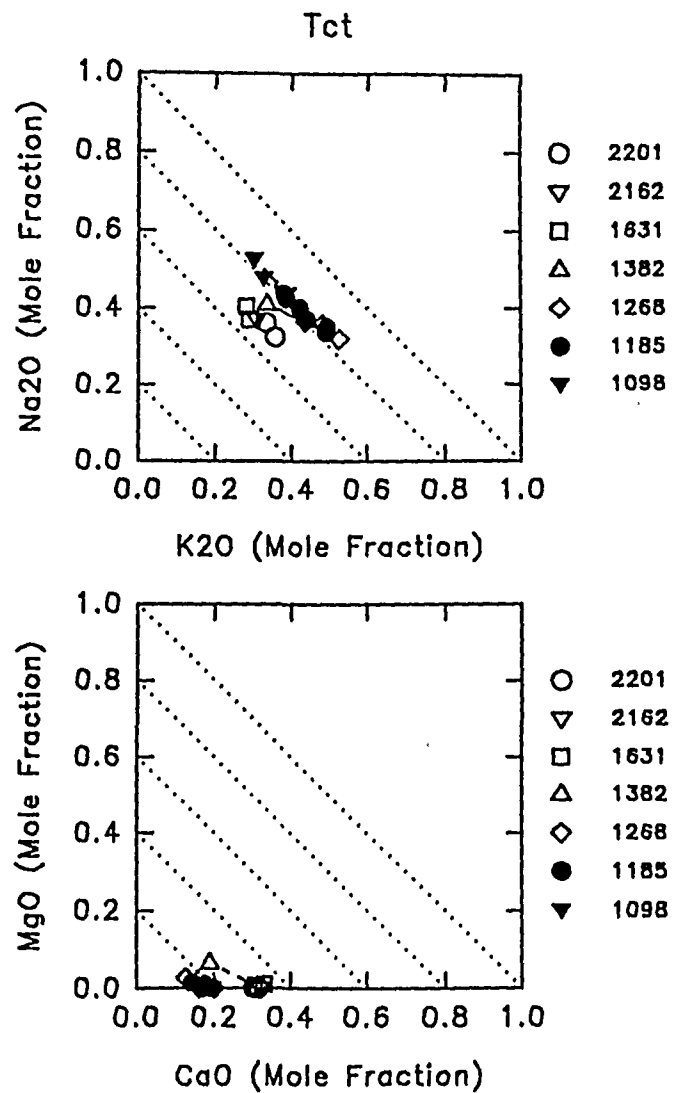
For lefthand diagram: The solid, dashed and dotted lines represent MgO, MgO+CaO and MgO+CaO+K2O respectively divided by (MgO+CaO+K2O+Na2O). Horizontal dotted line = water table. Horizontal dashed line = land surface.

Figure 8b. USW G-3, Clinoptilolite Chemistry, Detail, Tcp and Tcb.



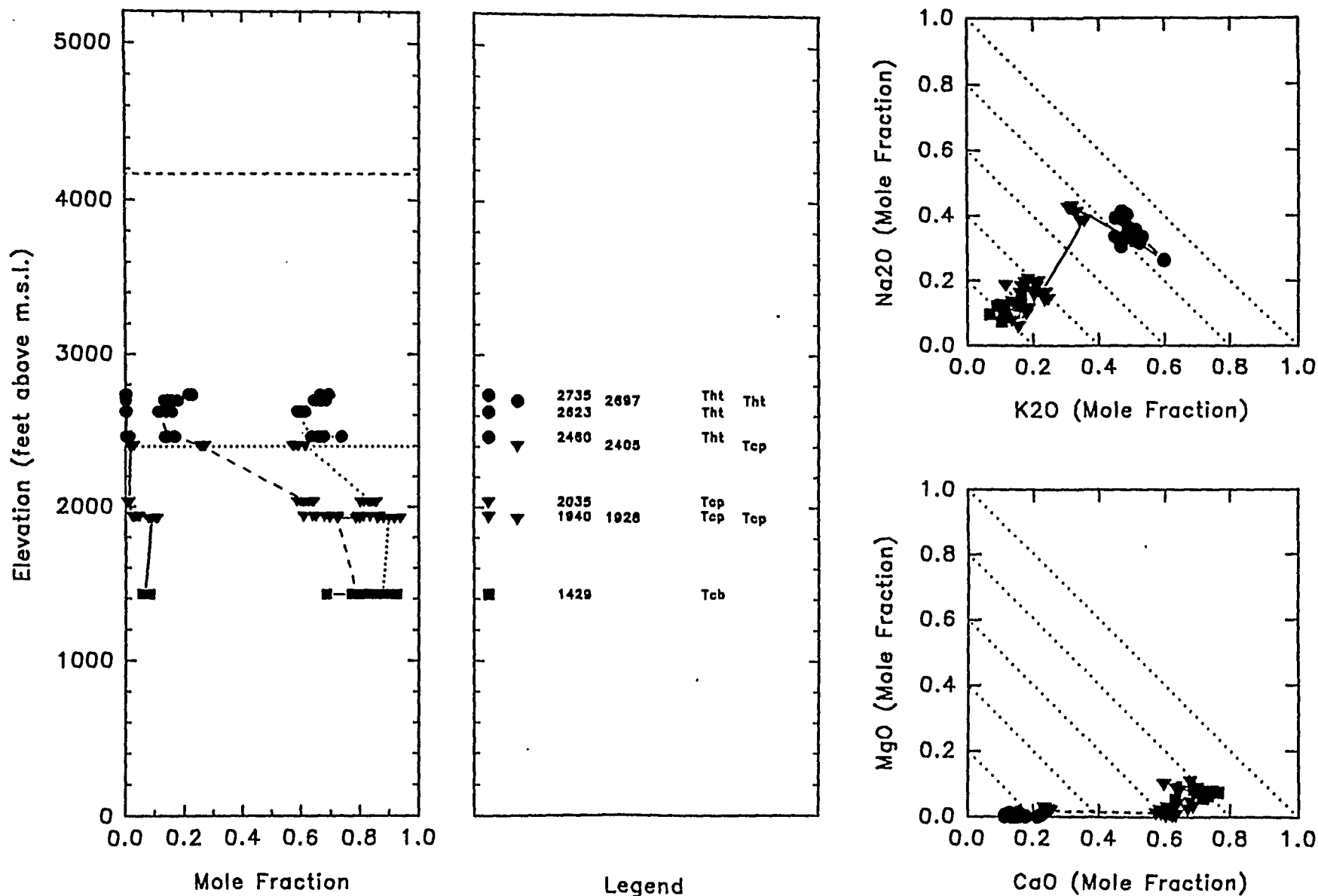
Detailed crossplots by elevation of samples for stratigraphic units, borehole USW G-3.

Figure 8c. USW G-3, Clinoptilolite Chemistry, Detail, Tct.



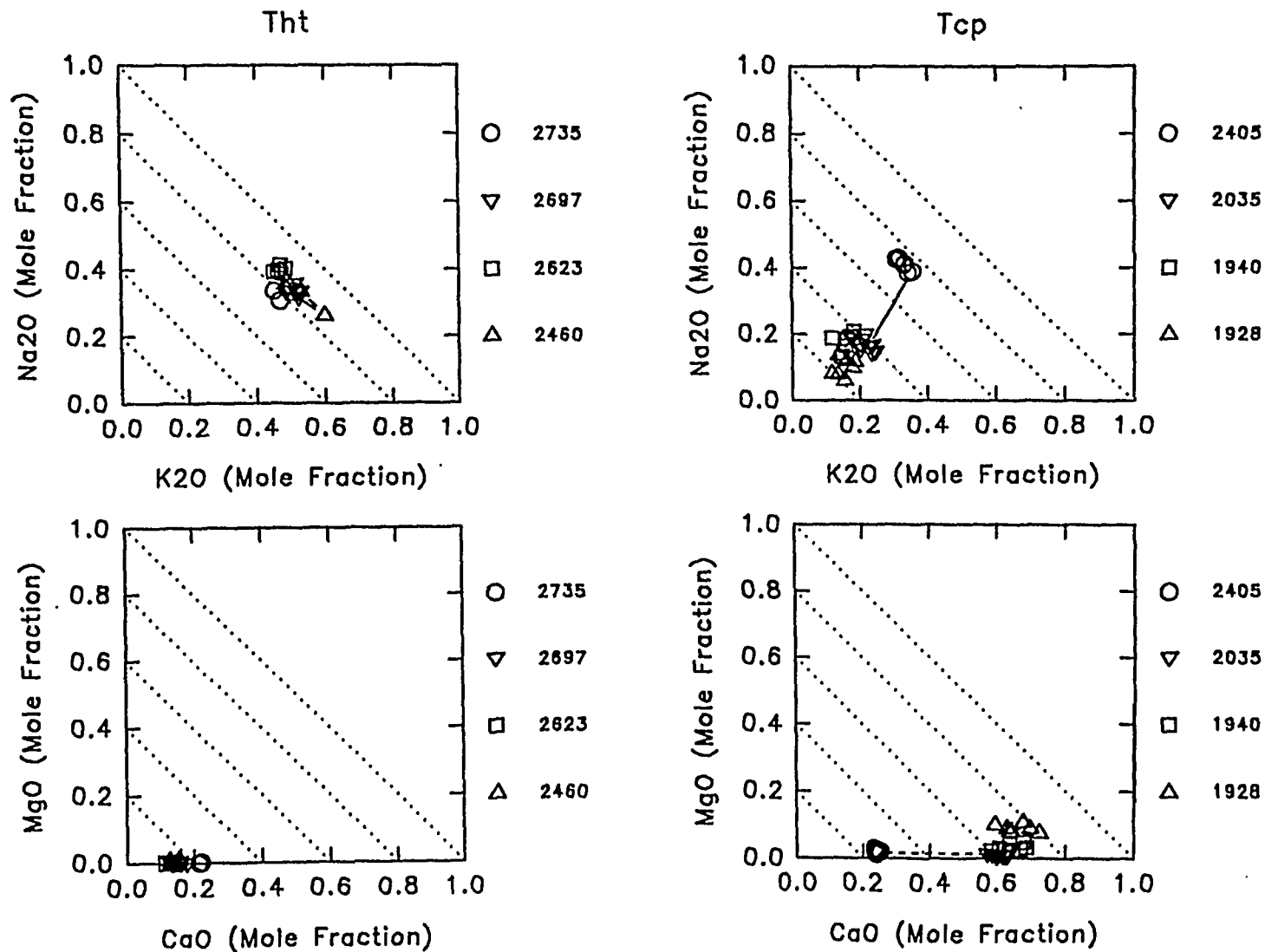
Detailed crossplots by elevation of samples for stratigraphic units, borehole USW G-3.

Figure 9a. USW G-4, Clinoptilolite Chemistry.



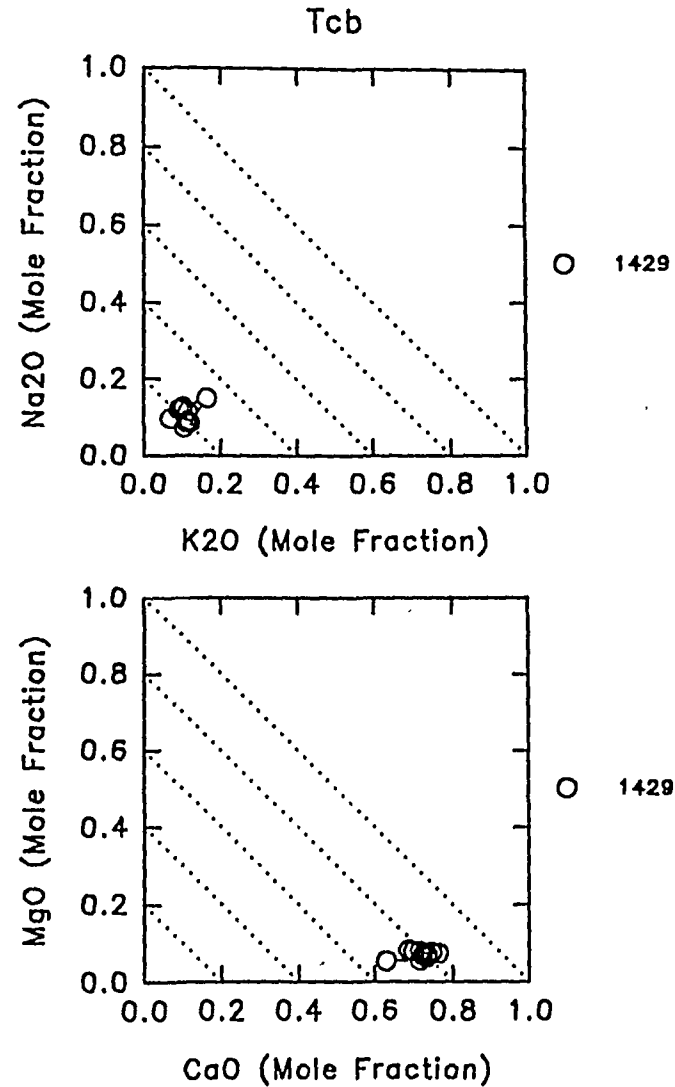
For lefthand diagram: The solid, dashed and dotted lines represent MgO, MgO+CaO and MgO+CaO+K2O respectively divided by (MgO+CaO+K2O+Na2O). Horizontal dotted line = water table. Horizontal dashed line = land surface.

Figure 9b. USW G-4, Clinoptilolite Chemistry, Detail, Tht and Tcp.



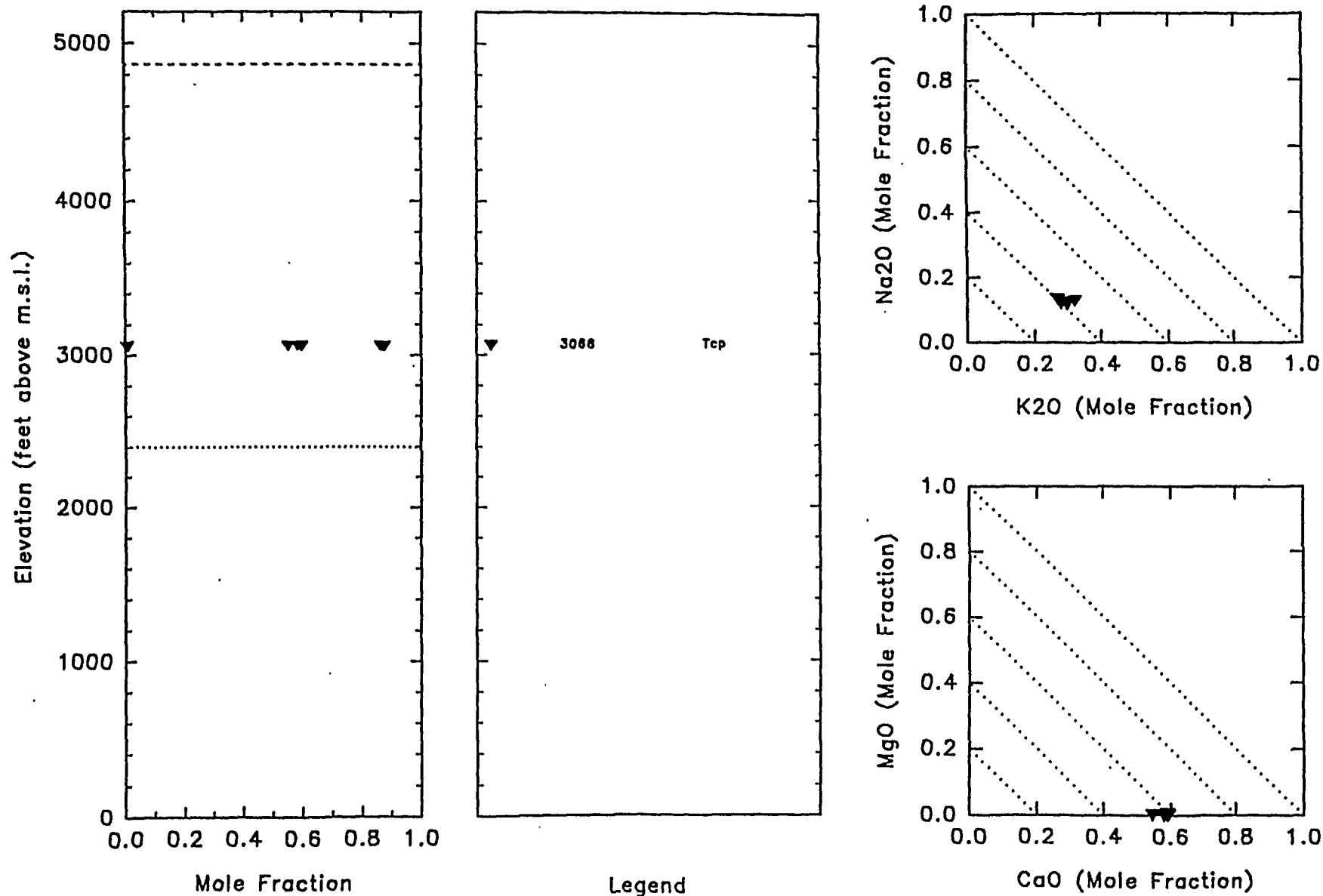
Detailed crossplots by elevation of samples for stratigraphic units, borehole USW G-4.

Figure 9c. USW G-4, Clinoptilolite Chemistry, Detail, Tcb.



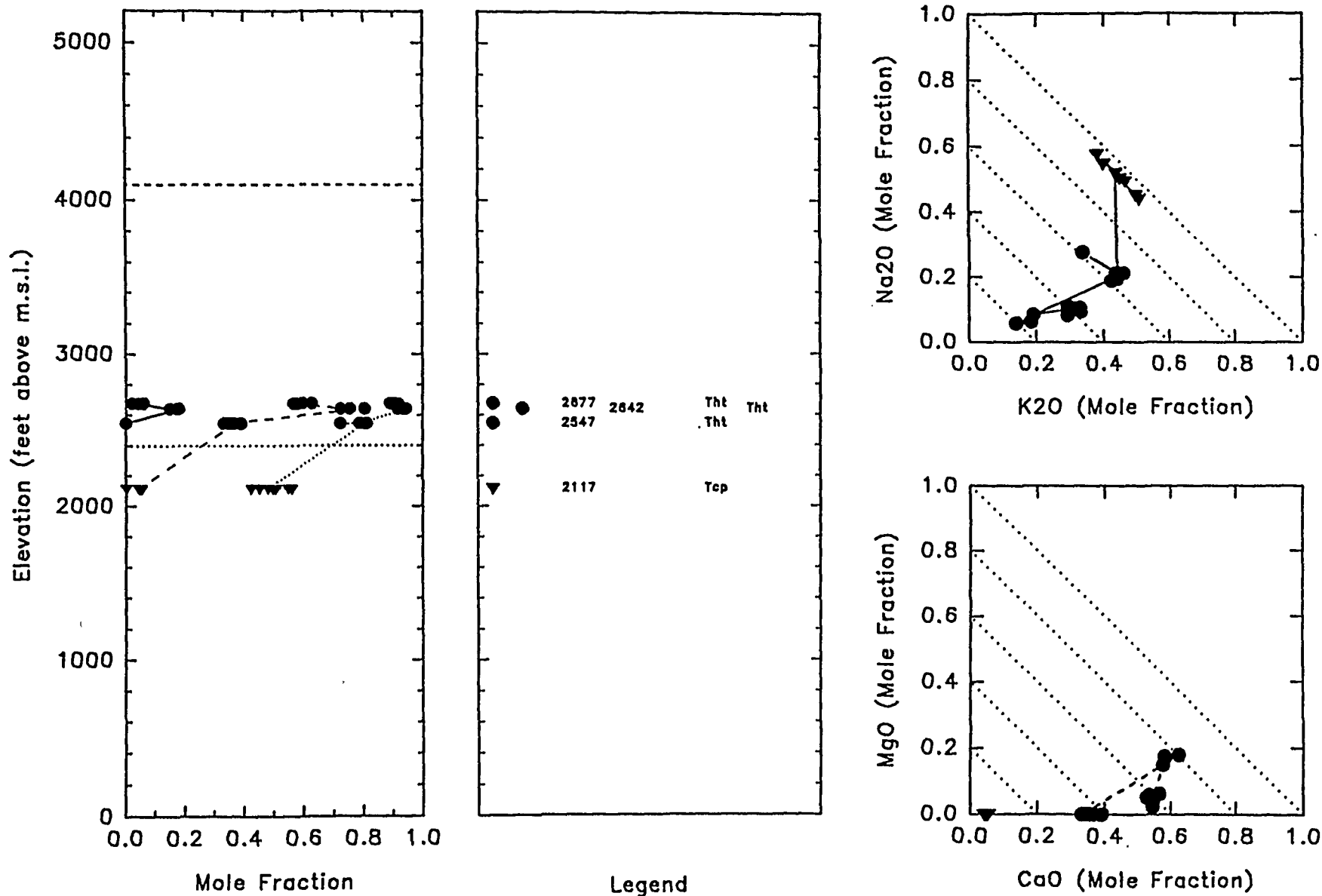
Detailed crossplots by elevation of samples for stratigraphic units, borehole USW G-4.

Figure 10. USW H-3, Clinoptilolite Chemistry.



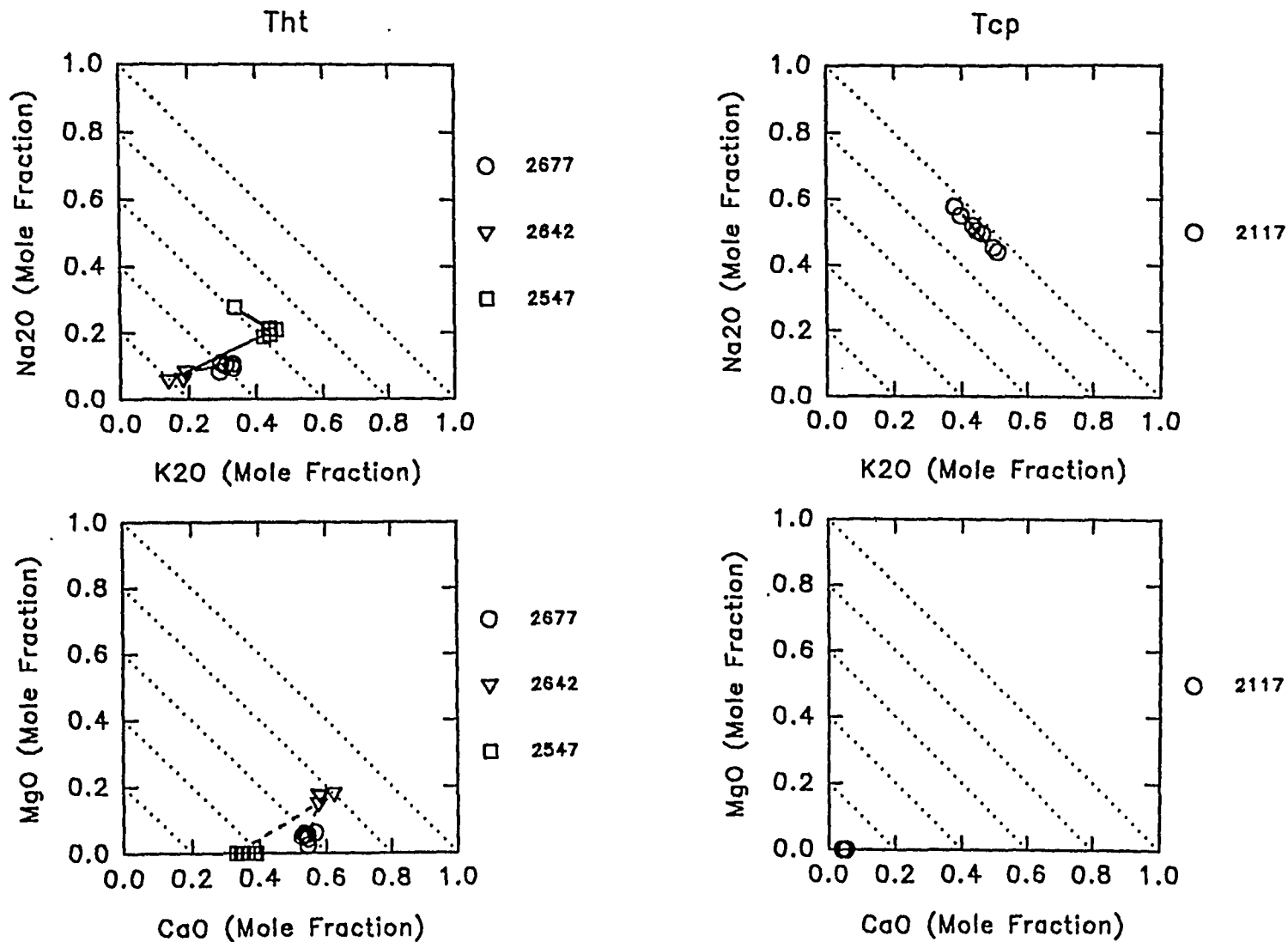
For lefthand diagram: The solid, dashed and dotted lines represent MgO, MgO+CaO and MgO+CaO+K₂O respectively divided by (MgO+CaO+K₂O+Na₂O). Horizontal dotted line = water table. Horizontal dashed line = land surface.

Figure 11a. USW H-4, Clinoptilolite Chemistry.



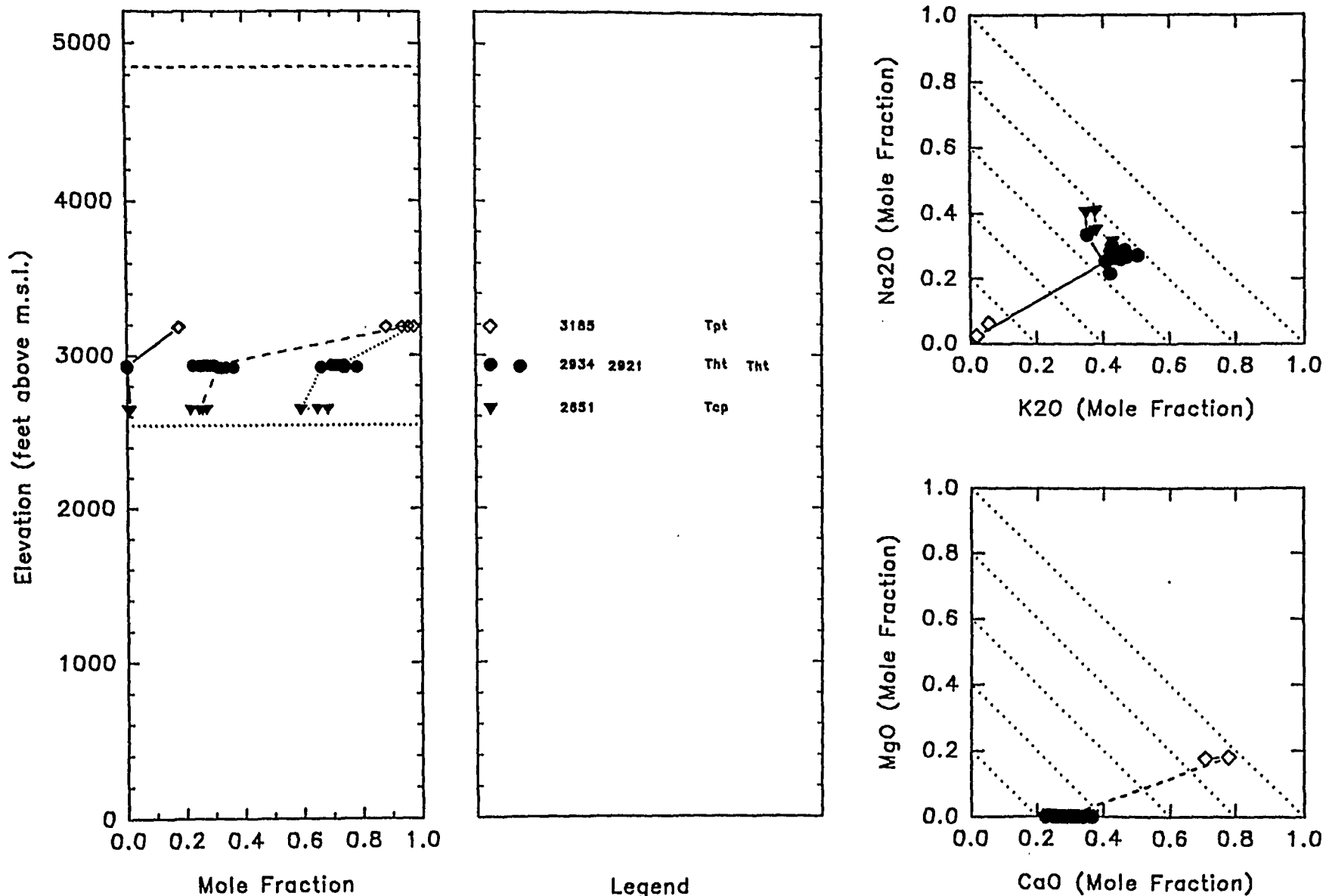
For lefthand diagram: The solid, dashed and dotted lines represent MgO, MgO+CaO and MgO+CaO+K2O respectively divided by (MgO+CaO+K2O+Na2O). Horizontal dotted line = water table. Horizontal dashed line = land surface.

Figure 11b. USW H-4, Clinoptilolite Chemistry, Detail, Tht and Tcp.



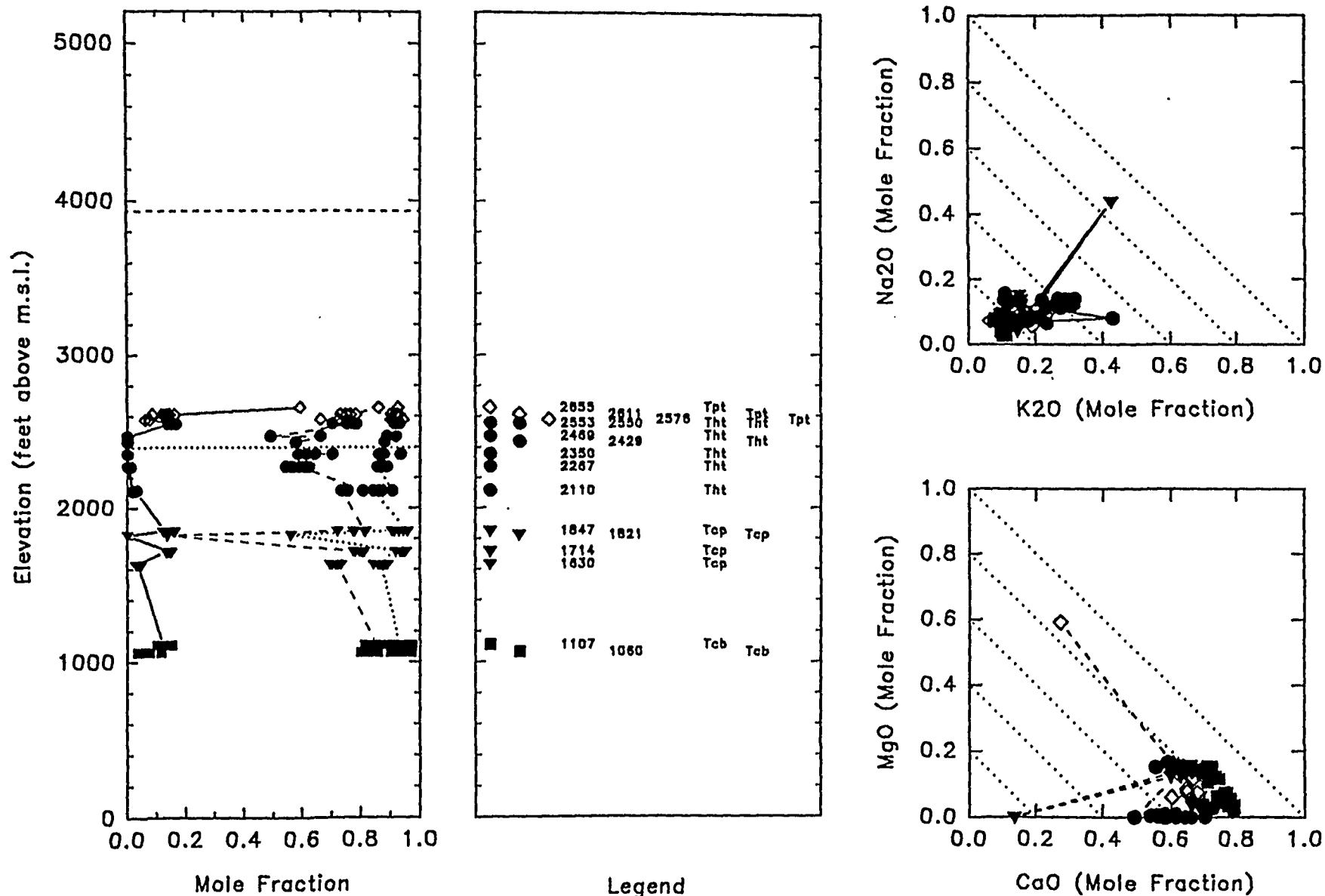
Detailed crossplots by elevation of samples for stratigraphic units, borehole USW H-4.

Figure 12. USW H-5, Clinoptilolite Chemistry.



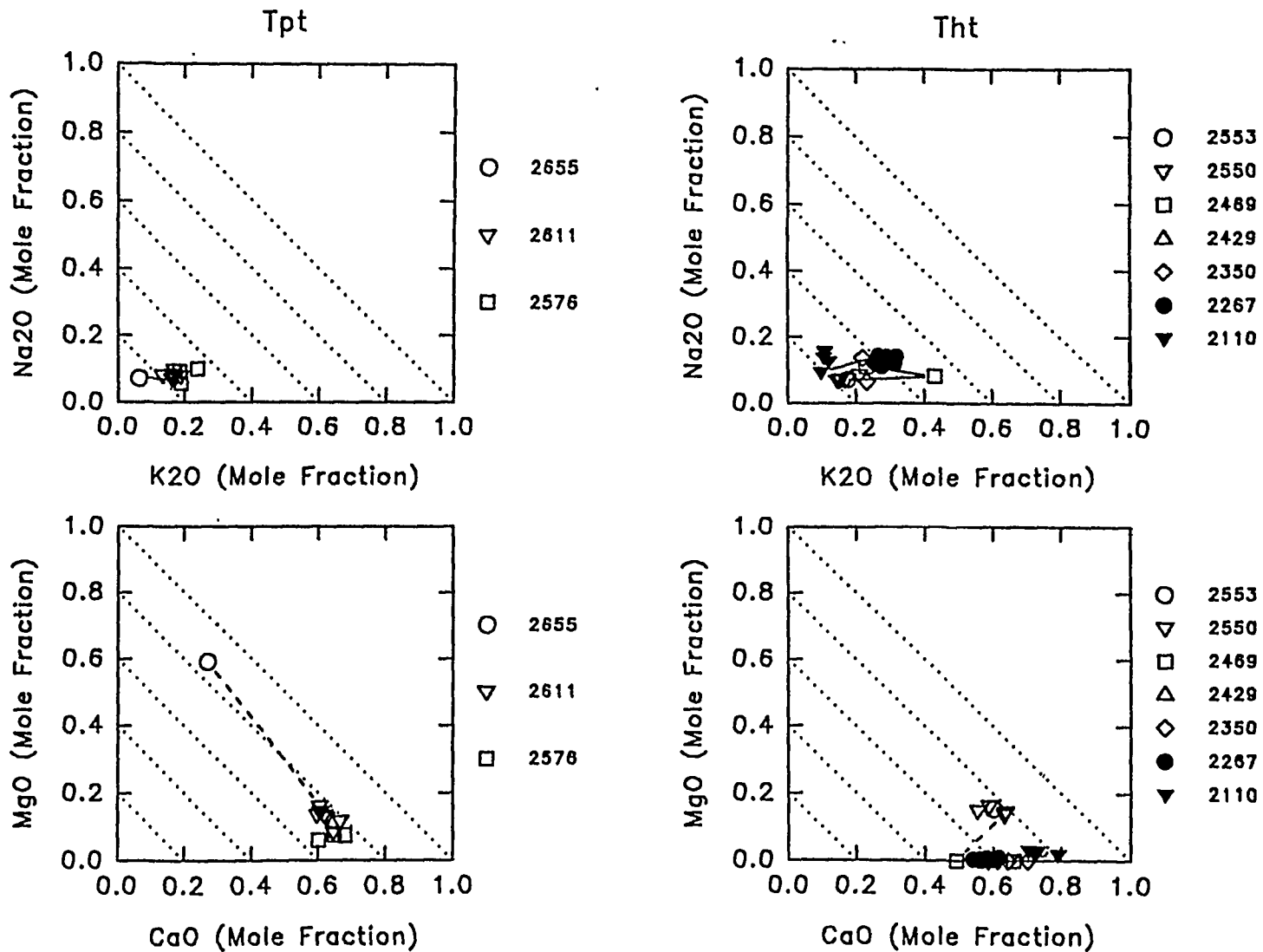
For lefthand diagram: The solid, dashed and dotted lines represent MgO, MgO+CaO and MgO+CaO+K₂O respectively divided by (MgO+CaO+K₂O+Na₂O). Horizontal dotted line = water table. Horizontal dashed line = land surface.

Figure 13a. UE-25 a&b#1, Clinoptilolite Chemistry.



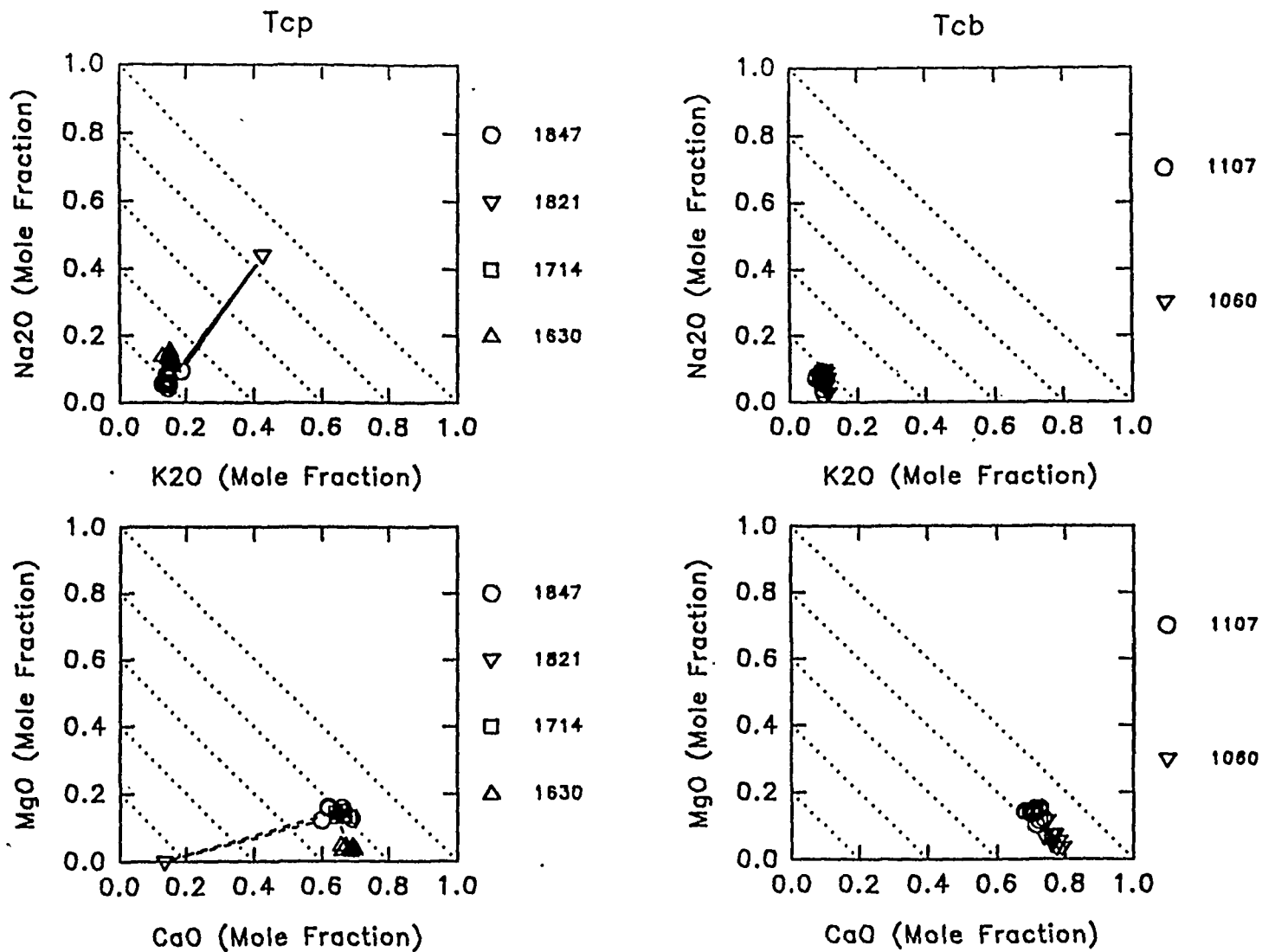
For lefthand diagram: The solid, dashed and dotted lines represent MgO, MgO+CaO and MgO+CaO+K2O respectively divided by (MgO+CaO+K2O+Na2O). Horizontal dotted line = water table. Horizontal dashed line = land surface.

Figure 13b. UE-25 a&b#1, Clinoptilolite Chemistry, Detail, Tpt and Tht.



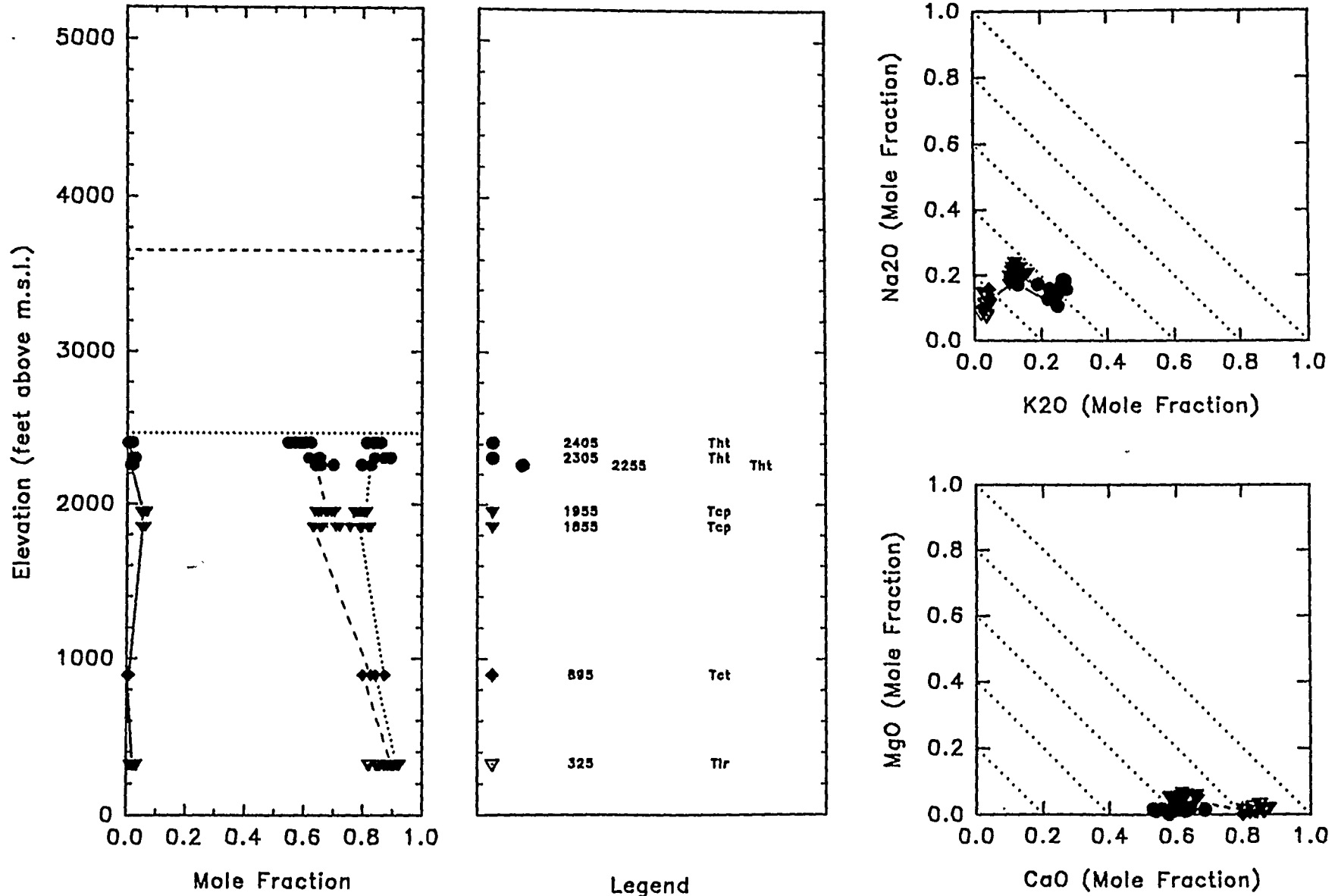
Detailed crossplots by elevation of samples for stratigraphic units, borehole UE-25 a&b#1.

Figure 13c. UE-25 a&b#1, Clinoptilolite Chemistry, Detail, T_{cp} and T_{cb}.



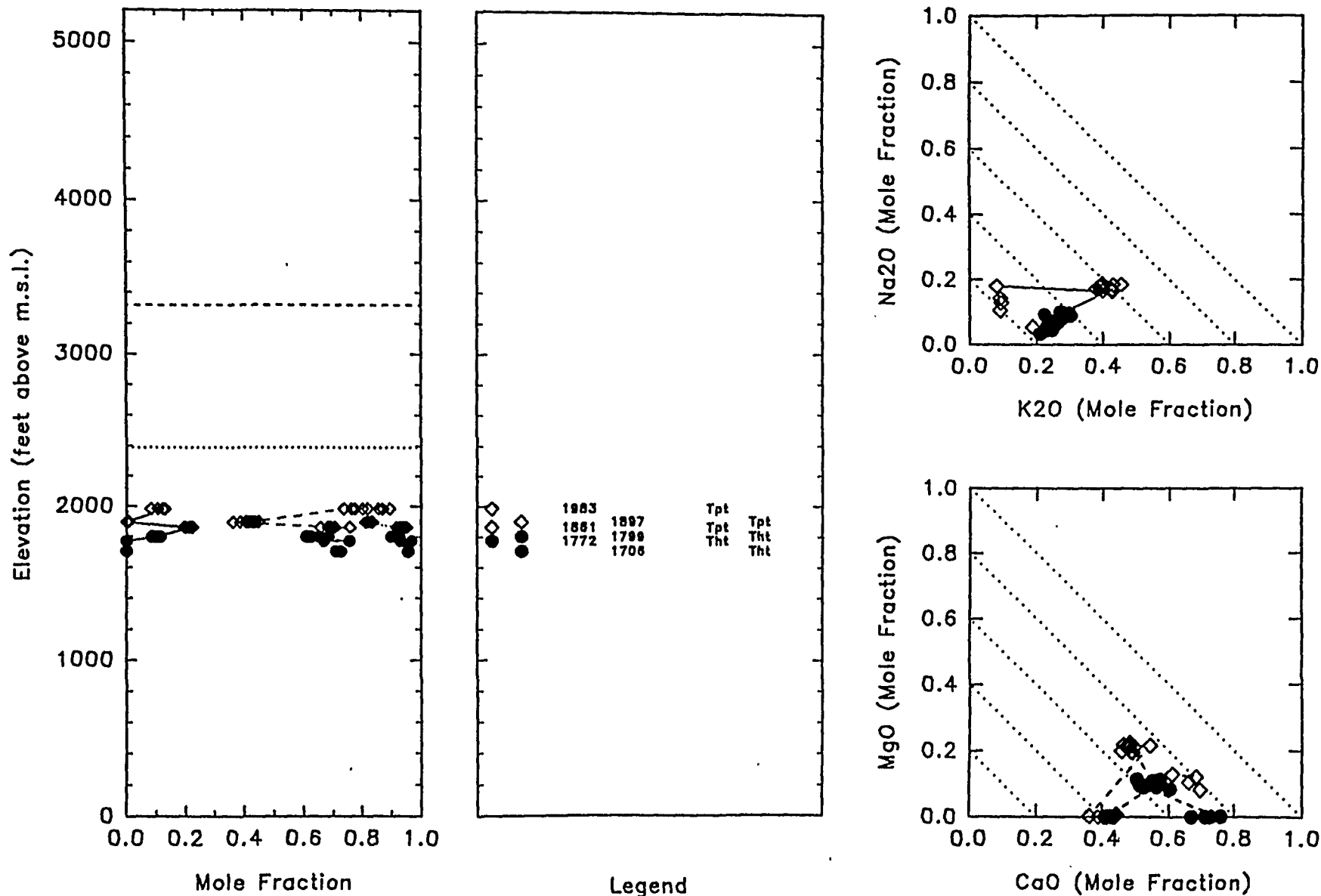
Detailed crossplots by elevation of samples for stratigraphic units, borehole UE-25 a&b#1.

Figure 14. UE-25 p#1, Clinoptilolite Chemistry.



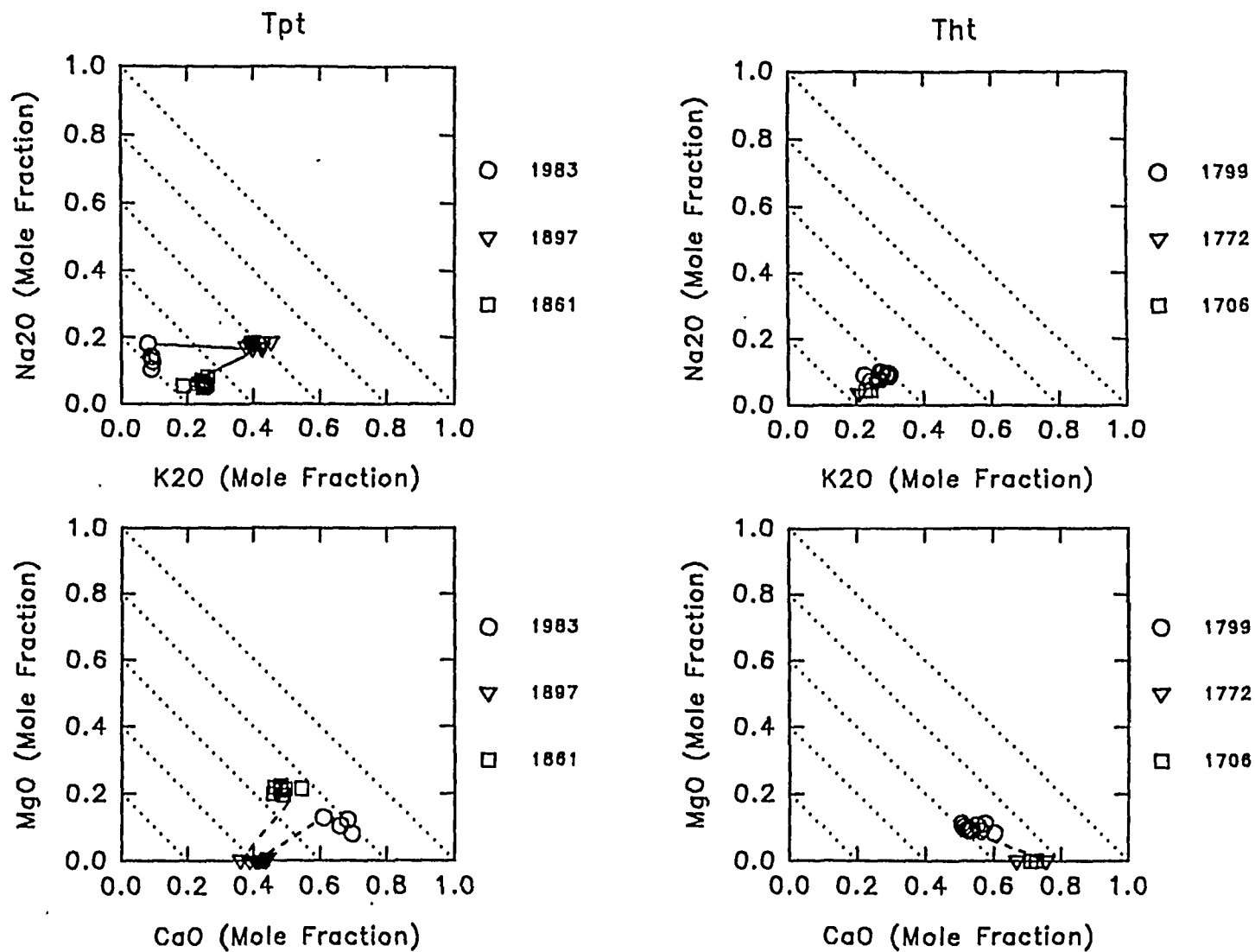
For lefthand diagram: The solid, dashed and dotted lines represent MgO, MgO+CaO and MgO+CaO+K2O respectively divided by (MgO+CaO+K2O+Na2O). Horizontal dotted line = water table. Horizontal dashed line = land surface.

Figure 15a. J-13. Clinoptilolite Chemistry.



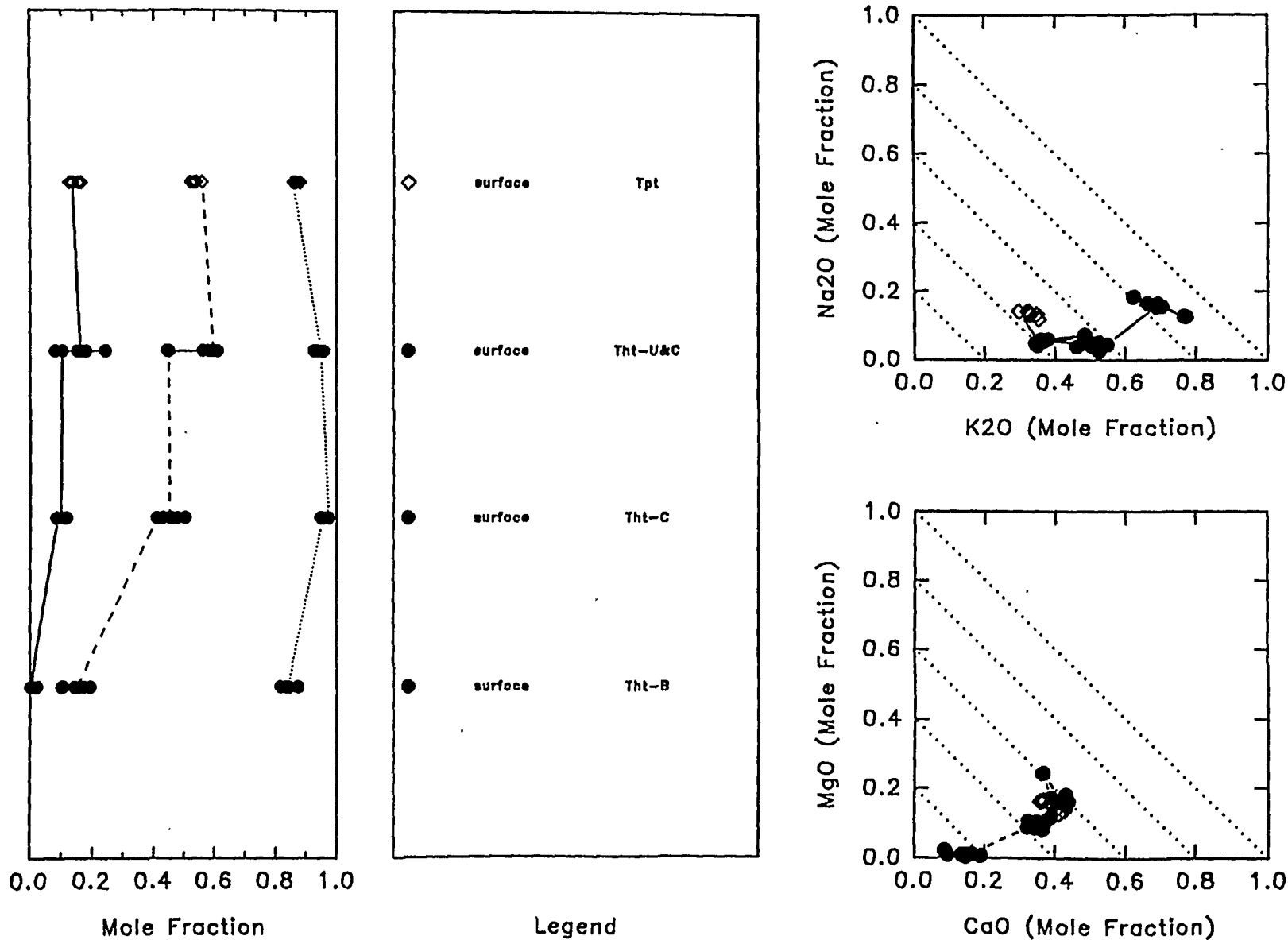
For lefthand diagram: The solid, dashed and dotted lines represent MgO, MgO+CaO and MgO+CaO+K2O respectively divided by (MgO+CaO+K2O+Na2O). Horizontal dotted line = water table. Horizontal dashed line = land surface.

Figure 15b. J-13, Clinoptilolite Chemistry, Detail, Tpt and Tht.



Detailed crossplots by elevation of samples for stratigraphic units, borehole J-13.

Figure 16. Prow Pass, Clinoptilolite Chemistry.



57

For lefthand diagram: The solid, dashed and dotted lines represent MgO, MgO+CaO and MgO+CaO+K2O respectively divided by (MgO+CaO+K2O+Na2O).

Large Scale Spatial and Chemical Diversity of Clinoptilolites

Geographic Diversity

Figures 17, 18 and 19 present the same chemical information as the main group of figures, in abbreviated form, and grouped according to location at Yucca Mountain. The curves given in each diagram are the same as those shown previously.

North-South Cross Section along Yucca Mountain

From Figure 17, also see map of Figure 2, a north-south cross section along Yucca Ridge, it can be seen that there is a general increase of Na_2O with increasing depth for the boreholes in the western portions of Yucca Mountain. Whether or not this generalization would hold with increased sample coverage is not clear. There is a general decrease of CaO and MgO with increasing depth but K_2O is variable, showing no regular variation with increasing depth.

Central Yucca Mountain

In Figure 18, for the central portion of Yucca Mountain, it can be seen that both USW G-4 and UE-25 contain clinoptilolites that are more calcic rich than clinoptilolites in the other boreholes, especially as depth increases. The other two boreholes, USW G-1 and USW H-4, are similar to those on Yucca Ridge in that Na_2O increases with depth, CaO and MgO decrease with depth and K_2O is variable with increasing depth.

Southern Yucca Mountain

In Figure 19 it can be seen that CaO rich clinoptilolites in boreholes UE-25 p#1 and J-13 predominate at depth while CaO rich clinoptilolites occur at discrete intervals in borehole USW G-3.

Deep Calcium Rich Clinoptilolite

Calcium rich clinoptilolites predominate at depth in boreholes USW G-4, UE-25 p#1, UE-25 a&b#1 and J-13. Other boreholes, where data is sufficient, show that CaO generally decreases with increasing depth. This relation has been noted by Broxton, *et al.* (1986) and Szymanski (1992).

Relation to the Water Table

Examination of Figures 17 through 19 show that changes in chemical composition of clinoptilolite do not have a systematic relation to the present day water table.

Relation to Elevation

Examination of Figures 17 through 19 show that changes in chemical composition of clinoptilolite do not have a systematic relation to elevation.

Relation to Stratigraphy

Figures 20a, 20b and 20c show the chemical diversity of each stratigraphic unit as cross plots of Na₂O vs. K₂O and MgO vs. CaO. With the exception of the Pah Canyon member (Tpp) of the Paintbrush tuff and the flow breccia (Tfb), all

stratigraphic units display a diversity of chemical compositions of the indigenous clinoptilolites. Most units include numerous samples of CaO rich clinoptilolites. Most units show multiple clustering of chemical compositions. No systematic correlated relation can be discerned for chemical composition and stratigraphy other than that the members of the Paintbrush tuff, the Pah Canyon (Tpp) and the Topopah Spring (Tpt), are dominantly lime rich.

Summary of Large Scale Spatial and Chemical Diversity of Clinoptilolites

1. Calcic rich clinoptilolites occur at depth in boreholes USW G-4, UE-25 a&b#1, UE-25 p#1 and J-13 in the southeastern portions of Yucca Mountain..
2. Clinoptilolites in the western boreholes, along Yucca Ridge increase in Na₂O with increasing depth.
3. Calcic rich and calcic poor clinoptilolites occur both above and below the present day water table. Marked changes in the chemistry of clinoptilolite have no systematic relation to the present day water table or to elevation.
4. Clinoptilolites of the Paintbrush tuff are predominantly CaO rich.
5. Clinoptilolites of the dacite flow breccia, Tfb, are Na₂O rich.
6. With the above two exceptions there is no systematic relation of chemistry or chemical variations with stratigraphic position. Within each stratigraphic unit the clinoptilolites tend to cluster into small groups of distinctly different composition.

The above listing of large scale chemical characteristics mostly have been recognized in previous reports, Broxton, *et al.* (1986) and Broxton, *et al.* (1987) and Szymanski (1992). Though Broxton, *et al.* (1987) recognize that the calcium component of clinoptilolites, in the southeastern part of Yucca Mountain, as having a source in the subjacent Paleozoic carbonates they still adhere to the concept of diagenesis rather than epigenesis. In contrast to Szymanski (1992), these authors do not consider the source of the alkaline earth elements in the clinoptilolites that occur in the Paintbrush tuff. In this regard, Hoover (1968) states: "*...the source of the calcium and magnesium to account for the increase is not known.*"

Authigenic Analcime and Feldspar

The major element compositions of authigenic analcime and feldspar are reported in Appendices G and H of Broxton, *et al.* (1986). A summary of their spatial distribution is included here and shown graphically in Figure 21.

Analcime and Feldspar in USW G-1

Analcime occurs in Tot, Tlr and Tct, in borehole USW G-1, from an elevation of -1,397.6 to 977.4 feet (depth = 5,746 to 3,371 feet), see left-hand diagram of Figure 21. Except for the shallowest reported analcime (Tct), they all occur below the clinoptilolites shown in Figure 6. Albite and adularia occur in Tlt and Tot from an elevation of -1,598.6 to 140.4 feet (depth = 5,947 to 4,208 feet), all below the reported clinoptilolites.

Analcime in J-13

Analcime occurs in Tcp and Tpc at elevations of 1,323 and 2,710 feet (depth = 1,995 and 608 feet) respectively, both above and below the reported analyses of clinoptilolites, see second from left diagram of Figure 21. The occurrence of analcime as shallow as 608 feet in the Tiva Canyon (Tpc) member of the Paintbrush tuff, and in the vadose zone, at borehole J-13 is very remarkable and maybe unique. The implications of this occurrence have not been discussed by any of the investigators of Yucca Mountain. This occurrence indicates a notable inversion of "diagenetic zones II and III." For the significance of this occurrence of analcime see the discussion concerning Broxton, *et al.* (1986) and Broxton, *et al.* (1987) in the section on Discussion of Genetic Implications below.

Analcime in UE-25 b#1

Analcime occurs in UE-25 b#1 at 433 and 546 feet of elevation. Both occurrences are in the Tram member (Tct) of the Crater Flat tuff and below all of the reported occurrences of clinoptilolite, see second from right diagram of Figure 21.

Analcime in UE-25 p#1

Analcime occurs in borehole UE-25 p#1 in the tuff of Lithic Ridge (Tlr) at 201.6 feet of elevation and in the Bull Frog member (Tcb) of the Crater Flat tuff at an elevation of 1,434 feet, see second from right diagram of Figure 21. The lower occurrence is below all of the reported clinoptilolite occurrences but the upper occurrence is above the two lower occurrences of clinoptilolite.

Albite and Adularia in USW G-2

Albite occurs in USW G-2 in the older tuffs (Tot) at elevations of -893.6, -796.6, -721.6 and -597.6 feet. It also occurs at 260.4 and 293.4 feet of elevation in the tuff of Lithic Ridge (Tlr). Adularia occurs at -893.6 feet in the older tuffs (Tot), at 293.4 feet in the tuff of Lithic Ridge (Tlr) and at 2,668.4 and 2,773.4 feet in the tuff of Calico Hills. All but the two uppermost occurrences of feldspar are below the reported occurrences of clinoptilolite.

Feldspar in Boreholes USW G-3 and USW G-4

Two individual analyses of adularia below the reported clinoptilolites are reported in USW G-4, at 1,428 feet in the Bull Frog member of the Crater Flat tuff and in USW G-3, at 148 feet in the tuff of Lithic Ridge (Tlr), see right-hand diagram of Figure 21.

Adularia at Prow Pass

Two analyses of adularia are reported from surface outcrops of the tuff of Calico Hills at Prow Pass, see right-hand diagram of Figure 21.

Summary of the Spatial Distribution of Analcime and Feldspar

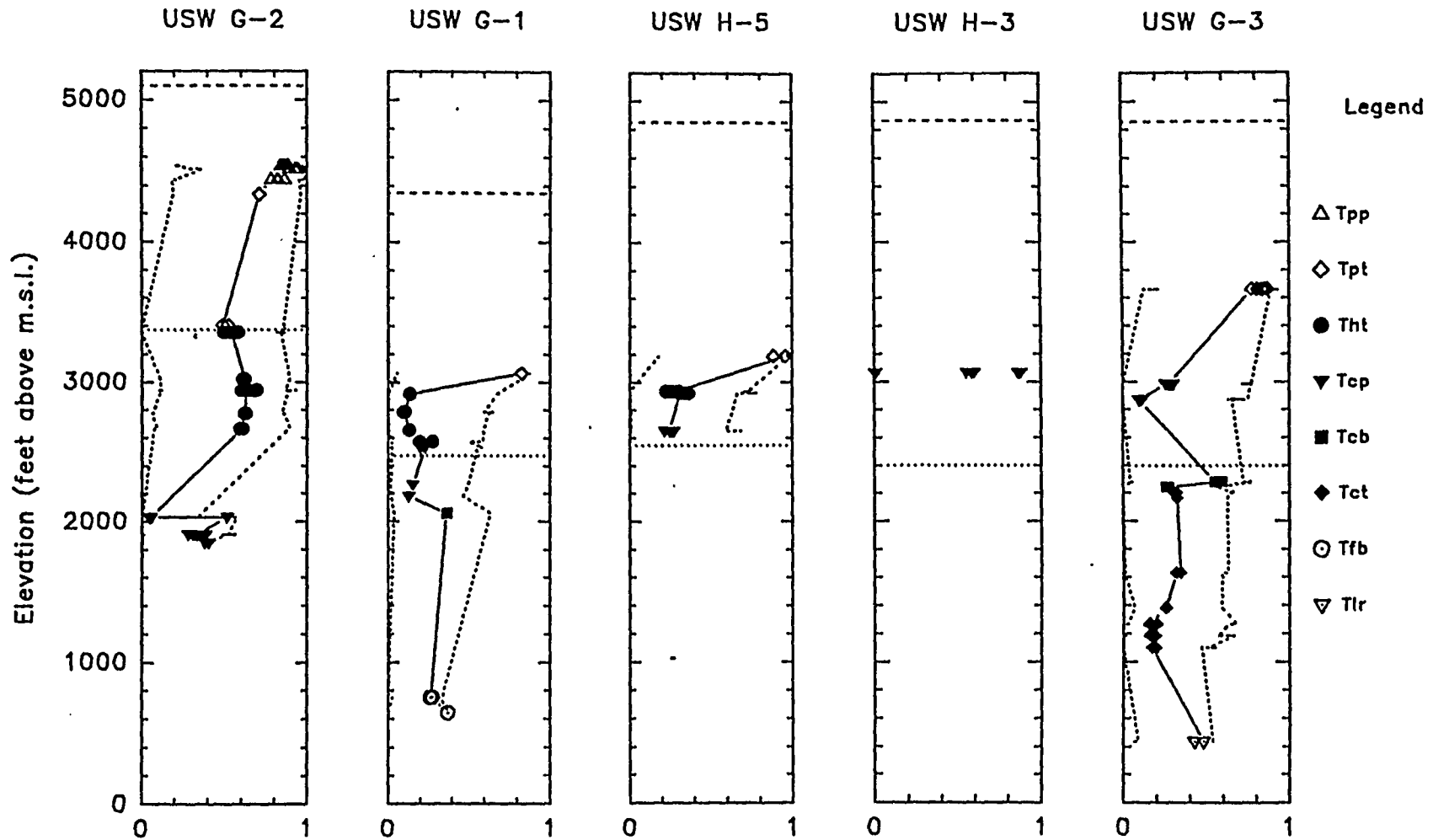
At Yucca Mountain, authigenic analcime, albite and adularia generally occur at greater depths than clinoptilolite, however, in borehole J-13 analcime occurs 1,000 feet higher than the lowest reported occurrence of clinoptilolite. At USW G-2 adularia occurs about 1,000 feet higher than the lowest reported occurrence of clinoptilolite. These specific occurrences are not discussed in either Broxton, *et al.*

(1986) or Broxton, *et al.* (1987). At borehole J-13, "*the first appearance of analcime*" occurs in the Tiva Canyon member (Tpc) of the Paintbrush tuff placing all of the clinoptilolites reported from this borehole in "*Diagenetic Zone III.*" Such occurrences deserve further consideration beyond the concept of diagenesis.

N

Figure 17, North-South Cross Section Along Yucca Ridge.

S

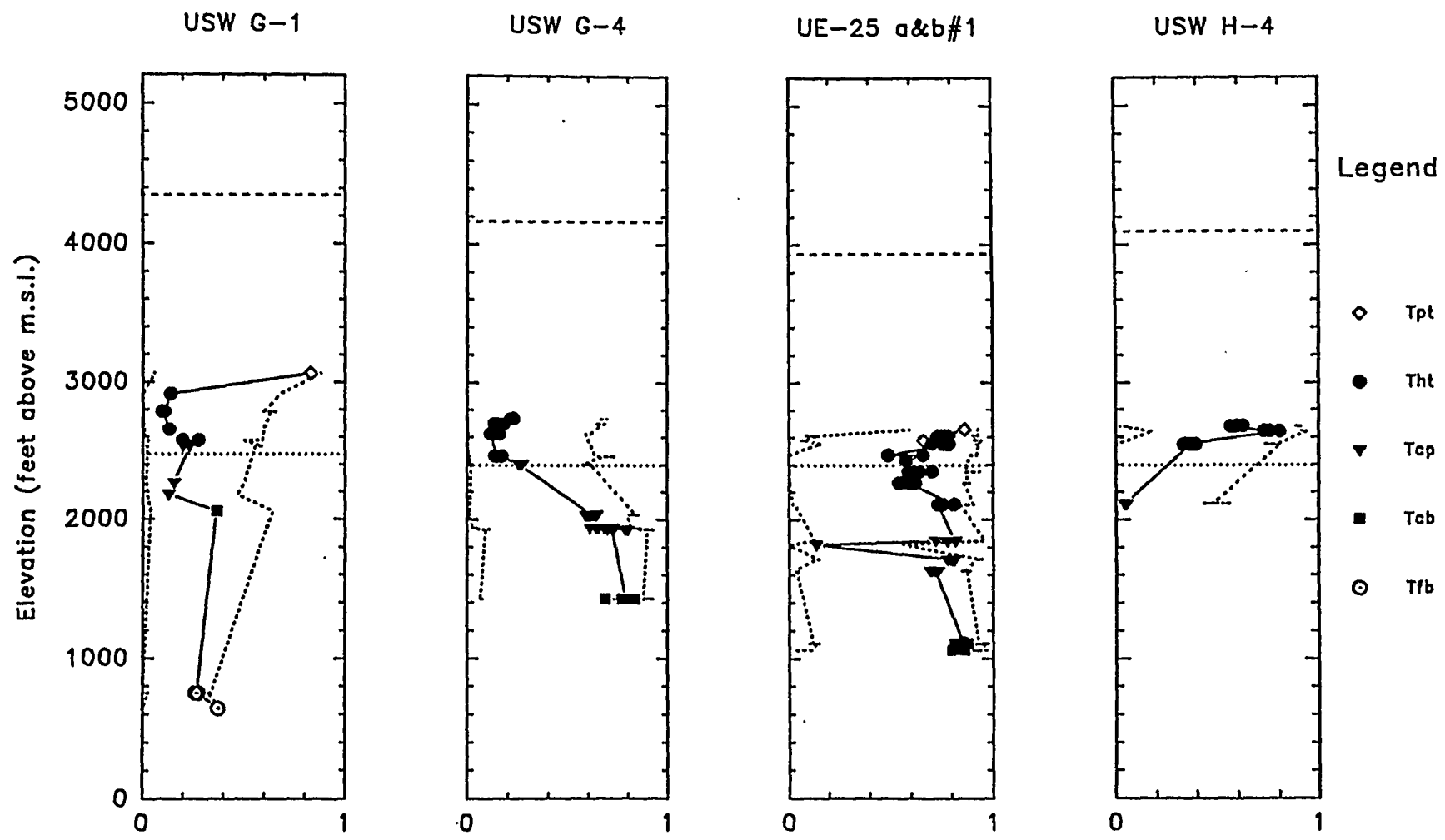


Plots of mole fraction $(MgO+CaO)/(Na_2O+K_2O+MgO+CaO)$ vs. elevation for bore holes of N-S cross section along Yucca Ridge. Dotted line = water table, dashed line = land surface.

NW

Figure 18, Boreholes of Central Yucca Mountain

SE

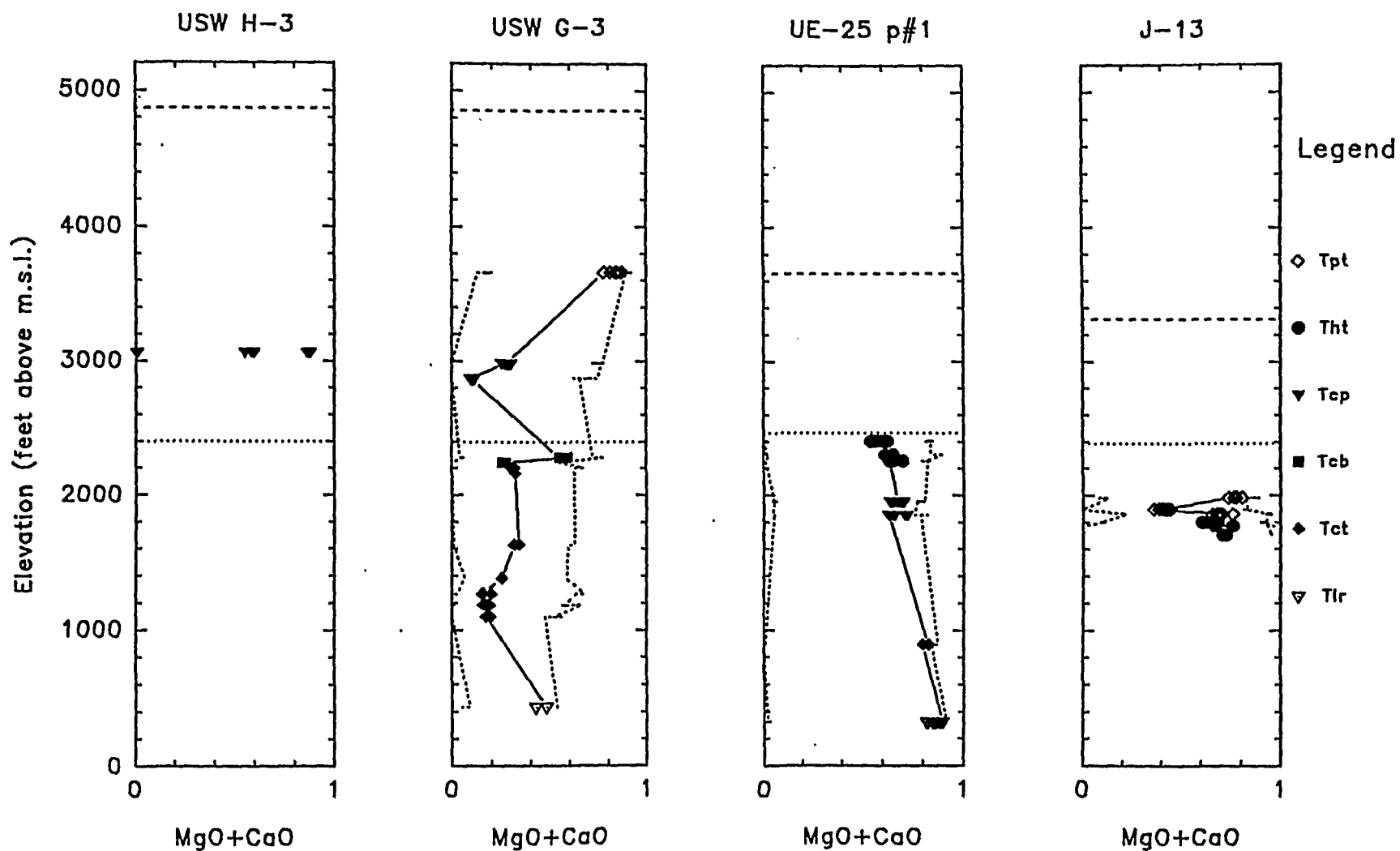


Plots of mole fraction $(MgO+CaO)/(Na_2O+K_2O+MgO+CaO)$ vs. elevation for bore holes of central Yucca Mountain. Dotted line = water table, dashed line = land surface.

W

Figure 19, Boreholes of Southern Yucca Mountain

E



Plots of mole fraction $(\text{MgO} + \text{CaO}) / (\text{Na}_2\text{O} + \text{K}_2\text{O} + \text{MgO} + \text{CaO})$ vs. elevation for bore holes of southern Yucca Mountain. Dotted line = water table, dashed line = land surface.

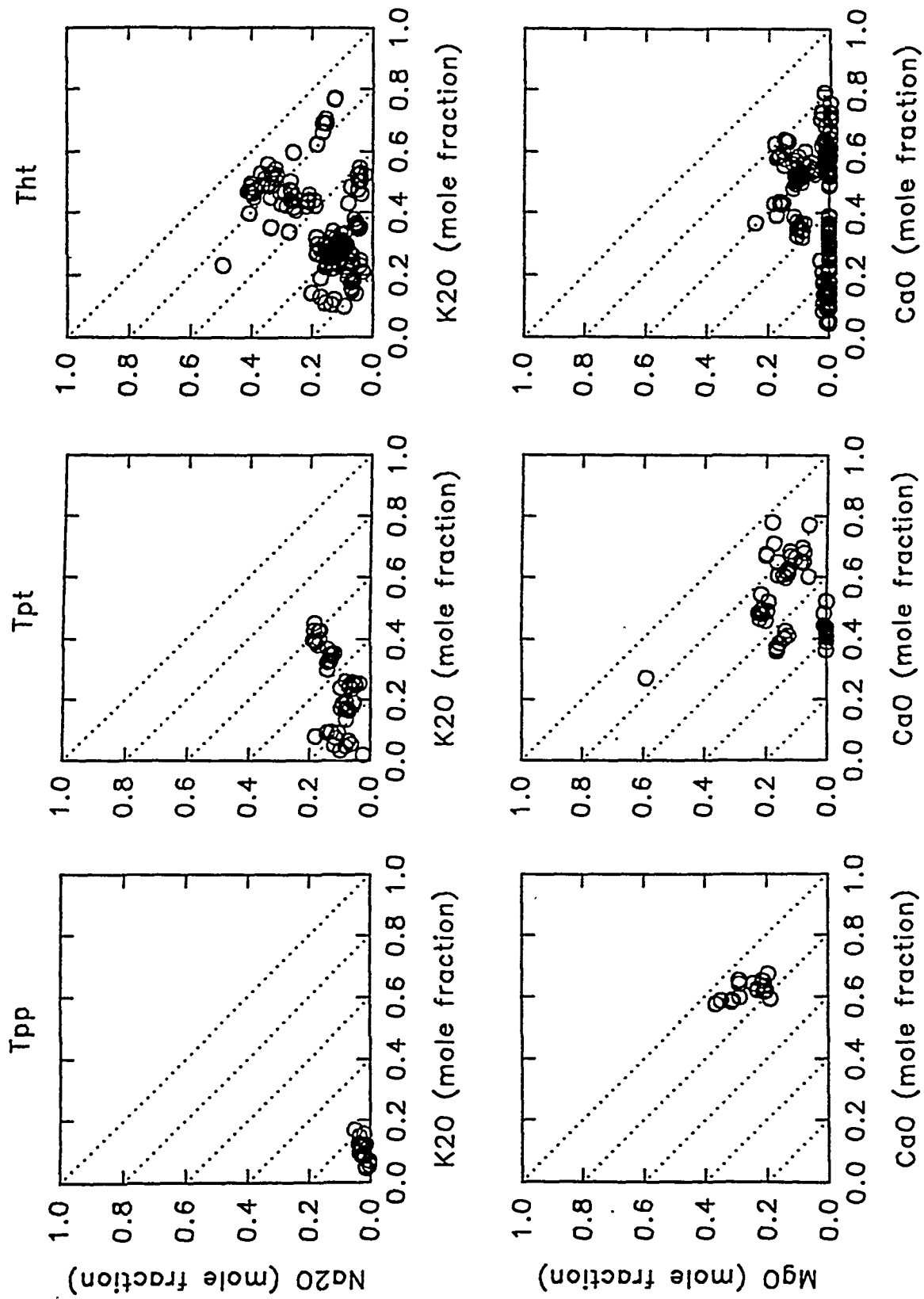


Figure 20a. Cross plots of interstitial cation oxides for Tpp, Tpt and Tht.

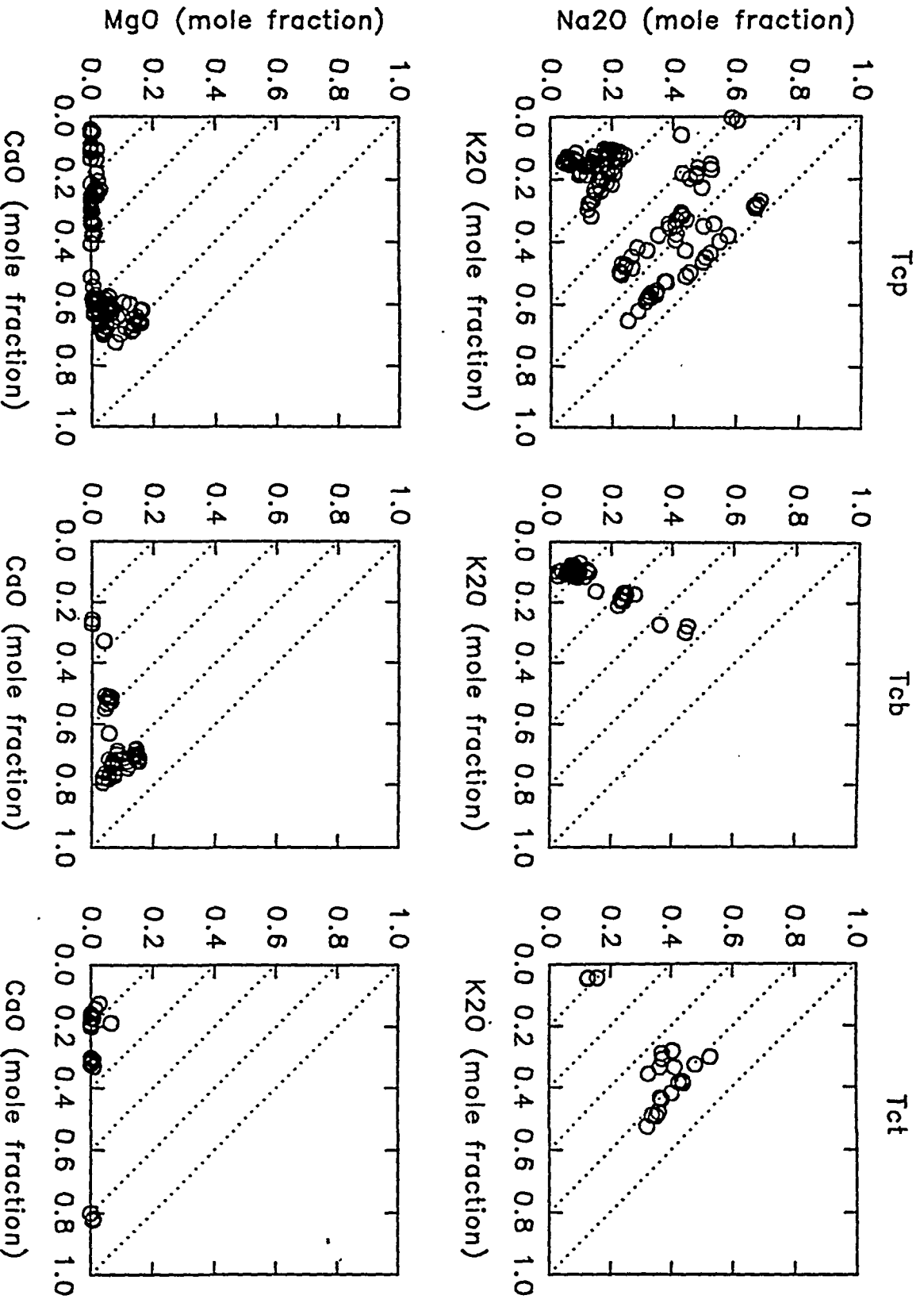


Figure 20b. Cross plots of interstitial cation oxides for Tcp, Tcb and Tct.

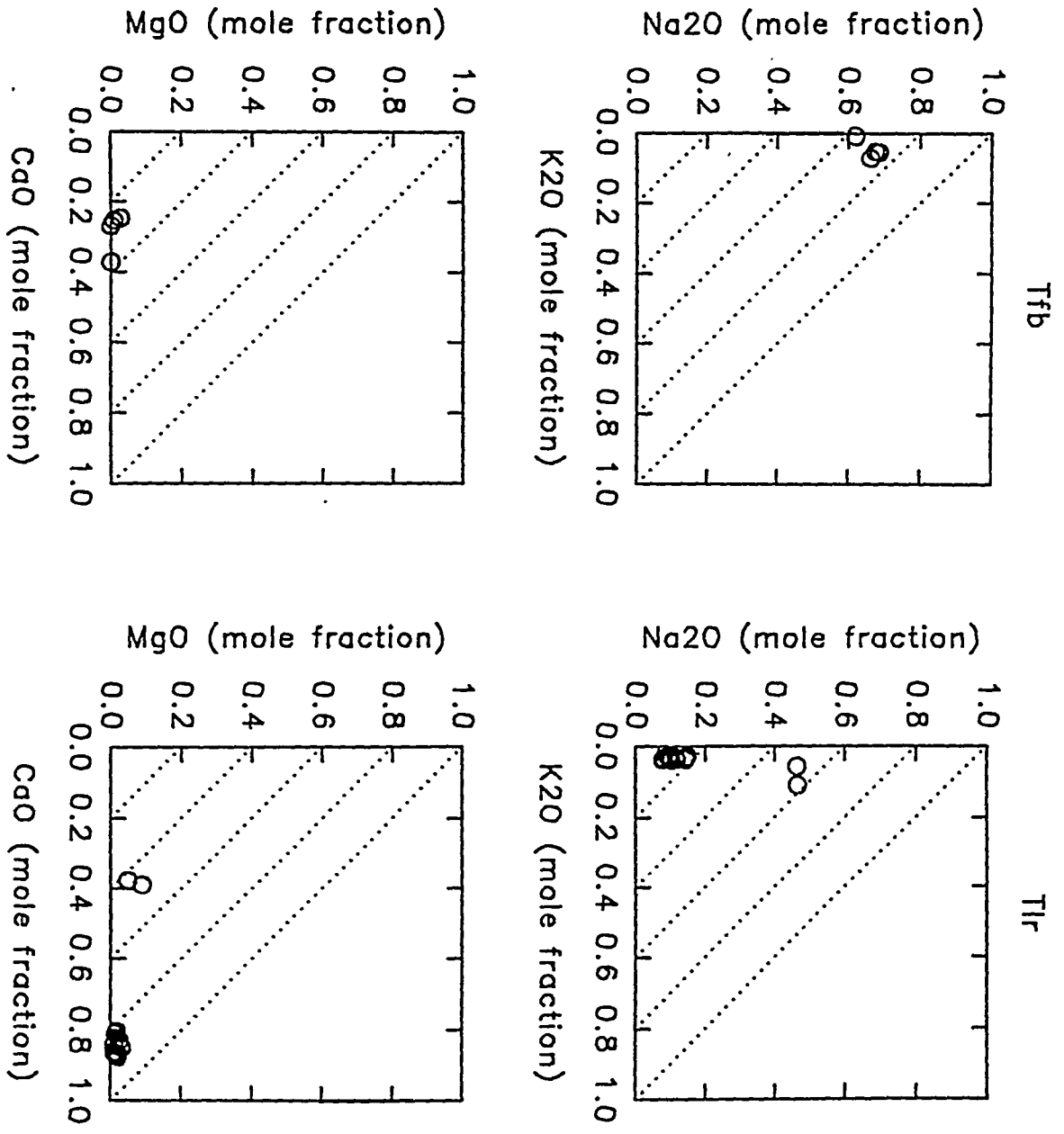


Figure 20c. Cross plots of interstitial cation oxides for Tfb and Tir.

SUMMARY OF RESULTS, CHEMICAL AND SPATIAL DIVERSITY AT YUCCA MOUNTAIN

Spatial diversity of the chemistry of clinoptilolites persists at all scales at and near Yucca Mountain for all of the major interstitial cation elements. At the largest scale, from Prow Pass on the northwest to USW G-3 on the southwest and to J-13 on the southeast the chemistry of clinoptilolites ranges from K_2O rich, to Na_2O rich, to CaO rich and to MgO rich. Stratigraphically, the most Na_2O rich unit is the dacite flow breccia (Tfb) in borehole USW G-1, the most K_2O rich units are the basal beds of the tuff of Calico Hills (Thc) at Prow Pass and the most MgO rich analysis is from a sample of the Topopah Spring member (Tpt) of the Paintbrush tuff in borehole UE-25 a#1 at an elevation of 2,655 feet. All samples of both members of the Paintbrush tuff, the Tiva Canyon (Tpc) and the Topopah Spring (Tpt) are very CaO rich at all localities except at Prow Pass. CaO rich clinoptilolites occur in all stratigraphic units of boreholes UE-25 a#1, UE-25 p#1 and J-13 from the Topopah Spring (Tpt) member of the Paintbrush tuff to the tuff of Lithic Ridge (Tlr). This diversity of chemistry ignores any systematic relation with the stratigraphic boundaries and the present day water table. At the smallest scale, this spatial diversity is manifest by discrete and marked differences of the chemistry of clinoptilolite within a single elevation in at least one borehole, for example: USW G-2, at an elevation 2,031 feet. Numerous markedly different and distinct chemical changes in the composition of clinoptilolite occur within zones of distinctly different chemical composition. This great range in the spatial diversity of the chemistry of zeolitic alteration at Yucca Mountain is a significant characteristic that must be accounted for by any genetic model under consideration.

DISCUSSION OF GENETIC IMPLICATIONS

Historical Perspective

In his paper on the genesis of zeolites, Hoover (1968) states: *"At the Nevada test Site, zeolites, cristobalite, quartz, feldspar, and clay minerals were deposited by ground water that leached vitric volcanic rocks in the unsaturated zone..."* Further, he notes: *"...Ca and Mg are concentrated in the uppermost part of the zeolitized rocks, K in the middle part and Na in the lowermost part."* The zonation he describes is not unlike the vertical zonation of zeolites along the western side of Yucca Mountain. He notes that zeolites can form by: *"(1) hydrothermal alteration, (2) burial metamorphism (Coombs, 1961), (3) reaction of glass and water in a saturated system (below a water table), and (4) leaching and deposition in an unsaturated system (above a water table)."* In his description of the hydration of glass, the first step in the formation of zeolites, he comments: *"Relative changes in calcium and magnesium during hydration are the largest changes of any of the constituents, but the source of the calcium and magnesium to account for the increase is not known"* (emphasis added). Without knowing the source of the calcium and magnesium he dismisses hydrothermal alteration and burial metamorphism with the statement: *"Temperatures in the zeolitized rocks measured in drill holes are 25° to 65° C., and there is no evidence for higher temperatures during zeolitization. This temperature range is below the presently known stability field of analcime and is very narrow for the zoning. Thus, a hydrothermal or burial metamorphic (Coombs, 1961) origin is unlikely."* He dismisses zeolite formation below the water table by a spate of *"Geologic evidence..."*, pages 278 and 279. Hoover, apparently, is the first to have

dealt with the origin of zeolites that occur in the vadose zone of the Nevada Test Site.

In their report, Broxton, *et al.* (1986), discuss the distribution of chemical alteration in the context of the diagenetic zones of Vaniman, *et al.* (1984). Broxton, *et al.* (1986) state: *"The nonwelded tuffs... ..were highly susceptible to alteration because of the instability of glass in the presence of groundwater. During diagenesis, glass was replaced primarily by the zeolites clinoptilolite, heulandite, and mordenite."* Furthermore they state *"These mineralogical zones are similar to those described by Iijima (1975, 1978, and 1980) for burial diagenesis of volcanic ash beds in thick sedimentary sequences"* (emphasis added). They recognize four zones of diagenesis:

"Zone I, the shallowest zone, is characterized by tuffs that contain substantial unaltered volcanic glass."

"Zone II is characterized by complete replacement of volcanic glass by clinoptilolite +/- mordenite, with minor quartz, potassium feldspar, and smectite."

"Diagenetic Zones III and IV are confined to the deeper structural levels of Yucca Mountain. Zone III is characterized by the progressive replacement of clinoptilolite and mordenite by analcime, potassium feldspar, quartz, and minor calcite and smectite. Zone IV, the deepest diagenetic zone penetrated by drill holes, is characterized by the replacement of analcime by authigenic albite."

They note exceptions to this generalization in zone I by the occurrence of calcic zeolites and other alteration minerals in the Paintbrush tuff of borehole USW G-2 at the northern part of Yucca Mountain. They state that zeolite-rich tuffs are laterally

extensive beneath Yucca Mountain in three well defined intervals within the interval extending from the base of the Topopah Spring member of the Paintbrush tuff to the top of the Tram member of the Crater Flat tuff.

Broxton, *et al.* (1987), provide a more extensive discussion of the possible genesis of the several types of chemical alteration while still using the concept of diagenetic zonation and including the spatial distribution of mineral phases reported in Bish and Vaniman, 1985. Unfortunately, their analysis of the distribution of the mineralogy and chemical alteration seems to be restricted by rigorous adherence to the concept of diagenetic zones. They consider hypogene sources only for the deep calcic rich alteration in the southeastern part of Yucca Mountain. Though they recognize many of the occurrences of markedly distinctive chemical anomalies, they explain them by downward percolation of local rainwater. In addition, several of the marked chemical anomalies noted in this review are not discussed. They do however state: *"Alteration of volcanic glass to clinoptilolite-group minerals occurred in an open chemical system, resulting in significant rearrangement of mobile cations in the host tuffs"* (emphasis added). An *"...open chemical system..."* would seem to contradict the more traditional concept of diagenesis. In this fashion they have missed the most significant implications of the locally discrete spatial and chemical diversity of the zeolitic alteration. This implication is that much, if not all, of the chemical alteration may have been the result of polygenetic and epigenetic upwelling and lateral incursions of hypogene ground water, at least some of which may have been of geothermal origin.

Similarly, Peterman, et al. (1993) state: *"In agreement with earlier studies, zeolitization is shown to have occurred under wholesale open-system conditions. Calcium was increased by up to two to three times the baseline values and strontium up to twenty times"* (emphasis added). These words refer to chemical comparisons between rocks from borehole UE-25 a&b#1 and relatively unaltered rocks collected from Raven Canyon in the southern part of Yucca Mountain just north of U. S. Highway 95. In addition these authors state: *"Much of the section of nonwelded to partially welded tuffs in the unsaturated zone, including the rhyolite of Calico Hills and part of the Prow Pass and Bullfrog Members of the Crater Flat Tuff, was extensively altered to clinoptilolite and mordenite during regional diagenesis"* (emphasis added). The fact that the sections studied by these workers in Raven Canyon, at the southern end of Yucca Mountain, and in Paintbrush Canyon just north of Yucca Wash, and immediately north of Yucca Mountain, are relatively unaltered indicates that this alteration of which they write is more local in nature than regional. They go on to state: *"However, K-Ar dating of zeolites, which are less retentive for Ar than illite, yields a wide spectrum of ages suggesting that the rock has continued to be susceptible to low-temperature alteration long after the main episode of diagenesis."* This statement seems to acknowledge that at least some of the alteration of the tuffs is epigenetic and post dates the hydrothermal stages of the activity associated with the formation of the Timber Mountain Caldera. However, the obvious question of the genesis of the *"...low-temperature alteration long after the main episode of diagenesis"* is left unanswered. In this regard, Peterman, et al. (1993) state: *"Future detailed isotopic studies of these units will hopefully contribute*

to a better understanding of the ultimate source of Ca and Sr added to the Calico Hills and of the degree of water-rock interaction necessary to accomplish this immense mass transfer."

Contrary to the above, Szymanski (1992, pages 7-32 to 7-34) has proposed that the zeolitic alteration of the tuffs at Yucca Mountain is the product of two distinctly different hydrothermal systems as follows. One system is alkaline in character and it could be zoned, potassic at shallower depths and sodic at deeper depths. This system is localized to the northwestern portions of Yucca Mountain and is related to the later stages of the development of the Timber Mountain Caldera which was the source of the Timber Mountain tuff. This hydrothermal system was driven by the thermal energy of the waning igneous activity of that eruptive center. The hydrothermal activity of this system occurred about nine to eleven million years ago and was responsible for the formation the younger argillic alteration dated at about 10 million years, Aronson and Bish (1987). It was also responsible for the older of the zeolitic alteration dated between nine and eleven million years by WoldeGabriel (1991). The chemical and isotopic characteristics of the rocks altered by this system would be similar to those of the unaltered tuffs. The zeolitic alteration of this older system was over printed by a second younger hydrothermal system of much different character.

The younger system is a fault based hydrothermal system that occurs southeast of Yucca Mountain. This system is the one which is responsible for the alkaline earth

variety of zeolitic alteration that is so abundant to the southeast. The likely major conduits of this system were the Stage Coach Road Fault and splays related to this fault such as the Paintbrush Canyon Fault and the Bow Ridge Fault. Upwelling along these faults, through the underlying Precambrian and Paleozoic bedrock, spread out through and above the previously altered tuffs taking advantage of permeable fracture zones, fault zones, breccias and as yet unaltered bedded tuffs. The alteration products of this system would take on the characteristics of the various basement rocks. The chemical character of the alteration products would be due, in part, to the underlying Paleozoic carbonate rocks and, in part, due to the Precambrian basement rocks. The large scale shape of the alteration zone would be that of a giant mushroom if unconstrained in any lateral direction, of if constrained it would have the shape of a segment of a mushroom. Laterally to the west and northwest it would have been responsible for the calcium rich zeolitization of the of the Paintbrush tuff in and near the base of the unaltered or slightly altered "diagenetic zone I." This fault based system is believed to have continued to operate, intermittently through the Pliocene and into the Quaternary. This is the system that is responsible for the younger K/Ar ages, ~2 to ~8 million years, of clinoptilolites reported by WoldeGabriel (1990) and the calcite silica occurrences cross cutting and on top of unconsolidated Quaternary deposits.

Interpretive Options

Two distinct options for the interpretation of the zeolitic and spatially related alteration are advocated by two different groups of investigators of Yucca Mountain.

These two options regard the source of the water that has carried the exotic (alkaline earth) chemical constituents of the alteration into Yucca Mountain. It should be noted that the disagreement focuses on alteration that may have occurred during Pliocene and Quaternary time because this is the time frame of direct regulatory concern for the siting of a high level nuclear waste repository. The alterations of specific concern are the calcite-silica deposits that form veins and cements within, and on top of, Quaternary and late Tertiary (Pliocene ?) alluvium. These calcitic deposits have a calcic affinity with the calcium rich clinoptilolites and may be cogenetic with them. If cogenetic with the calcite-silica veins then the calcium rich clinoptilolites are also of direct regulatory concern.

The Supergene (Pedogenic) Hypothesis

The supergene (pedogenic) hypothesis for the formation of the Quaternary calcite-silica deposits includes the deposition of aeolian dust to provide calcium (and perhaps silica as well), the direct infiltration of rain water to dissolve and transport the aeolian components, and respiration from plant roots, to provide carbon dioxide to form the deposits of concern. With this hypothesis, most of the zeolitic alteration is considered to be unrelated to the calcite-silica deposits of Quaternary age. The zeolitic alteration is considered to be diagenetic, similar to *"...burial diagenesis of volcanic ash beds in thick sedimentary sequences"* (Broxton, *et al.*, 1986), and to have formed soon after the deposition of the tuffs during the late Miocene. The deep calcium rich clinoptilolites of southeastern Yucca Mountain may have been formed by upwelling of hypogene fluids from the subjacent Paleozoic carbonates. The same

may have been true for the carbonate veins which cross cut the tuffs at depth. These veins also are considered to have been formed in late Miocene time. The carbonate veins within the tuffs of the vadose zone and within (and on top of) deposits of Quaternary alluvium are largely attributed to formation from water of local meteoric precipitation and direct infiltration as also are the calcic clinoptilolites that also occur in tuffs of the vadose zone. With this hypothesis the regulatory implications of both the Quaternary calcite-silica deposits and the alkaline earth zeolitization are dismissed.

The Hypogene Hypothesis

The hypogene hypothesis calls upon upwelling and lateral incursions of ground water as the agent for the introduction and precipitation of the calcite-silica veins and surficial deposits as well as the zeolitic alteration of the tuffs. Once introduced by ground water discharge at spring sites, as tufas and spring aprons, the surficial calcite deposits would be subject to supergene remobilization and re-precipitation within one or two meters of the ground surface. It is, perhaps, the products of such supergene processes that have added to the confused situation at Yucca Mountain. It would be expected, by the hypogene hypothesis, that calcite-silica deposits would be formed in faults, fractures and breccia zones in the sub surface and, if formed from groundwater discharge at the surface, would form tufas and spring aprons on the surface down slope from the points of discharge. This relationship is commonly observed in the vicinity of Yucca Mountain. Examples of this relationship occur on the sand ramps on the western slope of Busted Butte.

Supergene vs. Hypogene

From the supergene point of view, Broxton, *et al.* (1987) acknowledge the role of hypogene upwelling to form the deep calcic clinoptilolites of southeastern Yucca Mountain and Vaniman (1993) recognizes at least two modes of calcite precipitation in veins but declines to discuss their genesis. Marshall, *et al.* (1993) also recognize two groups of veins *"...corresponding to their location in either the saturated or unsaturated zones."* They comment that for samples collected from the upper part of the vadose zone: *"...the strontium came from the surface during infiltration events."* For samples deeper in the vadose zone *"...they are interpreted as the result of a higher water table stand... ..in the past."*

From the hypogene point of view, an early alkaline alteration can not be ruled out but this does not account for *"...wholesale open-system..."* introduction of calcium and strontium into either the vadose zone or below the water table. Repetitively intermittent, low to moderate temperature, polygenetic alteration seems to best describe the origin of the spatially and chemically diverse alteration of the tuffs of Yucca Mountain and the affinitive, coextensive, calcite-silica deposits.

REFERENCES

- Aronson, J. L., and D. L. Bish, 1987. Distribution, K/Ar Dates, and Origin of Illite/Smectite in Tuffs from Cores USW G-1 and USW G-2, Yucca Mountain, Nevada, a Potential High-Level Radioactive Waste Repository. Clay Mineral Society, 24th Annual Meeting. Socorro, New Mexico.
- Bish, D. L. and S. J. Chipera, 1989. Revised Mineralogic Summary of Yucca Mountain, Nevada. LA-11497-MS, Los Alamos National Laboratory, Los Alamos, New Mexico.
- Bish, D. L., and Vaniman, D. T., 1985. Mineralogic Summary of Yucca Mountain, Nevada. LA-10543-MS, Los Alamos National Laboratory, Los Alamos, New Mexico.
- Broxton, D. E., R. G. Warren, R. C. Hagan and Gary Luedemann, 1986. Chemistry of Diagenetically Altered Tuffs at a Potential Nuclear Waste Repository, Yucca Mountain, Nye County, Nevada. LA-10802-MS, Los Alamos National Laboratory, Los Alamos, New Mexico.
- Broxton, D. E., D. L. Bish, and R. G. Warren, 1987. Distribution and Chemistry of Diagenetic Minerals at Yucca Mountain, Nye County, Nevada. Clays and Clay Minerals, Vol. 35, No. 2, pp. 89-110.
- Hoover, D. L., 1968. Genesis of Zeolites, Nevada Test Site. Geol. Soc. Am., Memoir 110, pgs. 275 to 284.
- Livingston, Donald E. 1992. Some Aspects of Alteration and Metasomatism at Yucca Mountain, Nevada. Presentation to: The Association Of Engineering Geologists, Southwestern Section, Las Vegas, Nevada, Nov. 10, 1992.
- Livingston, Donald E. 1993. A Review of the Major Element Geochemistry of Yucca Mountain, Nevada. Report No. 4, Quarterly Report submitted to the Nuclear waste Project Office of the State of Nevada. Technical and Resource Assessment Corporation, Boulder, Colorado, 89 pp.
- Marshall, B. D., Z. E. Peterman and J. S. Stuckless, 1993. Strontium isotopic Evidence for a Higher Water Table at Yucca Mountain. High Level Radioactive Waste Management, Proceedings of the Fourth International Conference, Las Vegas, Nevada, April 26-30. American Nuclear Society, La Grange, Ill. and American Society of Civil Engineers, New York, NY.

- Peterman, Z. E., R. W. Spengler, F. R. Singer and R. P. Dickerson, 1993. Isotopic and Trace Element Variability in Altered and Unaltered Tuffs at Yucca Mountain, Nevada. High Level Radioactive Waste Management, Proceedings of the Fourth International Conference, Las Vegas, Nevada, April 26-30. American Nuclear Society, La Grange, Ill. and American Society of Civil Engineers, New York, NY.
- Szymanski, J. S., 1989. Conceptual Considerations of the Yucca Mountain Groundwater System with Special Emphasis in the Adequacy of this System to Accommodate a High-Level Nuclear Waste Repository. DOE Internal Report. U. S. Department of Energy. Las Vegas, Nevada.
- Szymanski, J. S., 1992 The origin and History of Alteration and Carbonization of the Yucca Mountain Ignimbrites. DOE Internal Report. U. S. Department of Energy. Las Vegas, Nevada.
- Vaniman, D. L., 1993. Calcite Deposits in Fractures at Yucca Mountain, Nevada. High Level Radioactive Waste Management, Proceedings of the Fourth International Conference, Las Vegas, Nevada, April 26-30. American Nuclear Society, La Grange, Ill. and American Society of Civil Engineers, New York, NY.
- Vaniman, D., D. Bish, D. Broxton, F. Byers, G. Heiken, B. Carlos, E. Semarge, F. Caporuscio, and R. Gooley, 1984. Variations in Authigenic Mineralogy and Sorptive Zeolite Abundance at Yucca Mountain, Nevada, Based on Studies of Drill Cores USW GU-3 and G3. LA-9707-MS, Los Alamos National Laboratory, Los Alamos, New Mexico.
- WoldeGabriel, G., 1990. Diagenetic Minerals, K/Ar Data, and Alteration History in the Yucca Mountain, Nevada: A Candidate High-Level Radioactive Waste Repository. Draft Report, Los Alamos National Laboratory, Los Alamos, New Mexico.

PART 8

**Isotopic and Fluid Inclusion Study of Yucca
Mountain Samples**

TRAC *Technology and Resource Assessment Corporation*

3800 Arapahoe Avenue, Suite 225
Boulder, Colorado 80303
(303) 443-3700 FAX No. (303) 443-8626

**ISOTOPIC AND FLUID INCLUSION STUDY OF YUCCA
MOUNTAIN SAMPLES**

QUARTERLY REPORT No.6
CONTRACT No. 92/94.0004

QUARTERLY REPORT Submitted to the
Nuclear Waste Project Office
State of Nevada

August, 1993

Authored by:

R. S. Harmon
Geochemisches Institut
der Universität Göttingen
Goldschmidtstrasse 1
D-37077 Göttingen, Germany

ISOTOPIC AND FLUID INCLUSION STUDY OF YUCCA MOUNTAIN SAMPLES

TABLE OF CONTENTS

Introduction	1
1. Strontium Isotope Results	3
2. Carbon and Oxygen Isotope Results	8
3. Fluid Inclusion Study	19
4. U-Series Disequilibrium Analysis and Geochronology	27

LIST OF TABLES

Table 1. Sr-, C-, and O- Isotope Data	7
Table 2. U-Series Disequilibrium Data	29

LIST OF FIGURES

Figure 1. Distribution of Measured Sr-Isotope Ratios	5
Figure 2. Distribution of Measured C- and O- Isotope Ratios	11
Figure 3. Plots of $\delta^{18}\text{O}$ vs $\delta^{13}\text{C}$ and $\delta^{18}\text{O}$	12
Figure 4. Plots of $\delta^{18}\text{O}$ and $\delta^{13}\text{C}$ as a function of $^{87}\text{Sr}/^{86}\text{Sr}$	13
Figure 5. Distribution of Fluid Inclusion Temperatures	24
Figure 6. Distribution of U and Th Concentrations	32
Figure 7. Distribution of U-series Isotope Activity Ratios	33

Figure 8. Plots of [$^{234}\text{U}/^{238}\text{U}$] and [$^{230}\text{Th}/^{234}\text{U}$] Ratios vs U	34
Figure 9. U-series Isochron Diagram	37

APPENDIX

Appendix 1 - Detailed List of Samples Collected at Each Stop	38
--------------------------------------------------------------	----

ISOTOPIC AND FLUID INCLUSION ANALYSIS PROGRAM

SUMMARY REPORT

This report presents (i) the analytical data obtained for a suite of samples collected during a 5-day field visit to the Yucca Mountain area by TRAC scientists in December 1992 and (ii) the interpretations of this data. The sample suite selected for isotopic and fluid inclusion study was chosen to be representative of the 203 samples collected. A major objective of this aspect of the geochemical program undertaken by TRAC was to obtain, on the same geological samples, different types of analytical data, deemed to be important to elucidating the origin of the mixed carbonate/silica vein deposits which occur throughout the Yucca Mountain area. Such an integrated analytical approach was not a feature of previous studies undertaken by USGS and the State of Nevada scientists.

Four different analytical approaches were utilized in this study: (i) determination of $^{87}\text{Sr}/^{86}\text{Sr}$ ratios; (ii) determination of $^{13}\text{C}/^{12}\text{C}$ and $^{18}\text{O}/^{16}\text{O}$ ratios; (iii) determination of U and Th concentrations, U-series isotope activity ratios, and U-series disequilibrium radiometric ages; and (iv) fluid inclusion analysis.

The Sr-isotope measurements were made by thermal ionization mass spectrometry in the laboratory of Prof. S. Moorbath (FRS) of the Department of Earth Sciences at Oxford University, Oxford (UK). The C- and O- isotope measurements were made

by gas-source mass spectrometry in the stable isotope laboratory of Prof. Dr. J. Hoefs of the Geochemistry Institute at the University of Göttingen (Germany) under the direction of Dr. R. S. Harmon. The U-series analyses were made by alpha spectrometry in the laboratory of Prof. D. C. Ford (FRSC) of the Department of Geography at McMaster University in Hamilton (Canada), and the fluid inclusion study was conducted by Dr. D. M. H. Alderton of the Department of Geology at Royal Holloway and Bedford New College of the University of London in Egham (UK).

1. STRONTIUM ISOTOPE PROGRAM

SUMMARY REPORT AND INTERPRETATION

Introduction

Strontium is an alkaline earth element that has a geochemical behavior similar to that of calcium, except that in most geological situations it occurs as a trace element and therefore its distribution and isotopic composition can be used as petrogenetic tracers. Because carbonate minerals form essentially free of Rb, $^{87}\text{Sr}/^{86}\text{Sr}$ ratio of a carbonate will not change as a result of radioactive decay so that at any subsequent time, the measured ratio will reflect directly the ultimate source or sources from which the dissolved Sr was derived.

Analytical Procedures

Twenty-five (25) samples were submitted for Sr-isotope analysis as follows: 14 carbonates (4d, 5c, 10a, 14g, 16c, 19a, 28d, 30c, 36n, 36z, 38f, 39a, 40b, and 41b), a single sample of the Wahmonie paleo-spring gypsum mound (32d), 6 Paleozoic sedimentary rocks (2a, 2b, 4a, 11c, 26a, and 34a), 2 samples associated with Tertiary mineralization (24c and 24d), and 2 volcanic samples (20a and 29d). For a complete listing of the location, brief description, and identification of each sample, refer to Appendix 1.

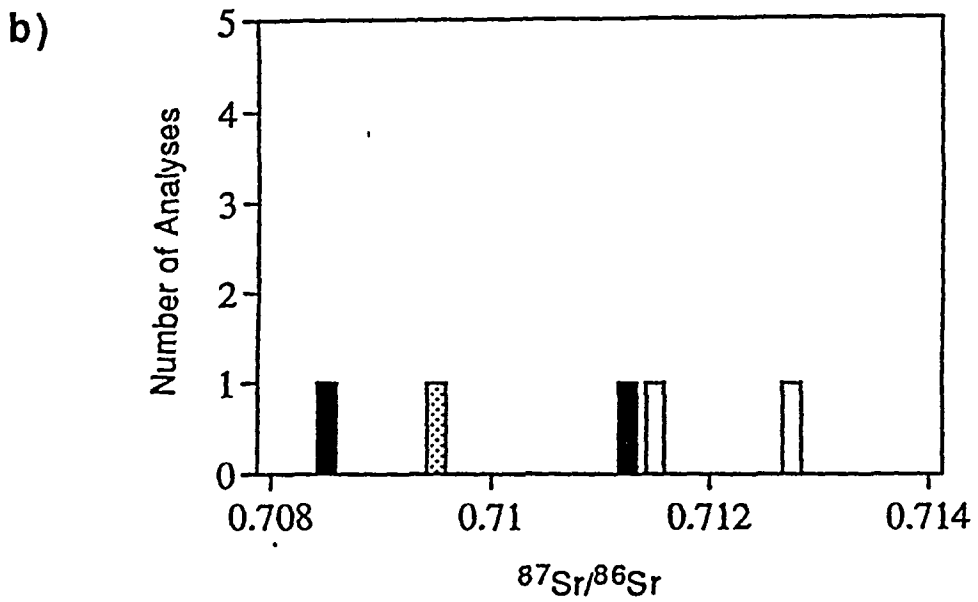
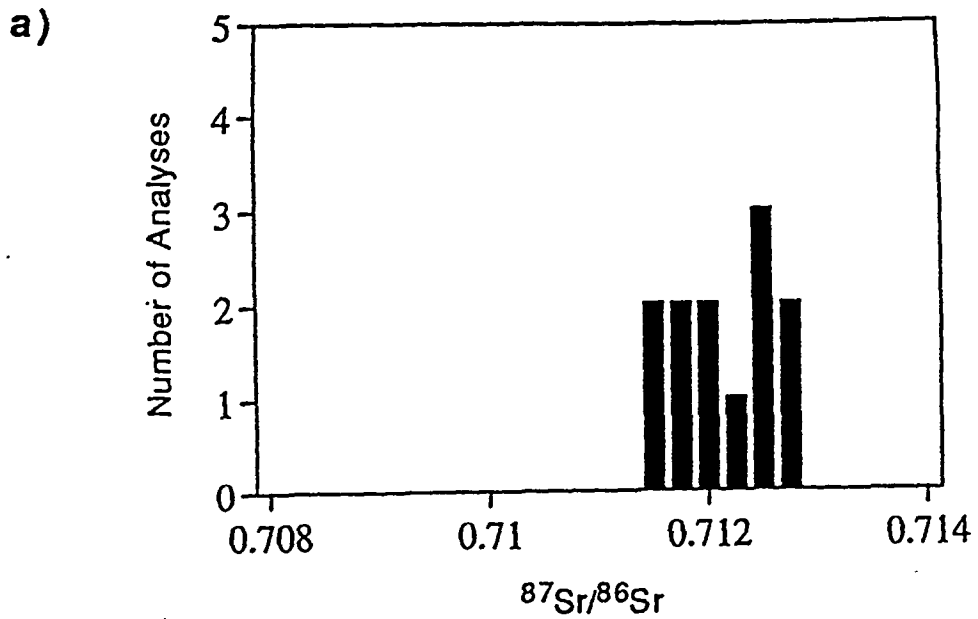
Samples were dissolved using conventional approaches appropriate to the sample type, and Sr separated and purified using an anion exchange resin. Purified Sr was

evaporated onto a metal filament and the $^{87}\text{Sr}/^{86}\text{Sr}$ ratio determined by thermal ionization mass spectrometry. Measured Sr-isotope ratios were normalized to a value of $^{86}\text{Sr}/^{88}\text{Sr} = 0.1194$ and $^{87}\text{Sr}/^{86}\text{Sr} = 0.70800$ for the Eimer and Amend SrCO_3 standard. The analytical uncertainty for the normalized $^{87}\text{Sr}/^{86}\text{Sr}$ ratios is better than ± 0.00005 at the ± 2 -sigma confidence level.

Seven (7) samples turned out to have Sr contents lower than indicated by the chemical analyses provided. Because these samples (2a, 2b, 11c, 19a, 29d, 36n, and 39a) did not give acceptable results in terms of beam stability and internal reproducibility during analysis and presently are being reanalyzed, the data for them is not included in this report, but will be forwarded as soon as it becomes available.

Results

Sr-isotope data are reported in Table 1. The 11 carbonates are characterized by quite uniform $^{87}\text{Sr}/^{86}\text{Sr}$ ratios of 0.71137 to 0.71260 (Figure 1), with a mean value of 0.71205 ± 0.00045 . This is a range of only 1.73‰, from +3.06 to +4.79 in the $\delta^{87}\text{Sr}$ notation occasionally utilized by the USGS. The Paleozoic sediments span the range of Sr-isotope composition observed for the carbonate; the limestones tending to be slightly depleted in ^{87}Sr with ratios of 0.70932 and 0.71162, whereas the shale is more ^{87}Sr rich with a ratio of 0.71345. Carbonate associated with the Tertiary mineralization at Bonanza King, with $^{87}\text{Sr}/^{86}\text{Sr}$ ratios of 0.71137 to 0.71274, has a Sr-isotopic composition which falls within the range of the Yucca Mountain carbonates. By contrast, the carbonate coating on volcanic material at Lathrop cone and carbonate from the Wahmonie gypsum mound both have Sr-isotope ratios



- Wahmonie gypsum mound carbonate
- Carbonate coating at Lathrop Cone
- ▨ Paleozoic limestone
- Carbonate associated Tertiary mineralization

Figure 1. Distributions of measured Sr-isotope ratios for: a) carbonate and mixed carbonate/silica veins, and b) other deposits.

which are lower than all other carbonate samples measured, with $^{87}\text{Sr}/^{86}\text{Sr}$ ratios of 0.71120 and 0.70830, respectively.

Conclusions

The restricted range of Sr-isotopic variation for the carbonates suggests that the Sr in the carbonates was derived from a single source or from proportionally constant mixtures of components derived from two sources. Whether the Sr was of local origin, near-surface derivation, or had been mobilized at depth by groundwaters remains unanswered. At the present time, the potential sources for the Sr in the carbonate deposits are too poorly constrained in terms of their Sr-isotopic composition to permit a definitive interpretation of the data. However, the data do not exclude a groundwater source for the Sr in the vein carbonates and, importantly in the context of the fluid inclusion results reported in Section 4, the Tertiary mineralization at Bonanza King has equivalent Sr-isotope ratios to the carbonate deposits. Therefore, both could have been deposited from hydrothermal fluids derived from the same source - possibly Paleozoic sedimentary rocks - now that such an epithermal component has been recognized as the youngest event in the depositional history of the carbonate deposits. Alternatively, the carbonates could be precipitates from groundwaters, a possibility consistent with the $^{234}\text{U}/^{238}\text{U}$ data for the carbonates reported in Section 5.

Sample #	$^{87}\text{Sr}/^{86}\text{Sr}$	$\delta^{87}\text{Sr}$	$\delta^{13}\text{C}_{\text{PDB}}$ (carbonate)	$\delta^{18}\text{O}_{\text{PDB}}$ (carbonate)	$\delta^{18}\text{O}_{\text{SMOW}}$ (carbonate)	$\delta^{18}\text{O}_{\text{SMOW}}$ (opal)	$\Delta^{18}\text{O}$ (opal-carb)
carbonate and mixed carbonate/silica deposits							
4a	0.71162	3.41	-0.81	-9.07	21.51		
4d	0.71217	4.19	-3.41	-7.27	23.26	28.17	4.91
5c	0.71231		-6.59	-9.97	20.58		
10a	0.71164	3.44	-6.54	-10.28	20.19	28.19	8
14g	0.71179	3.65	-5.39	-6.27	24.4		
16c	0.71142	3.13	-5.28	-10.67	19.12		
19a	0.71257	4.75	-7.08	-10.69	19.84	28.17	8.33
28d	0.71137	3.06	-4.77	-9.2	21.38		
30c	0.71249	4.64	-5.14	-10.31	20.23	29.91	9.68
36n			-7.2	-10.57	19.79		
36z	0.7126	4.79	-7.84	-10.69	19.83		
38f	0.71188	3.78	-3.97	-10.43	20.11		
39a			-5.84	-9.33	21.25		
40b	0.71231	4.38	-4.76	-9.38	21.19		
Wahmonie Gypsum mound							
32d	0.7083	-1.27	-4.4	-10.68	19.85		
Lathrop Cone carbonate coating							
41b	0.7112	2.82	0.47	-5.82	25.04		
Paleozoic limestones							
26a	0.70932	0.17	-1.02	-8.89	21.7		
other Paleozoic sedimentary rocks							
34a	0.71345	5.99					
Tertiary mineralization							
24c	0.71137	3.06	-0.43	-7.37	23.26		
24d	0.71274	4.99	-2.77	-10.64	19.91		

Table 1. Strontium, carbon, and oxygen isotope data for samples from Yucca Mountain and vicinity.

2. C- & O- ISOTOPE ANALYSIS PROGRAM

SUMMARY REPORT AND INTERPRETATION

Introduction

The stable isotopes of carbon and oxygen are useful as geochemical tracers because fractionations of the light stable isotopes occur due to physio-chemical processes in the natural environment but isotope ratios do not change as a function of time. Hence, different environments tend to be characterized by distinct stable isotope compositions. Also, because isotope fractionation between coexisting phases at equilibrium is temperature dependent, there is an important potential for geothermometry.

Analytical Procedures

Nineteen (19) samples were submitted for C- and O- isotope analysis as follows: 14 carbonates (4a, 4d, 5c, 10a, 14g, 16c, 19a, 28d, 30c, 36n, 36z, 38f, 39a, and 40b), single sample of carbonate from the Wahmonie (paleo-spring) gypsum mound (32d) and a carbonate coating from volcanic debris at the Lathrop cone (41b), a Paleozoic limestone (26a), and 2 samples associated with Tertiary mineralization (24c and 24d). A subset of four mixed carbonate/silica samples (4d, 10a, 19a, and 30c) was selected for an O-isotope geothermometry feasibility study. Refer to Appendix 1 for a complete sample description. Carbon and oxygen were liberated from the carbonate samples using conventional vacuum preparation techniques. After overnight outgassing under vacuum, the carbonate samples were reacted at 25°C

with 100% phosphoric acid and the CO₂ produced was purified cryogenically. For the opal samples, oxygen was liberated by reaction with ClF₃ at 650°C, converted to CO₂ by reaction with hot platinized graphite, and the CO₂ purified cryogenically. Isotope ratios of ¹³C/¹²C and ¹⁸O/¹⁶O were determined by gas-source mass spectrometry and are reported in Table 1 in the conventional δ-notation as per mil (‰) variations relative to either the PDB standard (carbonate C and O) or the SMOW standard (carbonate and opal O). Analytical uncertainties are less than ±0.1‰ for ¹³C/¹²C ratio determinations and on the order of ±0.15‰ for ¹⁸O/¹⁶O ratios.

Results and Interpretation

C- and O- isotope data are reported in Table 1. The 14 carbonates are characterized by large ¹³C/¹²C and ¹⁸O/¹⁶O variations of c. 7‰ and c. 5‰, respectively (Figure 2). These ranges are slightly greater than those documented by previous studies; δ¹³C_{PDB} = -7.8 to -0.8‰, as compared with c. -8 to -3‰, δ¹⁸O_{PDB} = -6.3 to -10.7‰, as compared with c. -11 to -8.5‰. The C- and O- isotopic compositions of the other carbonates and country rocks analyzed overlap those of the carbonate veins, but there is a tendency for the carbonate veins to have slightly lower δ¹³C_{PDB} values. Carbonate of the Wahmonie gypsum mound is similar in C- and O- isotope composition to the carbonate veins, whereas that of the carbonate coating at Lathrop cone is enriched in ¹³C and ¹⁸O relative to all other samples measured. For the Paleozoic limestone and carbonates associated with Tertiary mineralization, C- and O- isotope ratios fall with the ranges of the carbonate veins, but lie toward the ¹³C- and ¹⁸O- rich portions of the distributions.

Figure 3 presents plots of $\delta^{13}\text{C}_{\text{carb}}$ and $\delta^{18}\text{O}_{\text{opal}}$ vs. $\delta^{18}\text{O}_{\text{carb}}$; Figure 4 displays C- and O- isotope ratios as a function of Sr-isotope ratio. In each of these figures, isotopic variations for the carbonate veins are compared with those of the other types of samples from the Yucca Mountain region that were analyzed; also identified is carbonate sample 4d, for which two independent lines of evidence from this study indicate a hydrothermal origin related to an epithermal environment (see Sections 3 and 4 below). In Figure 3a, most of the carbonate samples cluster in the lower left portion of the diagram in a field between the $\delta^{13}\text{C}_{\text{PDB}} = \text{c. } -8 \text{ to } -4\%$ and $\delta^{18}\text{O}_{\text{PDB}} = \text{c. } -11 \text{ to } -9\%$. Likewise, the majority of samples from the "Trench 14" and "Busted Butte" localities analyzed in other studies plot in this same region, but a few are displaced to higher $\delta^{18}\text{O}$ and $\delta^{18}\text{O}$ values. Sample 4d is also distinct from this main group of carbonates in the same manner, as are samples 4a (a sample of limestone related to a fault-associated alteration at the "Pull-Apart Fault" locality) and 14g (a mixed carbonate/opal vein sample from the "Trench 8" site). As seen in Figure 4, sample 14g is also similar to sample 4d in terms of its Sr-isotopic composition and, therefore, would be a high-priority sample for future fluid inclusion study. It is important to note that the $\delta^{18}\text{C}_{\text{PDB}}$ value of -3.4% for sample 4d is similar to the C-isotope composition of dissolved carbonate in the waters of the Paleozoic aquifer, $\delta^{13}\text{C}_{\text{PDB}} = -5 \text{ to } -2\%$, but distinctly different from the lower $\delta^{13}\text{C}_{\text{PDB}}$ values of $-11 \text{ to } -5\%$ that characterize waters of the Tertiary aquifer.

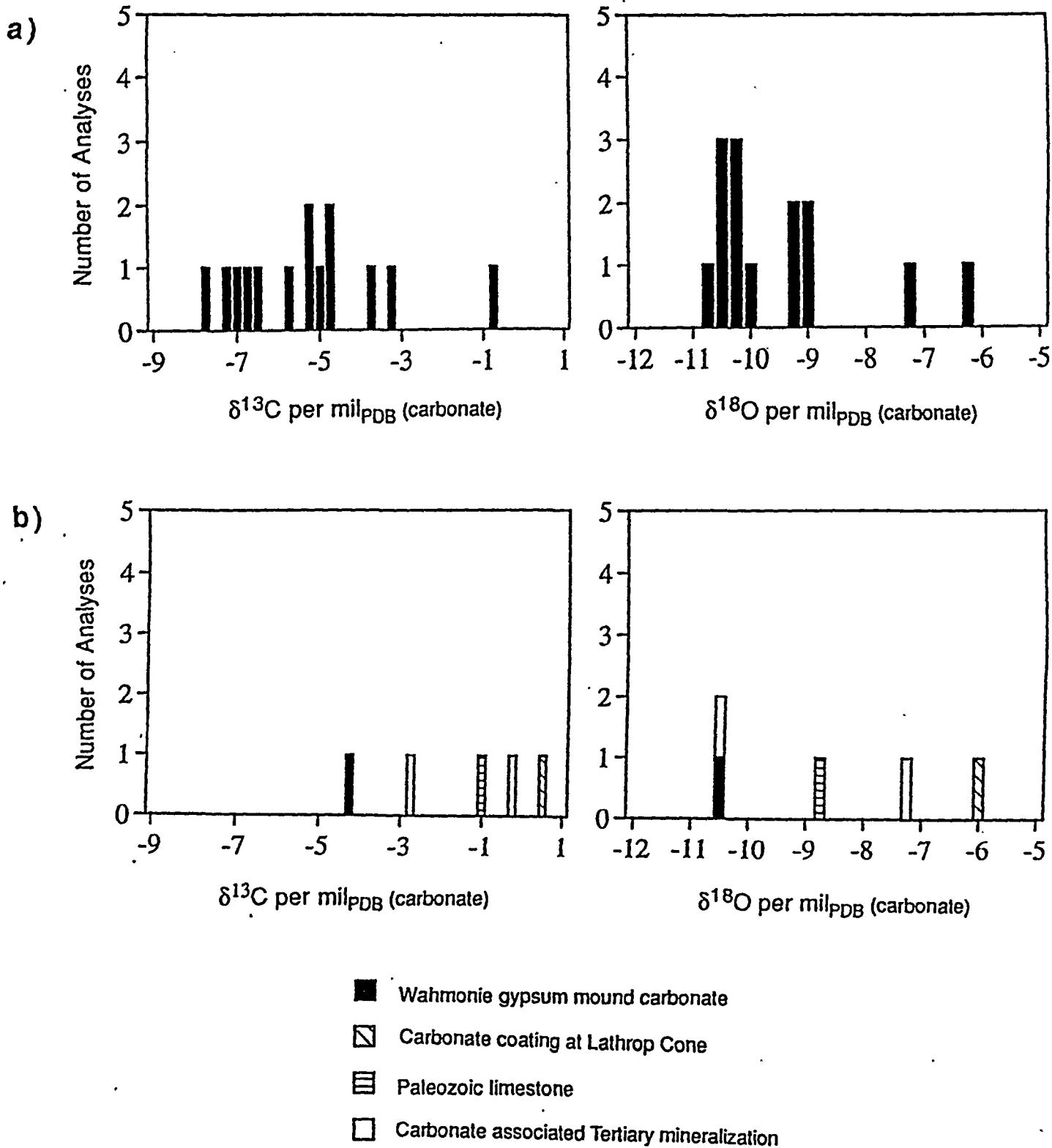
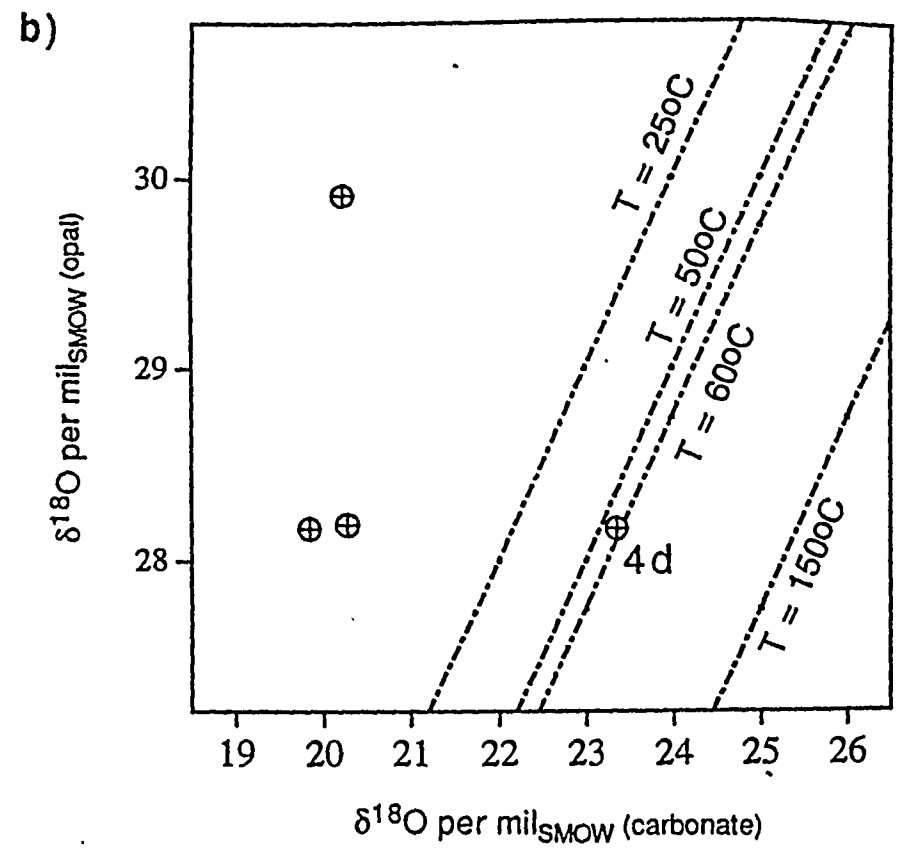
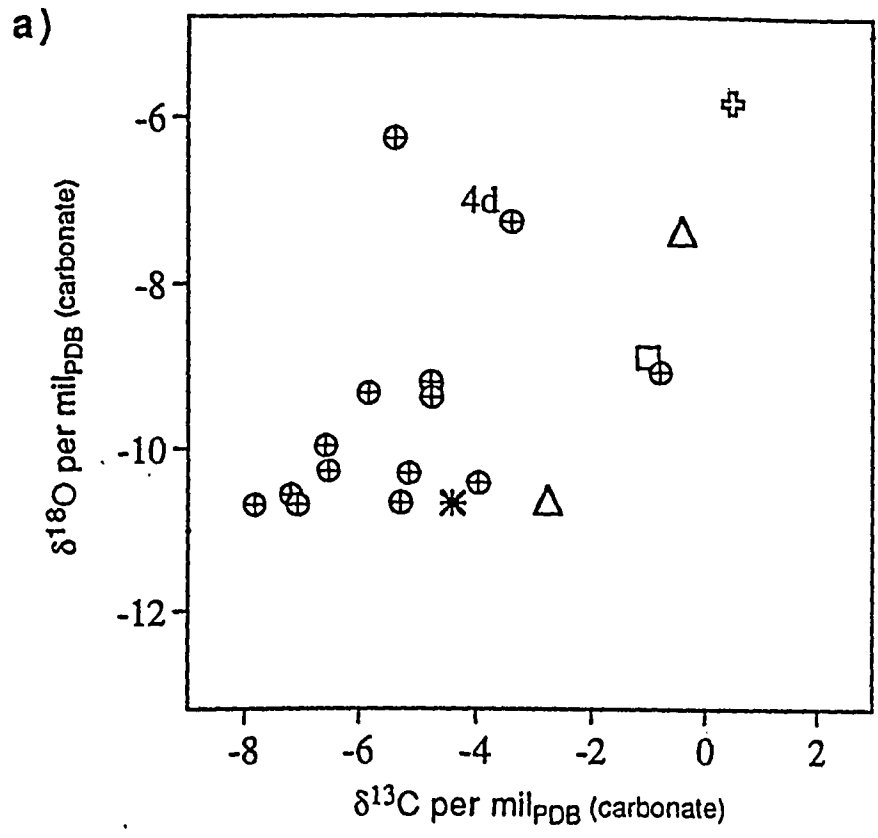
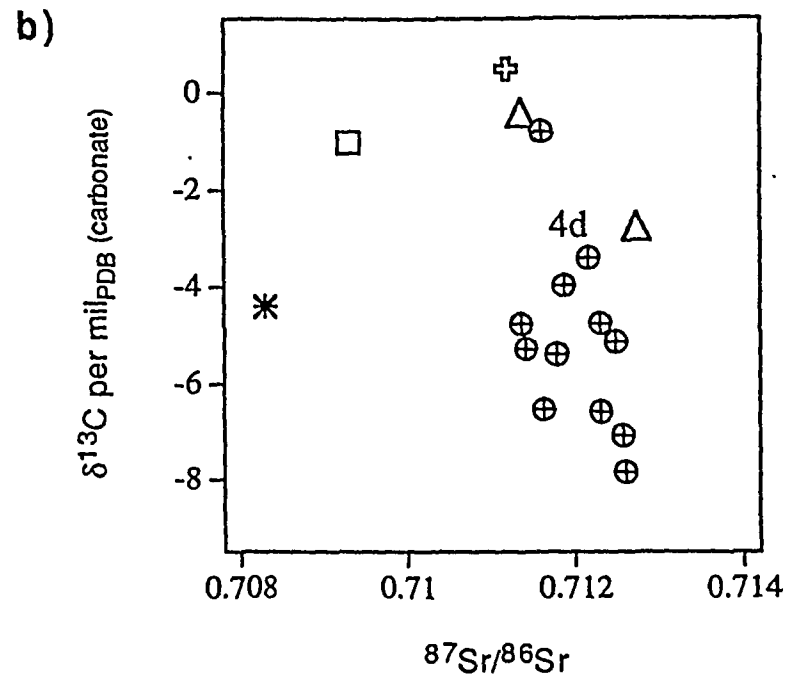
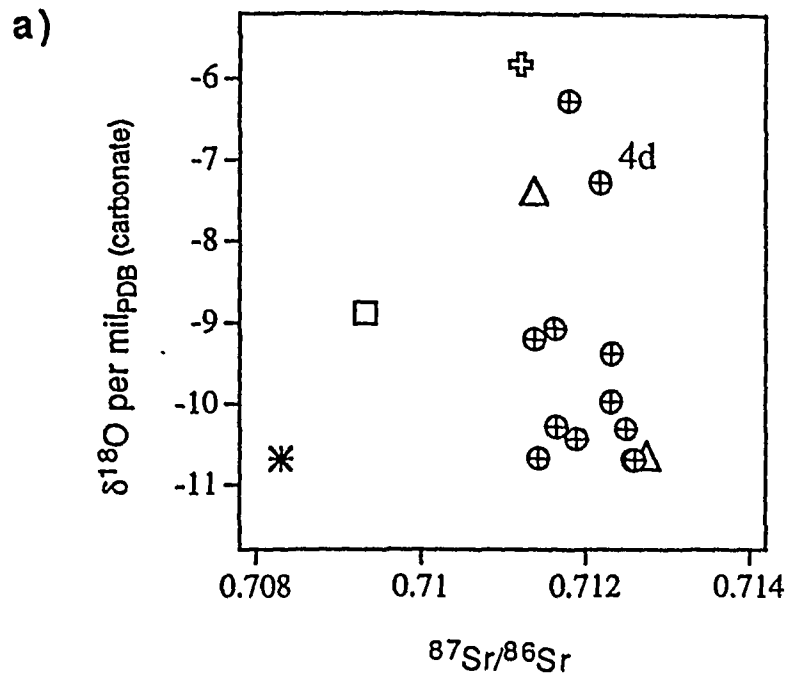


Figure 2. Distribution of measured C- and O- isotope ratios for: a) carbonate and mixed carbonate/silica veins, and b) other samples.



- ⊕ Carbonate and mixed carbonate/silica veins
- * Wahmonie gypsum mound carbonate
- △ Carbonate associated with Tertiary mineralization
- ⊕ Carbonate coating at Lathrop Cone
- Paleozoic limestone

Figure 3. Comparisons between: a) $\delta^{18}\text{O}$ (carbonate) vs. $\delta^{13}\text{C}$ (carbonate), and b) $\delta^{18}\text{O}$ (opal) vs. $\delta^{18}\text{O}$ (carbonate).



- ⊕ Carbonate and mixed carbonate/silica veins
- * Wahmonie gypsum mound carbonate
- ⊕ Carbonate coating at Lathrop Cone
- Paleozoic carbonate
- △ Carbonate associated with Tertiary mineralization

31 **Figure 4.** Comparisons between: a) $\delta^{18}\text{O}$ (carbonate) as a function of $^{87}\text{Sr}/^{86}\text{Sr}$, and $\delta^{13}\text{C}$ (carbonate) as a function of $^{87}\text{Sr}/^{86}\text{Sr}$.

If the carbonate coating on volcanic debris at Lathrop cone, which is strongly enriched in both ^{13}C and ^{18}O relative to the vein carbonates, can be considered typical of "pedogenic" carbonates that form in the Yucca Mountain area, then the stable isotope data lead to the conclusion that different processes have been responsible for the deposition of these two carbonate types. This distinct isotopic composition must either characterize a particular source or result from a process, such as evaporation, which is characterized by a kinetic fractionation that produces isotope enrichment in the solid phase. As a marine carbonate, the most isotopically enriched geological reservoir of the region has a C- and O- isotopic composition that falls within the range of $\delta^{13}\text{C}$ and $\delta^{18}\text{O}$ variation observed for the carbonates, evaporation is considered the most likely mechanism for producing the enriched C- and O- isotopic character of the Lathrop cone carbonate.

Further constraints on the origin of various carbonates of the Yucca Mountain area are provided by the Sr-C and Sr-O isotope plots shown in Figure 4. In these diagrams, distinct differences are observed for the carbonate veins, the Paleozoic limestone, and carbonate of the Wahmonie gypsum mound. A striking feature of these figures is the similarity of the vein carbonates (particularly samples 4d, 14g, and 4a) to the carbonates associated with hydrothermal mineralization at the "Bonanza King" locality.

Conclusions

Considered in the context of stable isotope data from previous studies, the stable

isotope data for the carbonate vein deposits of the Yucca Mountain area can be interpreted in terms of mixing between two fluid components, a higher temperature component characterized by high and variable C- and O-isotopic compositions (the sample 4d source) and a second less variable low-temperature component having low $\delta^{13}\text{C}$ and $\delta^{18}\text{O}$ values. Deep groundwaters are possible source for the elevated temperature fluid.

There is a similarity in isotopic composition between the carbonate veins, particularly sample 4d, to carbonates associated with Tertiary mineralization.

O-ISOTOPE GEOTHERMOMETRY

Introduction

O-isotope ratios were determined for four carbonate-opal pairs to assess the potential of this approach for geothermometry. Assuming that two coexisting phases have been deposited under conditions of O-isotope equilibrium from a common fluid phase, then the distribution of ^{18}O between the two phases will be a direct function of the temperature of deposition.

Recently, the results of direct, O-isotope exchange experiments have been reported for the system quartz-calcite over the temperature range 600-800°C. Because there is good thermodynamic data for these two mineral phases in the literature, it is possible to extrapolate the results of these experiments to temperatures outside of

the experimental range using reduced partition coefficient ratios obtained from statistical mechanics calculations. For the system quartz-calcite, this approach predicts the O-isotope fractionations over the low-temperature interval from 25-250°C listed below. The term $\Delta^{18}\text{O}_{\text{qtz-calc}}$ is the intermineral O-isotope fractionation and is equivalent to the difference between isotope ratios measured for two coexisting minerals (e.g. $\delta^{18}\text{O}_{\text{qtz}} - \delta^{18}\text{O}_{\text{calc}}$).

T (°C)	$\Delta^{18}\text{O}_{\text{qtz-calc}}$
25	6.03
36	5.69
51	5.04
60	4.76
70	4.49
105	3.53
135	3.21
153	2.73
204	2.10
254	1.64

Results and Interpretation

The O-isotope results for the four Yucca Mountain sample pairs analyzed are presented in the table below. Two important conclusions can be drawn from this comparison of the analytical and experimental data and from the plot of $\delta^{18}\text{O}_{\text{opal}}$ vs $\delta^{18}\text{O}_{\text{carb}}$ shown in Figure 3b.

sample	$\delta^{18}\text{O}_{\text{opal}}$ (‰ SMOW)	$\delta^{18}\text{O}_{\text{carbonate}}$ (‰ SMOW)	$\delta^{18}\text{O}_{\text{op-carb}}$ (‰)
4d	28.17	23.36	4.81
10a	28.19	20.27	7.92
19a	28.17	19.84	8.33
30c	29.91	20.23	9.68

1. The measured $\Delta^{18}\text{O}_{\text{qtz-carb}}$ values range from +4.8 to +9.7‰, as compared with the +6.0 to +16‰ fractionations expected for equilibrium deposition under surface to epithermal/hydrothermal temperatures of 25-250°C. Thus, for only one of the four samples, 4d, it is likely that deposition of carbonate and silica was contemporaneous and possibly occurred under conditions of O-isotope equilibrium. Assuming this to be the case, a depositional temperature of 50-60°C is indicated for this sample.

2. The ^{18}O variation observed for opal is much less than for calcite, ($\delta^{18}\text{O}_{\text{opal}} = +28.17$ to $+29.91$ vs $\delta^{18}\text{O}_{\text{calc}} = +19.84$ to $+23.36$), with three of the four opal samples having identical $\delta^{18}\text{O}$ values. This suggests that, in addition to sample 4d, samples 10a and 19a were deposited under essentially equivalent environmental conditions from an isotopically similar epithermal/hydrothermal solution. The displacement of these two samples (and sample 30c) far to the left of the 25°C isotherm in Figure 3b implies isotopic disequilibrium between opal and calcite in these samples. Quartz and opal are known to be essentially insensitive to post-depositional isotope exchange under low-temperature conditions, whereas fine-grain calcite will readily undergo isotope exchange. Therefore, the O-isotope relationships displayed in

Figure 3b are interpreted to indicate that the carbonate component of samples 10a, 19a, and 30c (and also other carbonate vein samples of similar composition) has been affected by post-depositional O-isotope exchange with a fluid phase having significantly lower ^{18}O content than that which precipitated the coexisting opal, such as meteoric precipitation.

Conclusion

This feasibility study of coexisting carbonate-opal pairs has raised the possibility of obtaining direct information about temperatures of deposition of these pairs.

3. FLUID INCLUSION STUDY

SUMMARY REPORT & INTERPRETATION

Introduction

Three small hand specimens of carbonate rich material formed the basis of this study (samples 4d, 5h, and 19e). Refer to Appendix 1 for a complete sample description. The objective of the study was to examine these samples for the presence of fluid inclusions. If found, and amenable to analysis, the fluid inclusions were to be subjected to thermometric analysis in order to obtain information concerning their environment of formation (i.e. homogenization temperature and fluid composition).

The three samples are intergrowths of carbonate and opal, but contain numerous quartz veinlets, brecciated zones, and small vugs partially infilled with gradations of cryptocrystalline-crystalline quartz. The fluid inclusion study was restricted to the quartz because of its universal value in fluid inclusion studies compared to carbonate minerals.

Sample Preparation and Analysis

Doubly-polished thin sections, 100-150 μ m in thickness were made using routine techniques for such "wafers" and the thin sections examined using a standard petrographic microscope at magnifications up to 600x. Thermometric study was undertaken using a Linkham TH600 heating-freezing stage, which previously had

been calibrated with synthetic standards. Because of the presence of opaque phases, the samples were also viewed under reflected light at a magnification of up to 600x. The fluid inclusions in the samples were not amenable to photography due to their size.

Petrographic Examination

SAMPLE 5h

This sample consists of predominantly of carbonate in which there are numerous sub-parallel veinlets of quartz. Under high magnification, the veinlets quartz is observed to be zoned, the central portions of consisting of clear euhedral quartz crystals and the outer zone being comprised of fine-grained cryptocrystalline quartz (opal). Some of the veinlets contain unfamiliar tubular structures of undetermined composition. Neither their origin nor their significance is known, they could be organic, or could represent a low-temperature epithermal fluid flow structures. The latter explanation is preferred as there are mammillated surfaces on some of the voids which appear to consist of similar material.

The clear euhedral quartz crystals are totally lacking in fluid inclusions, except for a few very small (<1 μ m) monophase (?) inclusions. However, the sample does contain relatively abundant very small grains and microveinlets of pyrite and chalcopyrite. The pyrite tends to occurs as small, discrete grains scattered throughout the sample, whereas the chalcopyrite occurs either as solitary grains or

as microveinlets. All of the sulfides occur as particles on the order of a few microns diameter. Some of the microveinlets exhibit a clear association with zones of brecciation in the carbonate host. Together, the occurrence of sulfides in this sample and their introduction by solutions during or after a minor phase of brecciation, suggest an origin related to an epithermal environment.

SAMPLE 19e

This is a mixed carbonate/silica sample containing numerous small void spaces which have been infilled with secondary silica. The silica deposited within the "vuggy" areas is zoned from an early fine-grained microcrystalline silica (opal) to a later clear crystalline quartz which forms subhedral to euhedral crystals with doubly-terminated bipyramidal forms. These appear to be isolated within the carbonate component of the sample, so their relationship to the vug-filling quartz in the sample is unclear. Some of these isolated crystals are cross-cut by micro-fractures.

In places, the quartz crystals contain abundant, but minute ($<1\mu\text{m}$) fluid inclusions not suitable for thermometric analysis. Many are not easily resolved, but appear as solid "specks" within the host quartz. Two kinds of the inclusions appear to be present in the sample, a monophasic gaseous type and a 2-phase liquid-vapor variety. The latter have a high degree of fill (i.e. ratio of liquid to total volume of about 0.9). Small pyrite grains are also present in this sample, scattered throughout the host carbonate, and microveinlets consisting of chalcopyrite are observed to crosscut some of the euhedral-subhedral quartz crystals.

SAMPLE 4d

This is a mixed carbonate/silica sample that contains three distinct types of quartz:

- (i) solitary crystals of a bipyramidal form,
- (ii) veins of fibrous quartz,
- and
- (iii) euhedral crystals infilling "vugs".

The fibrous quartz is inclusion free, but the other two varieties contain inclusions sufficiently large for detailed study and analysis. The solitary, bipyramidal crystals have rounded margins, some are crosscut by fractures, and all appear to be incorporated in a breccia zone within the sample. The inclusions in the solitary crystals contain immobile bubbles that commonly do not have a spherical shape. In the vug-filling quartz, the inclusions are 2-phase, liquid-bearing inclusions with a high degree of fill (c. 90%) and in these samples the bubble is spherical in shape and mobile. These latter inclusions occur in small groups and on planes which cut across the host quartz. Their size is on the order of 5 μ m in diameter. There is no evidence of whether they are of primary or secondary origin. Several of the liquid inclusions also contain an opaque crystal. Presumably this is a cogenetic mineral phase captured during inclusion growth, rather than a true "daughter" mineral that crystallized inside the inclusion after its formation, and is most likely a sulfide such as pyrite or chalcopyrite.

Thermometric Analysis

Sample 4d was the only one of the three samples which contained fluid inclusions of adequate size for thermometric analysis. However, even in this sample, fluid inclusions are small and relatively rare, so that only 22 were located that were of a sufficient size for thermometric analysis. The heating measurements were confined to the temperature of homogenization of the inclusion (T_h), which always was measured at a time of the disappearance of the vapor bubble. The freezing measurements were confined to a recording of the last melting temperature of the ice formed inside the inclusions upon freezing. Only two reliable measurements could be obtained because of the small size of the inclusions.

As illustrated in Figure 3, thermometric analysis of the liquid inclusions in the euhedral, vug-filling quartz of sample 4d yielded a temperature of homogenization (T_h) range of 118 to $>216^\circ\text{C}$, with a mean of 147°C . One inclusion had not homogenized at 220°C , but was not heated further to avoid decrepitation of the inclusion. The T_h determinations are considered accurate to about $\pm 3^\circ\text{C}$, given the small size of the inclusions. The number of measurements is inadequate to ascertain if the observed temperature distribution is bimodal or not. Some necking down of inclusions was observed, resulting in abnormally large vapor bubbles, but such inclusions were not utilized for the thermometric study.

Although the fluid inclusions within the subhedral-euhedral quartz of sample 19e were not of adequate size to permit thermometric analysis, the similarity of the

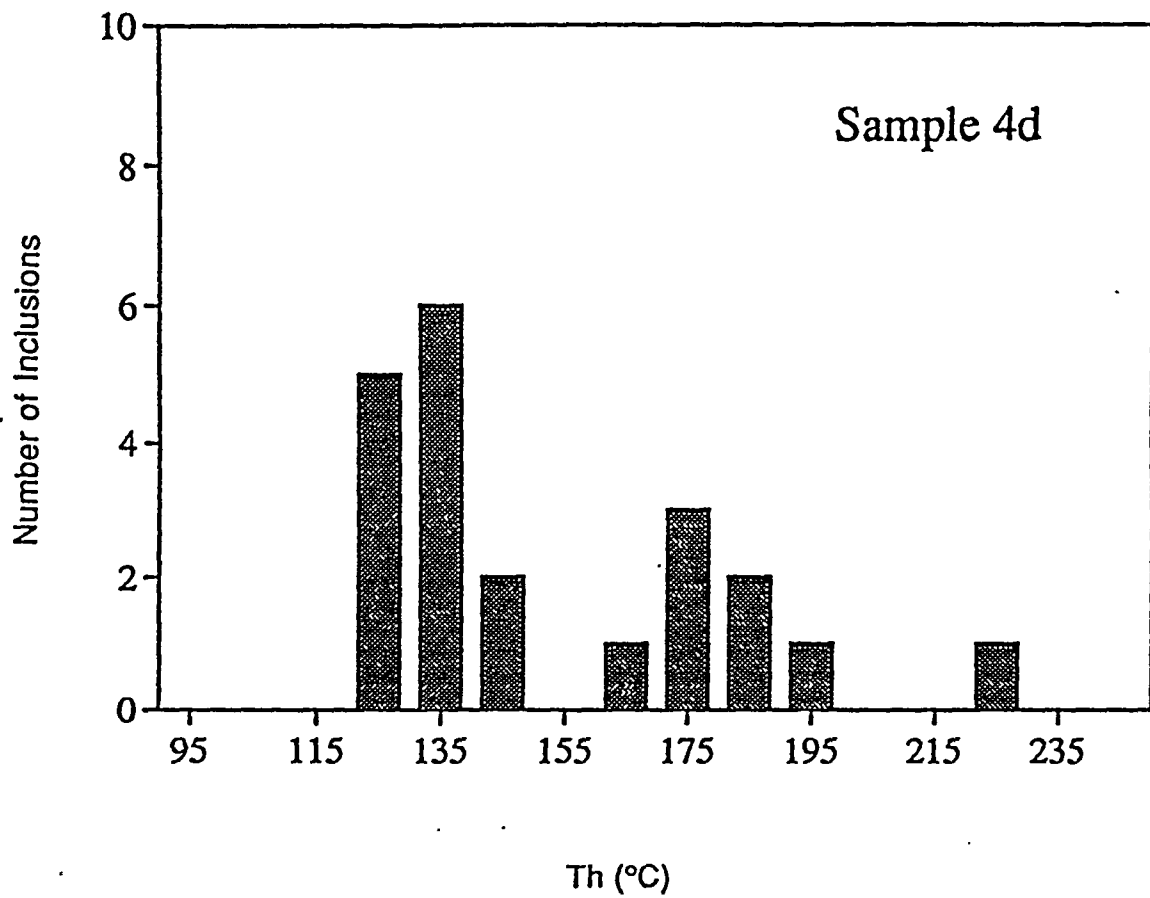


Figure 5. Distribution of fluid inclusion temperatures of homogenization (Th).

quartz in this sample to that in sample 4d, and the similar degree of fill of the inclusions, would suggest a similar range of homogenization temperatures to that observed in sample 4d.

No evidence of boiling was observed in the inclusions analyzed. Therefore, the T_h values measured for sample 4d represent a minimum temperature for hydrothermal activity. A pressure-based temperature correction, which would be controlled by the depth of formation, is necessary to define precise fluid inclusion filling temperatures. However, a rough approximation of the depth of formation of the quartz in sample 4d (i.e. the depth necessary to prevent boiling of the fluid) is c. 150 meters.

Only two inclusions were located in sample 4d which were of an adequate size for freezing studies. The last melting temperatures of ice translates to salinities of 0.1 and 0.5 wt % NaCl (equivalent) for these two inclusions.

The inclusions in the solitary, bipyramidal quartz crystals were heated to 400°C, but neither movement of the vapor bubble nor a change in phase proportions was noted. This observation, coupled with the distorted vapor bubbles and the bipyramidal form of the quartz crystals, suggest that these inclusions consist of glass (i.e. that they represent a trapped silicate melt phase). This rounded quartz is undoubtedly of magmatic origin and detrital in character: therefore, it has been derived from a different source than the host carbonate in which it occurs. This is an important sign that caution must be exercised in any future fluid inclusion studies of this type of

material; it will be crucial to recognize such glass inclusions and the volcanic origin of such host quartz.

Conclusions

At least three types of quartz have been identified in the Yucca Mountain carbonate and mixed carbonate/opal vein deposits: (i) a fibrous vein quartz that is inclusion free, (ii) vug and void space infillings within the carbonate material of cryptocrystalline silica and euhedral quartz that contains fluid inclusions amenable to thermometric analysis, and (iii) bipyramidally-terminated quartz crystals of presumably volcanic derivation.

Thermometric measurements indicate that the temperature of formation of the fluid inclusions in sample 4d was c. 150°C, last melting temperatures for ice in the inclusions indicates that the fluids involved were of a dilute character (<1 wt% NaCl equivalent), and the fact that evidence for boiling was not observed in the inclusions implies a depth formation for the fluid inclusions of around 150m.

Thus, the vug-filling quartz in sample 4d appears to have been deposited from a moderate-temperature, low-salinity fluid or, at least, was subjected to an episode of interaction with such a fluid some time after its formation. These facts, together with the presence of microbreccia veinlets and sulfides in the Yucca Mountain samples, points to a hydrothermal environment with a low-temperature character (i.e. epithermal origin).

4. U-SERIES PROGRAM

SUMMARY REPORT AND INTERPRETATION

Introduction

Naturally-occurring disequilibrium within the ^{238}U decay series is one of the most important means of obtaining geochronologic information for geological deposits of late Quaternary age. The $^{238}\text{U}/^{238}\text{U}$ ratios and concentrations of U and Th determined as a part of a U-series geochronological investigation also have utility as geochemical tracers.

Analytical Procedures

U-series analysis by conventional alpha spectrometry was undertaken on nine (9) samples: 28d, 28e, 30a, 36d, 36g, 36k, 36n, 36p2, and 39a. Refer to Appendix 1 for a complete sample description. The samples were ground to a fine powder and dissolved in nitric acid, spiked with a $^{232}\text{U}/^{228}\text{Th}$ in isotopic equilibrium, and U and Th isotopes separated and purified using anion exchange resins. For analysis by alpha spectrometry, the purified U and Th were plated onto stainless steel discs and counted for 2-8 days to determine ^{238}U , ^{234}U , ^{232}Th , and ^{230}Th activities. U and Th concentrations were calculated from yield-corrected ^{228}Th and ^{232}U activities and, where appropriate, absolute ages were calculated from measured $^{230}\text{Th}/^{234}\text{U}$ and $^{234}\text{U}/^{238}\text{U}$ activity ratios according to standard radioactive decay equations, after correcting for the presence of detrital Th in the silica component of the samples, and assuming that the deposits had remained closed systems to U and Th since the time

of their deposition.

Results

Analytical data, in the form of measured isotope activities, chemical yields and concentrations of U and Th, calculated isotope activity ratios, and $^{230}\text{Th}/^{234}\text{U}$ ages are given in Table 2 and displayed graphically in Figures 6-9. Three repeat analyses were made: for sample 36d because of the very low chemical yields obtained on the first analysis, for sample 36k because Th portion of the sample was lost during the chemical separation procedures, and for sample 36n to confirm the high, finite age obtained from the first analysis.

The Yucca Mountain sample suite is characterized by uniformly low U and Th contents, respective ranges being 0.12-0.87 ppm for U and 0.15-1/16 ppm for Th. Concentrations of U approach a normal distribution (Figure 6), whereas Th contents exhibit a marked positive distribution that, in general, reflects the amount of insoluble residue remaining after acid dissolution of the carbonate sample. This indicates that the majority of Th in the Yucca Mountain samples resides in the detrital component.

Measured $^{230}\text{Th}/^{234}\text{U}$ and $^{234}\text{U}/^{238}\text{U}$ activity ratios range from 0.91-3.97 and 0.55-1.95, respectively (Figure 7). Ratios of $^{230}\text{Th}/^{232}\text{Th}$, an indication of the amount of Th associated with the detrital component of the carbonate samples, are exceptionally variable, ranging over nearly three orders of magnitude from 0.22 to 19.3 (Figure 7). For pure carbonate samples, free of any contamination, $^{230}\text{Th}/^{232}\text{Th}$ ratios should be high (>10-15). Low ratios are an indication that some

Sample #	^{238}U (cpm)	^{234}U (cpm)	^{232}U (cpm)	^{232}Th (cpm)	^{230}Th (cpm)	^{228}Th (cpm)	yield U (%)	yield Th (%)
28d	0.117±0.001	0.194±0.014	0.460±0.140	0.170±0.010	0.720±0.003	0.128±0.004	28.8	7.8
28e	0.020±0.004	0.110±0.180	0.716±0.18	0.025±0.002	0.018±0.003	0.537±0.010	42.1	30.8
30a	0.097±0.005	0.142±0.010	0.274±0.010	0.960±0.005	0.459±0.008	0.837±0.011	17.7	54.7
36d	0.170±0.004	0.022±0.003	0.037±0.004	0.016±0.003	0.137±0.006	0.132±0.005	2.4	8.3
36d (repeat)	0.040±0.003	0.061±0.005	0.097±0.005	0.121±0.005	1.116±0.011	1.143±0.011	6.3	65.4
36g	0.074±0.005	0.118±0.023	0.849±0.023	0.091±0.005	0.617±0.009	1.149±0.012	53.1	65.8
36k	0.119±0.004	0.108±0.005	0.517±0.008		Th sample lost			
36k (repeat)	0.110±0.005	0.71±0.025	0.976±0.025	0.092±0.003	0.191±0.005	0.549±0.007	57.4	33.4
36n	0.027±0.003	0.47±0.004	0.080±0.004	0.012±0.002	0.103±0.004	0.177±0.005	5.3	11.5
36n (repeat)	0.055±0.003	0.107±0.014	0.498±0.014	0.020±0.003	0.165±0.005	0.748±0.009	31.1	42.8
36p2	0.048±0.002	0.079±0.005	0.126±0.005	0.033±0.003	0.637±0.009	0.937±0.010	7.9	53.6
39a	0.108±0.003	0.183±0.009	0.265±0.009	0.031±0.002	0.134±0.005	0.219±0.007	17.7	14.2

Table 2. Results of U-series analyses.

Sample #	U (ppm)	Th (ppm)	$^{234}\text{U}/^{238}\text{U}$	$^{230}\text{Th}/^{234}\text{U}$	$^{230}\text{Th}/^{232}\text{Th}$	corrected age (ka)	uncorrected age (ka)	$(^{234}\text{U}/^{238}\text{U})_i$
28d	0.33	0.54	1.658 ± 0.134	1.37 ± 0.13	4.23 ± 0.38	>350 or indet.		
28e	0.12	0.65	0.550 ± 0.910	2.39 ± 3.72	0.72 ± 0.12	>350 or indet.		
30a	0.47	0.49	1.464 ± 0.123	1.09 ± 0.08	4.78 ± 0.24	>350 or indet.		
36d	0.48	0.4	1.294 ± 0.383	1.79 ± 0.43	8.56 ± 1.54	>350 or indet.		
36d (repeat)	0.38	0.31	1.525 ± 0.163	1.60 ± 0.14	9.22 ± 0.38	>350 or indet.		
36g	0.22	0.63	1.593 ± 0.332	3.97 ± 0.79	6.78 ± 0.36	>350 or indet.		
36k	0.32		1.560 ± 0.071					
36k (repeat)	0.25	1.16	1.555 ± 0.239	2.04 ± 0.30	2.08 ± 0.09	>350 or indet.		
36n	0.57	0.36	1.714 ± 0.219	1.106 ± 0.117	8.58 ± 1.31	246 (+135/-75)	258 (+145/-71)	2.48 ± 0.48
36n (repeat)	0.42	0.32	1.945 ± 0.278	1.054 ± 0.142	8.25 ± 1.17	265 (+99/-94)	276 (+120/-89)	2.99 ± 0.55
36p2	0.51	0.15	1.646 ± 0.128	1.11 ± 0.78	19.30 ± 1.92	>350 or indet.		
39a	0.87	0.96	1.694 ± 0.098	0.910 ± 0.066	4.32 ± 0.39	168 (+42/-34)		2.11 ± 0.12

Table 2 (continued).

proportion of the measured ^{230}Th activity is not of authigenic origin (within the carbonate from the radioactive decay of U), but instead is of detrital origin. Therefore, the $^{230}\text{Th}/^{234}\text{U}$ determined for samples with low $^{230}\text{Th}/^{232}\text{Th}$ ratios have been corrected for their detrital Th component. Based upon previous experience of the McMaster laboratory in the analysis of travertines, "dirty" archeological carbonate deposits, and speleothems, a correction factor of $[\text{}^{230}\text{Th}/\text{}^{232}\text{Th}]_i = 1.25$ was used in this study.

The relationships between measured U-series isotope activity ratios and U concentrations are illustrated in Figure 8. The lowest $^{234}\text{U}/^{238}\text{U}$ activity ratio occurs in the sample with lowest U content, indicating substantial post-depositional leaching of U from this sample. For other samples, the $^{234}\text{U}/^{238}\text{U}$ activity ratios vary independently of U content, although an important observation from Figure 8 is that the samples which either are at isotope equilibrium or yield finite $^{230}\text{Th}/^{234}\text{U}$ ages are those having the highest U contents and highest $^{234}\text{U}/^{238}\text{U}$ activity ratios. The other five samples display a negative correlation of $^{230}\text{Th}/^{234}\text{U}$ and Th content with U concentration, a clear indication that these samples also have experienced some degree of U loss at some time after their deposition, which has resulted in an induced negative correlation between $^{234}\text{U}/^{238}\text{U}$ and $^{230}\text{Th}/^{234}\text{U}$ ratios with U concentration (Figure 8).

The maximum $^{230}\text{Th}/^{234}\text{U}$ activity ratio for a system at radioactive equilibrium, and subsequently closed to radioisotope migration, is c. 1.0-1.2 (Figure 9), depending on

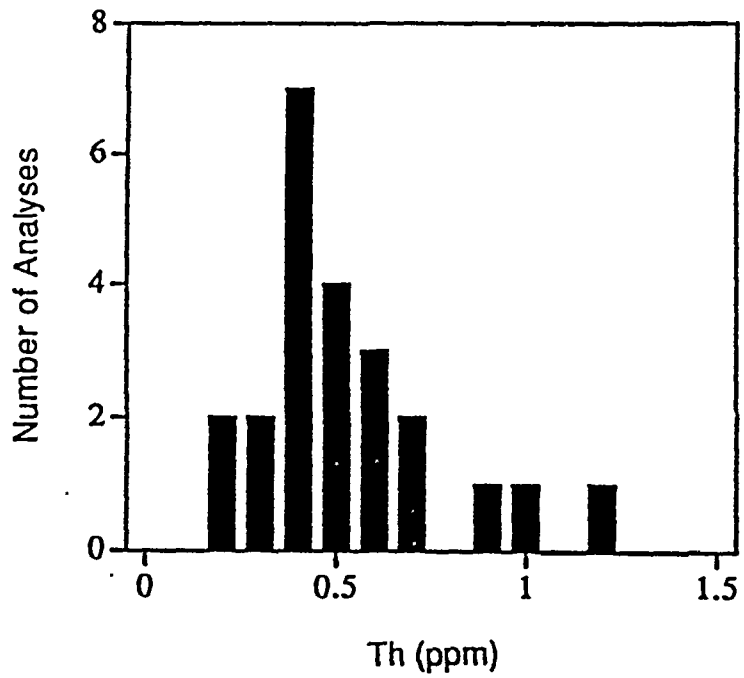
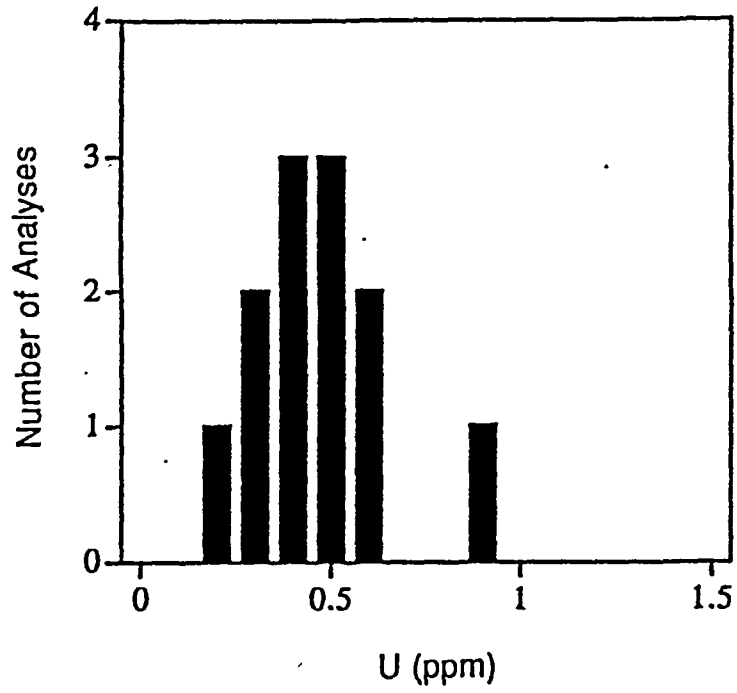


Figure 6. Distributions of measured: a) U concentrations, and b) Th concentrations.

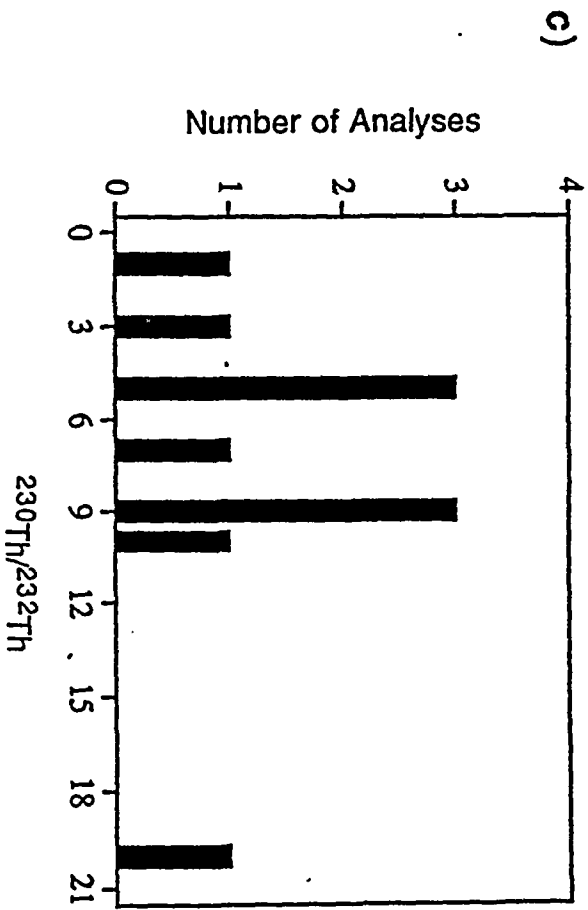
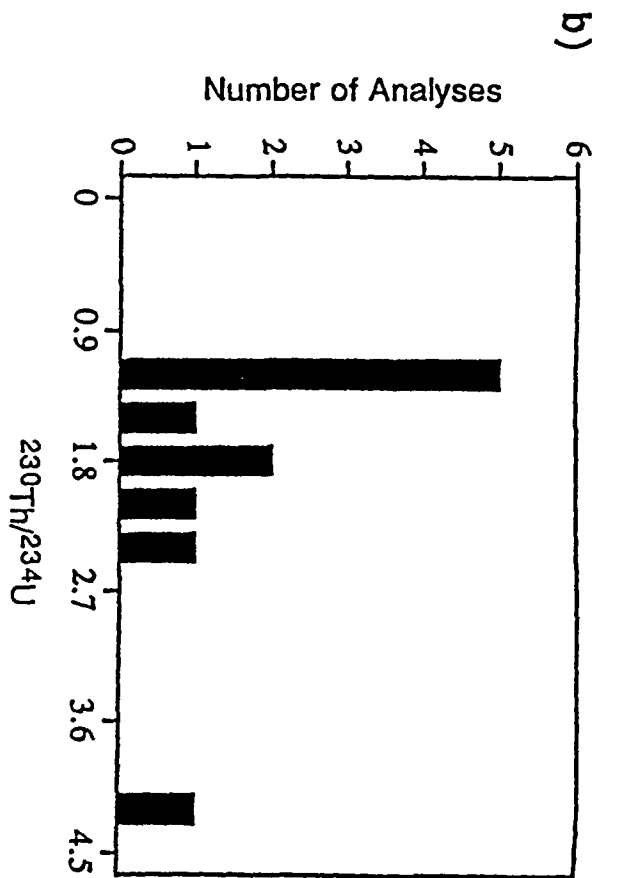
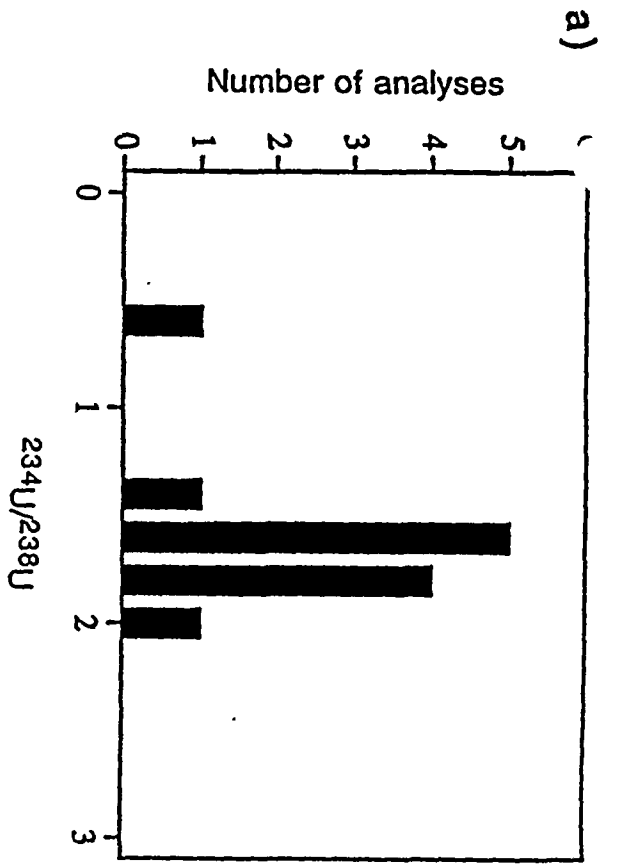


Figure 7. Distributions of measured U-series isotope activity ratios. a) $^{234}\text{U}/^{238}\text{U}$, b) $^{230}\text{Th}/^{234}\text{U}$, and c) $^{230}\text{Th}/^{232}\text{Th}$.

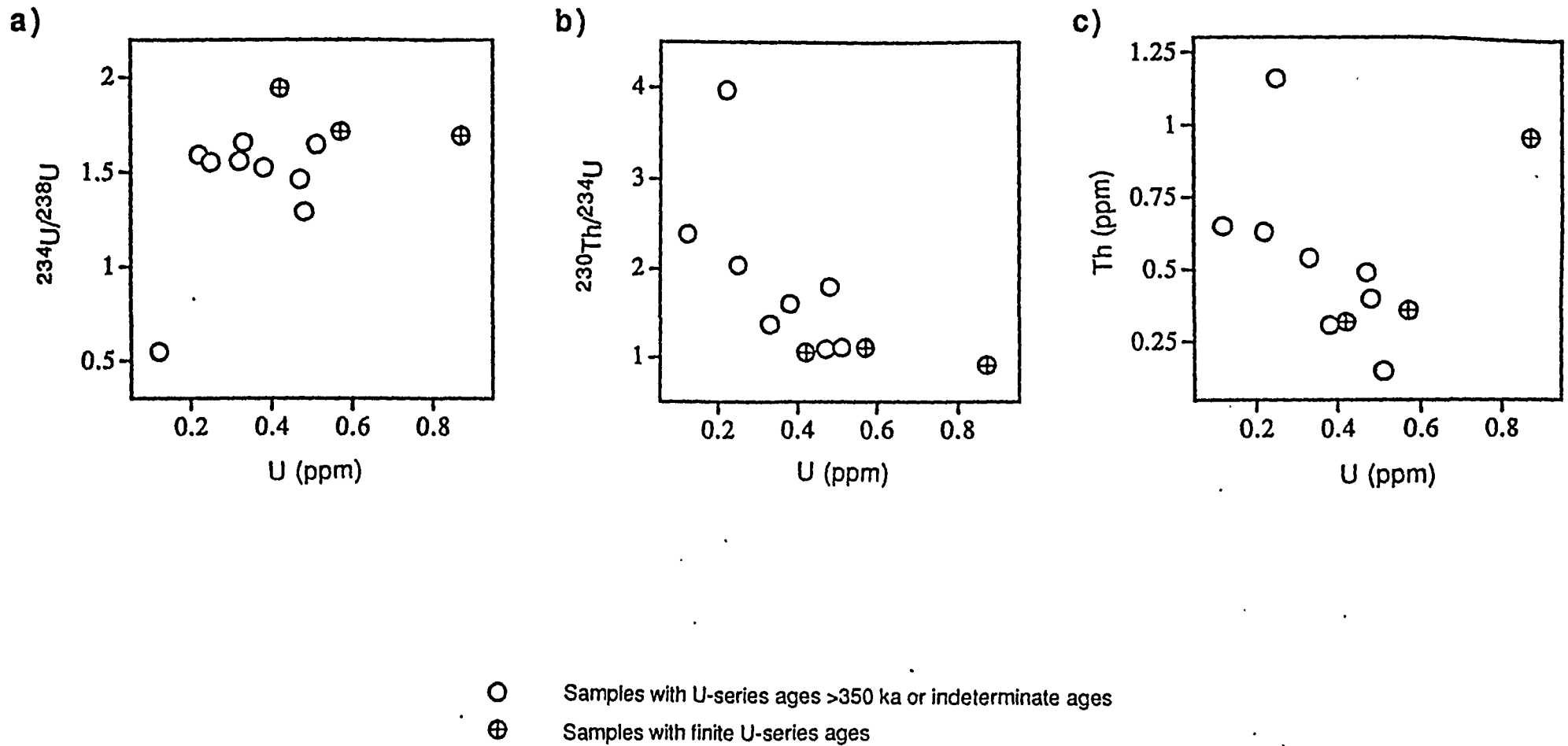


Figure 8. Activity ratios of: a) $^{234}\text{U}/^{238}\text{U}$, b) $^{230}\text{Th}/^{234}\text{U}$, and c) Th (ppm) as a function of sample U concentration.

its initial $^{234}\text{U}/^{238}\text{U}$ ratio. Four of the Yucca Mountain samples have measured $^{230}\text{Th}/^{234}\text{U}$ activity ratios of less than 1.2. Two of these samples (36n and 39a) yield finite $^{230}\text{Th}/^{234}\text{U}$ ages and two samples (30a and 36p2) are observed to be at isotopic equilibrium (i.e. >350,000 years old). The remaining five samples (28d, 28e, 36d, 36g, and 36k) have $^{230}\text{Th}/^{234}\text{U}$ ratios that are too high and, therefore, reflect the post-depositional leaching of U from the samples.

The other important information that can be obtained from the four pristine samples (36n, 39a, 30a, and 36p2) is their initial (at the time of deposition) $^{234}\text{U}/^{238}\text{U}$ ratio, which is a direct reflection of that in the solution from which the carbonates were precipitated. For these four samples, calculated $^{234}\text{U}/^{238}\text{U}$ ratios fall between 2.2 and 3.2. This range is distinctly higher than that of 1.0 to 1.7 reported by USGS investigations for "pedogenic" carbonates of the Yucca Mountain region, but brackets the $^{234}\text{U}/^{238}\text{U}$ activity ratio of 2.5 to 3.0 for deep carbonate groundwaters that periodically supplied springs near the southern end of Crater Flat during the Late Pleistocene.

Conclusions

Of the nine samples submitted for U-series disequilibrium analysis, four (30a, 36n, 36p2, and 39a) appear to have remained closed systems to radionuclide migration since the time of their deposition; the other five samples (28d, 28e, 36d, 36g, and 36k) have been subjected to variable degrees of fluid-rock interaction which has leached U from the samples. Of the four pristine samples, finite $^{230}\text{Th}/^{234}\text{U}$ ages

(corrected for the presence of detrital Th) of c. 245-265ka and 170ka. were obtained for two samples (36n and 39a) and two samples (30a and 36p2) were observed to be in isotopic equilibrium and thus have an age of >350ka. The two ages determined fall within two of the three time intervals of calcite deposition recognized to have occurred in southern Nevada during the late Pleistocene.

Initial $^{234}\text{U}/^{238}\text{U}$ activity ratios for the four pristine carbonate samples vary from 2.2 to 3.2. Such values are comparable to those that have characterized the regional groundwater system in southern Nevada over the last 500,000 years. Because U-series measurements were not, in general, made on the same samples analyzed for Sr-, C-, and O-, it has not been possible to examine interrelationships between $^{234}\text{U}/^{238}\text{U}$ activity ratios and these other geochemical tracers.

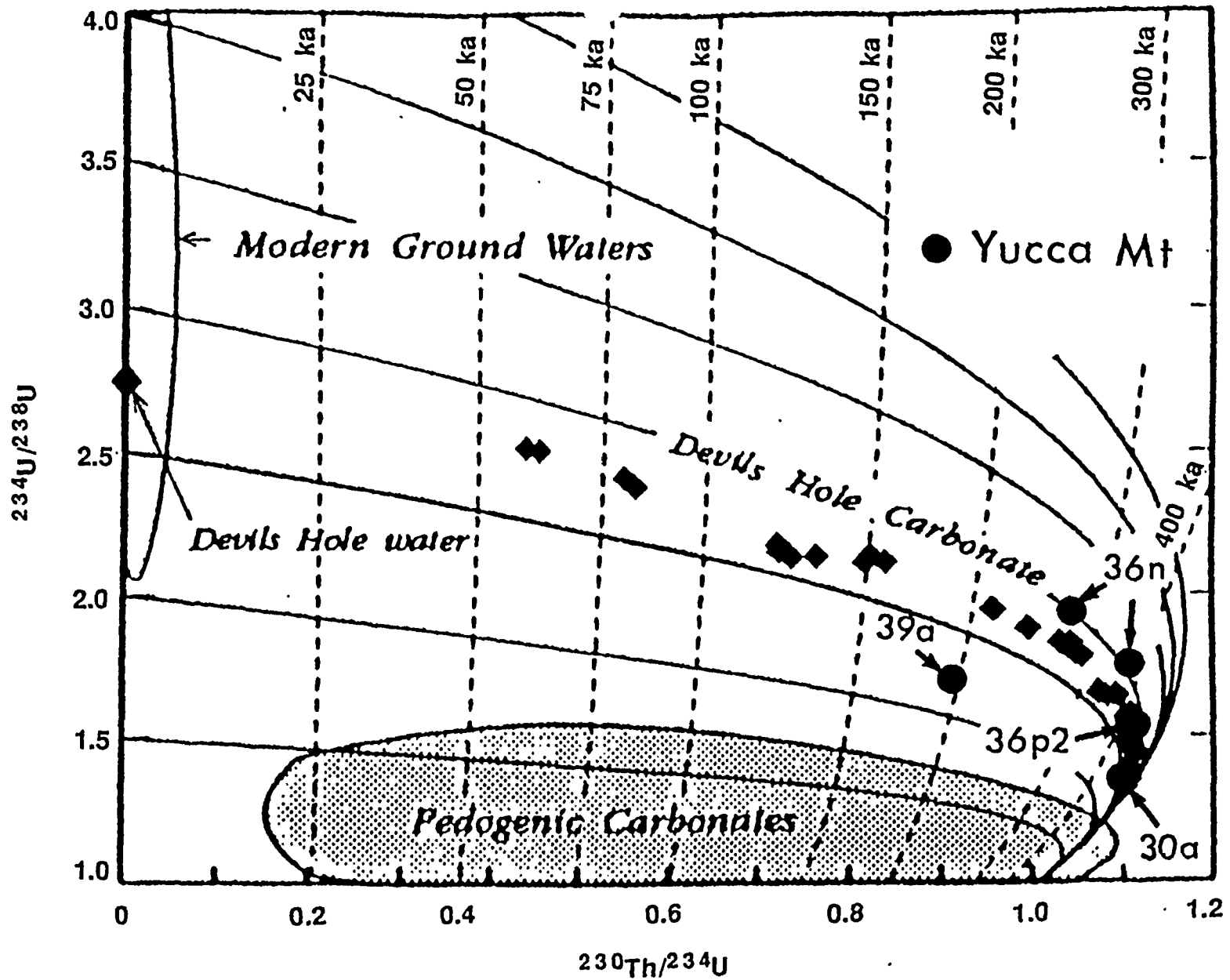
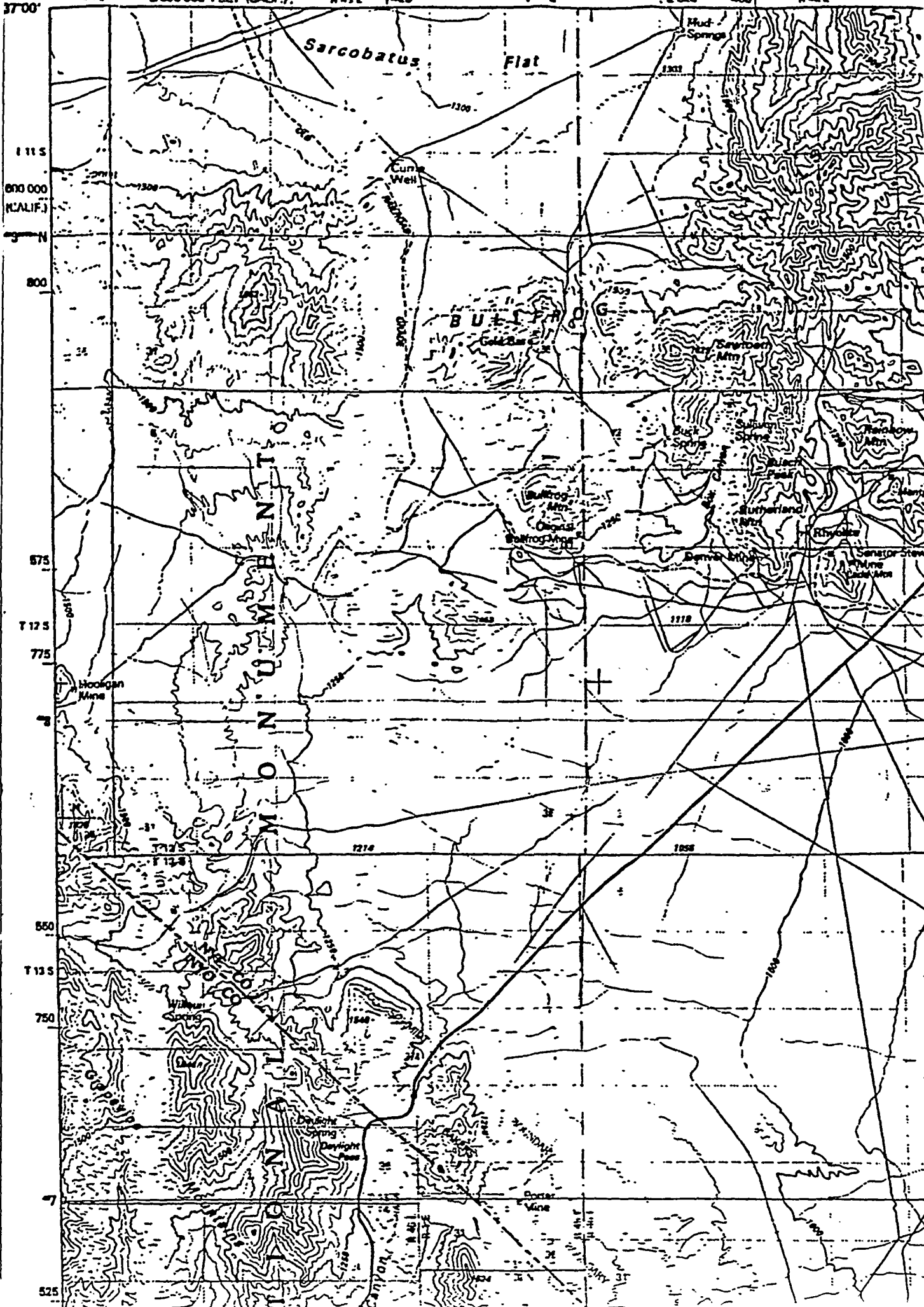


Figure 9. U-series isochron diagram. Taken from Paces et al., 1993.

STOP #	SAMPLE	TYPE	STOP #	SAMPLE	TYPE
STOP #1	US 95 mile 10		STOP #10	Bare Mountain	
1a	dolomite	Nopah Fromation	10a	calcite-opal	loose material
1b	silica	breccia zone	10b	lmst/opal	brecciated, cemented
1c	calcite		10c	calcite-lmst	
1d	dolomite	organic lithofacies	10d	limestone	Ely Springs
1e	silica	vein	10e	opal	siliceous
1f	calcite	vein	10f	carbonate	in stream bed
1g	calcite				
			STOP #11	Diamond Queen M.	
STOP #2	US 95 mile 12.47		11a	white mineral	filling, metamorphosed
2a	quartzite (clean)	Stirling Quartzite	11b	calcite	float sample
2b	quartzite (dirty)	Stirling Quartzite	11c	phyllite	Johnnie Formation
2c	epidote	vein	11d	carbonate	incrustations
2d	calcite	vein	11e	Nopah formation	
			11f	Iceland spar	massive
STOP #3	US 95 mile 18.8		11g	calcite	vein
3a	dolomite/lmst		11h	quartz	
			11j	fluorite	
STOP #4	Pull Apart Fault		11k	fluorite	
4a	limestone	fault related alteration	11m a	calcite	coating
4b	calcite	coating	11m b		
4c	calcite-opal-breccia		11n	calcite	crust
4d	calcite-opal	bulk samples	11o	kaolinite clay	from breccia pipe
4e	opal breccia		11p	chert nodule	in fluorite breccia
4f	calcite	riverbed	11q	porphyry	volcanic breccia
4g	carb.-coated rock		11r	fluorite breccia	
			11s	chert nodule	
STOP #5	WT - 7				
5a	calcrete-coated rock		STOP #12	Chuckwalla Canyon	
5b	calcite-opal	surficial deposit	12a	Iceland spar	massive
5c	opaline layer	on breccia	12b	opal-calcite	inter-layers
5d	calcite-silica		12c	carbonate	white & black minerals
5e	calcite	fracture fill	12d	dolomite	Lone Mt.
5f	breccia		12e	calcite	
5g	breccia		12f	calcite	fracture filling
5h	calcium crystals	Carol's sample	12g	calcite	columnar crystals
STOP #6	USW H - 6		STOP #13	Tarantula Canyon	
6a	carbonate crust	surficial coating	13a	limestone	Meiklejohn
			13b	rhyolite	
STOP #7	roadside (WT-7)				
7a	calcite	caliche?/calcrete	STOP #14	Trench 8	
7b	silica-calcite		14a	calcite	root casts
7c	opal		14b	ash	
7d	indurated layer	coating on surface rock	14c	calcite-opal-silica	
			14d	calcite-opal	fault infilling
STOP #8	Plug Hill		14e	black glassy material	in altered vitrophyre
8a	carbonate	coating on colluvium	14f	carb., some silica	cement
			14g	silica-calcite	vein
STOP #9	roadside (WT-7)				
9a	calcite	coating			

STOP #	SAMPLE	TYPE	STOP #	SAMPLE	TYPE
STOP #15	roadsie (trench 8)		STOP #26	roadside (FOC)	
15a	carbonate	matrix	26a	lmst, dolomite	Bonanza King
STOP #16	New Trench		STOP #27	roadside (FOC)	
16a	carbonate	vein	27a	calcite	secondary
16b	ash		27b	carbonate? in basalt and	ccment filling
16c	carbonate	matrix	27c	travertine	surficial cap
STOP #17	Site 106		STOP #28	East Busted Butte	
17a	tufa	spring	28a	silica	vein
17b	carbonate	spring	28b	sand	
STOP #18	Livingston Scarp		28c	carbonate?	root casts
18a	carbonate	fracture fillings	28d	carbonate?	vert. vein
18b	opal-carbonate	vein	28e	opaline-coral	slope deposit
STOP #19	Wailing Wall		28f	travertine	upslope
19a	opal-calcite	coating	STOP #29	East Busted Butte	
19b	carbonate	vein	29a	calcrete	
19c	carbonate	coating	29b	rat midden	
19d	algal?		29c	sheet deposit	
19e	opal-calcite	Carol's sample	29d	vitrophyre	
STOP #20	roadside ("scarp")		29e	travertine, breccia	sheet deposit
20a	glass	volcanic	29f	carbonate?	root casts
STOP #21	Red Cliff Gulch		STOP #30	West Busted Butte	
21a	carbonate	surface coatings	30a	carbonate?	vert. vein
STOP #22	Stagecoach Trench	(North)	30b	carbonate?	root casts
22a	carbonate	root casts	30c	opal-calcite	
22b	tuff	calcite overlies	30d	carbonate?	vein
22c	quartz?	calcite overlies	30e	carbonate?	vein
22d		full of clasts	30f	calcite	vein
22e	carbonate	surficial	30g	carbonate?	punchbowl
STOP #23	Stagecoach Trench	(South)	30h	carbonate?	root casts
23a	carbonate	root casts	STOP #31	roadside (Mercury)	
23b	glass	vitrophyre	31a	calcite	coating
STOP #24	Site 199		STOP #32	Wahmonie Mounds	
24a	silicified material	some clasts	32a	gypsum with calcite	
24b	breccia (Carrera)	conglomerate	32b	carbonate	
24c	breccia	Bonanza King	32c	calcite-gypsum	
24d	tufa	some brecciated carb.	32d	calcite	
JP #25	roadside (site 199)		32e	gypsum	crust on carbonate
25a	carbonate	root casts (burrows?)	STOP #33	Mines (Wahmonie)	
25b	seeds.	marsh/lake	33a	carbonate?	vein
			33b	fluorite? in quartz	
			33c	calcite crystal in quartz	

STOP #	SAMPLE	TYPE	STOP #	SAMPLE	TYPE
STOP #34	Calico Hills		STOP #37-2	Mercury	
34a	shale	Elcana	37-2a	dolomite	fault zone
34b	limestone	Elcana	37-2b	carbonate	vein
34c	pyrite	cubes			
34d	pumice and silicified	Calico Hills	STOP #38	West Busted Butte	
34e	kaolinitized clay		38a	sand	windblown
34f	ironized tuff	Calico Hills	38b	travertines	
34g	calcite	slslickenside	38c	opal-calcite	
34h	yellow hot rock		38d	pumice tuff	bedded tuff
			38e	tuff	red altered
STOP #35	Shoshone Mt. road		38f	travertine	
35a	kaolinite		38g	carbonate	caps tuff
35b	Topopah	red sample			
35c		cavity fillings	STOP #39	Harper Valley	
			39a	carbonate	in streambed
STOP #36	Trench 14		39b	silica	botryoidal (opalite)
36a	carbonate		39c	Tiva	partially welded
36b	opaline		39d	flowstone	laminated
36c	carbonate	finely laminated	39e	carbonate	vein filling
36d	carbonate	vein	39f	opal	botryoidal
36e	silica	vein	39g	calcite	vein
36f	carbonate	vein	39h	some opal	pinnacles
36g	carbonate	vein	39i	carb?-silica	"Z" veins
36h	silica	vein	39k	tuff	red altered
36i	carbonate	vein	39m	carbonate	vein
36j	opal	vein	39n	opal	Carol's sample
36k	opal-breccia-carbonate	finely laminated			
36m	calcite	vein	STOP #40	Trench 14	
36n	carbonate	vein	40a1	mostly carbonate	vein
36o	carbonate	vein	40a2	carbonate?	vein
36p1	calcite-opal	vein	40a3	carbonate?	vein
36p2	calcite-opal	vein	40b	calcite	vein
36r	carbonate	vein	40c	calcite	subsurface
36s	opal	vein			
36t	carbonate	vein	STOP #41	Lathrop Cone	
36v	carbonate	vein	41a	sulfur or jarosite	
36w	opal	vein	41b	carbonate	coatings
36x		Calico Hills?	41c	sulfur?	
36y	breccia-calcite				
36z	breccia		STOP #42	Lathrop Cone	
			42a	sand	
STOP #37-1	UE 25 p#1				
37-1a	opal	opaline			
37-1b	opal	Carol's sample			



Sarcobatus Flat

Mud Springs

Cuma Well

BULLROG

Sutherland Mtn

Bullfrog Mtn

Sutherland Mtn

Denver Mtn

Senator Stew. Mtn

Hoodigan Mine

Winters Spring

Daylight Pass

Dicker Mine

CANYON

1115
800 000
(CALIF.)

800

875

T 125

775

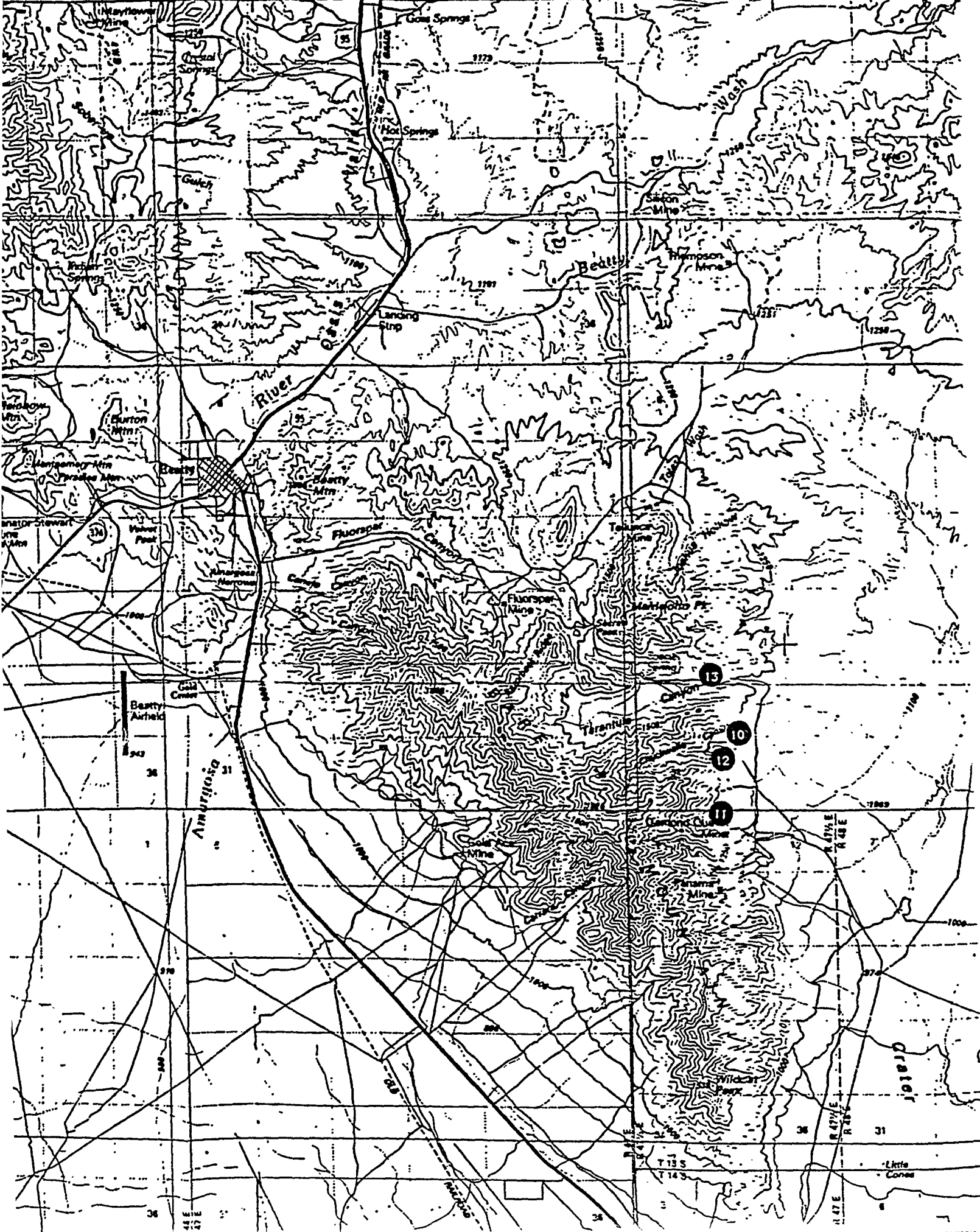
850

T 135

750

7

525



Mayflower Mine
Central Springs
1175

Goss Springs
1175
Hot Springs
1175

Wash
1175

1160
1160
1160

Landing Strip
1160

Betty
1160

Thompson Mine
1160

Burton Mtn
1160

River
1160

Florspar
1160

Florspar Mine
1160

Mahogany Pt.
1160

Betty Airfield
1160

Amargosa
1160

15

10

12

11

1160

1160

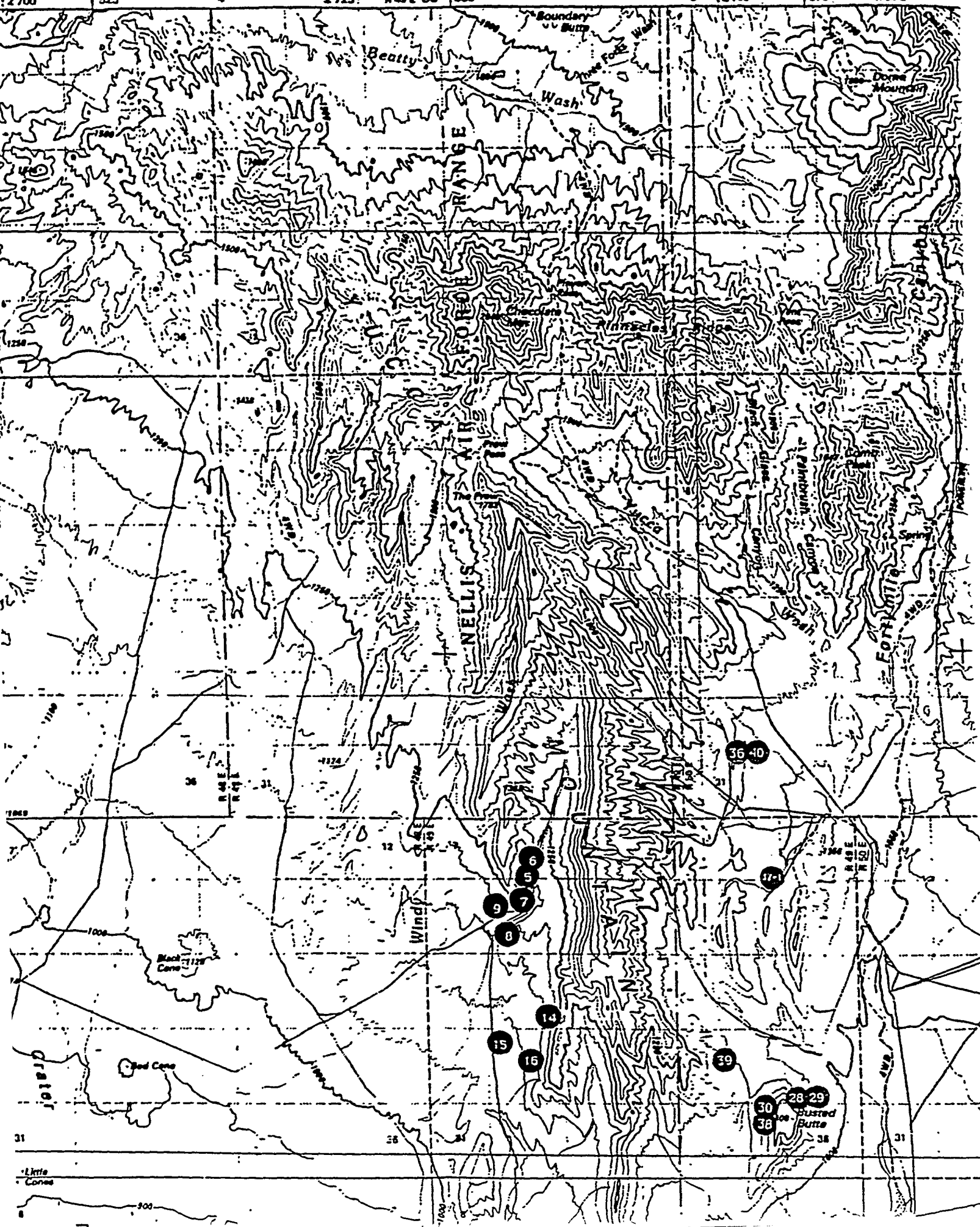
Crater
1160

1160

Little Cones
1160

T 13 S
T 14 S

R 47 E
R 48 E



Beatty

Boundary
Butte

Wash

RANGE

WASHO

WASHO

WASHO

WASHO

WASHO

WASHO

WASHO

WASHO

Dome
Mountain

Chocolate
Mtn

Washoe
Canyon

Fort
Milla

Fort
Milla

Fort
Milla

Fort
Milla

Fort
Milla

Fort
Milla

Black
Cone

Black
Cone

Black
Cone

Black
Cone

Busted
Butte

Busted
Butte

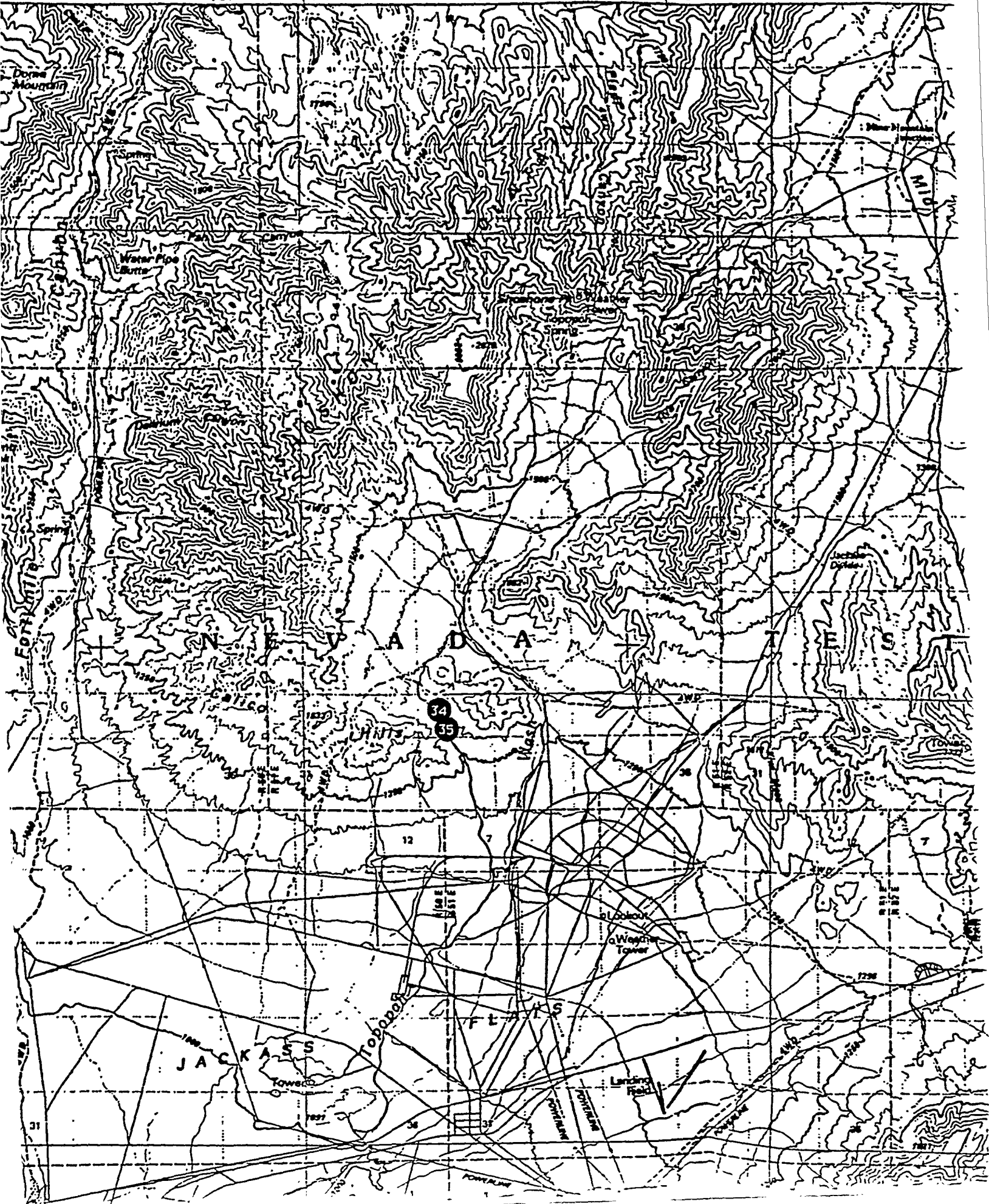
Busted
Butte

Little
Cove

Little
Cove

Little
Cove

- 1
- 2
- 3
- 4
- 5
- 6
- 7
- 8
- 9
- 10
- 11
- 12
- 13
- 14
- 15
- 16
- 17
- 18
- 19
- 20
- 21
- 22
- 23
- 24
- 25
- 26
- 27
- 28
- 29
- 30
- 31
- 32
- 33
- 34
- 35
- 36



Dome Mountain

Water Pipe Butte

Cottonwood Creek

JACKASS TOWNSHIP

FLACKS

Landing Field

Weather Tower

MID

34
35

31

12

36

35

7

7

36

35

30X60 MINUTE SERIES (TOPOGRAPHIC)

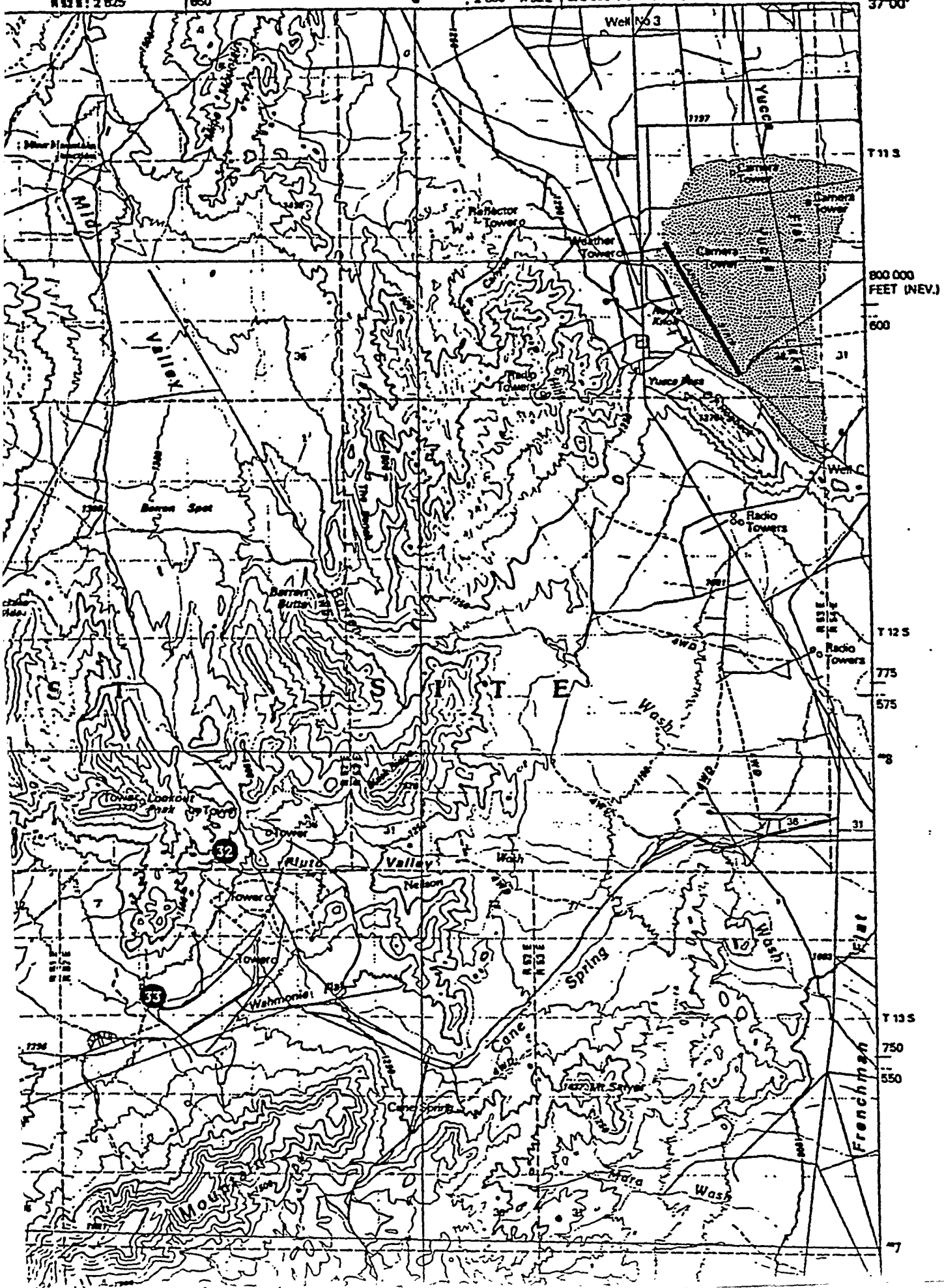
R 32 E : 2 825

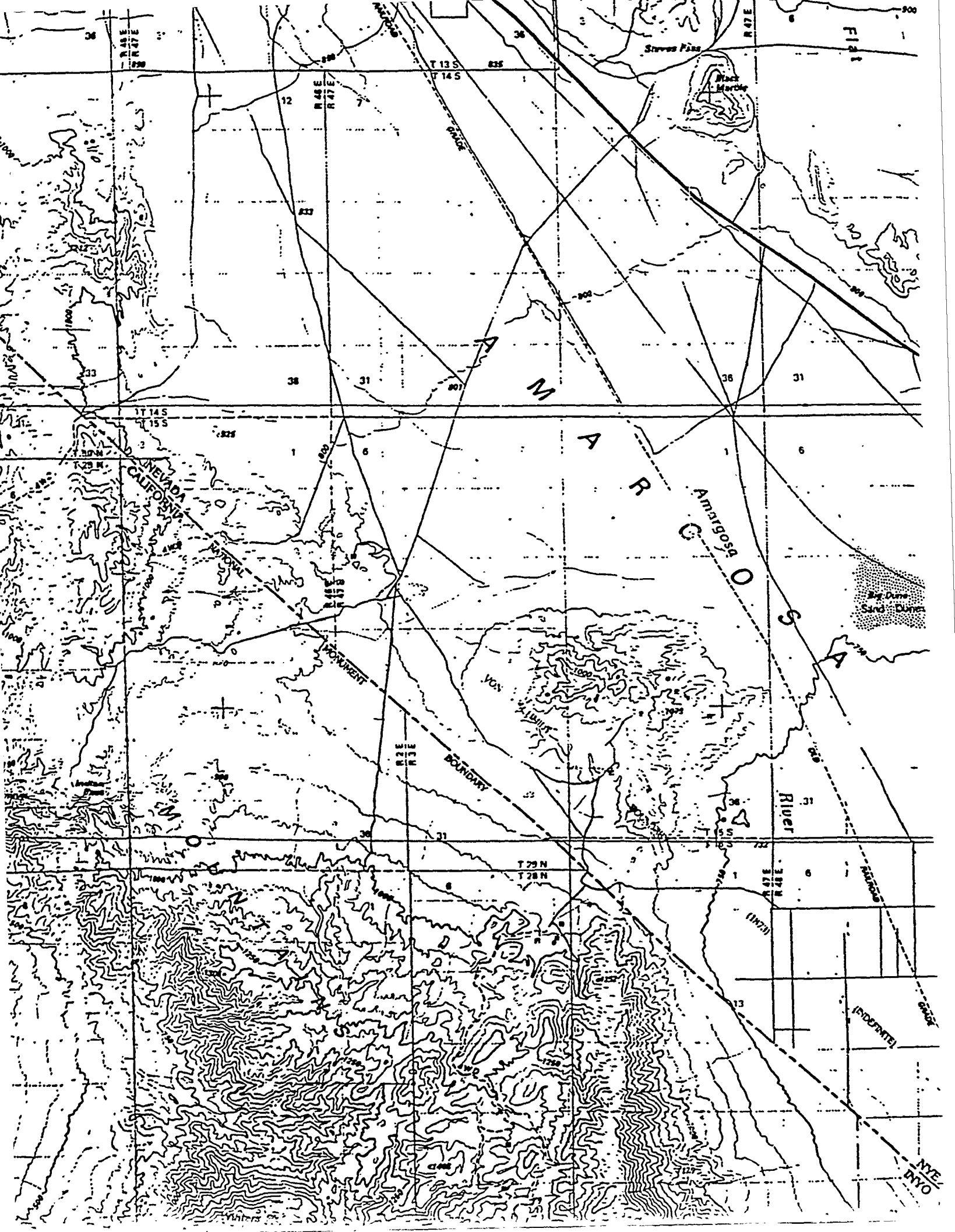
1 650

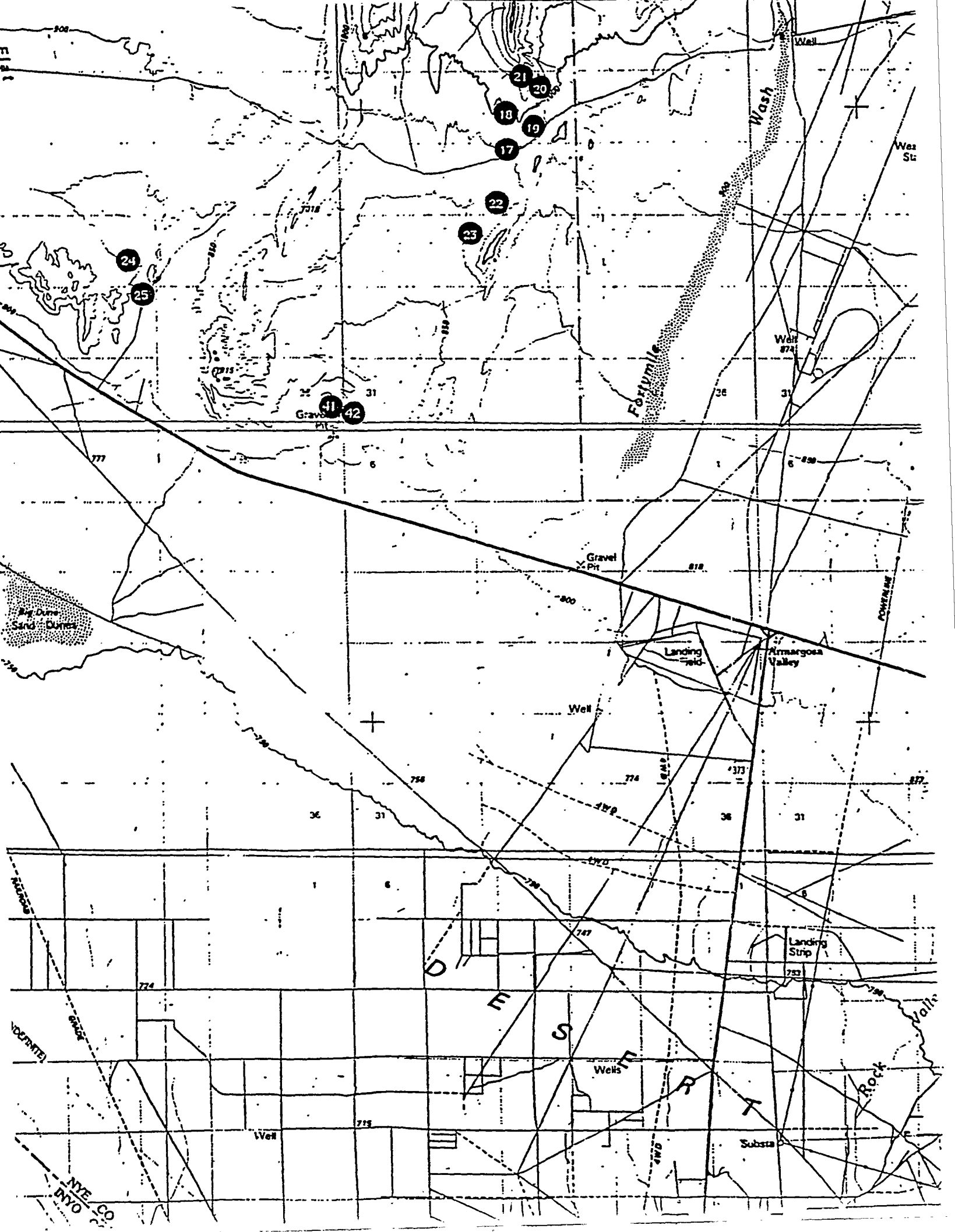
: 2 850 R 31 E | 875 000 FEET (NEV.)

135°00'

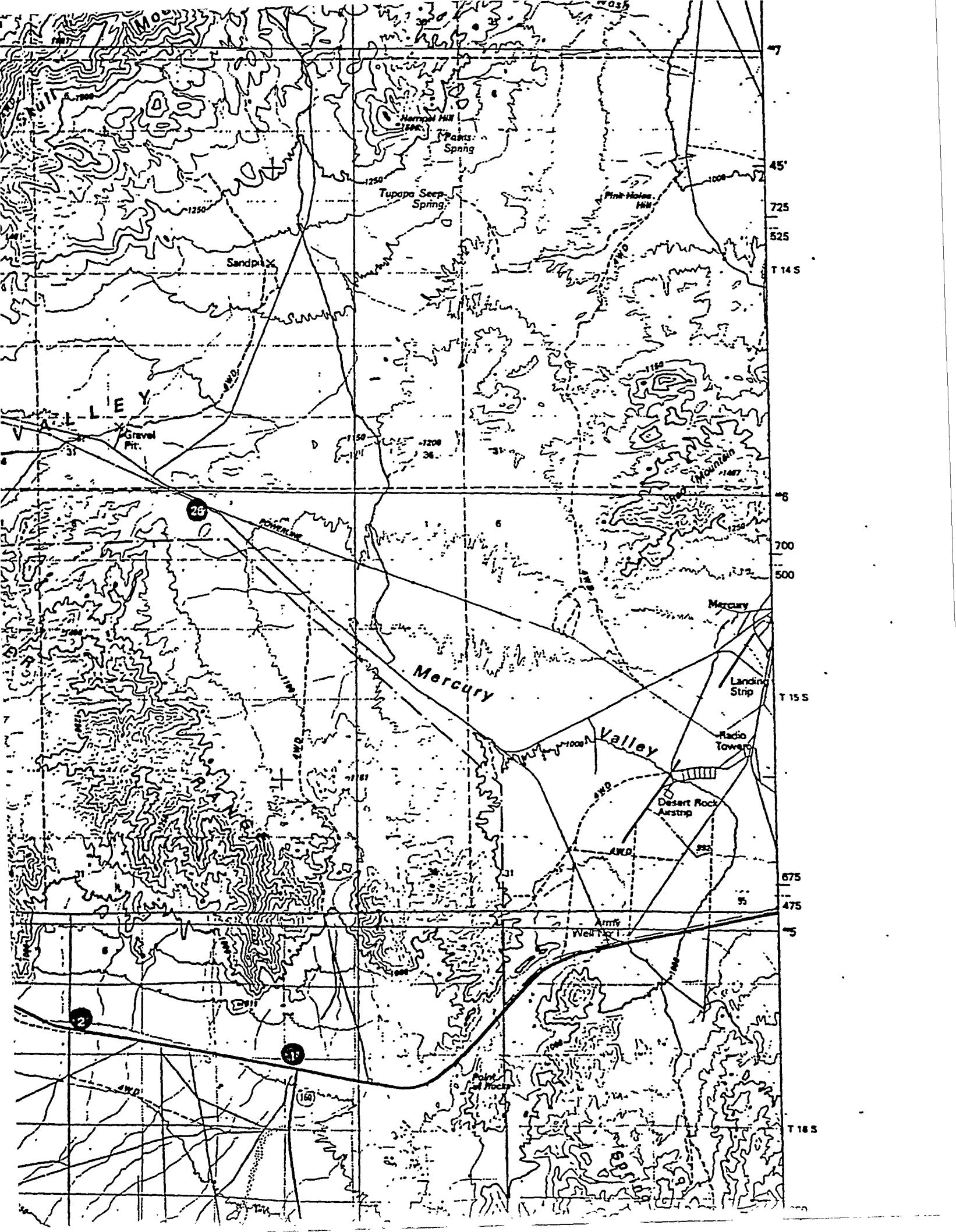
37°00'

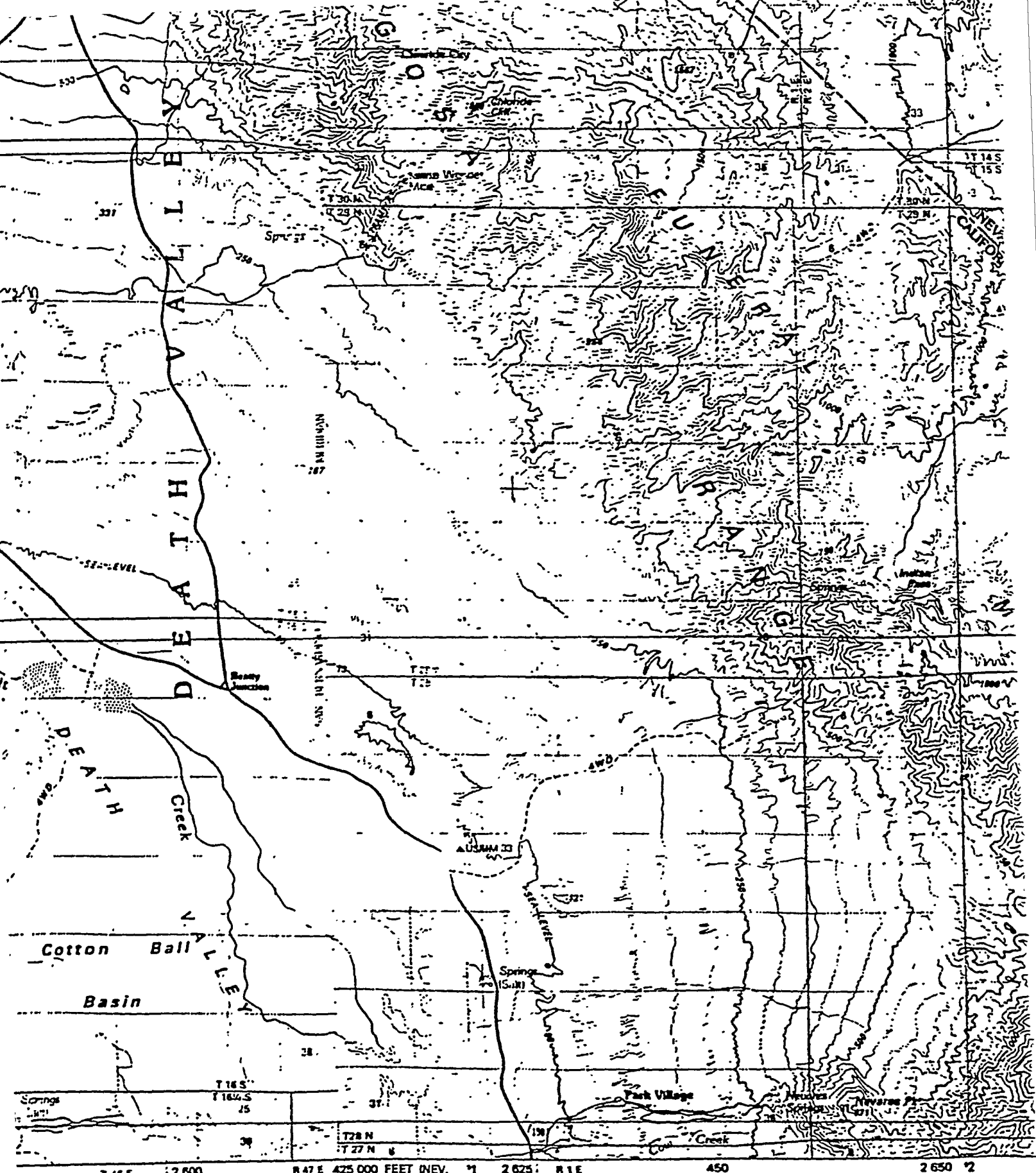




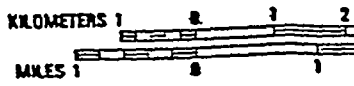








UNITED STATES GEOLOGICAL SURVEY, RESTON, VIRGINIA - 1968



746 E 12600 R47E 425 000 FEET (MEV. 1) 2625 R1E 450 2650 2

T16S
116W S
25

T28 N
117 W
6

Springs
117 W
25

Park Village

Spring
(S. 111)

Creek

Cotton Ball

Basin

DEATH VALLEY

DEATH VALLEY

DEATH VALLEY

CALIFORNIA

T14 S
T15 S

T29 N

T28 N

2650 2

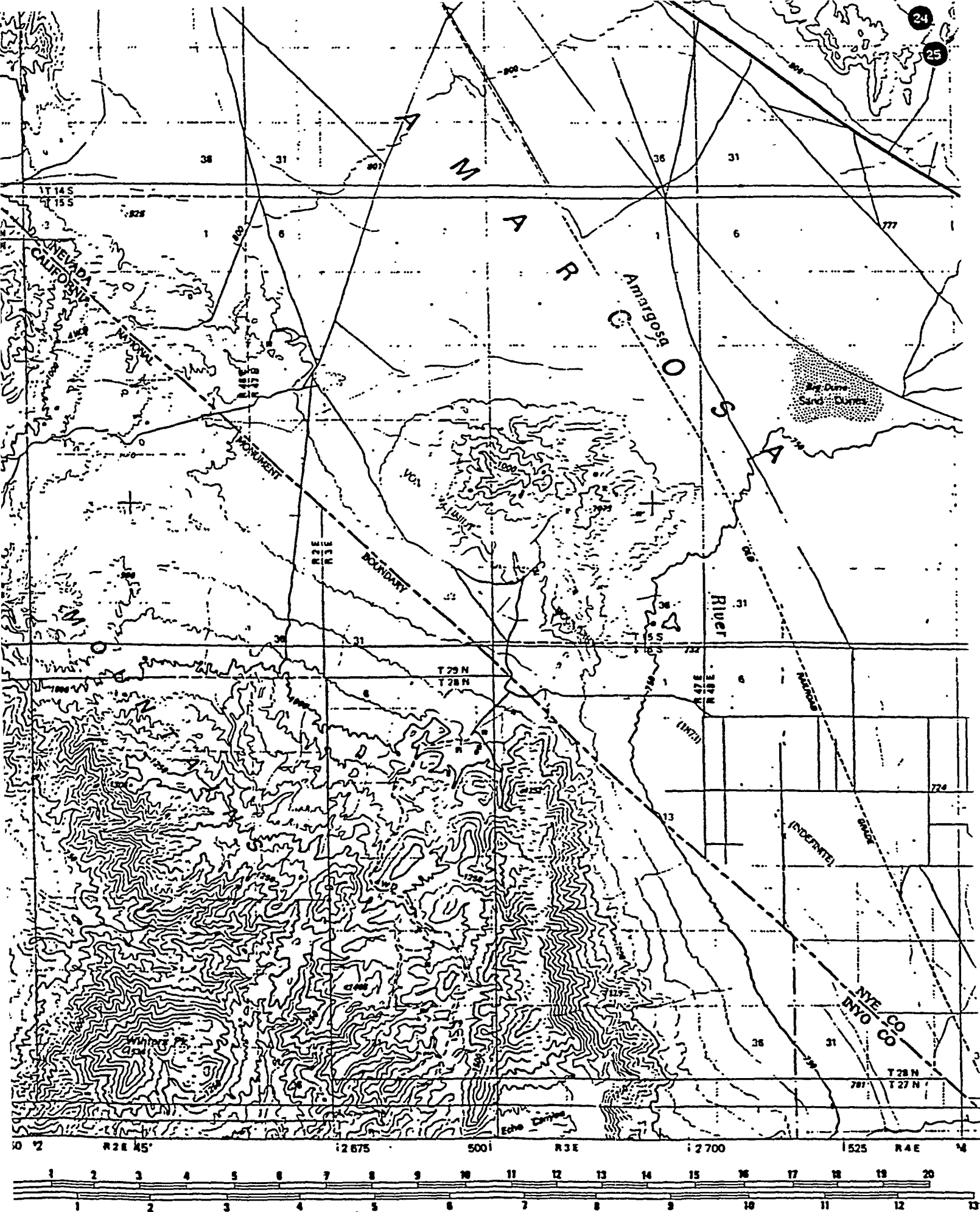
450

2625 R1E

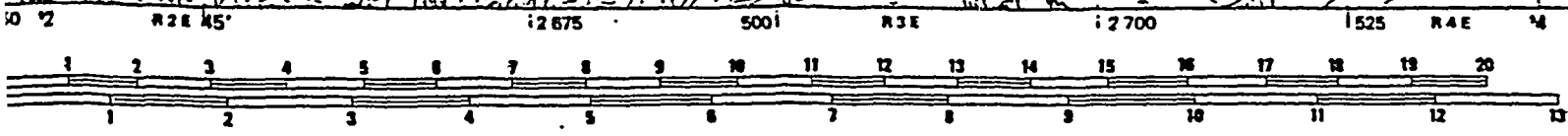
R47E 425 000 FEET (MEV. 1)

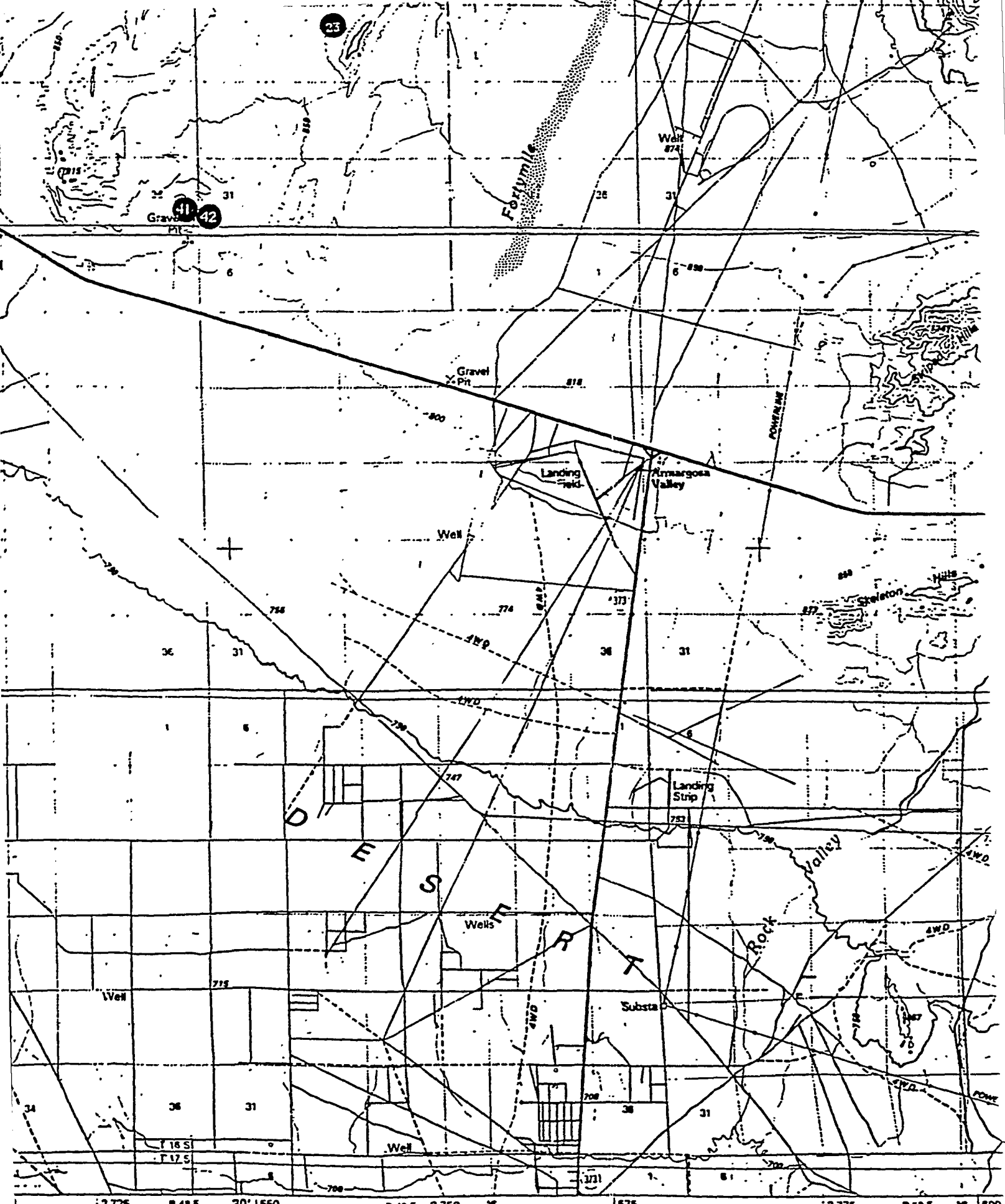
12600

746 E



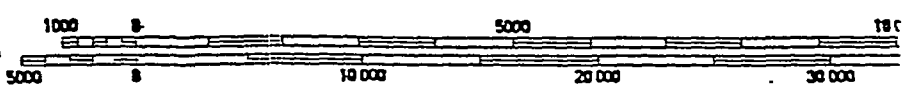
24
25

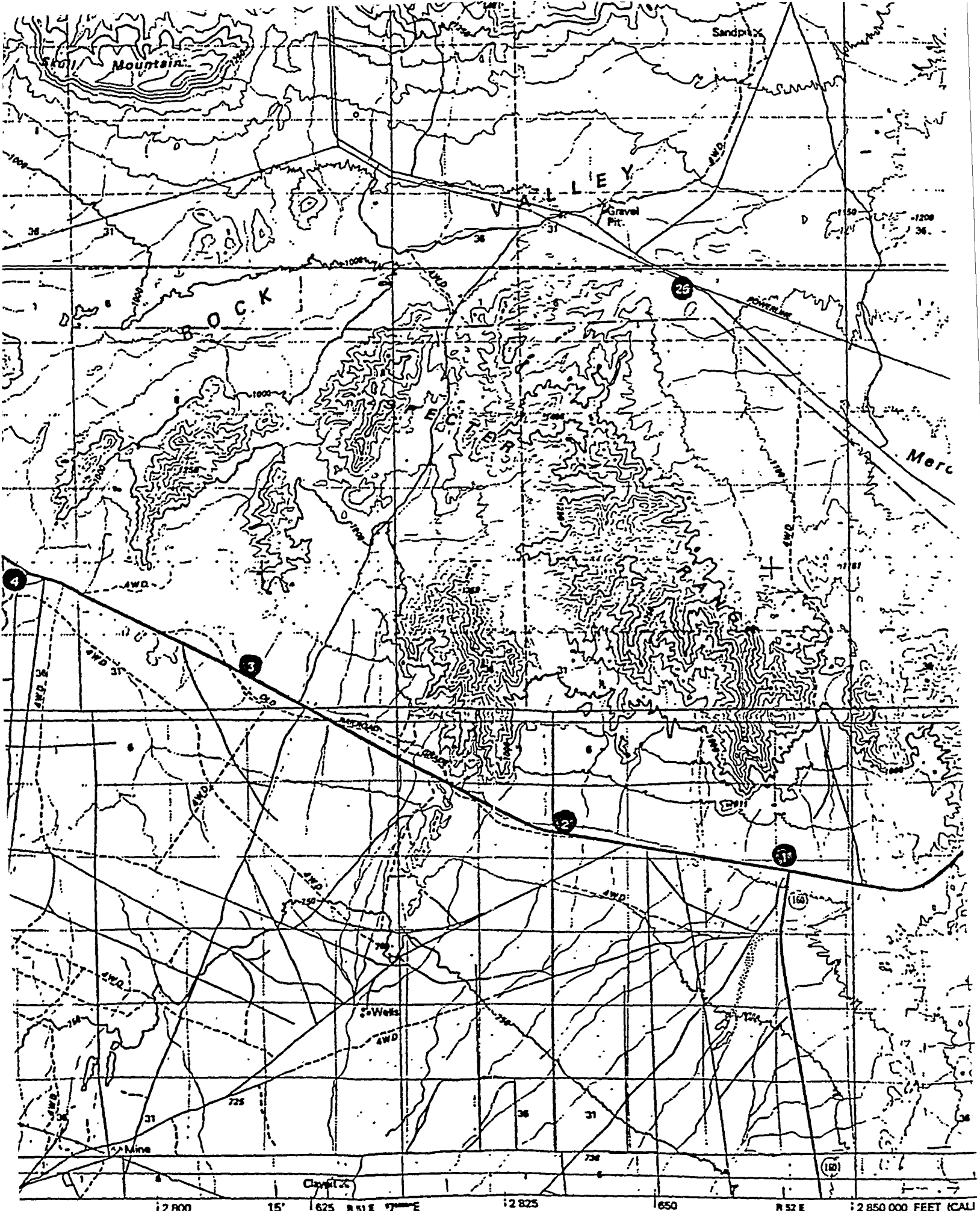




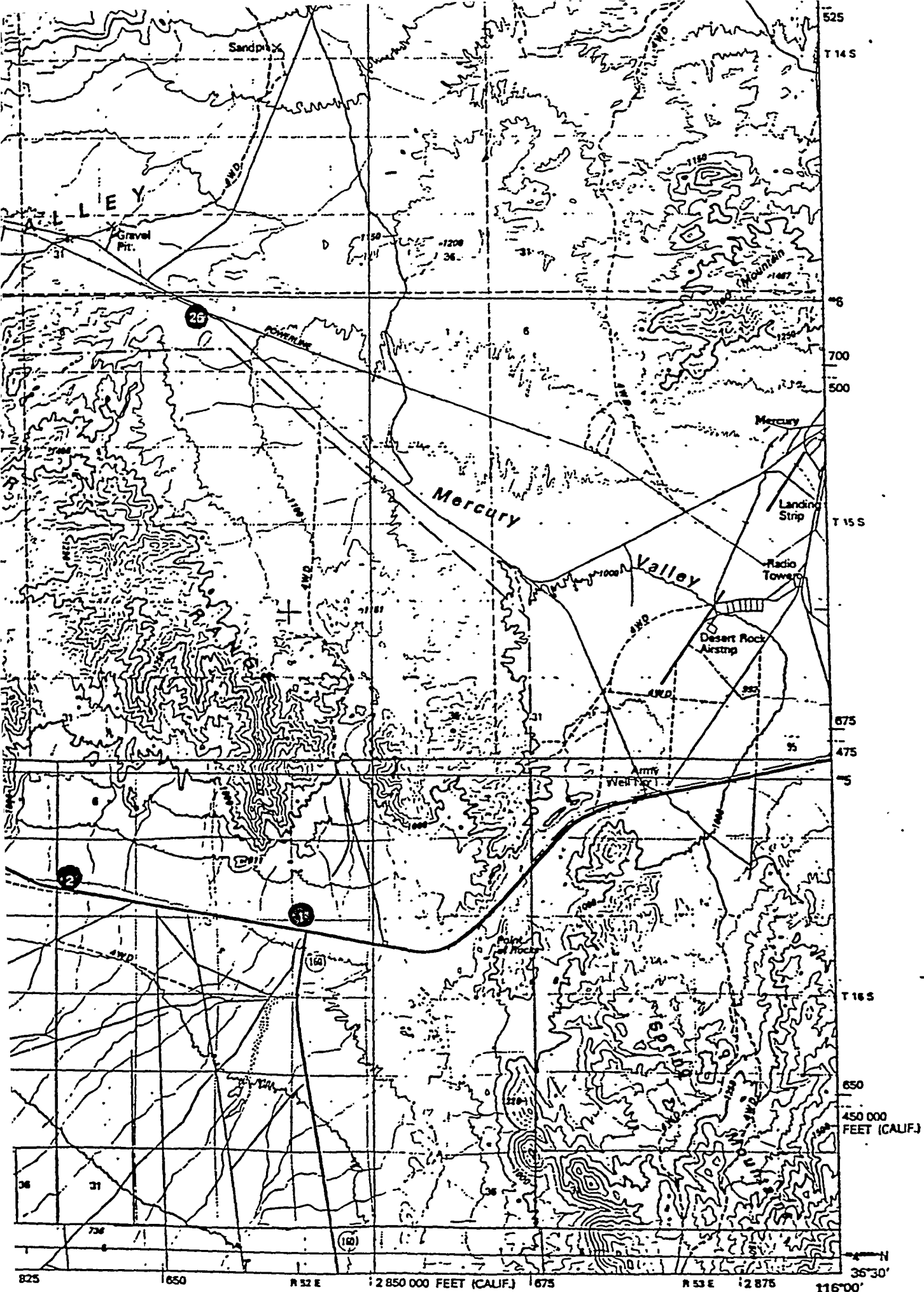
SCALE 1:100 000

1 CENTIMETER ON THE MAP REPRESENTS 1 KILOMETER ON THE GROUND
 CONTOUR INTERVAL 50 METERS





BEA



BEATTY, NEVADA—CALIFORNIA